Formation and reactions of *P*-amino substituted Li/Cl phosphinidenoid complexes

Dissertation

zur

Erlangung des Doktorgrades (Dr. rer. nat.)

der

Mathematisch-Naturwissenschaftlichen Fakultät

der

Rheinischen Friedrich-Wilhelms-Universität Bonn

Vorgelegt von

Philip Junker, M. Sc.

aus Bad Honnef

Bonn, 2020

Angefertigt mit Genehmigung der Mathematisch-Naturwissenschaftlichen Fakultät der Rheinischen Friedrich-Wilhelms-Universität Bonn

1. Gutachter: Prof. Dr. Rainer Streubel

2. Gutachter: Prof. Dr. Thomas Bredow

Tag der Promotion: 3. März 2021

Erscheinungsjahr: 2021

TO MY MOTHER DORIS, MY FATHER ROBERT † AND MY SISTER ALISSA

„Geniale Menschen beginnen große Werke, fleißige Menschen vollenden sie.“

Leonardo da Vinci

Publikationen und Konferenzbeiträge

Vorveröffentlichungen

1. *"Analysis of non-innocence of phosphaquinodimethane ligands when charge and aromaticity come into play."*; P. Junker, A. Rey Planells, A. Espinosa Ferao, R. Streubel, *Chem. Eur. J.* **2021**, *Accepted*. DOI: 10.1002/chem.202100420R2
2. *"A case study on the conversion of Li/Cl phosphinidenoid into phosphinidene complexes."*; P. Junker, Z.-W. Qu, T. Kalisch, G. Schnakenburg, A. Espinosa Ferao, R. Streubel, *Dalton Trans.* **2021**, *50*, 739.
3. *„ Formation and properties of phosphaquinomethane tungsten(0) complexes – isolation and conversion of primary radical coupling products."*; P. Junker, J. M. Villalba Franco, G. Schnakenburg, V. Nesterov, R. T. Boeré, Z.-W. Qu, R. Streubel, *Dalton Trans.* **2020**, *49*, 13544-13548.

Weitere Publikationen

1. *„Competitive or sequential reaction of an electrophilic terminal phosphinidene metal(0) complex with allyl halides? [2+1]-cycloaddition vs. C-X bond insertion."*; A. A. Khan, P. Junker, G. Schnakenburg, A. Espinosa Ferao, R. Streubel, *Chem. Commun.* **2019**, *55*, 9987.
2. *„Synthesis of P-CPh$_3$ Substituted Spirooxaphosphirane Complexes: Steric Effects Dominate the Product Formation."*; R. Streubel, P. Junker, A. W. Kyri, G. Schnakenburg, *Organometallics* **2017**, *36*, 2952-2955.

Konferenzbeiträge

1. "10. Deutsch-Österreichischer Mitarbeiter Workshop für Hauptgruppenelement Chemie" (MHC 10) in Tübingen (Deutschland) vom 15.-17.3.2019; **Vortrag** *"P-NR$_2$ substituted Li/Cl phosphinidenoid complexes – stability and reactivity."*
2. "13. International Conference on Heteroatom Chemistry" (ICHAC 13) in Prague (Tschechische Republik) vom 30.6.-5.7.2019; **Posterbeitrag** *"The remarkable difference in stability and reactivity of amino-substituted phosphinidenoid metal(0) complexes."*
3. "Bonn International Graduate Summer School" in Bonn (Deutschland) vom 10.-12.09.2019; **Posterbeitrag** *"Stability and reactivity of P-amino substituted phosphinidenoid metal(0) complexes – remarkable differences."*
4. "15. International Symposium on Inorganic Ring Systems" (IRIS 15) in Kyoto (Japan) vom 24.-29.6.2018; **Teilnahme**.

5. “15. European Workshop on Phosphorus Chemistry” (EWPC 15) in Uppsala (Schweden) vom 14.-16.3.2018; **Posterbeitrag** *„Formation and properties of phosphaquinomethane complexes.“*
6. “22. International Conference on Phosphorus Chemistry” (ICPC 22) in Budapest (Ungarn) vom 8.-13.7.2018; **Posterbeitrag** *“Phosphaquinomethane complexes – on the stabilization of radical anion formation.“*
7. “14. European Workshop on Phosphorus Chemistry” (EWPC 14) in Cluj-Napoca (Rumänien) vom 20.-22.3.2017; **Posterbeitrag** *“Study and Synthesis of P-CPh_3 substituted Small Ring Spirooxaphosphirane Complexes.“*
8. “12. International Conference on Heteroatom Chemistry” (ICHAC 12) in Vancouver (Kanada) vom 11.-16.06.2017; **Posterbeitrag** *“Study on the Formation of P-Trityl Phosphaquinomethane Complexes“.*
9. “Bonn International Graduate Summer School” in Bonn (Deutschland) vom 13.-15.09.2017; **Posterbeitrag** *“Study on the Formation of P-CPh_3 and P-NR_2 Phosphaquinomethane Complexes.“*
10. “14. International Symposium on Inorganic Systems” (IRIS 14) in Regensburg (Deutschland) vom 26.-31.07.2015; **Posterbeitrag**.
11. „7. Deutsch-Österreichischer Mitarbeiter Workshop für Hauptgruppenelement Chemie“ (MHC 7) in Freiberg (Deutschland) vom 19.-21.09.2014; **Vortrag** *„Synthesis and Ring Expansion of C-Acyl Oxaphosphirane Complexes.“*

DANKSAGUNG

Zu allererst danke ich Rainer für die Möglichkeit, meine Promotion in seinem Arbeitskreis anfertigen zu können, und für die Vergabe des interessanten Themas. Ebenfalls danke ich für die hervorragende Betreuung, die Diskussionen und die stets offene Tür bei Problemen. Die vielen und sehr lehrreichen Konferenzen und Auslandsaufenthalte in Spanien und Japan weiß ich zu schätzen. Ferner danke ich ihm für die vielen netten Abende mit ihm und dem Arbeitskreis, die unermüdlichen Versuche, auch mal Themen anzusprechen, die fernab von Chemie liegen über Personen, die ich natürlich nicht kannte, woraufhin wir auch viele anregende Diskussionen geführt und sehr viel gelacht haben!

Prof. Dr. Thomas Bredow danke ich natürlich für die freundliche Übernahme des Zweitgutachtens.

Weiterhin danke ich allen Kooperationspartnern, darunter Prof. Dr. Norihiro Tokitoh und seiner Arbeitsgruppe für den schönen Aufenthalt, René für die Unterstützung bei diversen CV-Messungen und die Auswertung dieser und natürlich Arturo für den schönen Aufenthalt in Murcia, die schöne morgendliche Espresso Runde, die gute Betreuung während diesem und die über mehrere Jahre stetige Zusammenarbeit und Bereitschaft, bei Problemen mit theoretischen Berechnungen zu helfen. In dem Zusammenhang danke ich auch Alicia für die Rechnungen und die nette Zeit, die wir zusammen in Murcia und Bonn hatten.

Ich danke dem Mulliken Centre und Prof. Dr. Stefan Grimme für die Bereitstellung der Rechenressourcen, Jens Mekelburger für die damit in Zusammenhang stehende Arbeit und natürlich Zheng-Wang für diverse sehr gute und detaillierte Rechnungen und die tolle Zusammenarbeit bei der Erstellung der Manuskripte.

Auch danke ich dem Institut für physikalische Chemie und Prof. Schiemann für die Möglichkeit der EPR Messungen und Hamed für die Durchführung dieser.

Ebenfalls danke ich der Universität Bonn, dem DAAD und BIGS für die finanzielle Unterstützung bei diversen Auslandsaufenthalten.

Vitaly danke ich für die tolle Betreuung bei der Bachelorarbeit und dass er mich damals in die anorganische Molekülchemie eingearbeitet hat. Ebenso danke ich Andreas für seine tolle Betreuung während der Masterarbeit.

Ebenso möchte ich mich bei meinem ehemaligen Bachelorstudenten Tim für die nette Zeit und den tollen Beitrag zur Chemie der Eisenkomplexe bedanken.

Ich danke allen Personen des AK Streubels, ob ehemalig oder aktuell, die mich während der Doktorarbeit begleitet haben. Insbesondere meinen Laborpartnern aus 1.013 - Alex, Philipp, Tim, Tatjana, Robert, Andreas - und aus 1.042 - Shahriar, Mridhul und Nabila.

Alex möchte ich noch einmal gesondert für eine tolle gemeinsame Zeit innerhalb aber auch außerhalb des Labors danken, er war der beste Laborpartner und unsere gemeinsame Zeit und vielen Auslandsaufenthalte werden mir in Erinnerung bleiben, ob nun das rote Pärchen Bett in Rumänien oder das gefängnisartige Zimmer in Schweden!

Ich danke allen Mitarbeitern des Instituts für Anorganische Chemie, vor allem Frau Dr. Rings und Frau Klein für die stets offene Tür. Dem analytischen Team der chemischen Institute danke ich für die reibungslose Zusammenarbeit, insbesondere gilt mein Dank Karin für diverse VT-NMR-Messungen, aber auch Frau Sondag, Frau Peters-Pflaumbaum und natürlich Gregor und Charlotte für die Vermessungen der Kristalle. Ebenfalls danke ich Tobias Schönberg für die guten und schnellen Glasbläserarbeiten und die stets offene Tür.

Mein größter Dank geht an meine Eltern, die mir das Studium und die Promotion ermöglicht haben, und an meine ganze Familie, die mich auf dem langen Weg begleitet und jederzeit unterstützt hat!

TABLE OF CONTENTS

1. Introduction

1.1 The element phosphorus, phosphanes and their applications in chemistry

Phosphorus is the 15. element in the periodic table of elements, thus being in the group of the *Pnictogens*.[1] It exists as a mononuclidic, or monotopic element with ^{31}P as the one stable isotope. It was first discovered in the year 1669 by *Hennig Brand*, coming from conversion of urine. He discovered a white chemiluminescent substance, the white phosphorus.[2] Phosphorus is deeply rooted in nature and life itself being essential for most organisms due to its occurrence in bones, deoxyribonucleic acid (DNA) and adenosine triphosphate (ATP). Moreover, as phosphates it plays an important role for agriculture as fertilizer. When paired with the right counterions it can also be found as minerals in nature, with the most important being Apatite $Ca_5(PO_4)_3X$ (X = OH, F or Cl). The generation of white phosphorus from such stable phosphates is costly. The reduction of potassium phosphate (K_3PO_4) takes place with coke at 1400 °C in an arc furnace yielding most probably transient P_2 moieties which form white phosphorus (P_4) upon condensation.[3] For elemental phosphorus four different modifications (allotropes) are known: The white phosphorus, consisting of P_4 tetrahedral molecules, is very reactive due to ring strain and quite toxic. Furthermore, there is the red phosphorus, a polymeric amorphous form, the violet or *Hittorf* phosphorus and the thermodynamically stable black phosphorus. Depending on the temperature and pressure some of these modifications can be converted into each other. For example, the heating of white phosphorus beyond 180 °C yields red phosphorus, which can be heated further to give the violet form (550 °C), whereas black phosphorus is formed under enormous pressure (12 kbar).

Due to its versatile behaviour phosphorus also plays an important role in chemistry since its discovery, and lead to various applications in the chemical industry. It forms stable compounds bearing oxidation states from -III to +V,[3] for example $P^{-III}H_3$, $P^{III}Cl_3$ and $H_3P^{V}O_4$. The most important property for organic and organometallic chemistry is its stability paired with manageable reactivity. Crucial for this can be the free electron pair, *e.g.* in phosphanes PR_3 (R as an organic substituent). It can easily be coordinated to a metal centre, forming a phosphane metal complex, altering its behaviour on the way. Due to the versatility of phosphorus ligands such metal complexes can be precisely tuned to find plenty of applications in the chemical industry for catalysis. Important examples are the *Wilkinson* catalyst $[RhCl(PPh_3)_3]$, which allows the hydrogenation of alkenes and alkynes at standard pressure and temperature,[4] or the *Grubbs* catalyst playing its role for the metatheses of olefins, advancing chemistry in a scale important to mankind.[5

1.2 Phosphorus as a centre of reactive molecules

Due to phosphorus being such a versatile element, in general, a great amount of interest and time has been put into the topic of forming reactive molecules containing phosphorus, either *closed*- or *open-shell*, which originates from the frontier orbital occupancy with electrons. *Open-shell* refers to molecules with orbitals containing unpaired electrons, *i.e.* radicals, while *closed-shell* compounds always contain either filled (2 electrons) or empty orbitals. In this context the terms *low-valent* and *low-coordinate* are important to distinguish. The former implies less than 8 electrons occupying the frontier orbitals, whereas the latter means that the corresponding atom has less than its normal amount of bonding partners, *e.g.* less than three for phosphorus. Examples are shown in figure 1.2.1.

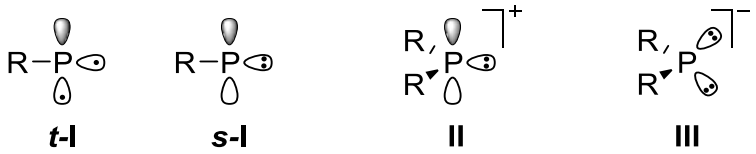

Figure 1.2.1 *Low-valent and -coordinated phosphorus compounds and* ***I-III****.*

The first class of compounds displayed in Fig. 1.2.1 are phosphinidenes **I**[6-8] which can exist either in a *triplet state* ***t*-I** or a *singlet state* ***s*-I**.[9,10] In all cases the triplet state ***t*-I** is energetically favoured due to spin-maximization, yet systematic computational studies by Nguyen showed that, as for carbenes and nitrenes, π-donor substituents, such as H_2N, H_2P and HS, can stabilized the singlet state by a small amount.[9] Yet, for a long time no example of a singlet state phosphinidene was known. Example **II** is a phosphenium ion, existing as a cation in a *singlet ground state*. Compound **III** is a so called phosphanide ion, which due to its completely filled orbitals is in a singlet state. To introduce the above-mentioned terms back, all compounds are low-coordinate with only one or two bonding partners and highly reactive, yet only compounds **I-II** are low-valent.

1.3 Syntheses and reactivity of phosphinidenes and their complexes

Phosphinidenes[6-8] **I** (P-R) are related to carbenes[11] (CR_2) and nitrenes[12] (N-R) and could, for a long time, only be detected in the gas phase or in glassy and cryogenic matrices.[13] In 2016 the first room temperature-stable derivative was synthesized by *Bertrand* as a singlet,[14] electrophilic (phosphino)-phosphinidene **IV** that displays some multiple bond character and can undergo reactions with CO and phosphanes (scheme 1.3.1).[15]

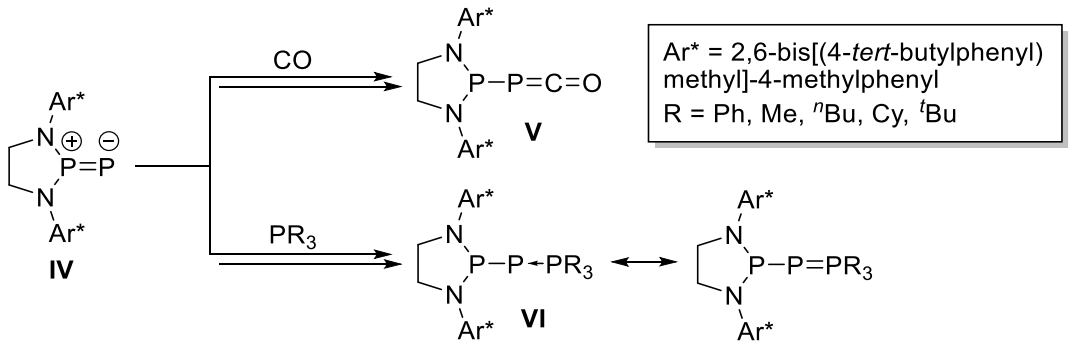

Scheme 1.3.1 *First room temperature-stable phosphinidene* ***IV*** *and its versatile reactivity.*[14,15]

It is important here to mention, that phosphinidene **IV** is stabilized due to mesomerism going formally from a P-P single up to a triple bond. This was evidenced by a short P-P bond distance (1.917 Å) and a large calculated *Wiberg bond index* (WBI 2.34), showing compound **IV** should be described with a P-P double bond. To kinetically stabilize phosphinidenes, *e.g.* against dimerization, very bulky substituents were used. Due to this partial electron donation from the phosphorus to the formally low-valent phosphorus in **IV** it mimics the reactivity of a singlet state phosphinidene with a vacant *p*-orbital at phosphorus contributing to its versatile reactivity. Such phosphinidenes can display electrophilic as well as nucleophilic properties. For example, the nucleophilic attack with its free electron pairs at the CO carbon atom forming a phosphaketene **V**, or the nucleophilic attack from a phosphane to the empty *p*-orbital forming a formal phosphinidene-phosphane adduct **VI**. Adduct **VI** can undergo ligand exchange reactions forming more stable adducts for example with CAACs (*cyclic(alkyl)(amino)-carbenes*).[14]

Around three decades ago *Niecke* and *Streubel* reported on the formation of three-membered phosphorus heterocycles via transfer of the phosphinidene $^{i}Pr_2NP$.[16] Later in 2006, *Mathey* postulated a "free" but imidazole-stabilized nucleophilic phosphinidene as RP-transfer reagent.[17] To obtain this a 7-phosphanorbornadiene complex was reacted with two equivalents of *N*-methylimidazole, first undergoing retrocyclization followed by decomplexation. Final products facilitated by this proposed intermediate were different kinds of oligomeric phosphorus ring systems, as was also shown recently by *Grützmacher* forming uncoordinated phosphorus heterocycles utilizing a sterically demanding N-heterocyclic carbene-phosphinidene adduct.[18]

A recent, very promising development was reported by *Cummins* in 2012 with the synthesis of a dibenzo-7-phosphanorbornadiene **VII,** which was further investigated and used as precursor for phosphinidene-transfer reactions (scheme 1.3.2).[19,20] It should be noted that not all product formations provide firm proof for the existence of a transient phosphinidene in these reaction as the phosphinidene group transfer can occur via higher coordinate intermediates that cleave in the reaction

course as it was first suggested by Quin,[21] and later also shown by Cummins for compound **VII** observing a charged intermediate **X** (scheme 1.3.2).[22]

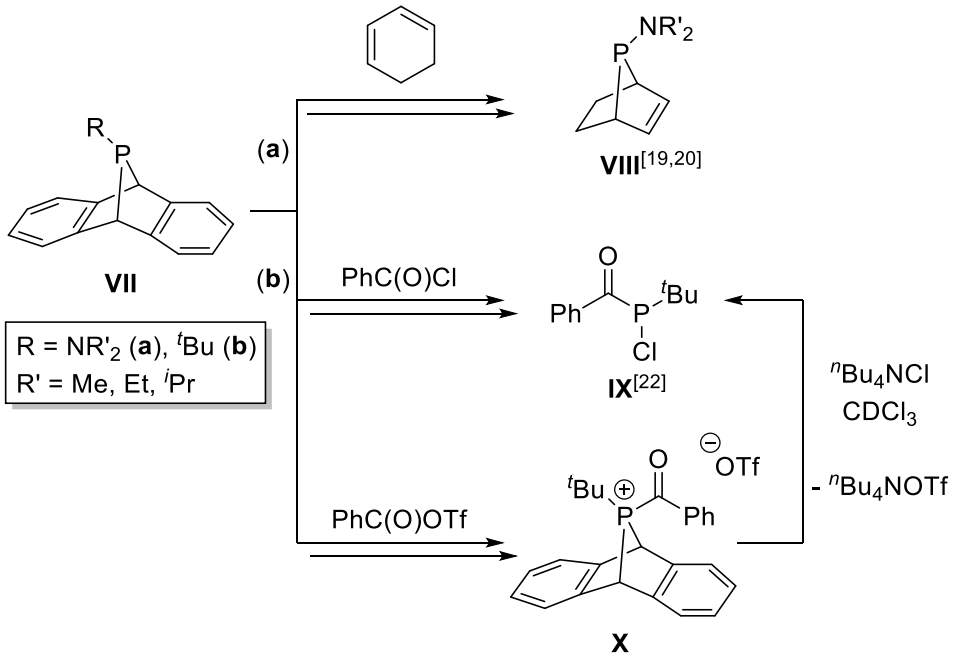

Scheme 1.3.2 *Phosphinidene-transfer reactions undergoing different reaction pathways.*[19,20,22]

In case of (**a**) evidence for a phosphinidene transfer was provided via direct detection of Me_2NP via *molecular beam mass spectrometry* (MBMS) in the gas phase and further backed by DFT calculations. It became clear, that π-donating dialkylamino groups and some steric bulk were mandatory for the success of the phosphinidene transfer.[20] The reaction of dibenzo-7-phosphanorbornadiene **VII** with acid chloride also yields a formal product of a phosphinidene that might have underwent oxidative addition (1,1-addition) into the polar C-Cl bond. Yet, in case of triflate as a weakly coordinating counterion (WCA)[23] a phosphonium ion **X** was postulated and then proven by spectroscopic evidence and theoretical calculations, which disproves the existence of a phosphinidene as the intermediate.

The formal complexation of RP to one metal centre yields terminal phosphinidene complexes, which have been known and/or postulated for a long time. The bonding situation in such complexes can be described in two ways,[7] depending on the amount of back bonding from the metal centre towards the phosphorus. Therefore, they can be divided into two categories depending on the polarity at the phosphorus atom resulting in vast differences in stability and reactivity (figure 1.3.1).

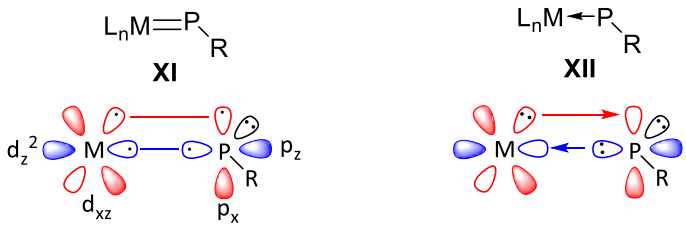

Figure 1.3.1 *Different bonding situations of phosphinidene complexes* ***XI, XII*** *(according to Mathey).*[7]

An extensive theoretical study by Lammertsma in 2002 revealed the main influence is coming from the co-ligands at the metal centre, with lesser influence by the metal centre itself, drastically changing the charge and electron density at the phosphorus going from -0.270 (Cp_2Ti=PH) to -0.060 ($(CO)_4Fe$=PH) (Table 1.3.1).[24] Therefore, nucleophilic phosphinidene complexes **XI** (L_nM=PR) are present in case of strong σ-donor co-ligands (*Schrock*-Type) or an electrophilic phosphinidene complex **XII** (L_nM-PR) in case of π-acceptor co-ligands (*Fischer*-Type).

Table 1.3.1. *Calculated VDD charges*[25] *on the phosphorus atom of phosphinidene complexes* L_nM=PH.

Cp_2Ti=PH	$Cp(PH_3)_3V$=PH	$Cp(CO)_3V$=PH	$(CO)_4Fe$=PH
-0.270	-0.210	-0.081	-0.060
Cp_2Hf=PH	$Cp(PH_3)_3Ta$=PH	$Cp(CO)_3Ta$=PH	$(CO)_4Os$=PH
-0.323	-0.234	-0.144	-0.124

These different bonding situations can also be seen due to an opposing reactivity coming from different HOMO (*highest occupied molecular orbital*) and LUMO (*lowest unoccupied molecular orbital*) localizations/contributions in **XI**, **XII**.

The first nucleophilic phosphinidene complex **XIII** was published by *Lappert* in 1987 (Cp_2W=PMes*) (Figure 1.3.2).[26] In general, there are many synthetic routes to such complexes, and they can be isolated due to a remarkable stability. Nowadays, a huge variety is known and have been reviewed.[8] Examples coming from different synthetic routes are shown in figure 1.3.2.

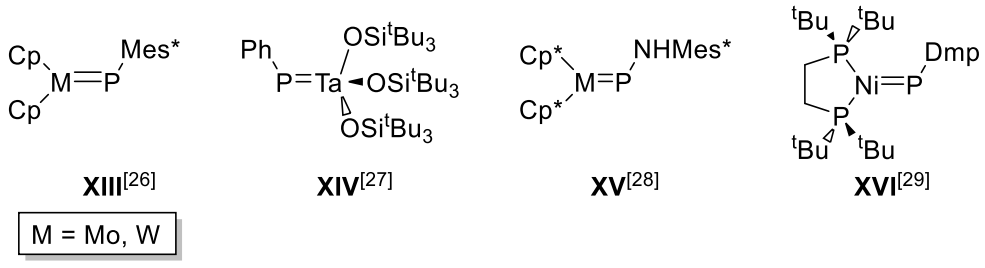

XIII[26] **XIV**[27] **XV**[28] **XVI**[29]

M = Mo, W

Figure 1.3.2 *Literature known nucleophilic phosphinidene complexes* ***XIII-XVI****.*

Complex **XIII** can be synthesized from a lithium metallocene hydride [{Cp_2MHLi}$_4$] reacting with the corresponding dichlorophosphane giving stable red crystalline materials with characteristic low field-shifted ^{31}P NMR signals of 779.5 ppm (W) and 661.1 ppm (Mo).[26] For the synthesis of complex **XIV** an insertion and elimination pathway was utilized through the oxidative addition of phenylphosphane to the "electron poor" tris(siloxy)tantalum complex followed by H_2 elimination.[27] In 1989 *Niecke* reported on an *α*-hydrogen migration where the initial salt-metathesis product generates complex **XV**, as evidenced by the low field ^{31}P NMR shift of 754 ppm at -40 °C.[28] The oxidation followed by deprotonation of a paramagnetic nickel(I) phosphido complex was reported to yield complex **XVI**,[29] yet even more synthetic protocols are known like phosphinidene group transfer[30] and dehydrohalogenation followed by ligation.[31,32] Nucleophilic phosphinidene complexes, in general, can (often) be isolated, crystallized and show the characteristic downfield-shifted ^{31}P NMR signals (> 500 ppm).

According to calculations and the Lewis formula for *Schrock*-type phosphinidene complexes **XI** the HOMO mainly consists of the π-bond displaying a typical reactivity; some examples are shown in scheme 1.3.3 using **XVII** as starting point.

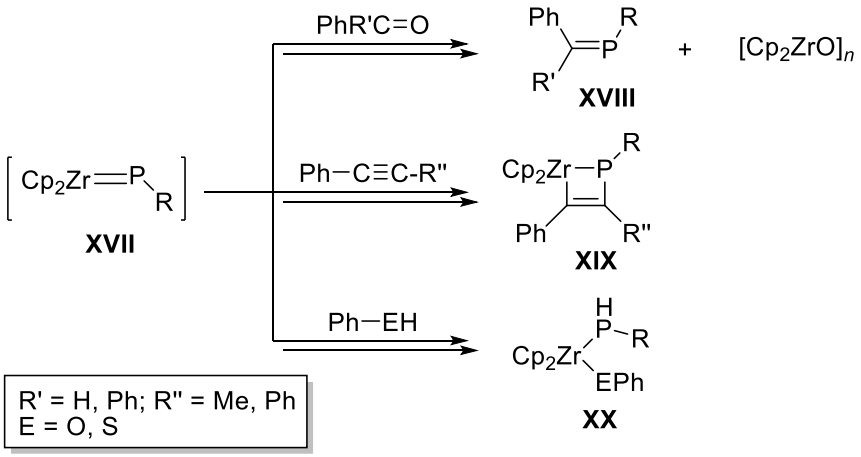

Scheme 1.3.3 *Reactivity of nucleophilic phosphinidene complex* ***XVII****.*[33-35]

Complex **XVII** was generated *in-situ* via the reaction of the mono- or dichloro(dicyclopentadienyl)-zirconium(IV) with a lithium phosphanide (LiPHR, R = C_6H_2-2,4,6-*tert*-Bu_3) followed by an elimination (of PH_2R or CH_4). With ketones complex **XVII** undergoes a *phospha-Wittig* type reaction forming the corresponding phosphaalkene **XVIII**.[33] With an alkyne the zirconaphosphet-2-ene **XIX** is formed through a [2+2]-cycloaddition,[34] and with polar EH bonds the 1,2-addition product **XX** can be found.[35] All these reactions support the description of complex **XVII** using a Zr-P double bond with HOMO and LUMO consisting of electron contributions from zirconium and phosphorus, which is in contrast to electrophilic phosphinidene complexes. To mention at his point is the observation done in 2003 by

Hillhouse, observing the formation of an unligated phosphirane with the nucleophilic phosphinidene complex **XVI**. In case of *P*-Dmp substitution (Dmp = 2,6-dimesitylphenyl) the expected [2+2]-cyclo-addition intermediate could be detected, yet in the end the corresponding phosphirane complex is formed, which normally is the reaction outcome when utilizing an electrophilic phosphinidene complex. This blurs the line even more between nucleophilic and electrophilic phosphinidene complexes and possibly being the first example of an isolated species undergoing this type of special nucleophilic phosphinidene group transfer.[36]

A large diversity of ancillary ligands is also available in cationic complexes $[L_nM{=}PR]^+$ of which stable ones have been reported.[37,38] These so called phosphenium complexes can be synthesised for example via chloride abstraction from a chloro(amino)phosphido complex with $AlCl_3$ yielding the *P*-amino substituted phosphenium complex.[38]

In contrast, neutral electrophilic terminal phosphinidene complexes (*Fischer*-type), having a metal(0) centre, have not been isolated, so far. The earliest entry to complexes of type **XII** was reported by *Mathey* in 1982, using a thermal retro-cyclization of 7-phosphanorbornadiene complex **XXI** (scheme 1.3.4).[39,40]

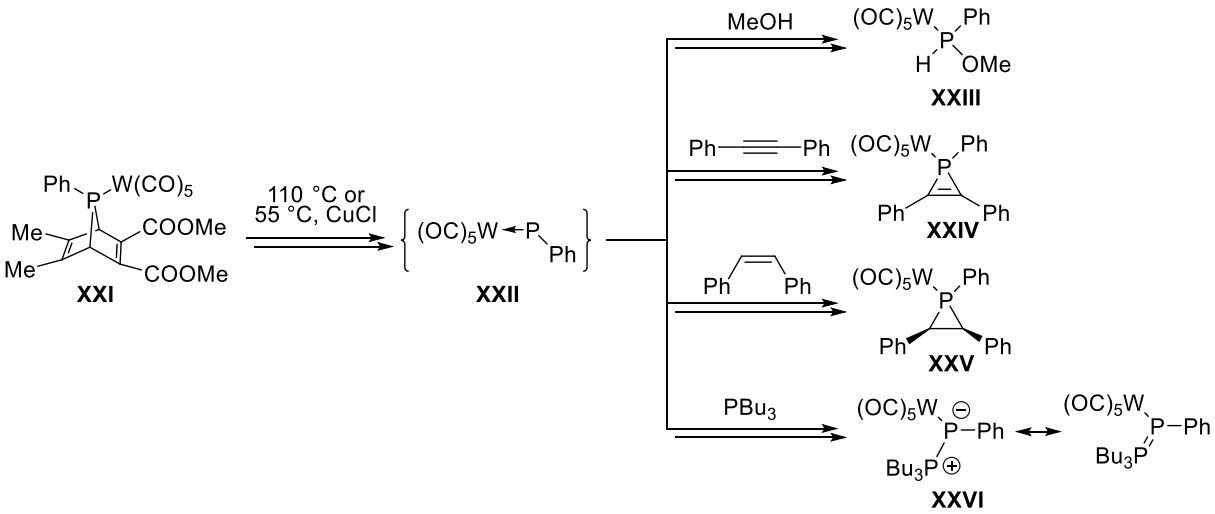

Scheme 1.3.4 *Entry to the transient terminal electrophilic phosphinidene complex* ***XXII****.*[39-41]

The *in-situ* generated singlet species **XXII** could then react, for example, with polar EH bonds,[39] alkynes[39] or σ-donors,[39,40] to form the corresponding 1,1-addition products **XXIII** (formal EH bond insertion), 1*H*-phosphirene complexes **XXIV** and formal phosphinidene adducts **XXVI**, respectively. When using the corresponding *cis*- or *trans*-isomers of an alkene a stereochemical selective ring-formation can be observed (**XXV**) in case of a singlet species showcasing the concerted mechanism.[41] Surprisingly, it was found by *Mathey* that the generation of **XXII** can be catalysed by CuCl to lower the

reaction temperature to 55 °C, an observation later theoretically investigated by *Lammertsma*.[42] Supported by theoretical calculations a Cu^{I}/Cl phosphinidenoid complex was discussed but, in fact, the latter is more closely related to a heterodinuclear complex that changes its bonding when a substrate is approached. Later a dimer could be crystallized which was derived from the reaction of CuCl with complex **XXI** in benzene.[42] This investigation also marks an important point regarding the importance of the solvent and even counterion for phosphinidene complexes and their reactivity.

Since then just a handfull of different routes have been established, they can be seen in scheme 1.3.5. These "high-temperature" routes take quite harsh conditions with > 50 °C to release the phosphinidene complex fragment from the corresponding precursor complexes **XXI, XXVII, XXVIII**.

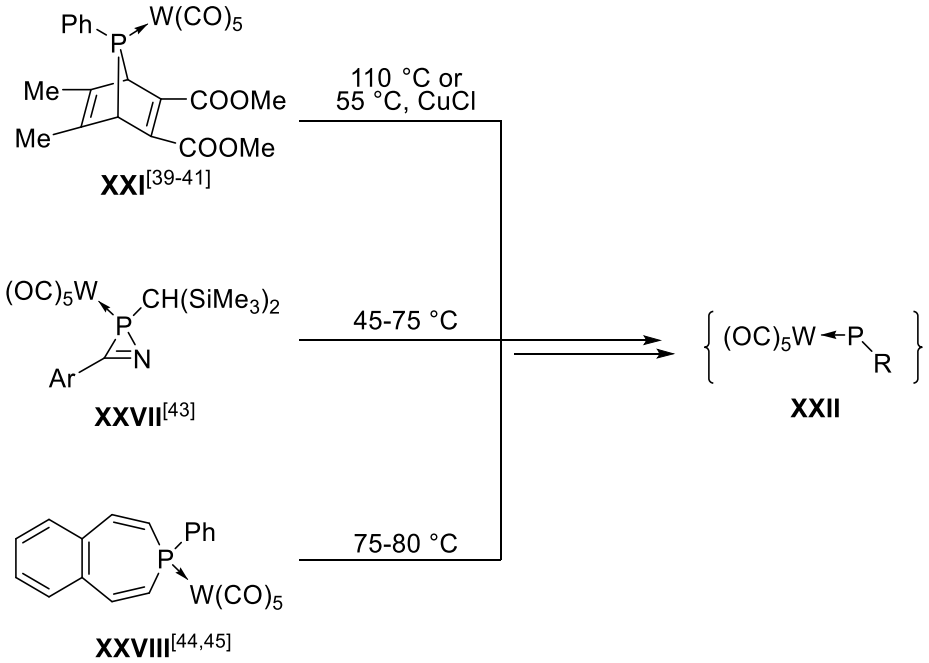

Scheme 1.3.5 *Established routes to transient terminal electrophilic phosphinidene complexes* ***XXII****.*

Another retro-cyclization was reported by *Streubel* in 1994 starting from the 1*H*-azaphosphirene complex **XXVII**, releasing the aryl nitrile as by-product.[43] Interesting was also the introduction of phosphepine complexes **XXVIII** to this chemistry by *Lammertsma* in 2005,[44,45] even though free phosphepines have been known for some time to decompose readily to the aromatic hydrocarbon and $(RP)_5$.[46] This happens presumably by expelling [RP] from the phospha-norcaradiene (NCD) which exists in an equilibrium with the phospha-cycloheptatriene (CHT) through a 6 electron electrocyclic reaction with a modest barrier.[44] Such phosphepine complexes can rather easily be synthesised in good yields.

There are also synthetic routes towards phosphinidene complexes under mild reaction conditions and taking advantage of a stabilization of the phosphinidene complex **XXXII** (scheme 1.3.6).

To lower the reaction temperature different metals and P-substituents were introduced, which started in 1987 when *Cowley* reported a salt elimination generating the iron(0) *P*-amino stabilized phosphinidene complex **XXXII**.[47] This complex **XXXII** ([M] = $Fe(CO)_4$, R = tris(pyrazol)borato) could be isolated and crystallized due to a very strong stabilization by the tris(pyrazol)borato ligand, yet the obtained ^{31}P NMR shift of 281 ppm is not low-field shifted enough for a "true" terminal electrophilic phosphinidene complex **XII**, and the high stability accompanied with a low reactivity shed doubt on the nature of this complex. In this context, very early work was also done by King, where the *in-situ* formed iron(0) phosphinidene complex **XXXII** was postulated and made responsible for the observed formation of several iron clusters.[48] During the course of the reaction a minor ^{31}P NMR shift of 401.2 ppm could be observed, presumably matching the formed trinuclear diphosphene complex $(Et_2NP)_2Fe_3(CO)_9$. Based on this work, in 1999 *Lammertsma* reported on another *P*-amino stabilized iron(0) phosphinidene complex.[49] Surprisingly, the trapping reaction worked only for a specific allene forming the methylene 1*H*-phosphirene complex which afterwards rearranges to the corresponding phospholene complex. Building up on this, *Lammertsma* then reported in 2016 the reactivity of the phosphinidene complex **XXXII** (R = N^iPr_2, [M] = $Fe(CO)_4$).[50] The corresponding phosphirane complexes could be obtained undergoing "phosphinidene hopping", *i.e.*, with alkynes the thermodynamically more stable 1*H*-phosphirene complexes were formed.

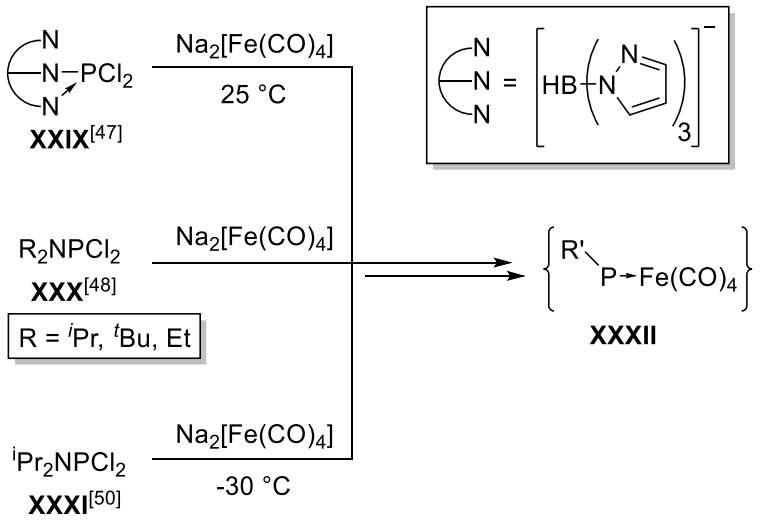

Scheme 1.3.6 *Further reported "low-temperature" synthetic routes to electrophilic phosphinidene complexes* ***XXXII****.*

1.4 Syntheses and reactivity of phosphinidenoid complexes

Another way to mimic the reactivity of neutral low-valent compounds like carbenes, nitrenes and their heavier homologues is by formally masking them with a salt, adding a coordinating counter cation to the anionic species (*e.g.* phosphanide **III**). So a formal addition of M'X to the (respective) low-coordinate compounds yields the so called carbenoids **XXXIII**,[51] silylenoids **XXXIV**[52] and phosphinidenoids **XXXV**[53] and their complexes **XXXVI** (Figure 1.4.1).

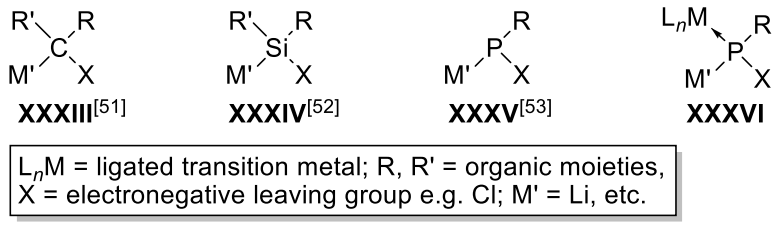

Figure 1.4.1 *Carbenoids **XXXIII**, silylenoids **XXXIV**, phosphinidenoids **XXXV** and their complexes **XXXVI**.*

In general, these compounds have the possibility to display ambiphilic behaviour as well, *i.e.,* to react with electrophiles and nucleophiles depending on the applied reactants and conditions. Phosphinidenoids **XXXV** remain unknown up to this date, and have only been assumed as possible reactive intermediates including the compound **XXXVIII** bearing no metal ion (figure 1.4.2).

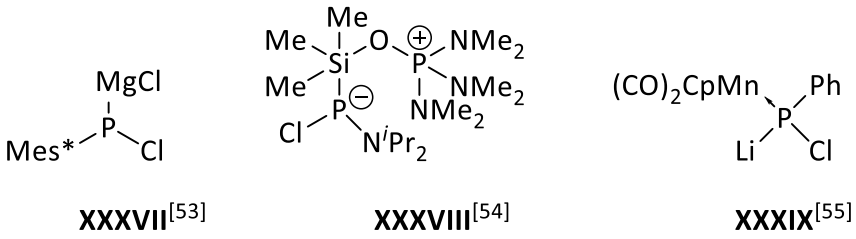

Figure 1.4.2 *First postulated M/X phosphinidenoid compounds **XXXVI, XXXVII** and complex **XXXVIII.***

The term "phosphinidenoid" has been proposed first by *Yoshifuji* to explain later the formation of the first diphosphene Mes*P=PMes* via reactions of Mes*PCl_2 with an excess of magnesium.[53] Around the same time, *Niecke* demonstrated that compound **XXXVIII** reacts as aminophosphinidene transfer reagent to polar π-bond systems, thus the formation of a transient nucleophilic phosphinidenoid seems reasonable.[16] An important fact here is that reactions with alkynes and alkenes were not successful, further supporting this ionic nucleophilic pathway.[55]

The first attempts to investigate lithium/chlorine exchange in dichlorophosphane complexes producing phosphinidenoid complexes **XXXIX** were reported in 1985 by *Huttner*.[54] The breakthrough in this field happened in 2007 with the synthesis of phosphinidenoid complexes **XLII-XLVI** by *Streubel*

(Scheme 1.4.1).[56] To stabilize the thermally unstable complex, a sterically very demanding substituent, namely $CH(SiMe_3)_2$ (bisyl), and 12-crown-4 was used. DOSY experiments[57] showed that the crown ether generates a solvent-separated ion pair thus lowering the possibility of unwanted side reactions due to LiCl elimination. In the following years, this methodical approach was transferred to generate many different derivatives bearing different transition metals, organic substituents and cations which is illustrated in scheme 1.4.1.

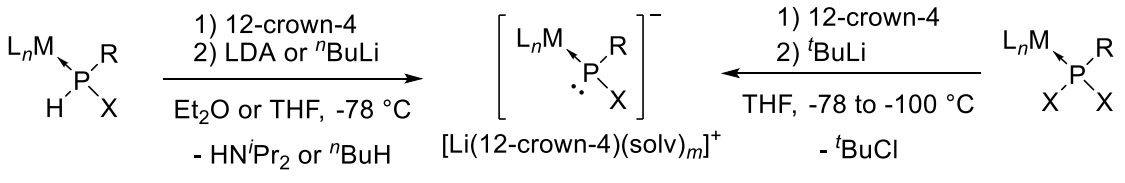

XL **XLII-XLVI** **XLI**

XLII: L_nM = $W(CO)_5$; R = $CH(SiMe_3)_2$; X = F (**a**), Cl (**b**), Br (**c**), I (**d**), CN (**e**)
XLIII: L_nM = $W(CO)_5$; R = Cp* (**a**), CPh_3 (**b**), *t*-Bu (**c**), 3,5-*t*-BuC_6H_3 (**d**); X = Cl
XLIV: L_nM = $Mo(CO)_5$; R = Cp* (**a**), CPh_3 (**b**), *t*-Bu (**c**), $CH(SiMe_3)_2$ (**d**); X = Cl
XLV: L_nM = $Cr(CO)_5$; R = Cp* (**a**), CPh_3 (**b**), *t*-Bu (**c**), $CH(SiMe_3)_2$ (**d**); X = Cl
XLVI: L_nM = $Fe(CO)_4$; R = CPh_3 (**a**), *t*-Bu (**b**), X = Cl

Scheme 1.4.1 *Preparation of Li/X phosphinidenoid complexes* ***XLII-XLVI****.*

The first established route utilized chlorophosphane complexes **XL** which was deprotonated at low temperature with LDA forming the corresponding complexes. This route was later replaced, and the new starting point used easier to access dichlorophosphane complexes **XLI** undergoing Li/Cl exchange with *t*-BuLi at low temperature also yielding complexes **XLII-XLVI**, facilitating access and removing (potentially) problematic side products such as $HNiPr_2$. It is to mention that a donor solvent like Et_2O or THF is also necessary to stabilize the Li/Cl phosphinidenoid complexes **XLII-XLVI** in solution, in general. These complexes are generally thermally unstable and decompose, yet the temperature and time span differ strongly, which depends largely on the nature of the P-substitution and the counterion (scheme 1.4.2).[58] For example, complex **XLIIa** (X = F, R = $CH(SiMe_3)_2$) is stable up to 10 °C in Et_2O,[59] while complex **XLIIb** (X = Cl, R = $CH(SiMe_3)_2$) starts decomposing already above -40 °C.[57] Furthermore, complexes with CPh_3-substitution (*e.g.* **XLIIIb** (M = W, R = CPh_3)) can be stable for hours at room temperature even without 12-crown-4.[60] Several different decomposition products could be identified like diphosphene complexes **XLVII**,[57] intramolecular [2+1]-cycloaddition products **XLVII**[61] and several ring systems, *e.g.* metalladiphosphiranes **XLIX,L**, cyclotriphosphanes **LI**.[62] Complex **L** represents a very interesting reaction between two molecules of the corresponding Li/Cl phosphinidenoid complex **XLIIId** forming a very labile transient phosphanylidene-phosphorane complex, which then forms complex **L** after loss of another equivalent of [Li(12-crown-4)]Cl and a shift of the $W(CO)_5$ fragment.[63]

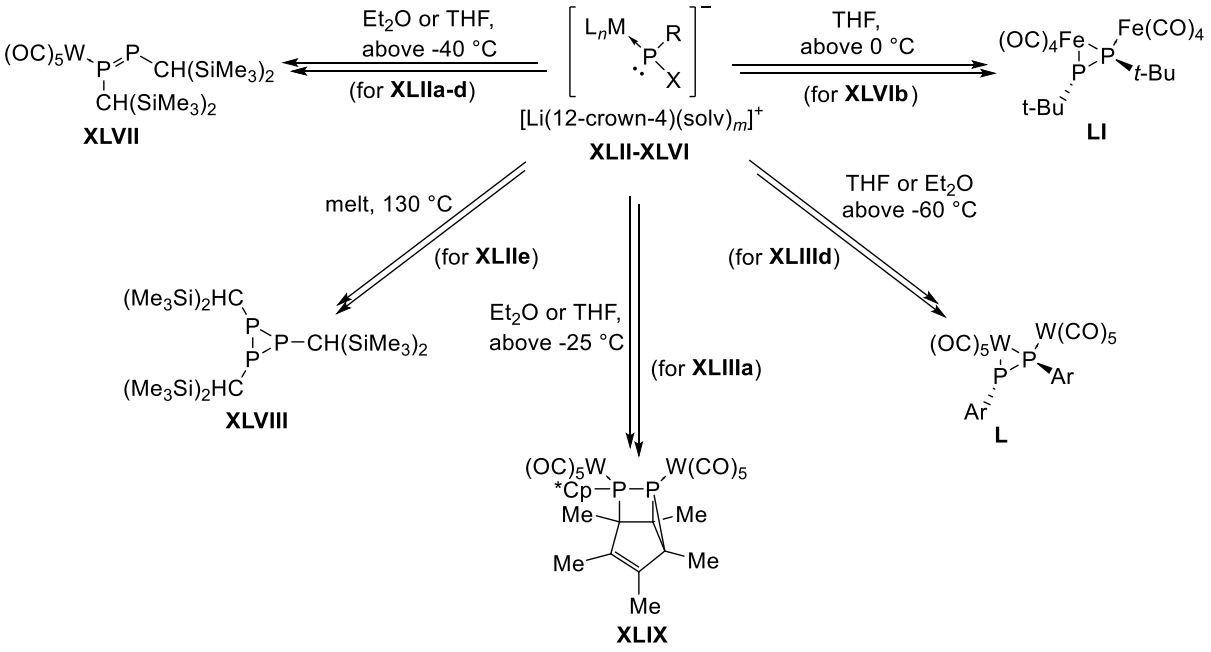

XLII: $L_nM = W(CO)_5$; R = $CH(SiMe_3)_2$; X = F (**a**), Cl (**b**), Br (**c**), I (**d**), CN (**e**)
XLIII: $L_nM = W(CO)_5$; R = Cp* (**a**), CPh_3 (**b**), *t*-Bu (**c**), 3,5-*t*-BuC_6H_3 (**d**); X = Cl
XLIV: $L_nM = Mo(CO)_5$; R = Cp* (**a**), CPh_3 (**b**), *t*-Bu (**c**), $CH(SiMe_3)_2$ (**d**); X = Cl
XLV: $L_nM = Cr(CO)_5$; R = Cp* (**a**), CPh_3 (**b**), *t*-Bu (**c**), $CH(SiMe_3)_2$ (**d**); X = Cl
XLVI: $L_nM = Fe(CO)_4$; R = CPh_3 (**a**), *t*-Bu (**b**), X = Cl

Scheme 1.4.2 *Decomposition-derived products of Li/X phosphinidenoid complexes* ***XLI-XLV****.*

Complexes **XLII-XLVI** display a characteristic low-field shift in the ^{31}P NMR spectrum (200 – 350 ppm) which somehow looks counterintuitive regarding the small ^{1}J(W-P) coupling (50 - 100 Hz) giving evidence for a strong anionic charge localization at the P-atom. A possible explanation can be done with the nature of the NMR shift or rather electronic shielding itself, which was intensively explored theoretically.[58] The general theory of *Ramsey* decomposes the shielding contributions into diamagnetic σ^d and paramagnetic σ^p portions.[64] The contributions to σ^p are largely due to *occ-vir* MO (*molecular orbital*) mixing between MO pairs. Symmetry allowed MOs yield a constructive overlap and therefore a positive shielding contribution, whereas symmetry forbidden MOs yield a destructive overlap and therefore a negative shielding contribution, also called *paramagnetic deshielding*. Depending on the energy separation (ΔE), the atomic character and the degree of mixing of the corresponding MOs the magnitude of the chemical shift contributions can strongly vary.[65]

The reactivity of Li/Cl phosphinidenoid complexes **XLII-XLVI** has been studied in great detail yielding a wide variety of reactions and, hence, broadened the access to new and novel structures (Scheme 1.6). These complexes can undergo [2+1]-cycloadditions forming the corresponding oxaphosphirane[66-68] **LII** and azaphosphiridine[69] **LIII** complexes.

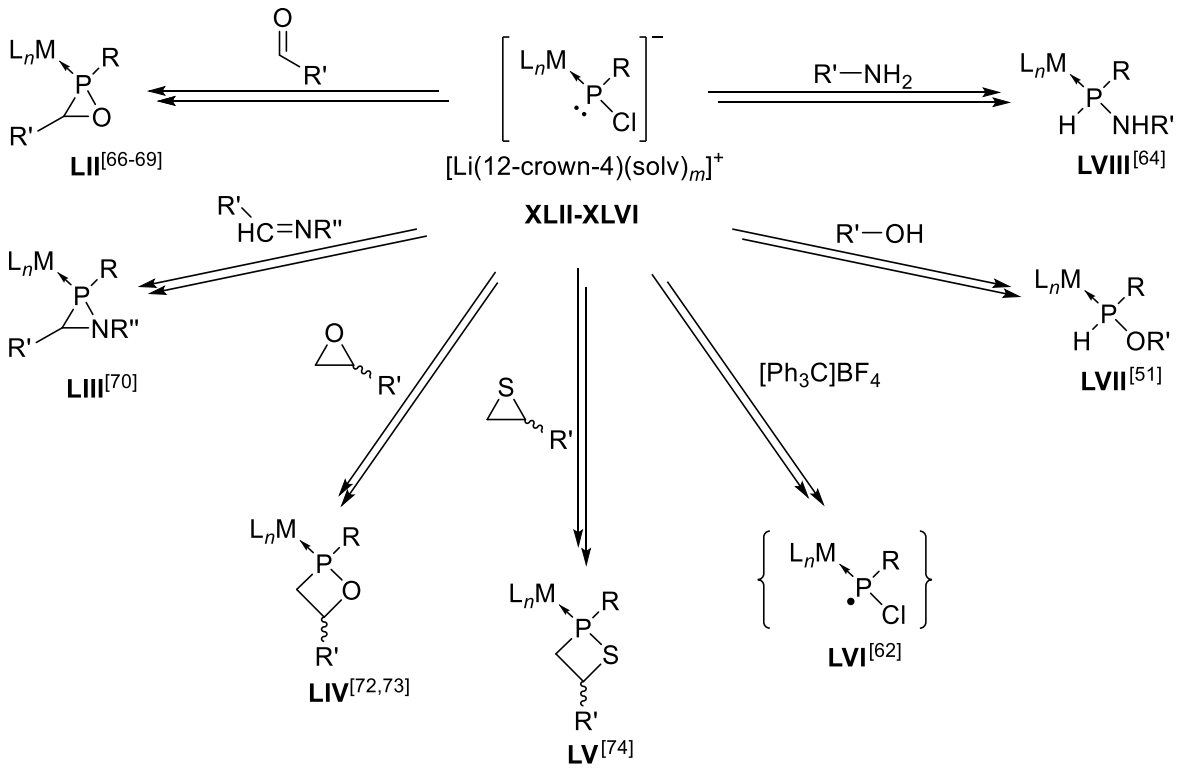

LII: L_nM = $W(CO)_5$, $Mo(CO)_5$, $Cr(CO)_5$; R = $CH(SiMe_3)_2$, CMe_3, Cp*, CPh_3; R' = alkyl, allyl, aryl, spiro; **LIII:** L_nM = $W(CO)_5$; R = alkyl, aryl; R' = alkyl, aryl, imino; R'' = alkyl, H; **LIV:** L_nM = $W(CO)_5$, $Mo(CO)_5$; R = $CH(SiMe_3)_2$, CPh_3, C_5Me_5; R' = alkyl, aryl; **LV:** L_nM = $W(CO)_5$, $Mo(CO)_5$, $Cr(CO)_5$; R = CPh_3; R' = alkyl; **LVI:** L_nM = $W(CO)_5$; R = $CH(SiMe_3)_2$, C_5Me_5; **LVII:** L_nM = $W(CO)_5$, $Mo(CO)_5$, $Cr(CO)_5$; R = $CH(SiMe_3)_2$, CPh_3, C_5Me_5; R' = alkyl, allyl; **LVIII:** L_nM = $W(CO)_5$, $Fe(CO)_4$, ; R = CPh_3; R' = alkyl, allyl

Scheme 1.4.3 *Reported reactions of various Li/Cl phosphinidenoid complexes* ***XLII-XLVI****.*

The former (**LII**) have been extensively studied, *e.g.*, their reactivity towards HCl, water and ammonia leading to ring opening reactions starting via C-O bond cleavage.[67] Furthermore, in 2018 the decomplexation of an oxaphosphirane molybdenum complex with dppe was reported, yielding the first isolated free P(III) oxaphosphirane.[68] Azaphosphiridine complexes also represent an interesting starting point, when increasing the ring strain via an exocyclic double bond (imino group) the ring can be opened with water while isonitriles form the corresponding formal RNC-to-phosphinidene adducts.[71] With epoxides and thiiranes the oxaphosphetane[72,73] **LIV** and thiaphosphetane[74,75] **LV** complexes can be obtained, respectively, through an insertion of the phosphinidenoid complexes into the corresponding three-membered ring system. For the former also ring opening reactions were reported, yet surprisingly via P-O bond cleavage.[73] Also reactions with alcohols and amines were reported yielding the formal EH-insertions products, the alkoxyphosphane[60] **LVII** and amino-phosphane[76-81] **LVIII** complexes, respectively. The calculated mechanism for the formal NH-insertion with ammonia starts with an approach of the hydrogen towards the formal phosphanide centre followed with the substitution of the chlorine by an ammonium ion. The rearrangement afterwards

yields the aminophosphane complex **LVIII**.[78] For these complexes also further deprotonation at the P/N has been reported forming either the phosphanido or amido complex, respectively.[76,79,80] A very remarkable reaction was the *single electron transfer* (SET) oxidation of **XLIIb, XLIIIa** with tritylium tetrafluoroborate forming *in-situ* a solvent-stabilized radical pair consisting of a trityl radical and the phosphanyl complex **LVI**, which could be detected via EPR spectroscopy.[82]

1.5 Syntheses of phosphaquinomethanes and their complexes

In general, quinoidal compounds have attracted considerable interest over a long time, due to their display of a unique structure resulting in interesting properties and a large potential for applications.[83] Therefore a variety of quinoidal compounds were investigated such as quinones, quinodimethanes and quinodiimines.[83] In 1999 the first heavier homologue of a quinomethane was reported with phosphorus, a so-called phosphaquinone **LIX** (figure 1.5).[84]

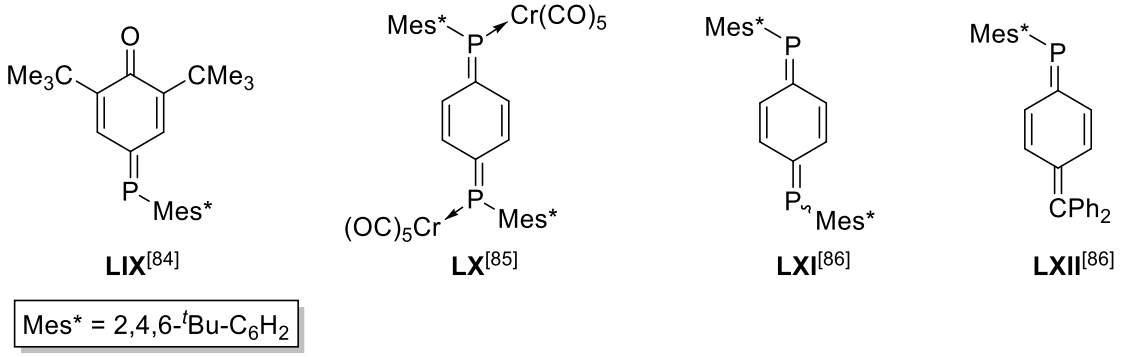

LIX[84] **LX**[85] **LXI**[86] **LXII**[86]

Figure 1.5.1 *Literature known quinoidal phosphorus compounds.*

Compound **LIX** has a strongly downfield-shifted ^{31}P NMR spectroscopic resonance at 327.4 ppm and can be easily reduced by Na forming the corresponding radical anion which could be confirmed by EPR spectroscopy. Cyclovoltammetric measurements showed a reversible one electron reduction at -1.43 V (vs. Ag/Ag$^+$).[84] *Märkl* already in 1996 reported the synthesis of the diphosphaquninone chromium complexes **LX**, via reduction of the bis(chloro)phosphino-*p*-benzene with zinc.[85] The reported ^{31}P NMR resonance signals, again, are downfield shifted in the region of 246-262 ppm.[85] In 2005, along with a free diphosphaquinone **LXI,** the first derivative of a phosphaquinomethane **LXII** was reported also displaying reversible one electron reduction (E_{red} = -1.83 V; in THF vs Fc/Fc$^+$) in the cyclic voltammograms, followed by an irreversible second process (scheme **1.5.1**).[86] It is to mention that for kinetical stabilization bulky P-substituents were used for all of these compounds.

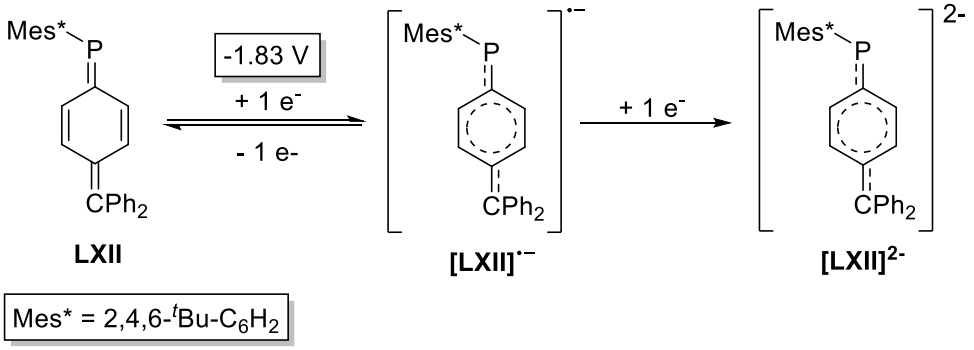

Scheme 1.5.1 *Reported reversible 1 e⁻ reduction of phosphaquinomethane* ***LXII****.*[86]

Bearing the property of reversible reduction these compounds gained interest regarding their possibility to become non-innocent ligands, stabilizing paramagnetic transition metal complexes. Paramagnetic compounds, in general, play an important role in chemistry, yet paramagnetic transition metal complex intermediates were studied the most regarding their important role in catalytic processes.[87] For example, group 6 transition metal complexes (Cr, Mo, W) can function as catalytic centres with the formation of radical anions.[88] Much of the chemistry of these radical complexes depends on the localization of the unpaired electron, either on the metal or the ligand. Known examples have common structural motives regarding π-stabilization or steric bulk for stability gain.[89] For most of these paramagnetic transition metal complexes, the unpaired electron is located at the metal centre, while complexes bearing most spin density at the ligand remain rare and, therefore, very interesting. These complexes contain so-called "non-innocent" ligands as they strongly participate in the chemistry of the corresponding paramagnetic complexes.[90] Various classes are known so far, most of them based on N-, O-, S-coordination of the ligands.[87] Yet until today there are only few complexes known bearing such kind of non-innocent P-ligands,[91] even though P-centred radicals have been recognized in reactions for a long time.[92] Accessible redox active ligands are, for example, phospha-alkenes and their complexes with group 6 transition metals.[93,94] The first tungsten phospha-quinomethane complex, reported by *Streubel* in 2010,[82] was the final result of a SET oxidation of the Li/Cl phosphinidenoid complex **XLIIa,b, XLIIIa** with tritylium tetrafluoroborate (scheme 1.5.2). A SET oxidation of these anionic complexes, most likely via an outer-sphere electron transfer mechanism, formed the corresponding phosphanyl complex **LVI** and the trityl radical. The radical could be determined by EPR spectroscopy and DFT calculations to be mostly phosphorus centred (87 %, R = C_5Me_5; 82 %, R = $CH(SiMe_3)_2$). After C,P coupling at the *para*-Ph position the dearomatized phosphane complex **LXIII** was postulated, undergoing either subsequent H-translocation to rearomatize and form complex **LXV**, or HCl elimination to yield complex **LXIV**. Complex **LXIV** displays a low-field shifted ^{31}P NMR shift of 189.6 ppm (comparable to phosphaalkene complexes)[95] and an intense purple color (λ_{max}: 372 – 440 nm), which stands in contrast to the colour of non-coordinated

phosphaquinomethanes.[86] Also SET oxidation with $[(p\text{-Tol})_3C]BF_4$ on **XLIIa** (Li/F phosphinidenoid complex) was reported undergoing C,P-coupling at the central C due to the Me-substituted *para*-Ph position.[96]

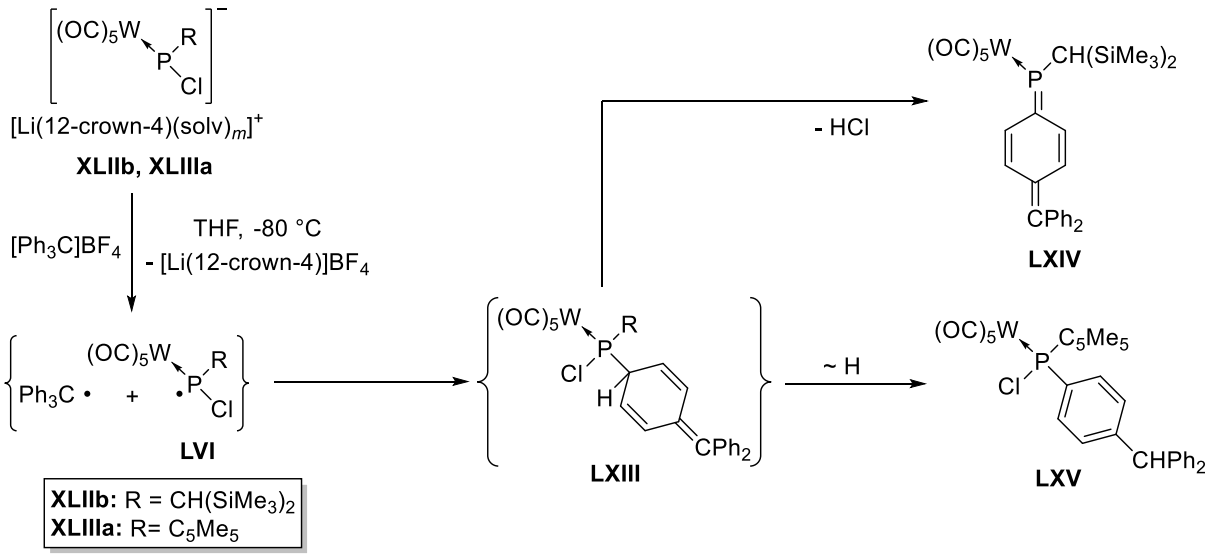

Scheme 1.5.2 *One electron oxidation of complexes* ***XLIIb, XLIIIa*** *and the substituent dependant formation of either the phosphaquinomethane* ***LXIV*** *or the phosphane complex* ***LXV****.*

2. Objectives of this PhD thesis

For this PhD Thesis three different questions of molecular chemistry were investigated:

1) The synthesis and investigation of *P*-amino substituted Li/Cl phosphinidenoid complexes. Here the influence of the amino substituents on stability and reactivity differences, especially towards established trapping reagents, was the focus.
2) The possibility to synthesize corresponding *P*-amino substituted terminal phosphinidene complexes.
3) Synthesis of phosphaquinomethane complexes with the special focus on the investigation of their non-innocence and the possibility to access *P*-amino substituted phosphaquinomethane complexes.

3. Results and discussion

As described in the introduction, Li/Cl phosphinidenoid complexes display a broad reactivity which can be used to synthesize different kinds of phosphorus-containing ligands, *e.g.,* a variety of phosphanes, phosphaalkenes and heterocyclic ligands such as oxaphosphiranes, oxaphosphetanes and others. Different sterically demanding substituents in combination with different transition metal carbonyls were introduced, often displaying selective reactions thus establishing “typical” Li/Cl phosphinidenoid complex-type reactions such as [2+1]-cycloadditions and oxidative additions with a broad variety of E-H containing reagents.

Yet, one crucial point hasn’t been investigated: P-heteroatom substitution (besides Cl) and, hence, the quest is still open which effect(s) on stability and reactivity of Li/Cl phosphinidenoid complexes the heteroatom might excert. To investigate this, it was planned to introduce a *P*-diorganoamino substitution into Li/Cl phosphinidenoid complex chemistry, focussing on $Fe(CO)_4$, $Cr(CO)_5$ and $W(CO)_5$ complexes. The lone pair at nitrogen of the amino group, capable of electron donation (+M-effect) and paired with the electron-withdrawing effect of the nitrogen (-I-effect) can provide an interesting starting point to investigate. Moreover, to see the influence of steric and electronic effects of the N-substituents, the diphenyl and dicyclohexyl substitution was targeted (NPh_2, NCy_2).

3.1 Synthesis of Li/Cl phosphinidenoid complex precursors $[M(CO)_n(R_2NPCl_2)]$

To start the investigation, diorganoaminophosphane complexes **2a-4b** were synthesized using dichloro(diphenylamino)phosphane **1a**[97] and dichloro(dicyclohexylamino)phosphane **1b**[98] as starting materials along with the corresponding metalcarbonyl complexes (Scheme 3.1.1). The complexation of the two phosphane derivatives was done differently for W and Cr, and Fe. In case of W, Cr the corresponding metal hexacarbonyls were first converted under photochemical conditions to yield the meta-stable $M(CO)_5(thf)$ (M = W, Cr) complexes.[98,99] With THF being a rather poor ligand concerning M-O bond strength, a ligand substitution took place upon addition of the corresponding phosphane at room temperature forming complexes **2a,b, 3a,b**. Complexes **4a,b** on the other hand where synthesized through thermal reaction of diironnonacarbonyl with **1a,b** in toluene. The complexes could be isolated - after filtration through a solid phase (SiO_2, Al_2O_3) with either Et_2O (**2b, 3a,b**) or toluene (**2a, 4a,b**) as solvents - with yields between 36% (**3a**) and 56 % (**3b**), yet complexes **2-4** can be synthesized in a gram scale (see also table 3.1.1).

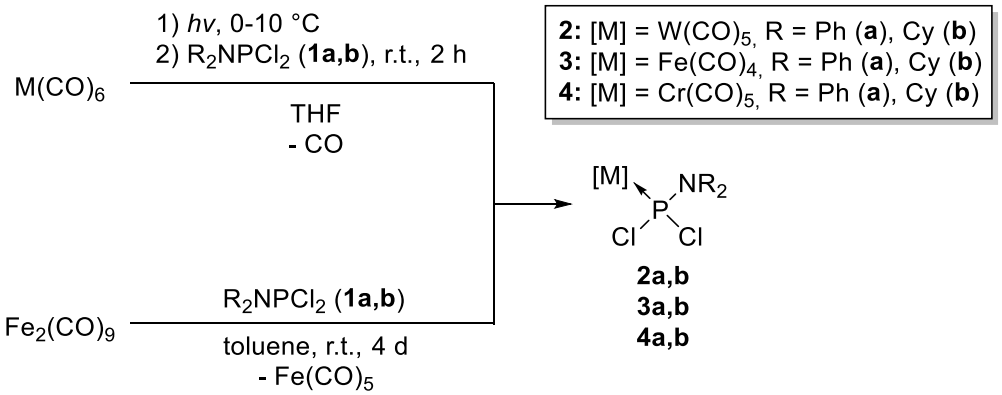

Scheme 3.1.1. *Syntheses of the dichloro(amino)phosphane complexes **2-4**.*

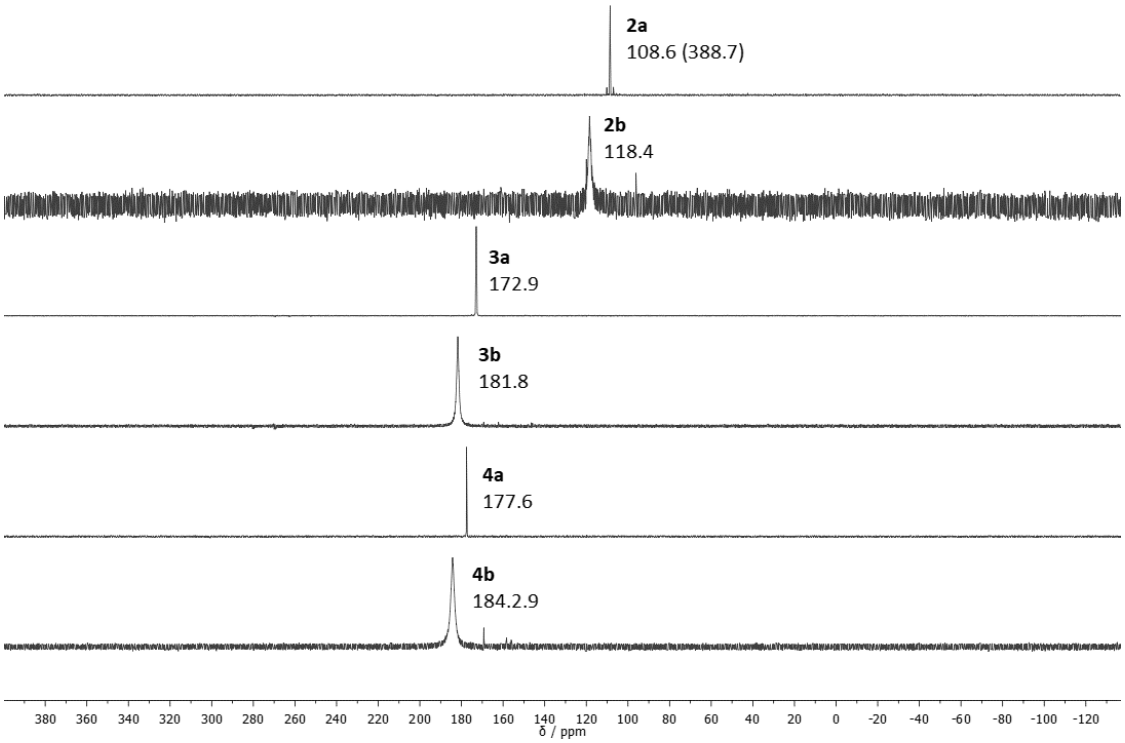

Figure 3.1.1. *^{31}P NMR spectra of complexes **2-4.** (Given values in ppm with the $^{1}J_{W,P}$ coupling constant in Hz in brackets).*

The influence of the amino-substitution is clearly visible in the ^{31}P NMR spectrum (figure 3.1.1) of **2-4**. For example, for **2a** a high-field shift by ~60 ppm to 108.6 ppm (compared to 166.2 ppm for $[W(CO)_5(Ph_3CPCl_2)]$[60]) is observed, indicating a net electron donation from the N towards the P centre resulting in a stronger P-shielding. In case of **2b** and **4b** very minor unknown side-products are visible. In case of *P*-NCy_2 substitution (**b**) a small downfield shift is observed (7 – 10 ppm), as well as a stronger signal broadening in general (FWHD ~ 50 – 150 Hz) resulting in a bad signal-to-noise ratio. Such broadened ^{31}P NMR signals indicate dynamic effects in solution on the NMR time scale and, therefore, VT-NMR measurements were conducted for **2b** in the range of -60 °C to r.t. (figure 3.1.3) showing the splitting into the two atropisomers **2b** and **2b'** along the P-N bond, at 110.8 ($^{1}J_{W,P}$ = 377.8 Hz) and 126.7 ppm ($^{1}J_{W,P}$ = 370.9 Hz) ($|\nu_A - \nu_B|$ = 1925.24 cm^{-1}), respectively (figure 3.1.2).

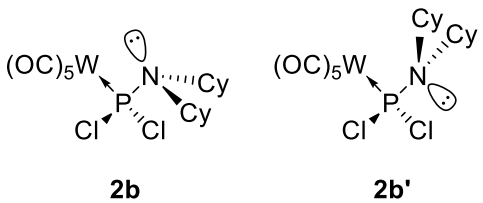

2b **2b'**

Figure 3.1.2. *Display of the two presumably formed atropisomers **2b** and **2b'** (s-cis and s-trans) regarding the relative orientation of the N lone-pair and the P-W bond).*

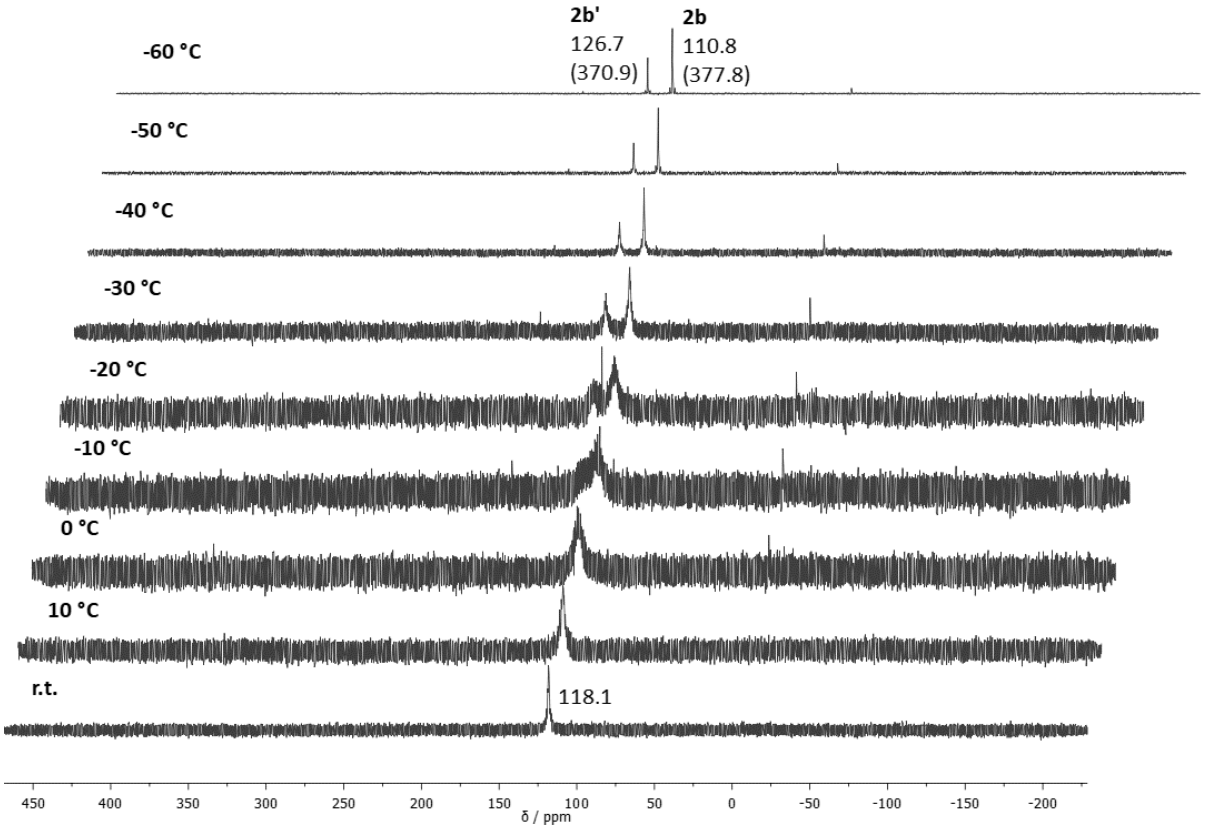

Figure 3.1.3. *$^{31}P\{^1H\}$ VT-NMR measurements of **2b** in solution. (Given values in ppm with the $^1J_{W,P}$ coupling constant in Hz in brackets).*

The measured coalescence temperature (T_c) lies at -10 °C. With the obtained data and the *Eyring* equation[100] a *Gibbs* free energy rotation of around 7.3 kcal/mol could be calculated (formula 3.1.1).[101] The obtained value appears reasonable when comparing for example with the rotation barrier for ethane of 2.7 kcal/mol.[102]

$$\Delta G^{\neq} = RT_c ln \frac{k_B T_c \sqrt{2}}{\pi h |v_A - v_B|}$$

Formula 3.1.1 *Eyring equation for the determination of the Gibbs free energy of rotation (R = 8.314 J K^{-1} mol^{-1}; k_B = 1.380 10^{-23} J K^{-1}; h = 6.626 10^{-34} J s).*

This kind of atropisomerism, due to hindered rotation at the P-R bond, was seen before in some cases of *P*-$CH(SiMe_3)_2$ substituted ligands in tungsten(0) complexes at room temperature, showing s-*cis* and s-*trans* isomers regarding the C-*H* bond and the P-W bond,[69] but which is due to steric effects only.

The ^1J(W-P) coupling constants lie in the expected range, *e.g.* $^1J_{W,P}$ = 388.7 Hz (**2a**), yet up to 70 Hz higher coupling constants are observed when compared to $[W(CO)_5(Ph_3CPCl_2)]$ ($^1J_{W,P}$ = 319.7 z).[60] This is the effect of the electronegative N as bonding partner for the phosphorus

and can be explained using *Bent's rule*.[103] According to this, orbitals with higher *p*-character will be directed towards bonding partners with higher electronegativity, in this case N, leaving higher *s*-character orbitals for the P-W bond. Since *s*-orbitals in general display a higher electronegativity (than *p, d*), due to their smaller nucleus spacing, electron back-bonding from tungsten to phosphorus increased and, hence, increasing the $^{1}J_{W,P}$ coupling constant; the latter becomes visible in a shorter P-W bond distance (see table 3.1.2).

The chromium and iron complexes (**3, 4**) show strong ^{31}P NMR downfield-shifted values by 60 – 70 ppm, which is a literature-known relation for various P-ligand metal complexes.[57] The obtained IR spectra show the expected absorptions due to CO stretch vibrations in the expected region (1912 – 2081 cm^{-1}) also fitting the calculated IR frequencies for CO stretch vibrations (1927.6 – 2068.6 cm^{-1}).

Table 3.1.1. *^{31}P NMR data, IR frequencies (experimental and calculated*) and isolated yields.*

	δ ^{31}P NMR ($^{1}J_{W,P}$) / ppm (Hz)	IR (exp) / cm^{-1}	IR (calc) / cm^{-1}	Yield / %
2a[a]	108.6 (388.7)	1931, 1980, 1997, 2081, 3061	1931.2, 2068.6, 3150.1	50
2b[b]	110.8 (379.6) 126.7 (368.2)	1912, 1948, 1970, 2080, 2857, 2933	1927.6, 2068.6, 3027.1	46
3a[a]	172.9	1946, 2067	1967.4, 2065.0, 3157.3	36
3b[a]	181.8	1951, 1985, 2080, 2850, 2930	1963.7, 2061.4, 3027.1	56
4a[a]	177.6	1932, 1986, 2005, 2079, 3040	1942.0, 2068.6, 3157.3	47
4b[a]	184.2	1920, 1993, 2074, 2931	1938.4, 2068.6, 3027.08	40
$[W(CO)_5$-$(Ph_3CPCl_2)]$[c][60]	166.2 (319.7)	1942, 1955, 2082	-	65

[a]C_6D_6; [b]THF, -60 °C; [c]$CDCl_3$; *TPSS-D3/CPCM(THF)/def2-TZVP.

Complexes **2a**, **3b** and **4a** could be crystallized and single crystal X-ray diffraction analyses were performed. The obtained crystal structures are displayed in figures 3.1.4 – 3.1.6 with their crystallographic data listed in table 3.1.2.

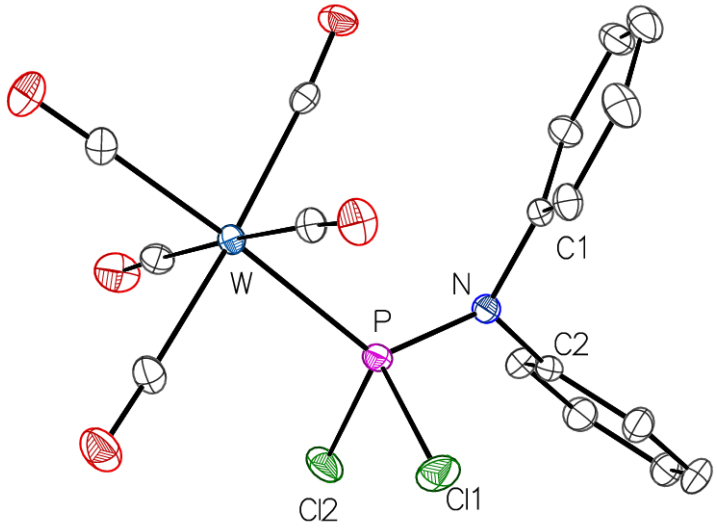

Figure 3.1.4. *Molecular structure of* ***2a*** *in the crystal. The ellipsoids were set to 50 % possibility and hydrogen atoms have been omitted.*

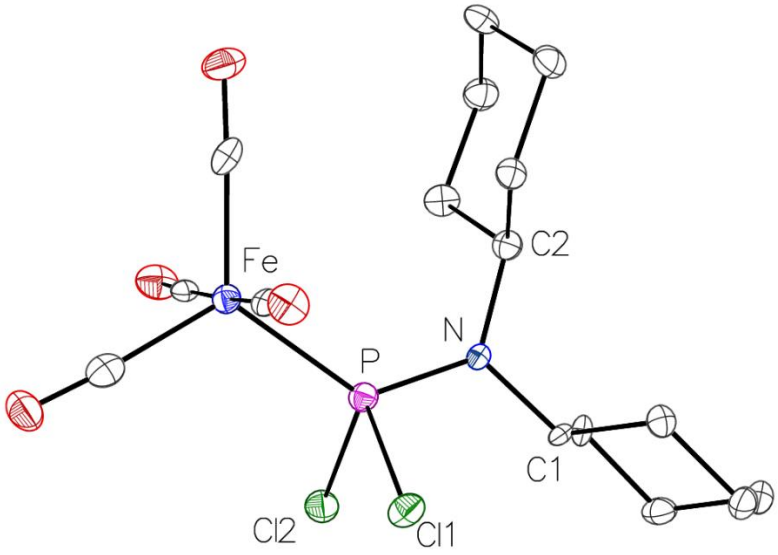

Figure 3.1.5. *Molecular structure of* ***3b*** *in the crystal. The ellipsoids were set to 50 % possibility and hydrogen atoms have been omitted.*

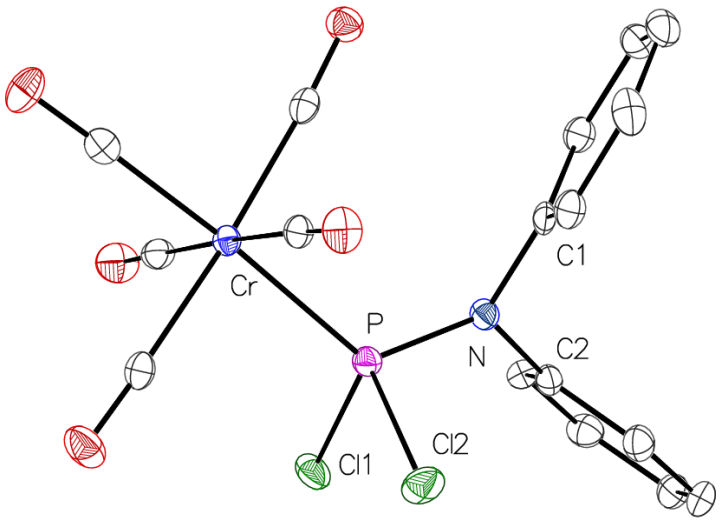

Figure 3.1.6. *Molecular structure of* ***4a*** *in the crystal. The ellipsoids were set to 50 % possibility and hydrogen atoms have been omitted.*

To get more insight into the structures of derivatives **2a-4b**, especially the ones with no x-ray diffraction analysis measured, calculations at the following level of theory (TPSS-D3/CPCM(THF)/def2-TZVP// PW6B95-D3/CPCM(THF)/def2-QZVP) were performed and selected structural details and bonding parameters listed in the table below (table 3.1.2). TPSS as a meta-GGA[104] yields reliable structure optimizations with reasonable resource demands (cores and computing time) in combination with a triple-ζ basis-set, yet tends to over-delocalize (and therefore overestimate bonding). A thorough benchmark for various DFT functionals showed a weighted total mean absolute deviation (WTMAD) of 4.6 kcal/mol (benchmark sets for properties, reaction energies and non-covalent interactions; (aug-)def2-QZVP).[105] This is why single-point calculations for these geometries were done using PW6B95 as a very robust hybrid-functional with a WTMAD of 2.5 kcal/mol.[105]

For comparison of the derivatives in table 3.1.2, also the literature-known complex $[W(CO)_5(Ph_3CPCl_2)]$ (**2-CPh$_3$**) was calculated, while the crystallographic data was taken from the literature.[60]

Table 3.1.2. *Bond lengths and angles obtained by X-ray diffraction studies and calculations* for complexes* ***2-4****.*

	d(M-P) (exp) / Å	d(M-P) (calc) / Å	d(P-N) (exp) / Å	d(P-N) (calc) / Å	d(P-Cl1) (exp) / Å	d(P-Cl2) (calc) / Å	Σ(<N) (exp) / °	Σ (<N) (calc) / °
2a	2.4396(19)	2.482	1.665(5)	1.670	2.088(2)	2.115	357.9	357.4
					2.051(3)	2.063		
2b	-	2.510	-	1.648	-	2.127	-	358.9
						2.086		
3a	-	2.162	-	1.676	-	2.110	-	357.5
						2.076		
3b	2.1925(17)	2.182	1.638(5)	1.647	2.103(2)	2.117	359.8	359.0
					2.086(2)	2.097		
4a	2.2891(8)	2.318	1.667(8)	1.671	2.0874(10)	2.117	357.5	357.3
					2.0421(10)	2.064		
4b	-	2.345	-	1.650	-	2.133	-	358.7
						2.084		
2-CPh_3	2.4685(6)	2.507	1.955(2) (P-C)	1.972 (P-C)	2.043(8)	2.076	-	433.6 (C)
					2.063(8)	2.076		

*TPSS-D3/CPCM(THF)/def2-TZVP.

The obtained crystallographic data for complexes **2a, 3b, 4a** are in the expected range, very well matching the computed structural data. Remarkable is that the sum of the bond angles at nitrogen is close to 360° for all cases, thus showing a planar nitrogen environment. This leads to the conclusion of a *p*-donation by N into the N-P bond thus yielding partial P-N double bond character.

To gain further evidence the corresponding *Mayer bond order* (MBO) values were calculated which are displayed in table 3.1.3.

Table 3.1.3. *Computed* MBO values, Loewdin charges (q^L) and HOMO-LUMO energy gaps for complexes **2-4**.*

	MBO(P-M)	MBO(P-N)	MBO(P-Cl)	$q^L(M(CO)_n)$	$q^L(P)$	$q^L(N)$	$\lvert\Delta E_{HOMO\text{-}LUMO}\rvert$ / eV
2a	0.667	1.229	1.049 0.950	-0.379	-0.191	0.245	4.76
2b	0.599	1.345	1.023 0.946	-0,410	-0.174	0.263	4.82
3a	0.841	1.196	1.016 0.957	-0,577	-0.094	0.279	5.04
3b	0.641	1.338	0.994 0.954	-0,638	-0.088	0.282	5.05
4a	0.610	1.210	1.048 0.944	-0,580	-0.074	0.257	5.18
4b	0.487	1.374	1.006 0.939	-0,629	-0.055	0.272	5.29
2a-CPh_3	0.531	0.896 (P-C)	1.070 1.041	-0,415	-0.001	-0.235 (C)	4.72

*PW6B95-D3/CPCM(THF)/def2-QZVP.

The obtained data support the notion of a partial P-N double bond as the MBO(P-N) averages are 1.212 (**a**) for NPh_2 and 1.352 (**b**) for NCy_2; the latter possess a 12 % higher bond order which correlates with the higher basicity of NCy_2 (**b**) compared to NPh_2 (**a**), which in the context of intramolecular electron donation better is called "π backbonding/-donation"[9] or stronger "resonance contribution".[75] Compared to **2-CPh_3** this is an increase of the MBO values by 0.316 (35 %) and 0.456 (50 %), respectively. Moreover, the calculated *Loewdin* atomic charges are showing more negative charge at the phosphorus, -0.191 for **2a** compared to -0.001 for **2-CPh_3**, showing that the +M-effect of the N outweighs its -I-effect. The average MBO(P-Cl) for NPh_2- and NCy_2-substituted complexes are 0.994 and 0.977, respectively, showing a small destabilization of the P-Cl bonds compared to **2-CPh_3** (average

MBO(P-Cl) 1.056). This will occur due to an electron donation that (partially) fills anti-bonding orbitals p(N)→σ*(P-X), which is consistent with the fact that the LUMO, additional to the metal fragment, has significant contributions from the P-Cl bonds (figure 3.1.7). In a computational study from 2019 regarding the NH-insertion of phosphinidenoid complexes also weakened bonds in the amino-phosphanide complex, compared to the neutral aminophosphane complex, were determined.[78]

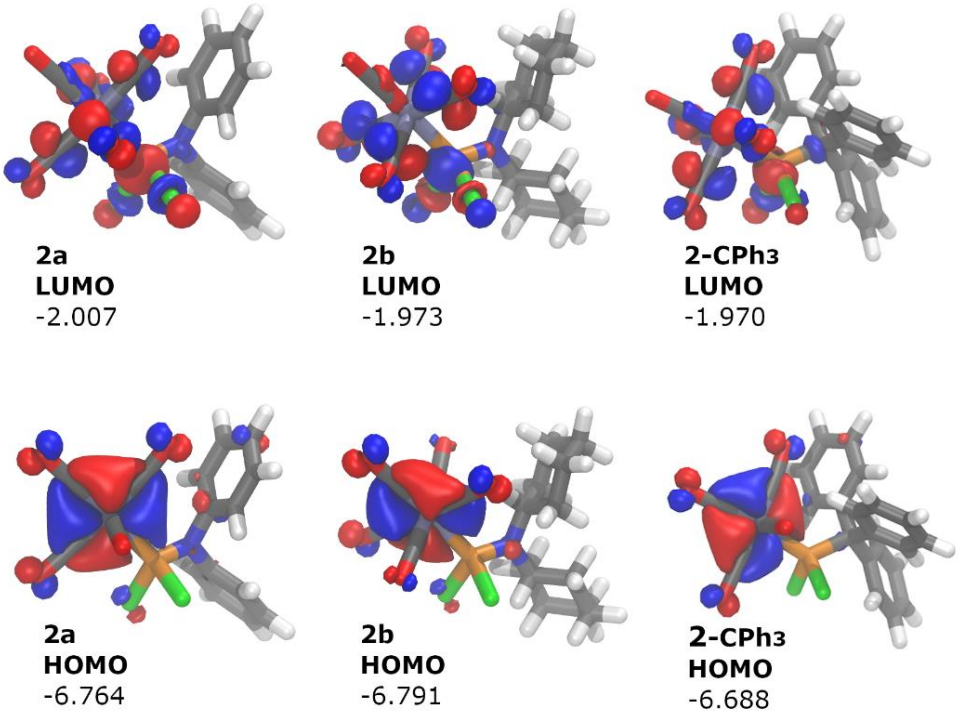

Figure 3.1.7 *Calculated HOMO and LUMO frontier orbitals of complex* ***2a,b*** *and for comparison* ***2-CPh₃*** *at the TPSS-D3/CPCM(THF)/def2-TZVP// PW6B95-D3/CPCM(THF)/def2-QZVP level of theory (a = ±0.04); energy values are given in eV.*

When comparing **2a, b** and **2-CPh₃** some small differences can be seen regarding frontier orbital distribution. The HOMO as well as the HOMO-1 are strongly metal centred in all cases, yet the differences can be seen regarding small contributions from the N in **2a, b** and Ph-rings in **2a** and very little for **2-CPh₃**. The stronger contributions of the P-Cl bonds for the LUMOs in **2a, b** are also visible, compared to the LUMO of **2-CPh₃**. The HOMO-LUMO gaps are very similar with 4.76, 4.82 and 4.72 eV for **2a, b** and **2-CPh₃**, respectively.

3.2 Generation and "self-condensation" of *P*-amino substituted Li/Cl phosphinidenoid complexes

Having the complexes **2-4** the corresponding *P*-amino substituted Li/Cl phosphinidenoid complexes were targeted (scheme 3.2.1), following the established protocol.[63,67,68] Complexes **2-4** were reacted with ^{t}BuLi at -80 °C in the presence of 12-crown-4 and VT-NMR studies were conducted for all derivatives to possibly observe the formation of the corresponding Li/Cl phosphinidenoid complexes **5-7** (figure 3.2.1-3.2.9). The numbering of the complexes was done according to the amount of usage W > Fe > Cr.

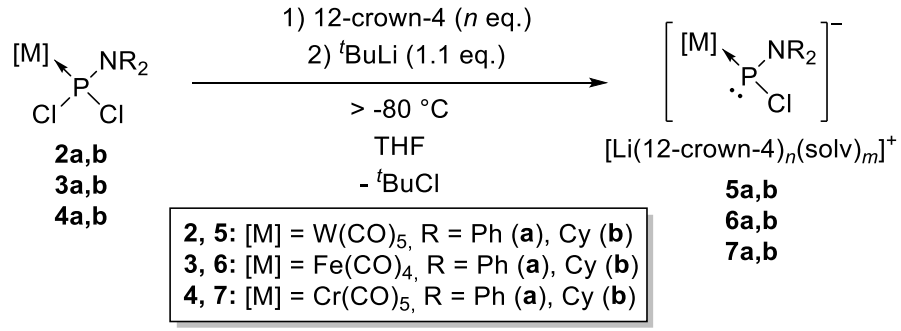

Scheme 3.2.1 *Generation of Li/Cl phosphinidenoid complexes* ***5-7*** *at low temperature.*

Complex **5a** was observed at -80 °C having an expected downfield-shifted signal at 339.3 ppm with a rather small $^{1}J_{W,P}$ coupling constant of 135.8 Hz, typical for Li/Cl phosphinidenoid complexes, or anionic P-ligand complexes in general (figure 3.2.1). Yet, **5a** appears to be much more strongly downfield-shifted with a significantly higher $^{1}J_{W,P}$ coupling constant magnitude than previously observed Li/Cl phosphinidenoid complexes, *e.g*. with a *P*-CPh_3 substitution, the signal appears at 252.1 ppm ($^{1}J_{W,P}$ = 77.6).[60] A remarkable good fitting ^{31}P NMR shift was calculated with 346.5 ppm, given that the electronic structure of such Li/Cl phosphinidenoid complexes is not trivial, thus leading to problems to calculate shielding parameters. First ^{31}P NMR shift calculations for Li/halogen phosphinidenoid complexes showed an overestimation of the ^{31}P NMR low-field shift of 103 ppm (by average) with strong contributions of paramagnetic contributions.[58] From their data, a persistent molecular complex or tight contact ion pair was also ruled out. This stands in agreement, since here the calculated 346.5 ppm is for the naked anion **5a^{-}**, whereas variations of the coordination of **5a** drastically change the shift (figure 3.2.3). It also appeared that complex **5a** is thermally much more labile (or reactive), compared to $[W(CO)_5(Ph_3CPCl)]^{-}$, with only 17 % at -80 °C and it had completely vanished at around -20 °C, mainly forming dinuclear diphosphane complex **8** as deduced from its ^{31}P NMR spectroscopic parameters.

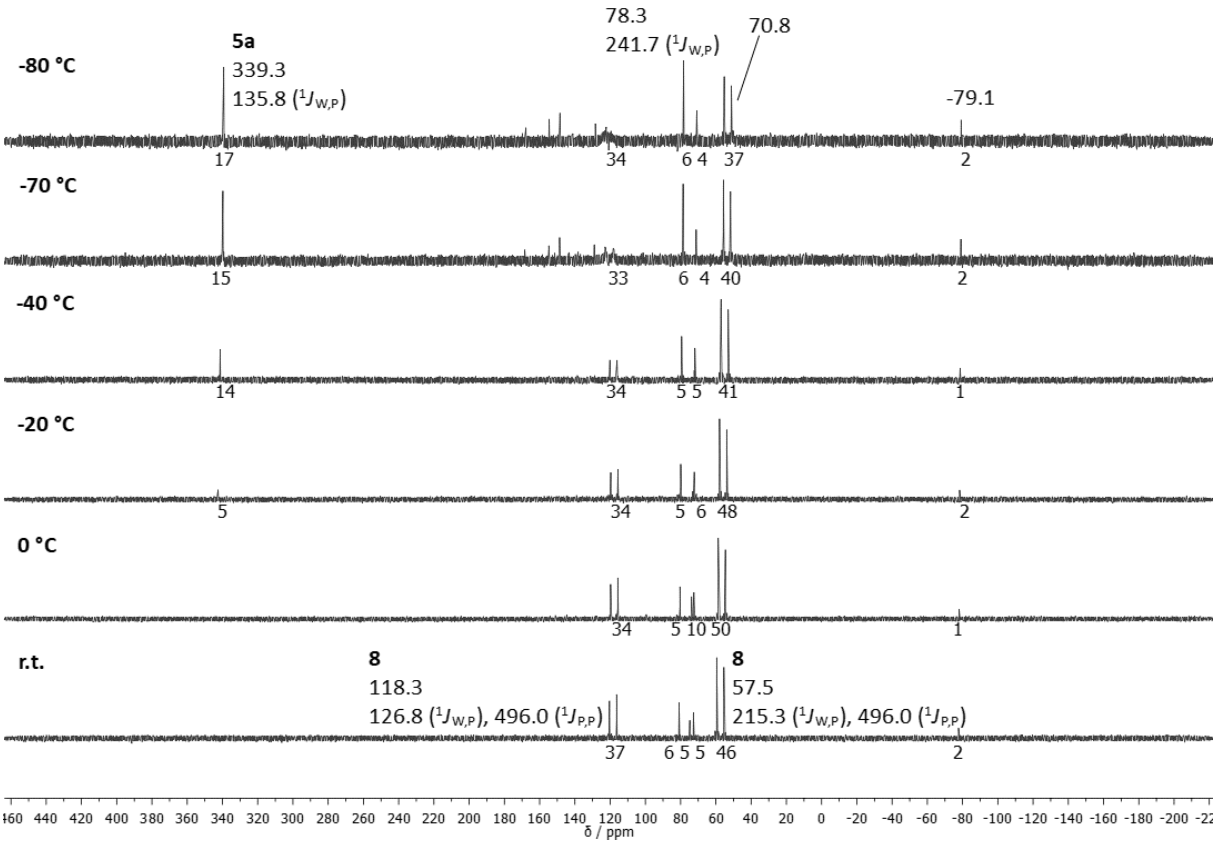

Figure 3.2.1. *$^{31}P\{^1H\}$ VT-NMR spectra of the reaction mixture of **2a** with ^{t}BuLi starting at -80 °C. (Given values in ppm with the coupling constant in Hz for the element couple in brackets. Integration values are given in % below the baseline).*

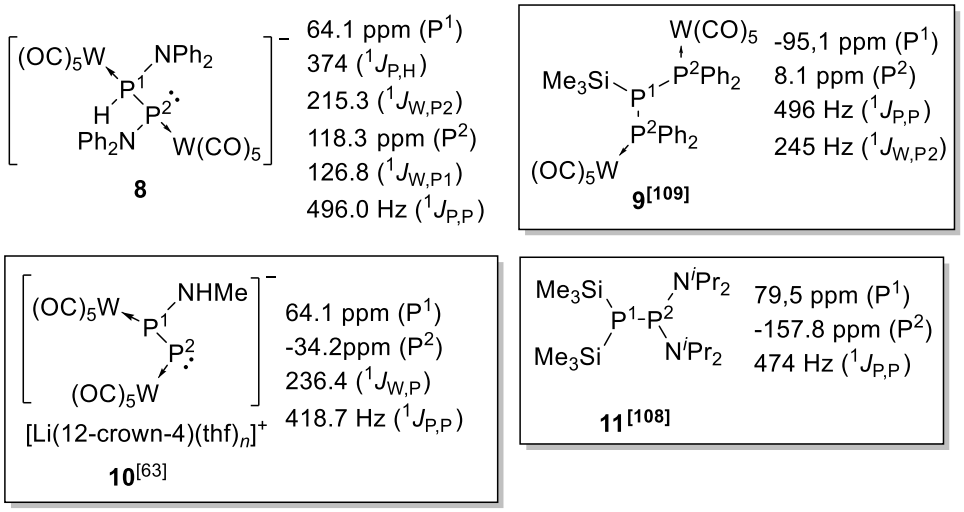

Figure 3.2.2. *Major side products deduced from their characteristic ^{31}P NMR spectroscopic data.*

Complex **8** displays very characteristic ^{31}P NMR data, with a large $^1J_{P,P}$ coupling constant of 496.0 Hz, one phosphorus at 118.3 ppm with a small $^1J_{W,P}$ = 126.8 Hz coupling and no P-H coupling, and the other

phosphorus with a $^{1}J_{W,P}$ = 215.3 Hz with a large $^{1}J_{P,H}$ coupling constant of 374.0 Hz. This is clearly indicating the phosphanido-type subunit (P2) combined with a P-H functional subunit directly bound (P1). Moreover, such large $^{1}J_{P,P}$ couplings can be seen in case of *σ-push-pull* substituted diphosphanes **11**,[106] triphosphanes[108] and their complexes such as **9**.[107] The large P-H coupling also indicates that the *P*-NPh_2 substitution stays intact over this coupling reaction, since an electronegative P-substituent is needed. Furthermore, a similar diphosphane complex **13** could be obtained and measured via x-ray diffraction analysis in case of **2b** (figure 3.2.6). The obtained ^{31}P NMR shifts are also in good agreement with the calculated ^{31}P NMR shifts (against **2a**, TPSS-D3/GIAO def2-QZVP) of 119.6 and 54.3 ppm for its anion, consisting with separated ions in solution.

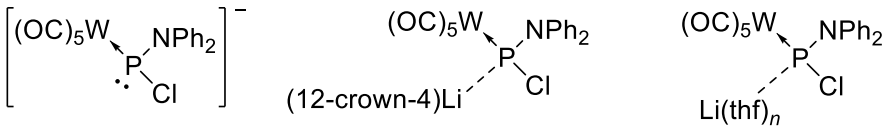

5a^{-} 346.5 Li(12-crown-4)-**5a** 281.3 Li(thf)$_2$-**5a** 406.1 Li(thf)$_3$-**5a** 280.2

Figure 3.2.3 *GIAO TPSS-D3/def2-QZVP computed ^{31}P NMR shifts (in ppm) for different coordination and solvent modii of complex **5a** using TPSS-D3/def2-TZVP/COSMO(THF) optimized geometries. Values are referenced against complex **2a** [W(CO)$_5$PCl$_2$NPh$_2$] at 108.6 ppm (computed shielding constant = σ_{iso}(**2a**) – δ_{exp}(**2a**) = 141.93 ppm).*

When reacting **2b** with ^{t}BuLi at low temperature, some unreacted complex can be seen even at room temperature (**2b, 2b'**: 126.7, 110.8 ppm), which may result from a sub-stoichiometric amount of ^{t}BuLi, or the reaction of the latter with some side-products formed. In figure 3.2.4, again, the formation of a diphosphane-type compound can be seen at 75.3 and 53.9 ppm, but due to a strong signal broadening, originating from *P*-NCy_2 substitution (FWHM ~ 50 Hz), no further conclusions could be drawn regarding a specific substitution pattern. The only clearly visible couplings are the $^{1}J_{P,P}$ with 508.5 Hz, again indicating a *σ-push-pull* substituted diphosphane, and the $^{1}J_{P,H}$ coupling of 350.1 Hz for one phosphorus nucleus.

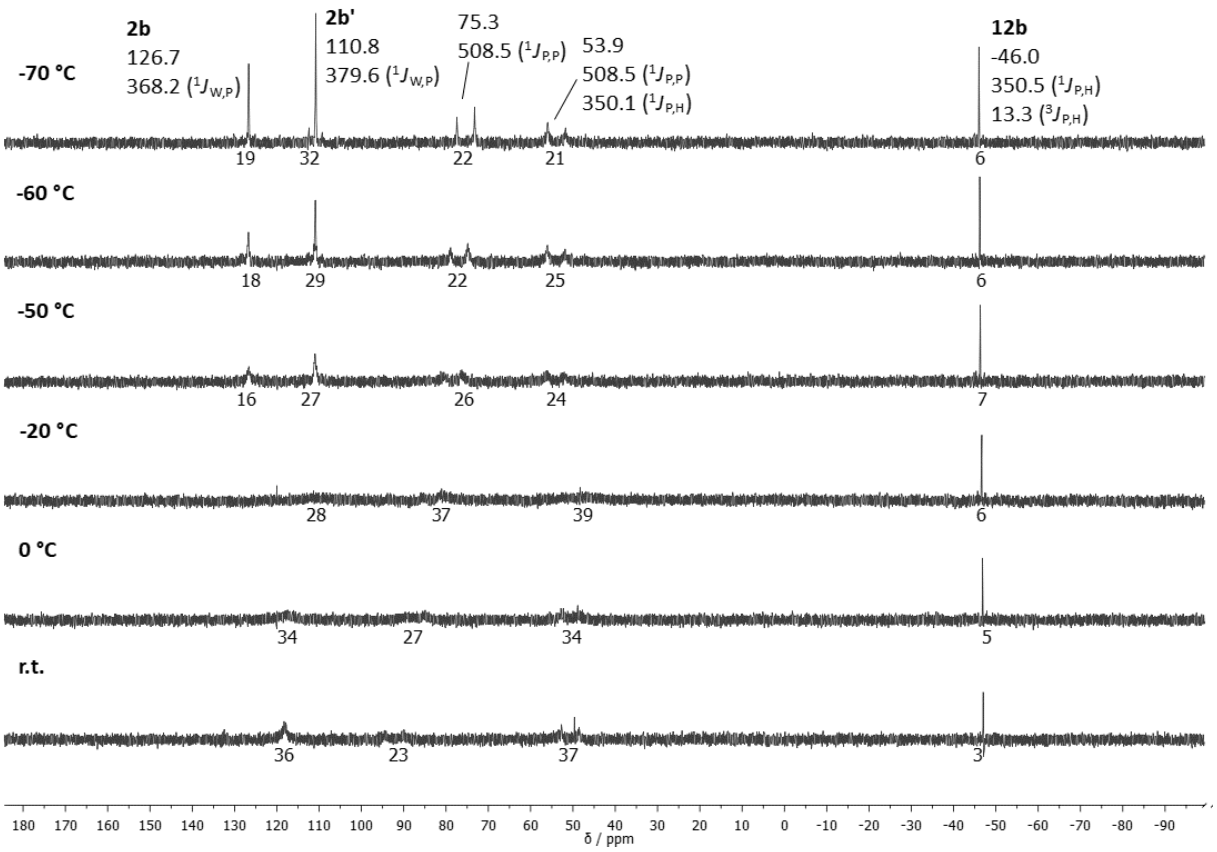

Figure 3.2.4. *$^{31}P\{^1H\}$ VT-NMR spectra of the reaction mixture of **2b** with ^{t}BuLi starting at -70 °C. (Given values in ppm with the coupling constant in Hz for the element couple in brackets. Integration values are given in % below the baseline).*

The signal at -46 ppm can be safely assigned to the reported complex $[W(CO)_5\{H_2PNCy_2\}]$ (**12a**) due to its characteristic P,H coupling pattern in the ^{31}P NMR spectrum: $^1J_{P,H}$ = 350.5 Hz, triplet (*PH*$_2$) and $^3J_{P,H}$ = 13.3 Hz, triplet (*P*-NC*H*) (figure 3.2.5).[98] It is to mention, that the strong broadened signals also result in unreliable ^{31}P NMR integration.

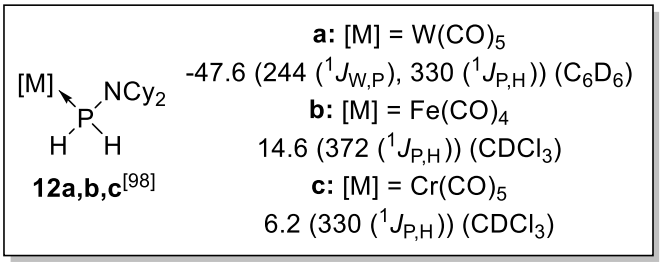

Figure 3.2.5 *Literature known dicyclohexylamino phosphane complexes **12**.[98]*

In case of the reaction of **2b,** the diphosphane complex **13** could be crystallized (from Et_2O) and single crystals measured via X-ray diffraction. The result (figure 3.2.6) showed, again, that bond angle sums

at the two N-atoms are Σ(<N1) 356.3° and Σ(<N2) 358.7°, *i.e.*, almost perfectly planar. Some small interactions between the H atoms (P*H*) with one O atom (C*O*) each of the opposite $W(CO)_5$ group can be found (d(H-O) = 2.67948(17) Å).

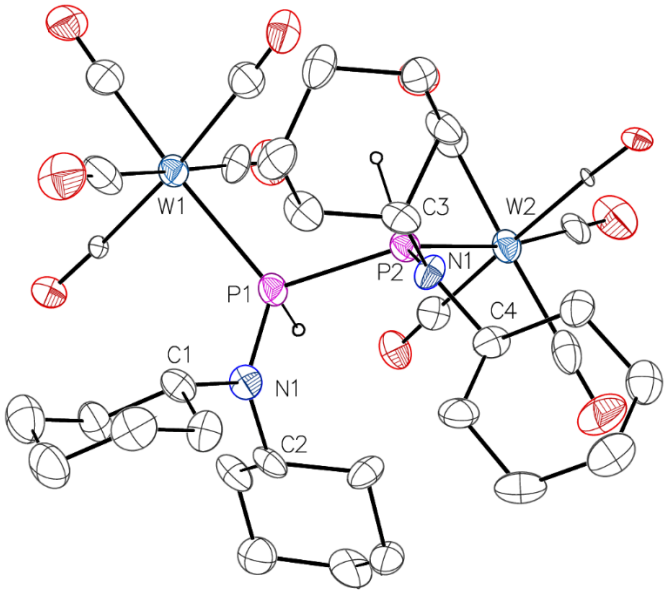

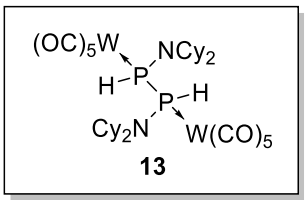

Figure 3.2.6. *Molecular structure of* ***13*** *in the crystal with its corresponding structural drawing. The ellipsoids were set to 50 % possibility and hydrogen atoms have been omitted, except for P-H. Selected bond lengths (in Å) and angles (in °): P1-W1 2.5115(10), P2-W2 2.5235(12), P1-P2 2.306(2), P1-N1 1.684(4), P2-N2 1.675(4), P1-N1-C1 117.0(4), P1-N1-C2 122.3(3), C1-N1-C2 117.0(4), P2-N2-C3 122.2(3), P2-N2-C4 119.2(3), C3-N2-C4 117.3(3).*

In case of **3a** (figure 3.2.7), the $^{31}P\{^{1}H\}$ NMR spectrum, having a rather bad signal to noise ratio, showed that a lot of unreacted starting material was still present. This might be due to undesired reactions of ^{t}BuLi with minor unknown side-products formed. Nevertheless, a diphosphane (complex) formation could be seen at 142.1 and 113.5 ppm with a large $^{1}J_{P,P}$ coupling of 495.5 Hz, which is similar to **8**. But due to the low quality spectrum and some signal broadening, no further information could be obtained; these signals showed no $^{1}J_{P,H}$ couplings.

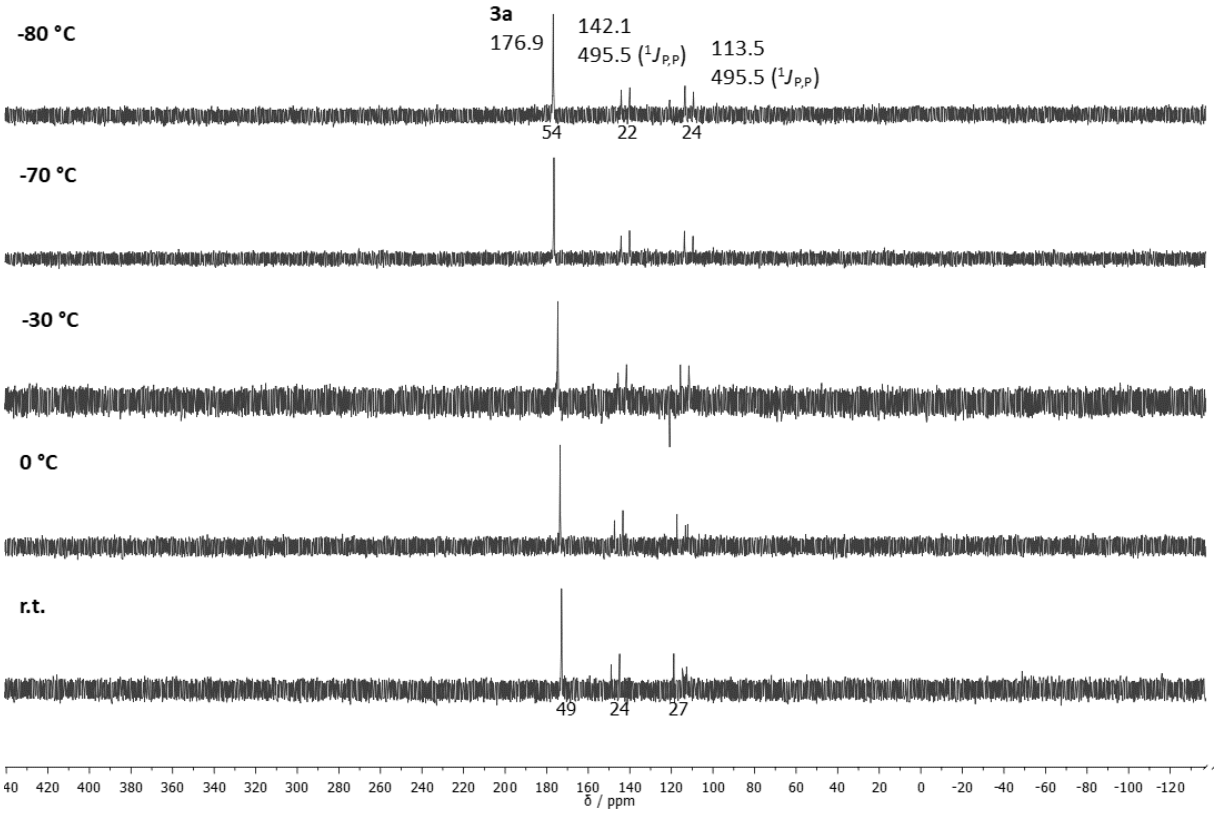

Figure 3.2.7. *$^{31}P\{^1H\}$ VT-NMR spectra of the reaction mixture of **3a** with ^{t}BuLi starting at -80 °C. (Given values in ppm with the coupling constant in Hz for the element couple in brackets. Integration values are given in % below the baseline).*

In case of the reaction of **3b** (figure 3.2.8), no Li/Cl phosphinidenoid complex **6b** could be observed in the time-scale of the $^{31}P\{^1H\}$ NMR measurements at -80 °C. At this temperature some starting material (181.1 ppm) also remained, but the general product pattern appears to be rather similar to the case of **2b** (figure 3.2.4). Here, a signal showed a rather characteristic P,H coupling for $[Fe(CO)_4PH_2NCy_2]$ in the ^{31}P NMR spectrum ($^1J_{P,H}$ = 380.4 Hz, triplet (*P*H_2) and $^3J_{P,H}$ = 14.2 Hz, triplet (*P*-NC*H*)) as well as signals of a diphosphane-type product at 97.9 and 64.9 ppm with a $^1J_{P,P}$ coupling constant of 488.5 Hz, but no further $^1J_{P,H}$ coupling in this case.

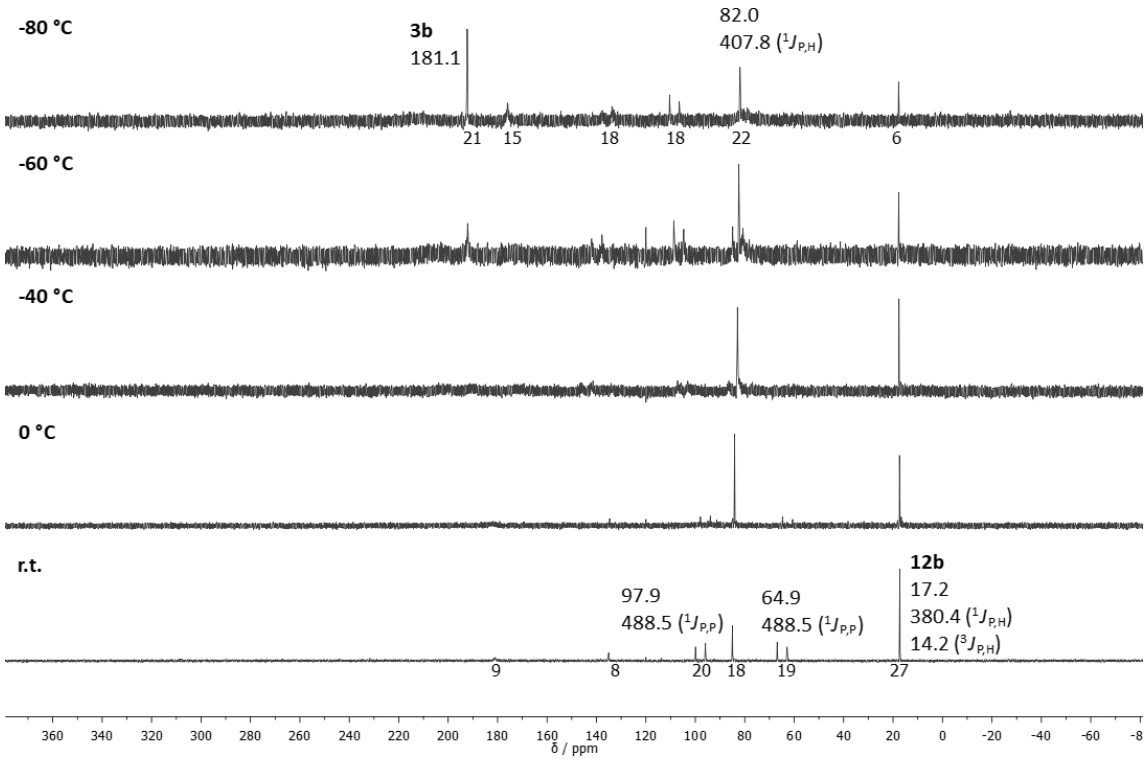

Figure 3.2.8. *$^{31}P\{^1H\}$ VT-NMR spectra of the reaction mixture of **3b** with ^{t}BuLi starting at -80 °C. (Given values in ppm with coupling constants in Hz for the element couple in brackets. Integration values are given in % below the baseline. P-H couplings were taken from the ^{31}P NMR spectrum).*

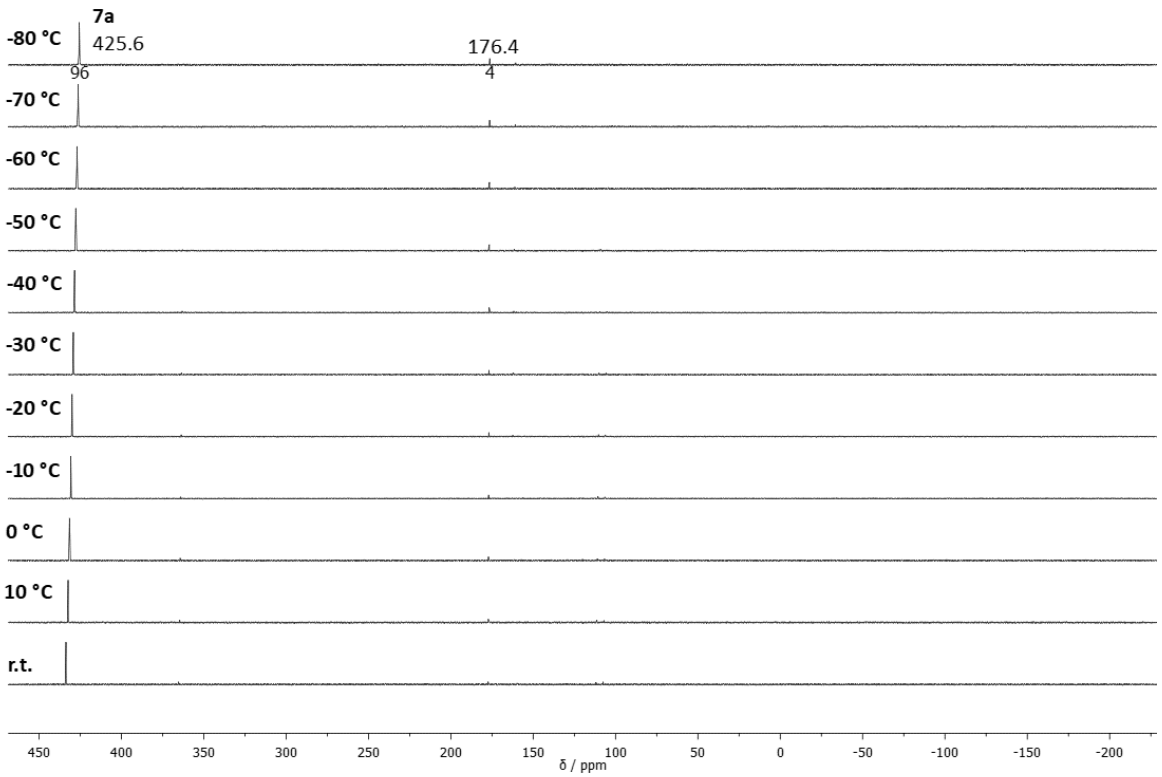

Figure 3.2.9. *$^{31}P\{^1H\}$ VT-NMR spectra of the reaction mixture of **4a** with ^{t}BuLi starting at -80 °C. (Given values in ppm with integration values in % below the baseline).*

Li/Cl phosphinidenoid complex **7a** was observed with a high product content > 95 % and a remarkable downfield-shifted signal at 425.6 ppm (no $J_{P,H}$ coupling). At ambient temperature the compound started to decompose. Unfortunately, crystallization attempts under fridge conditions yielded no measurable crystals. In contrast to the other *P*-amino substituted Li/Cl phosphinidenoid complexes, **7a** displayed a high thermal stability being one of the few examples stable up to room temperature.[60] Such a difference between tungsten and chromium has also be seen in case of Li/Cl phosphinidenoid complexes having a *P*-^{t}Bu substitution according to ^{31}P NMR VT-NMR measurements.[68]

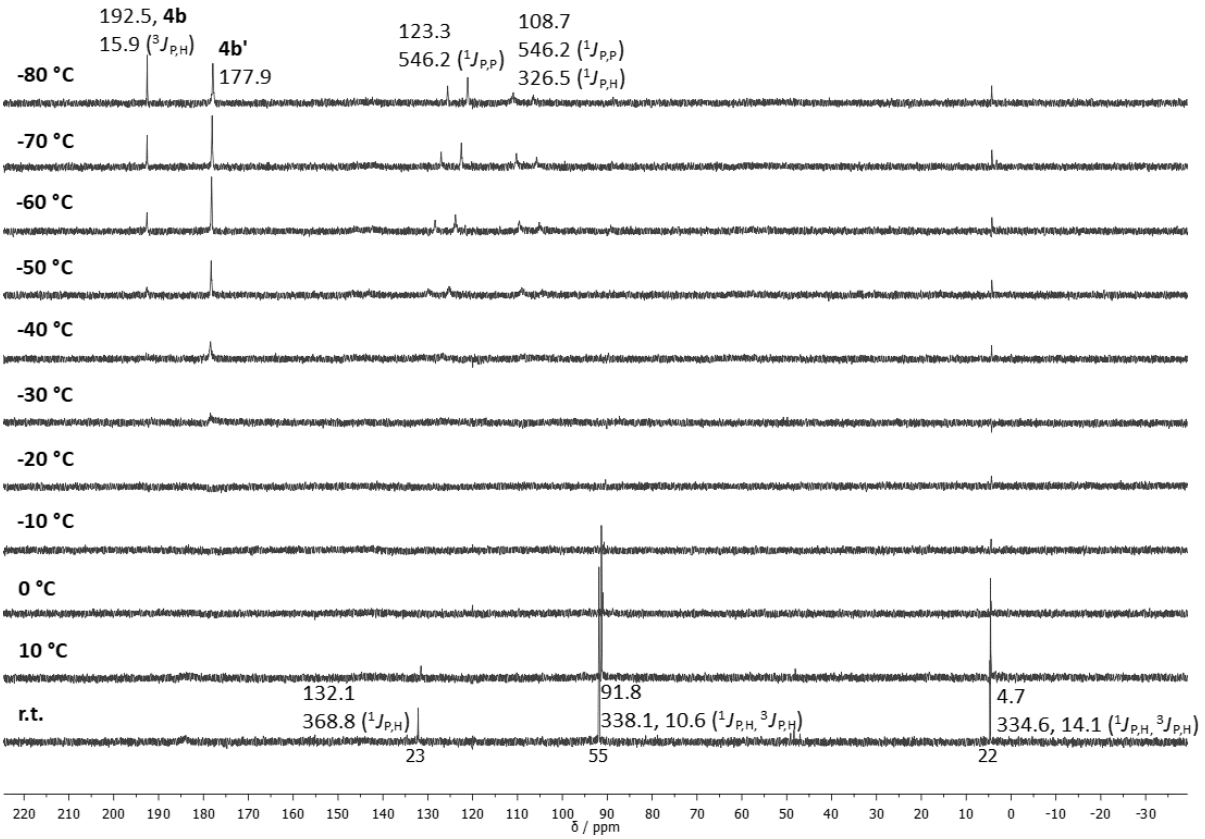

Figure 3.2.10. *^{31}P{^{1}H} VT-NMR spectra of the reaction mixture of **4b** with ^{t}BuLi starting at -80 °C. (Given values in ppm with the coupling constant in Hz for the element couple in brackets. Integration values are given in % below the baseline. P-H couplings were taken from the ^{31}P NMR spectrum).*

As it can be seen when figure 3.2.9 is compared to 3.2.10, the *P*-amino substituents NCy_2 and NPh_2 reveal a huge difference in terms of chromium complex product formation and stability. First of all, the signal **4b** was observed at low temperature, with strong signal broadening and splitting into two signals for the corresponding P-N bond atropisomers (see **2b** and compare figure 3.1.2). Regarding the product formation, the outcome for the other derivatives can be observed here as [$Cr(CO)_5PH_2NCy_2$] (**12c**) at 4.7 ppm – $^{1}J_{P,H}$ = 334.6 Hz, triplet (*PH*$_2$) and $^{3}J_{P,H}$ = 14.1 Hz, triplet (*P*-NC*H*) – and diphosphane, here at 123.3 and 108.7 ppm with $^{1}J_{P,P}$ coupling of 546.2 Hz and a $^{1}J_{P,H}$ of 326.5 Hz for the more high-field

shifted phosphorus can be seen. Although, in this case the corresponding diphosphane (complex) appeared to be not stable over the course of the reaction and formed two other side-products at 132.1 ppm ($^{1}J_{P,H}$ = 368.8 Hz) and 91.8 ppm ($^{1}J_{P,H}$ = 338.1 Hz, doublet (*PH*) and $^{3}J_{P,H}$ = 10.6 Hz, triplet (*P*-NC*H*)), respectively, additionally to the complex seen at 4.7 ppm.

First, simplified calculations were done to obtain HOMO and LUMO frontier orbitals for **5a,b** and **5-^{t}Bu** for comparison (figure 3.2.11). For this the cation Li or different solvation models containing 12-crown-4 were not taken into account.

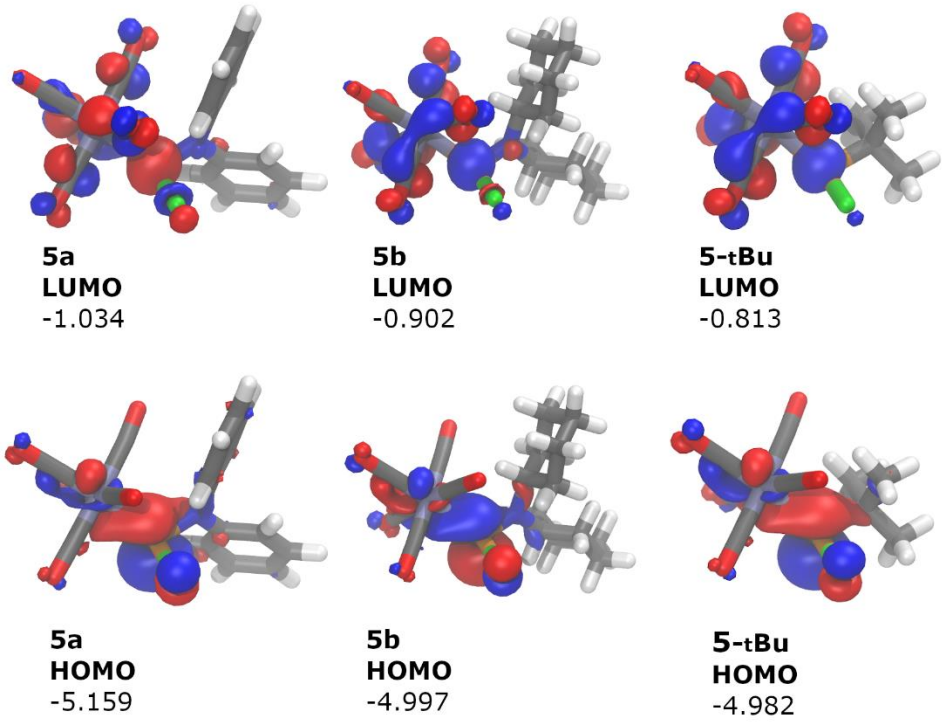

Figure 3.2.11. *Calculated HOMO and LUMO frontier orbitals of complex **5a,b** and for comparison **5-^{t}Bu** at the TPSS-D3/CPCM(THF)/def2-TZVP// PW6B95-D3/CPCM(THF)/def2-QZVP level of theory (a = ±0.04); energy values are given in eV.*

When comparing **5a,b** and **5-^{t}Bu** some small differences can be seen regarding frontier orbital distributions, yet large differences are visible when comparing with figure 3.1.6. The HOMOs are no longer metal centred yet strongly located at the P-centre with P-W and P-Cl bond contributions. The HOMO-1 only in case of **5a** is strongly located towards the Ph-rings. The LUMOs are similar when compared to figure 3.1.6, with stronger contributions of the P-Cl bonds for the LUMOs in **5a, b**. The HOMO-LUMO gaps are very similar with 4.13, 4.10 and 4.17 eV for **5a, b** and **5-^{t}Bu**, respectively

To get more insight, more complex calculations were done by *Qu* investigating the appearance and coordination of the *P*-amino substituted Li/Cl phosphinidenoid complex **5a** in solution (figure 3.2.12).[109] It was shown before that solvation effect have a great impact on the structure, and therefore stability and reactivity, of Lithium derivatives of organometallic and inorganic compounds.[110] This was recently shown for alkali metal carbenoids which are more stable in THF (as solvent stabilized monomers) and prone for facile salt elimination and decomposition in toluene (as dimers).[111]

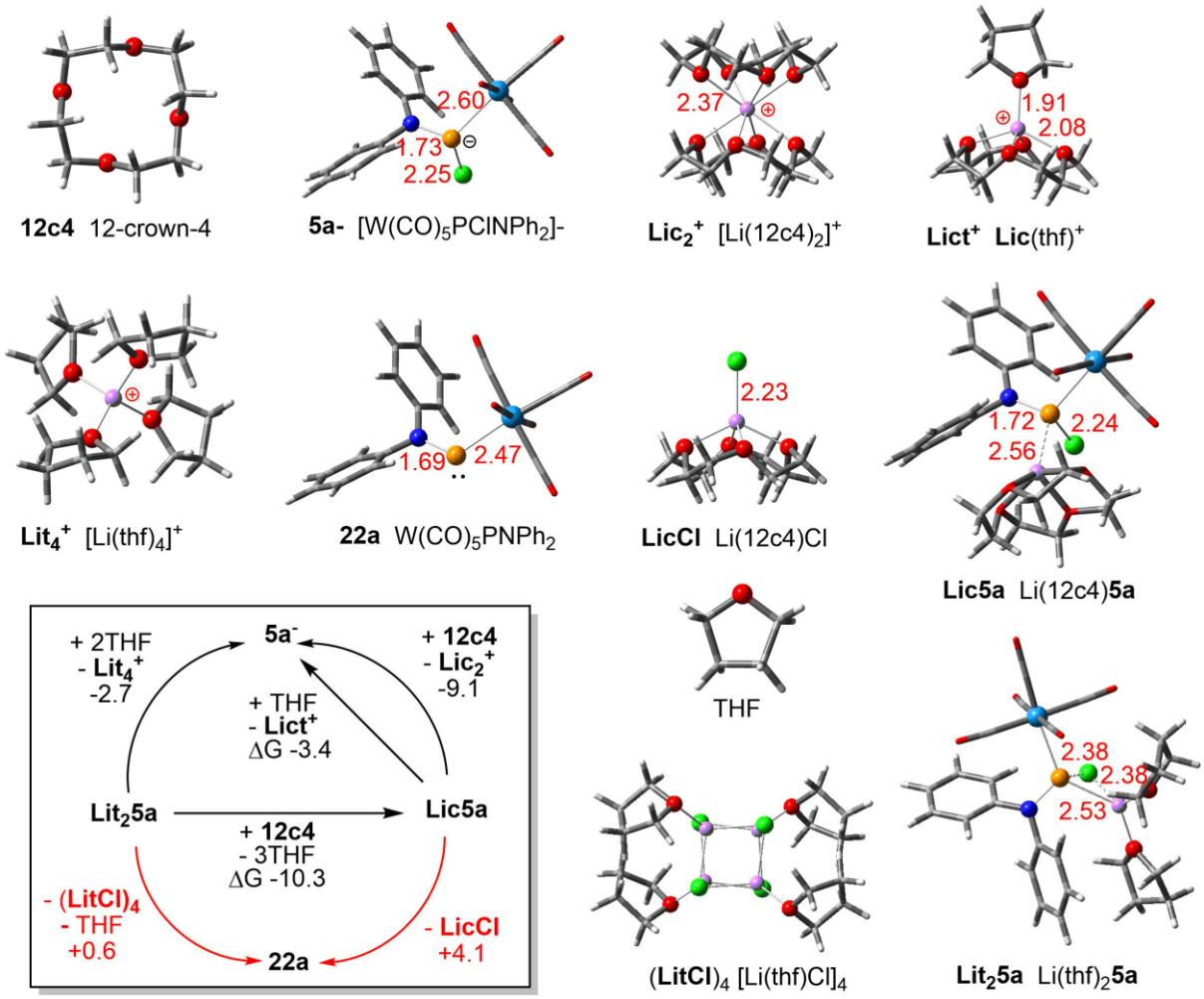

Figure 3.2.12 *DFT-optimized structures at the TPSS-D3/COSMO(THF)/def2-TZVP level. Crucial P, N, Cl, W, Li and O atoms are highlighted as orange, blue, green, cyan, violet and red balls; selected bond lengths are shown in Å. Reaction free energies are computed at the PW6B95-D3/COSMO-RS(THF)/def2-QZVP level (in kcal/mol, at 298 K and 1 mol/L reference concentration);* ***c/12c4****,* ***t*** *= 12-crown-4, THF.*

Following the lead of Espinosa,[60] the Li cation was calculated as differently solvated moiety with THF (**t**), 12-crown-4 (**c**) and Cl. Complex **5a** was optimized and calculated as a contact ion pair having a

separated Li cation unit. Even the terminal phosphinidene complex **22a,** having a chloride formally abstracted, was taken into account. Corresponding phosphinidene complex adducts were also investigated theoretically and reported recently.[112,113] In THF solution without strong coordination of 12-crown-4, the Li/Cl phosphinidenoid complex **5a** should exist as the separated ions of $[W(CO)_5P(Cl)NPh_2]^-$ (**5a$^-$**) and $[Li(thf)_4]^+$, which is 2.7 and 4.5 kcal/mol more stable than the P-Li contact ion-pair complexes $[Li(thf)_2][W(CO)_5P(Cl)NPh_2]$ (**Lit$_2$5a**) and $[Li(thf)_2][W(CO)_5P(Cl)NPh_2]$ (**Lit$_3$5a**), respectively. Surprisingly, the chloride transfer from **5a$^-$** to $[Li(thf)_4]^+$ via **Lit$_2$5a** is only 3.3 kcal/mol (**5a$^-$** → **Lit$_2$5a** (+2.7 kcal/mol) → **22a** (+0.6 kcal/mol)) endergonic to form the neutral, singlet-carbene-like phosphinidene complex $[W(CO)_5PNPh_2]$ (**22a**) along with tetrameric (**LitCl**)$_4$. This is consistent with the observed low thermal stability of complex **5a** in solution, compared to other Li/Cl phosphinidenoid complexes, having a low barrier to form the supposedly even more reactive phosphinidene complex **22a**. It is noteworthy that the N-P bond (1.69 Å, *Wiberg bond index* (WBI) 1.32) of **22a** is 0.04 Å shorter with an increased WBI of 1.32 than that of **5a$^-$** (1.73 Å, WBI 1.09), showing more double-bond nature due to N-electron-lone-pair donation into the empty P *3p* orbital (figure 3.2.13). It should be mentioned as well that the relative bond-shortening appears to be different for the P-N and P-W bonds with 0.04 and 0.22 Å, respectively. A theoretical study was report in 2017 regarding the phosphinidene complex adduct

The coordinating THF molecules in **Lit$_2$5a** can be replaced by a more strongly coordinating **12c4** ligand, with the resultant P-Li complex **Lic5a** being thermodynamically 10.3 kcal/mol more stable (**Lit$_2$5a** → **Lic5a** (10.3 kcal/mol)). In this case, elimination of **LicCl** from **Lic5a** is 4.1 kcal/mol endergonic forming complex **16a**. The formation of separated ion-pairs is even more favoured when 12-crown-4 is present. So complex **Lic5a** may react further with THF and **12c4**, eventually leading to the free anion **5a$^-$** along with the **Lict$^+$** and **Lic$_2^+$** cations that are 3.4 and 9.1 kcal/mol more stable in solution, respectively. When comparing with the **12c4**-stabilized cations [Li(**12c4**)(thf)]$^+$ (**Lict$^+$**) and [Li(**12c4**)$_2$]$^+$ (**Lic$_2$**) the solvated ion-pairs are 11.0 and 16.7 kcal/mol more stable (relative to **Lit$_2$5a**: **5a$^-$** + **Lict$^+$** (-13.7 kcal/mol); **5a$^-$** + **Lic$_2^+$** (-19.4 kcal/mol); **5a$^-$** + **Lit$_4^+$** (-2.7 kcal/mol)). The chloride transfers in these cases are now 7.5 and 13.2 kcal/mol endergonic to form the neutral complex **22a** (along with **LicCl** that does not oligomerize), respectively, matching the observation of **12c4**-enhanced thermal stability of Li/Cl phosphinidenoid complexes.

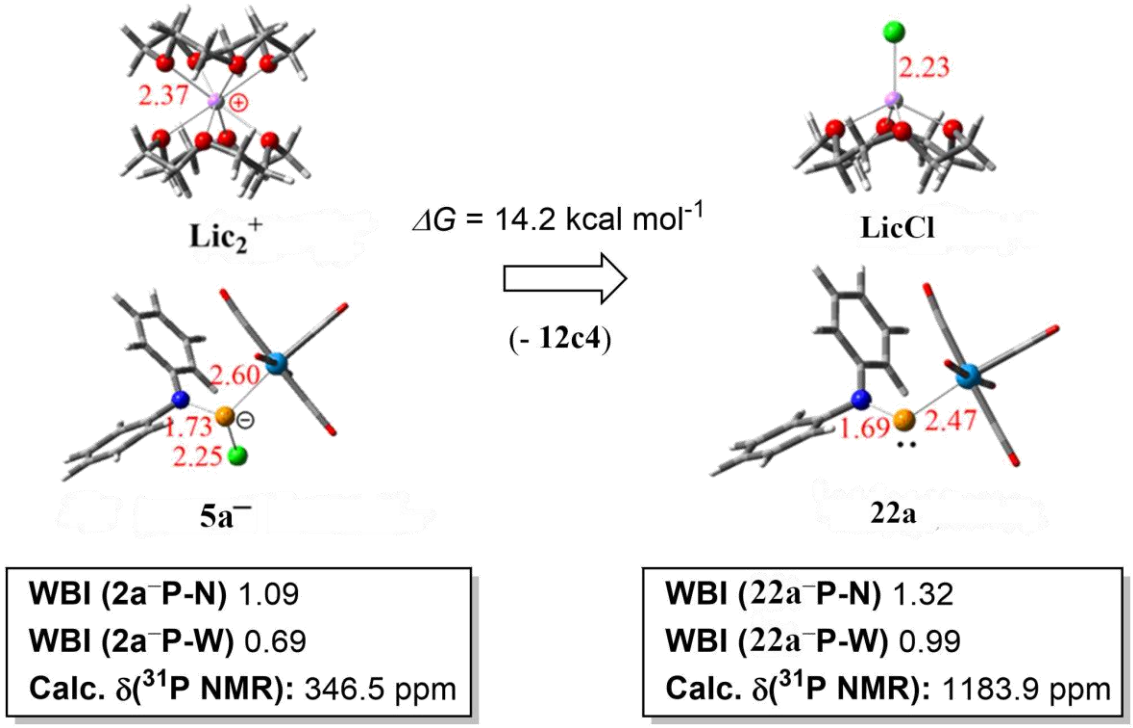

***Figure 3.2.13**. Free energy going from the solvent separated ions for complex **2a** to the “salt eliminated” phosphinidene complex **22a**. (Calculated Wiberg bond indices and ^{31}P NMR shifts are displayed in boxes).*

3.3 Trapping reactions of *P*-amino substituted Li/Cl phosphinidenoid complexes

Since it was not possible, in most cases, to get NMR spectroscopic evidence for the *in-situ* formed Li/Cl phosphinidenoid complexes **5-7**, trapping reactions were performed, first using methanol and then methylamine (scheme 3.3.1) as this has been shown before to be very effective.[63,67,68]

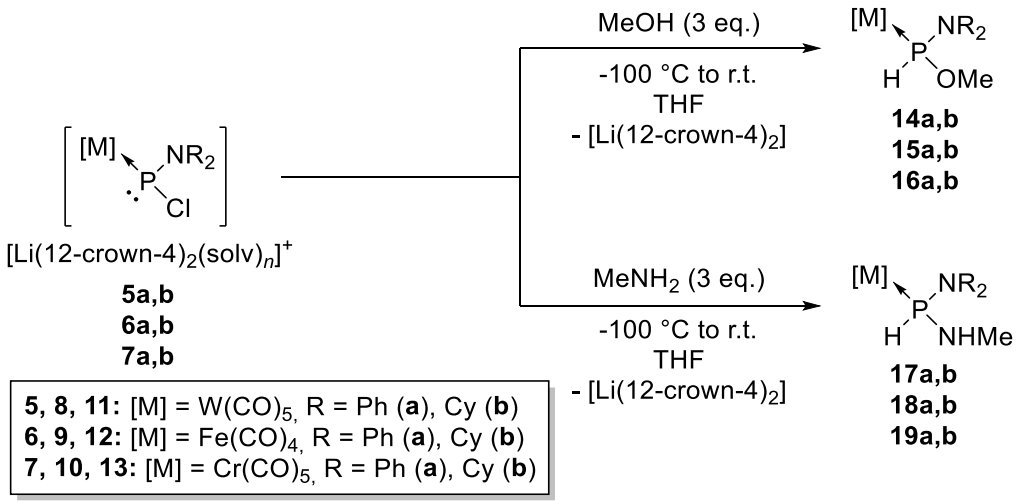

Scheme 3.3.1 *Trapping reactions of complexes* ***5-7*** *with MeOH and* $MeNH_2$.

In the reactions with methanol an excess (3-5 eq.) was added shortly (5 min) after the addition of ^{t}BuLi at -100 °C. Surprisingly, the reactions appeared not to be as selective as for the previously reported derivatives, which in most cases gave the alkoxyphosphane complexes almost quantitively.[60] The measured ^{31}P NMR spectra for complexes **14-16** are displayed in figure 3.3.1 with their corresponding NMR and IR data shown in table 3.3.1.

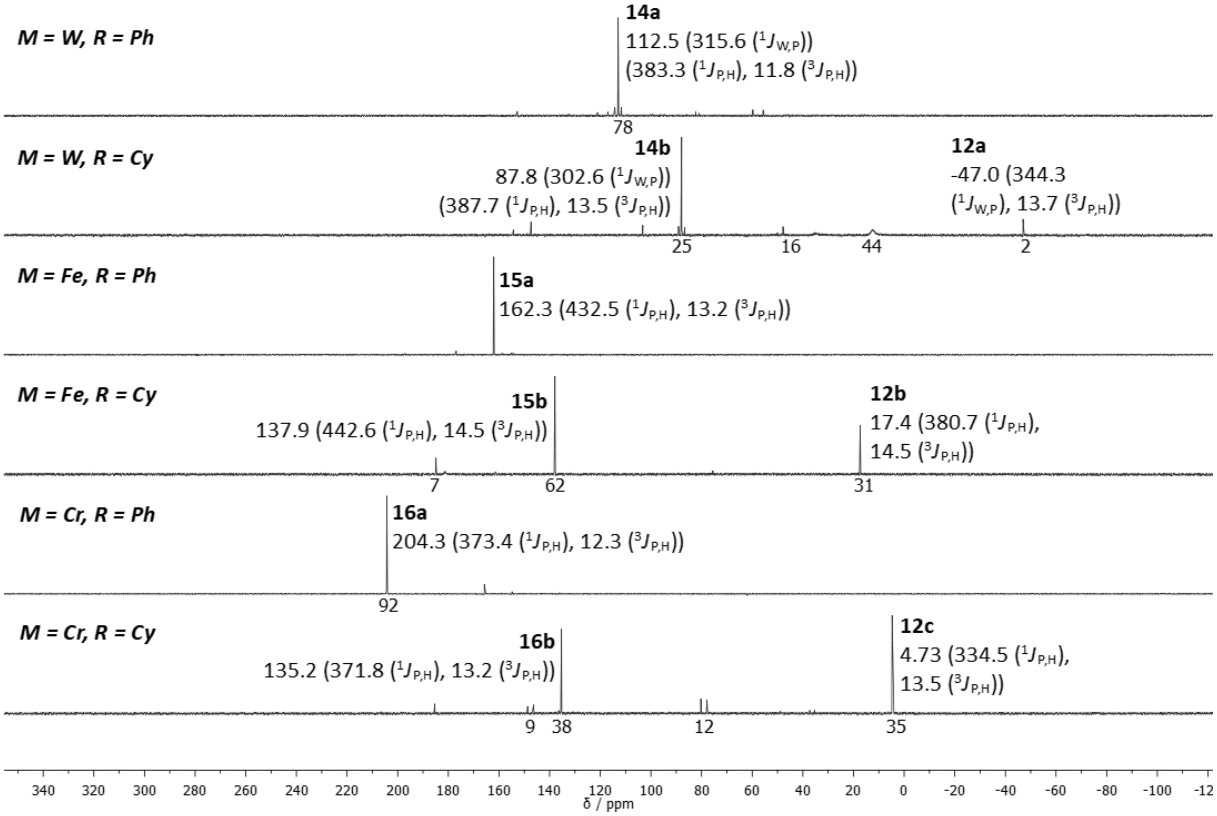

Figure 3.3.1 *$^{31}P\{^1H\}$ NMR spectra of the reaction mixtures of the trapping reaction of* ***5-7*** *with MeOH. (Given values in ppm with coupling constants in Hz for the element couple in brackets. Integration values are given in % below the baseline. P-H couplings were taken from the ^{31}P NMR spectrum).*

Table 3.3.1 *^{31}P NMR data for the trapping reactions with MeOH (scheme 3.3.1).*

	δ ^{31}P NMR ($^1J_{W,P}$) / ppm (Hz)	$^1J_{P,H}$ / Hz (^{31}P NMR)	$^3J_{P,H}$ / Hz (^{31}P NMR)
14a[a]	112.5 (315.6)	383.3 (d)	11.8 (q)
14b[b]	87.8 (302.6)	387.7 (d)	13.5 (q)
15a[a]	162.3	432.5 (d)	13.2 (q)
15b[b]	137.9	442.6 (d)	14.5 (q)
16a[b]	204.3	373.4 (d)	12.3 (q)
16b[b]	135.3	371.8 (d)	13.2 (q)
[W]P(H)(O^{i}Pr)CPh$_3$[60]	115.2 (278.5)	329.3 (d)	-

[a]C_6D_6; [b]THF

Table 3.3.2 *IR frequencies (experimental and calculated**) and yields for the trapping reactions with MeOH (scheme 3.3.1).*

	IR (exp) / cm^{-1}	IR (calc) / cm^{-1}	Yield / %
14a	1908, 2075, 2661	1913.1, 2061.4, 2415.8, 3001.8, 3153.7,	54
14b	-	1902.3, 2054.2, 2390.5, 3023.5	24*
15a	1921, 2054, 2585	1942.0, 2046.9, 2415.84, 3001.76, 3150.05	5
15b	-	1931.1, 2039.7, 2408.6, 3023.5,	45*
16a	-	1920.3, 2057.8, 2415.8, 3001.8, 3150.1	88*
16b	-	1913.1, 2054.2, 2390.5, 3019.8	35*

* via ^{31}P NMR integration from the reaction mixture; **TPSS-D3/CPCM(THF)/def2-TZVP

In the ^{31}P NMR spectra signals of complexes **14-16** can be found at a wide range of 87.8 – 204 ppm, the highest and lowest being **14b** and **15a**, respectively. All complexes display a very characteristic signal in the ^{31}P NMR spectra showing various P-H couplings such as the $^{1}J_{P,H}$ (range: 371 - 442 Hz) and $^{3}J_{P,H}$ (range: 11 - 14 ppm), which also matches literature data reported for complex [W]P(H)($O^{i}Pr$)CPh_3.[60] As for these complexes the *P*-amino substituent causes larger P-W and P-H coupling constants, 11 % (for $^{1}J_{P,W}$ average) and 21 % (for $^{1}J_{P,H}$ average). Problematic was that results were not always reproducible, especially the selectivity, but there were also problems during the work-up procedures, such as during column chromatography, presumably due to compound instability.

In general, very similar side products appeared in all reactions and, as an example, the ^{31}P NMR spectrum of the reaction of **7b** is displayed larger in figure 3.3.2.

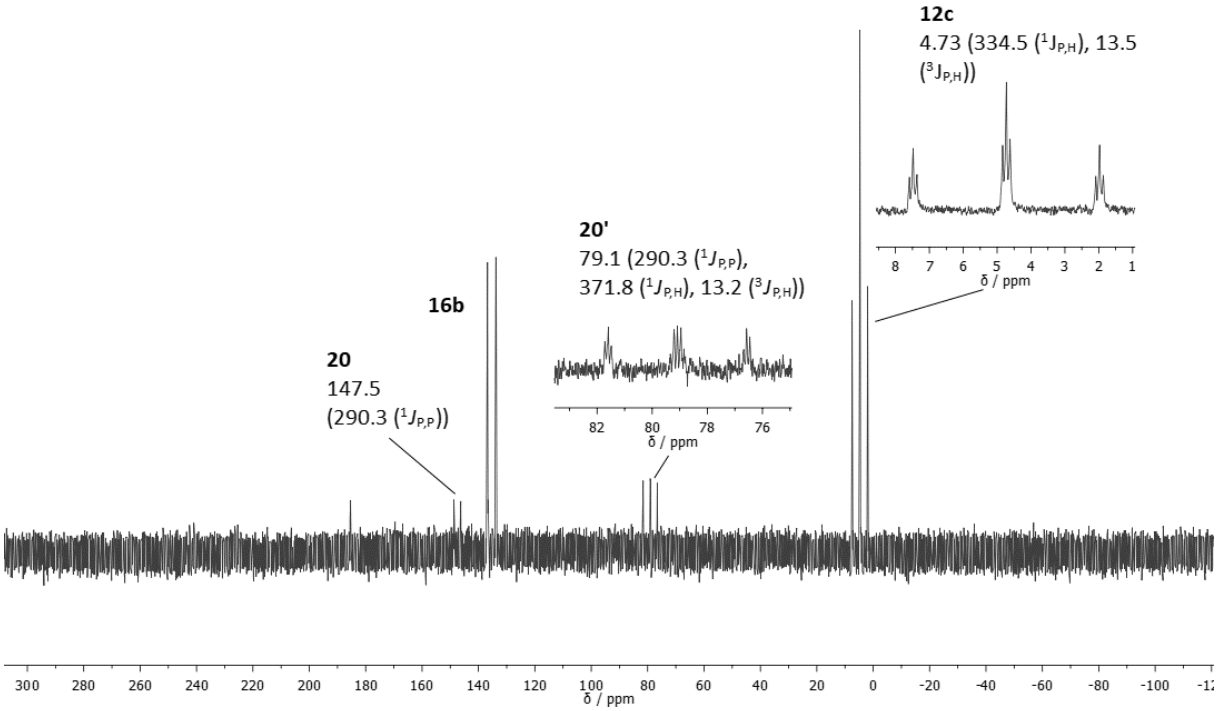

Figure 3.3.2. *^{31}P NMR spectrum of the reaction mixture of **7b**. (Given values in ppm with coupling constants in Hz for the element couple in brackets. Integration values are given in % below the baseline. P-H couplings were taken from the ^{31}P NMR spectrum).*

Due to some characteristic coupling patterns and constants in the ^{31}P NMR spectra the side products can be structurally assigned to complexes **12c** and **20** (figure 3.3.3). Again, the side product **12(c)** (figure 3.2.5) can be seen in all reactions of *P*-NCy_2 substituted complexes (**14b, 15b** and **16b)**. The other main side-product appears to be an asymmetrical diphosphane complex **15** with a visible $^1J_{P,P}$ coupling and the more high-field shifted phosphorus bearing a hydrogen atom. The low-field shift of the second phosphorus makes a chloride the most likely substituent. They can also be seen in case of **14a,b**.

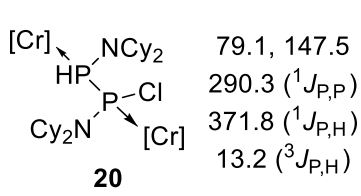

20

79.1, 147.5
290.3 ($^1J_{P,P}$)
371.8 ($^1J_{P,H}$)
13.2 ($^3J_{P,H}$)

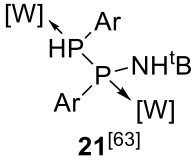

21[63]

4.8, 38.8
103.4 ($^1J_{P,P}$)
220.3, 268.0 ($^1J_{W,P}$)
327.2 ($^1J_{P,H}$)

Figure 3.3.3*. Side-products of the reaction of phosphinidenoid complex **7b** with MeOH in the reaction mixture (figure 3.3.2), along with literature known related compounds. (^{31}P NMR shifts are given in ppm with the corresponding coupling constant in Hz in brackets).*

In the end, only complexes **14a** and **15a** could be isolated. Whereas complex **14a** could only be isolated as a rather crude product via extraction with Et_2O, a small amount of complex **15a** was isolated via extraction with E_2O as a red oil (figure 3.3.4). The obtained IR spectra of complexes **14-16** showed the expected absorptions due to CO stretch vibrations in the region of 1908 – 2075 cm^{-1} fitting the calculated IR frequencies for CO stretch vibrations (1902.3 – 2061.4 cm^{-1}) (table 3.3.2). The absorption of the PH stretch vibrations can also be found at 2661 (**14a**) and 2585 (**15a**).

Moreover, single crystals of **15a** could be obtained from a Et_2O solution in the fridge and measured via X-ray diffraction analysis. The obtained crystal structure is displayed in figure 3.3.4 with its crystallographic data listed in table 3.3.2.

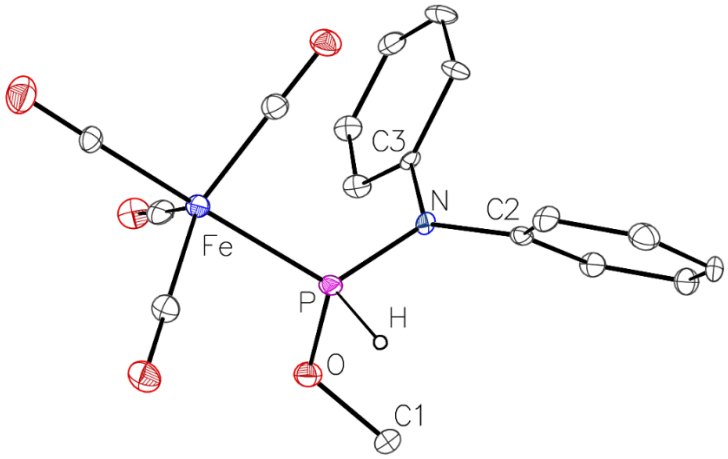

Figure 3.3.4 *Molecular structure of* ***15a****. The ellipsoids were set to 50 % possibility and hydrogen atoms have been omitted (except for PH). The relevant bond lengths and angles are displayed in table 3.3.2.*

To obtain insight into the structures of all derivatives **14-16**, especially those for which no X-ray diffraction analysis data were obtained, calculations at the following level of theory (TPSS-D3/CPCM(THF)/def2-TZVP//PW6B95-D3/CPCM(THF)/def2-QZVP) were performed, and the selected structural details and bonding parameters listed below (table 3.3.2). For comparison complex $[W(CO)_5P(H)(OMe)CPh_3]$ (**14-CPh$_3$**) was calculated as well.

Table 3.3.2 *Bond lengths and angles obtained by X-ray diffraction studies and calculations* for complexes* ***14-16****.*

	d(M-P) (exp) / Å	d(M-P) (calc) / Å	d(P-N) (exp) / Å	d(P-N) (calc) / Å	d(P-O) (exp) / Å	d(P-O) d(P-H) (calc) / Å	Σ(<N) (exp) / °	Σ (<N) (calc) / °
14a	-	2.494	-	1.706	-	1.631 1.410	-	360.0
14b	-	2.524	-	1.672	-	1.638 1.413	-	360.0
15a	2.181(3)	2.187	1.686(8)	1.707	1.620(8)	1.630 1.409	357.5	359.9
15b	-	2.213	-	1.664	-	1.636 1.410	-	359.0
16a	-	2.320	-	1.707	-	1.632 1.410	-	360.0
16b	-	2.348	-	1.668	-	1.644 1.412	-	359.8
14-CPh$_3$	-	2.531	-	1.915 (P-C)	-	1.638 1.417	-	441.0 (C)
[W]P(H)(O^{i}Pr)CPh$_3$ [60]	2.524(7)	-	1.913(3) (P-C)	-	1.608(2)	-	-	-

*TPSS-D3/CPCM(THF)/def2-TZVP.

The obtained crystallographic data for complex **15a** are in the expected range, very well matching the computed structural data. Again, in all cases of *P*-amino substitution a much shorter computed P-R bond was obtained, with an average of 1.69 Å for the P-N bond (1.706 Å for **2a**), compared to 1.915 Å for *P*-CPh$_3$, which in general for these complexes displays a rather long P-C bond.[60] Also, a planar

nitrogen could be found for all cases with an angle sum close to 360 ° for calculated and crystal data. It is to mention, that there is (very) little change regarding the P-O bond length between alkyl- and amino-substitution.

Table 3.3.3 *Computed* MBO (Mayer bond order) values, Loewdin charges (q^L) and HOMO-LUMO energy gaps for complexes* ***14-16****.*

	MBO(P-M)	MBO(P-N)	MBO(P-O) (P-H)	$q^L(M(CO)_n)$	$q^L(P)$	$q^L(N)$	$\lvert\Delta E_{HOMO-LUMO}\rvert$ / eV
14a	0.618	1.083	1.099 0.948	-0.432	0.347	0.294	4.80
14b	0.676	1.175	1.090 0.930	-0.494	0.324	0.278	4.85
15a	0.814	1.081	1.097 0.940	-0.620	0.430	0.310	5.61
15b	0.725	1.156	1.098 0.923	-0.700	0.406	0.299	5.65
16a	0.461	1.111	1.097 0.954	-0.610	0.442	0.304	5.30
16b	0.536	1.267	1.058 0.928	-0.662	0.423	0.293	5.66
14-CPh_3	0.487	0.931 (P-C)	1.090 0.897	-0.437	0.523	-0.218 (C)	4.90

*PW6B95-D3/CPCM(THF)/def2-QZVP.

The bond orders for the P-M bond are in the range of 0.461 (**16a**) to 0.814 (**15a**) with the chromium and iron complexes again displaying the lowest and highest MBO(P-M), respectively. The P-N bond orders are on average 23 % higher in comparison with **14-CPh_3** (P-C) showing values from 1.081 (**14a**) to 1.267 (**16b**). Again, derivatives having the NCy_2 substituent show higher bond orders regarding the

P-N bond, which is expected. Also, the average order of the P-N bond is smaller for complexes **14-16** than for complexes **2-4**.

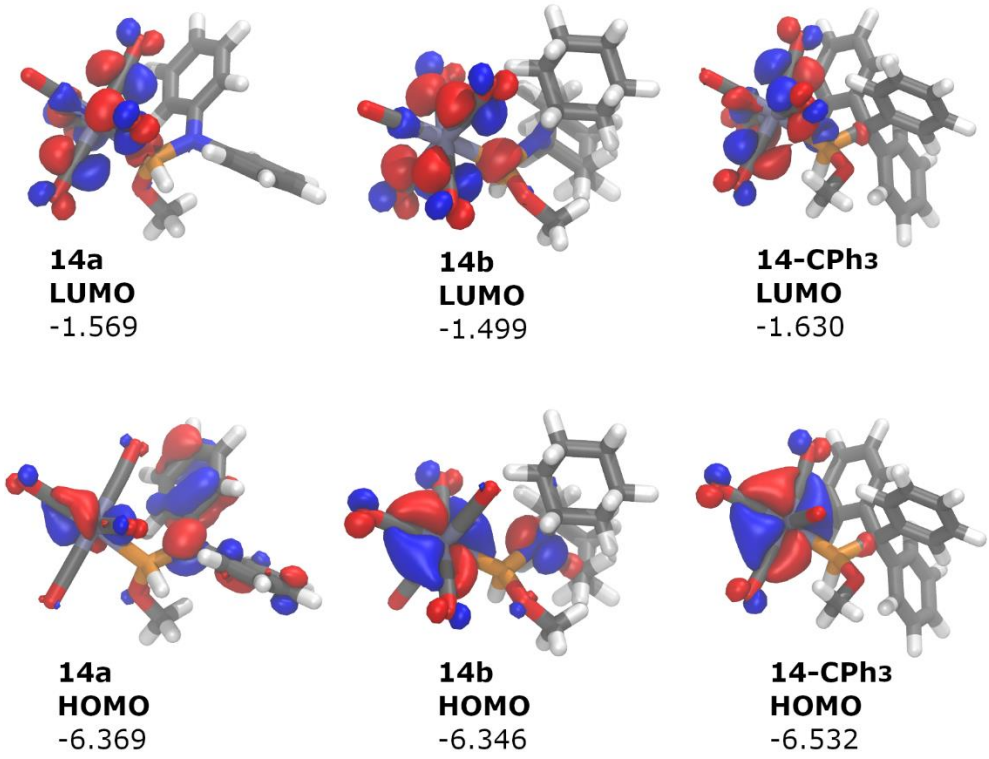

Figure 3.3.5 *Calculated HOMO and LUMO frontier orbitals of complex* ***14a,b*** *and for comparison* ***14-CPh₃*** *at the TPSS-D3/CPCM(THF)/def2-TZVP// PW6B95-D3/CPCM(THF)/def2-QZVP level of theory (a = ±0.04); energy values are given in eV.*

Tungsten complexes **14a,b** and **14-CPh₃** are displayed in figure 3.3.5 to visualize the differences regarding frontier orbital contributions. Surprisingly visible differences not only occur between amino- and trityl-substitution but also between NPh_2 (**a**) and NCy_2 (**b**). In **14a** the HOMO is almost completely located at the $W(CO)_5$-fragment, whereas for **14a,b** strong contributions from the N can be seen. Surprisingly, for **14a** suddenly the HOMO is mainly localized at the NPh_2-group with only small contributions from the $W(CO)_5$-fragment, which is something that could not be observed in this extend for example for the amino-substituted dichlorophosphane complex **2a** (figure 3.1.6). The HOMO LUMO gaps are rather similar in all cases with 4.80, 4.85 and 4.90 eV for **14a,b** and **CPh₃**, respectively. The HOMO-1 and LUMO+1 are almost completely localized around the $W(CO)_5$-group for all cases.

The next trapping reaction was done with $MeNH_2$ (scheme 3.3.1) which, many times before, has displayed almost quantitative reactions to give the N-H bond insertion product complexes.[77,78] It was

also added in an excess shortly (5 min) after the addition of ^{t}BuLi at low temperature (scheme 3.3.1). The outcome for the reactions can be seen in figure 3.3.6.

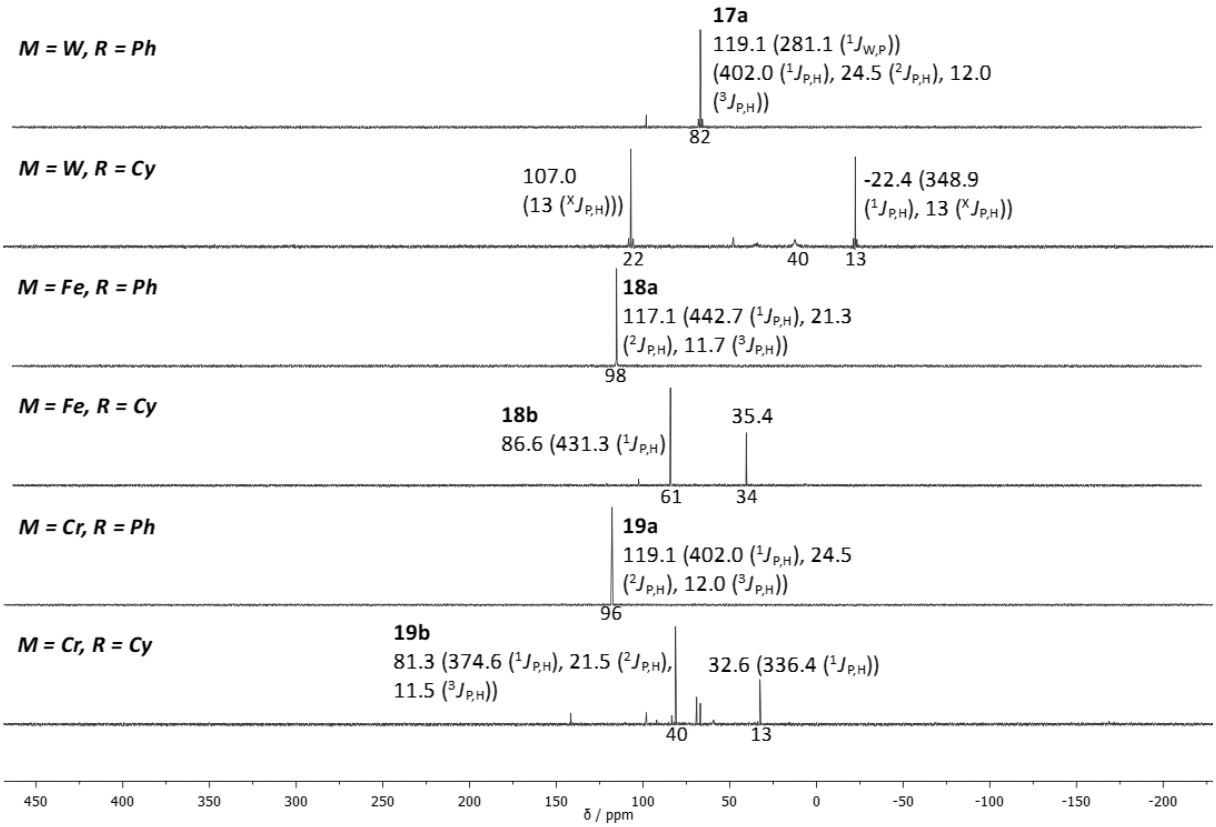

Figure 3.3.6 *$^{31}P\{^{1}H\}$ NMR spectra of the reaction mixtures of the trapping reaction of **5-7** with $MeNH_2$. (Given values in ppm with coupling constants in Hz for the element couple in brackets. Integration values are given in % below the baseline. P-H couplings were taken from the ^{31}P NMR spectrum).*

Signals of the corresponding N-H-insertion products (table 3.3.4) were measured in the range of 67.6 – 119.1 ppm in the $^{31}P\{^{1}H\}$ NMR spectra. All observed complexes display a very characteristic signal splitting (ddq) in the ^{31}P NMR spectra where the corresponding P-H coupling can be found with $^{1}J_{P,H}$ 374 – 443 Hz, $^{2}J_{P,H}$ 21 – 25 Hz and $^{3}J_{P,H}$ 11 – 12 Hz, matching the literature known NH-insertion products.[77.78] Surprisingly, the reaction mixture of **5b** showed no signal fitting the expected coupling pattern, yet two main signals at 107.0 and -22.4 ppm, along with some strongly broadened signals at around 12 and 35 ppm. The main signals show some hardly distinguishable splitting in the ^{31}P NMR spectra due to broadening, yet a triplet with a $^{1}J_{P,H}$ of 348.9 Hz could be seen for the signal at -22.4 ppm. Since the shift is far too different from **12a** for solvent effects, it gives some evidence for the cleavage of the former P-N bond. A rather unselective reaction was observed in case of **19b** with only 40 % of the expected product formed and some side products, being in the region of previously observed symmetrical diphosphane complexes (figure 3.3.3).

The obtained IR spectra show the expected absorptions from the CO stretch vibrations in the region 1895 – 2065 cm^{-1} being in good agreement with the calculated IR frequencies for CO stretch vibrations (1902.3 – 2061.4 cm^{-1}) (table 3.3.5).

For all NPh_2 (**a**) cases rather selective reactions could be obtained. **17a**, **18a**,**b** and **19a** could be isolated via extraction (**17a**, **18a**, **19a**) or via filtration through solid phase (**18b**) and were characterized by NMR, MS, IR and EA (**18a,b 19a**).

Table 3.3.4 *^{31}P NMR data and yields for the trapping reactions with $MeNH_2$ (scheme 3.3.1).*

	δ ^{31}P NMR ($^{1}J_{W,P}$) / ppm (Hz)	$^{1}J_{P,H}$ / Hz (^{31}P NMR)	$^{2}J_{P,H}$ / Hz (^{31}P NMR)	$^{3}J_{P,H}$ / Hz (^{31}P NMR)
17a[a]	67.6 (281.1)	407.0 (d)	22.1 (d)	11.1 (q)
17b	-	-	-	-
18a[a]	117.1	442.7 (d)	21.3 (d)	11.7 (q)
18b[a]	86.6	431.3 (d)	-[c]	-[c]
19a[a]	119.1	402.0 (d)	24.5 (d)	12.0 (q)
19b[b]	81.3	374.6 (d)	21.5 (d)	11.5 (q)

[a]C_6D_6; [b]THF, [c]not distinguishable

Table 3.3.5 *IR frequencies (experimental and calculated*) for complexes* ***17-19*** *(scheme 3.3.1).*

	IR (exp) / cm^{-1}	IR (calc) / cm^{-1}	Yield / %
17a[a]	1901, 1982, 2071, 2861, 3320	1909.5, 2061.4, 2477.3, 2987.3, 3153.7	59
17b	-	1902.3, 2054.2, 2423.1, 3016.2, 3468.3	-
18a[a]	1913, 1975, 2051, 2368, 3411	1934.8, 2043.3, 2473.7, 2976.4, 3066.9, 3150.1, 3486.4	29
18b[a]	1895, 1934, 2039, 2362, 2854, 3419, 3438	1924.0, 2036.1, 2455.6, 3023.5, 3472.0	8
19a[a]	1904, 1986, 2065, 2929, 3427	1916.7, 2054.2, 2470.1, 2987.3, 3153.7, 3482.8	28
19b[b]	-	1909.5, 2050.5, 2423.1, 3019.8, 3464.7	42**

*TPSS-D3/CPCM(THF)/def2-TZVP, ** via ^{31}P NMR integration from the reaction mixture.

Furthermore, complexes **18a** and **19a** could be crystallized and single crystals measured via X-ray diffraction. The obtained crystal structures confirm the connectivity and are displayed in figures 3.3.7 – 3.3.8 with their crystallographic data listed in table 3.3.5.

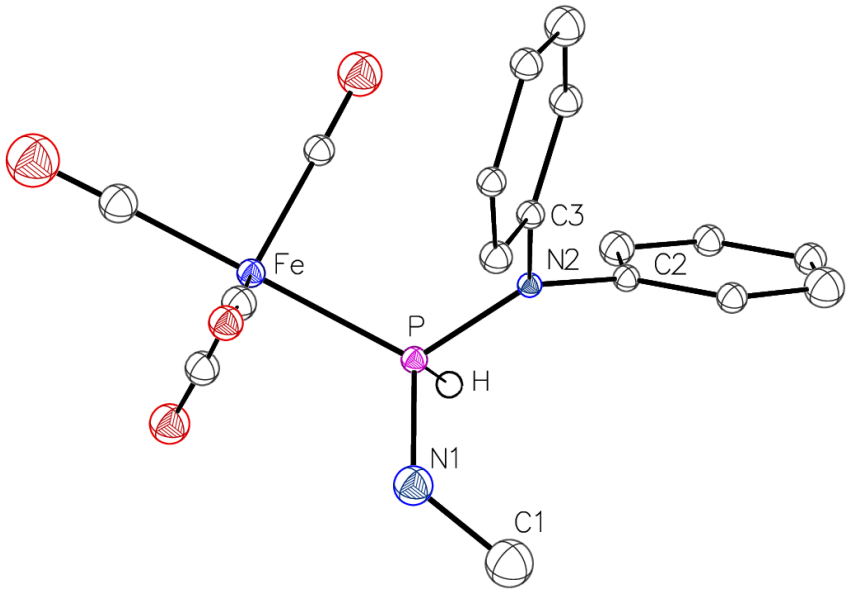

Figure 3.3.7 *Molecular structure of* ***18a*** *in the crystal. The ellipsoids were set to 50 % possibility and hydrogen atoms have been omitted (except for PH).*

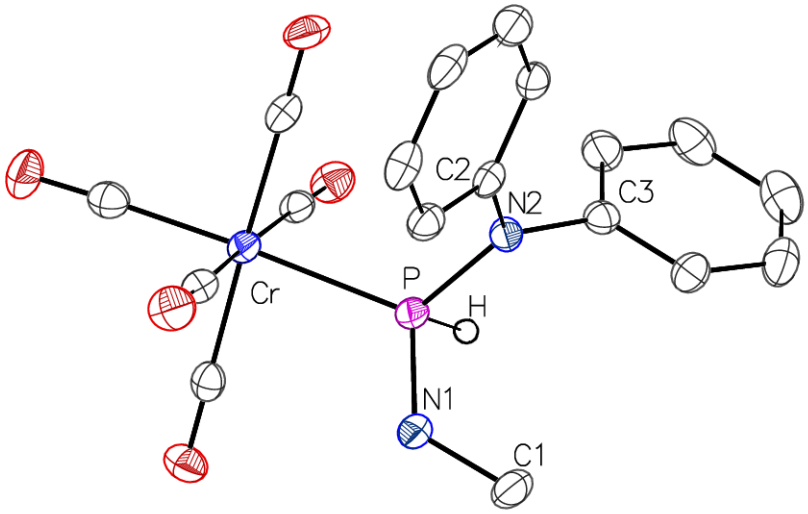

Figure 3.3.8 *Molecular structure of* ***19a*** *in the crystal. The ellipsoids were set to 50 % possibility and hydrogen atoms have been omitted (except for PH).*

Table 3.3.6 *Bond lengths and angles obtained by X-ray diffraction studies and calculations* for complexes* ***17-19****.*

	d(M-P) (exp) / Å	d(M-P) (calc) / Å	d(P-N) (exp) / Å	d(P-N) (calc) / Å	d(P-*N*H) (exp) / Å	d(P-*N*H) d(P-H) (calc) / Å	Σ(<N) (exp) / °	Σ (<N) (calc) / °
17a	-	2.494	-	1.706	-	1.631 1.410	-	360.0
17b	-	2.551	-	1.682	-	1.697 1.407	-	359.4
18a	2.2046(5)	2.216	1.6932(15)	1.728	1.6462(17)	1.677 1.401	359.8	359.5
18b	-	2.236	-	1.677	-	1.695 1.403	-	359.8
19a	2.3331(9)	2.366	1.716(2)	1.732	1.654(3)	1.677 1.402	359.8	359.3
19b	-	2.383	-	1.684	-	1.698 1.407	-	359.4
17-CPh_3	-	2.556	-	1.945 (P-C)	-	1.679 1.408	-	-

*TPSS-D3/CPCM(THF)/def2-TZVP.

The obtained crystallographic data for complexes **18a** and **19a** are in the expected range and in good agreement with the computed structural data (< 1 % average deviation). Again, in all cases of amino-substitution a much shorter P-R bond was observed, with a computed average of 1.702 Å (1.945 Å for **17-CPh_3**), which is a decrease of 12.5 %. This, together with the planar N-environment, points to the π-donation of the N atom to the P atom yielding partial double bond character. In all of these cases the *P-N*Ph_2 bonds appear to be the longest due to the lower π-backbonding of the N, compared to NCy_2 and NHMe, where the P-NCy_2 bonds appear to have the strongest P-N interaction and therefore

the shortest bonds (d(*P*-*N*Ph_2) > d(*P*-*N*HMe) > d(*P*-*N*Cy_2)). Bond orders, HOMO-LUMO energy gaps and partial charges are displayed in table 3.3.7.

Table 3.3.7 *Computed* MBO (Mayer bond order) values, Loewdin charges (q^L) and HOMO-LUMO energy gaps for complexes* ***17-19****.*

	MBO(P-M)	MBO(P-N)	MBO(P-*N*H) (P-H)	$q^L(M(CO)_n)$	$q^L(P)$	$q^L(N)$	$\lvert\Delta E_{HOMO-LUMO}\rvert$ / eV
17a	0.509	0.950	1.155 0.980	-0.454	0.473	0.287	4.64
17b	0.512	1.168	1.090 0.953	-0.493	0.434	0.277	4.87
18a	0.708	0.990	1.188 0.966	-0.658	0.555	0.303	5.42
18b	0.660	1.173	1.098 0.928	-0,720	0.526	0.295	5.79
19a	0.657	0.969	1.178 0.980	-0.646	0.568	0.297	5.08
19b	0.644	1.177	1.079 0.950	-0,687	0.531	0.287	5.54
17-CPh_3	0.436	0.859 (P-C)	1.096 0.930	-0.462	0.627	-0.219 (C)	4.75

*PW6B95-D3/CPCM(THF)/def2-QZVP.

The bond orders for the P-M bond appear in a range of 0.509 (**17a**) to 0.708 (**18a**), which is a much smaller region than for complexes **14-16** (0.461 – 0.814). The bond orders again display the different strength in π-backbonding of the different nitrogen atoms, with bond orders showing the same trend *P*-*N*Cy_2 > *P*-*N*HMe > *P*-*N*Ph_2. All the other values regarding partial charges and HOMO-LUMO energy gaps are quite similar to the OH-insertion products **8-10**, besides the Loewdin charges at phosphorus.

Here a significant increase of partial charge q^L(P) can be seen overall from 0.395 **(14-16**) to 0.514 (30 % increase)**,** indicating an electron rich phosphorus.

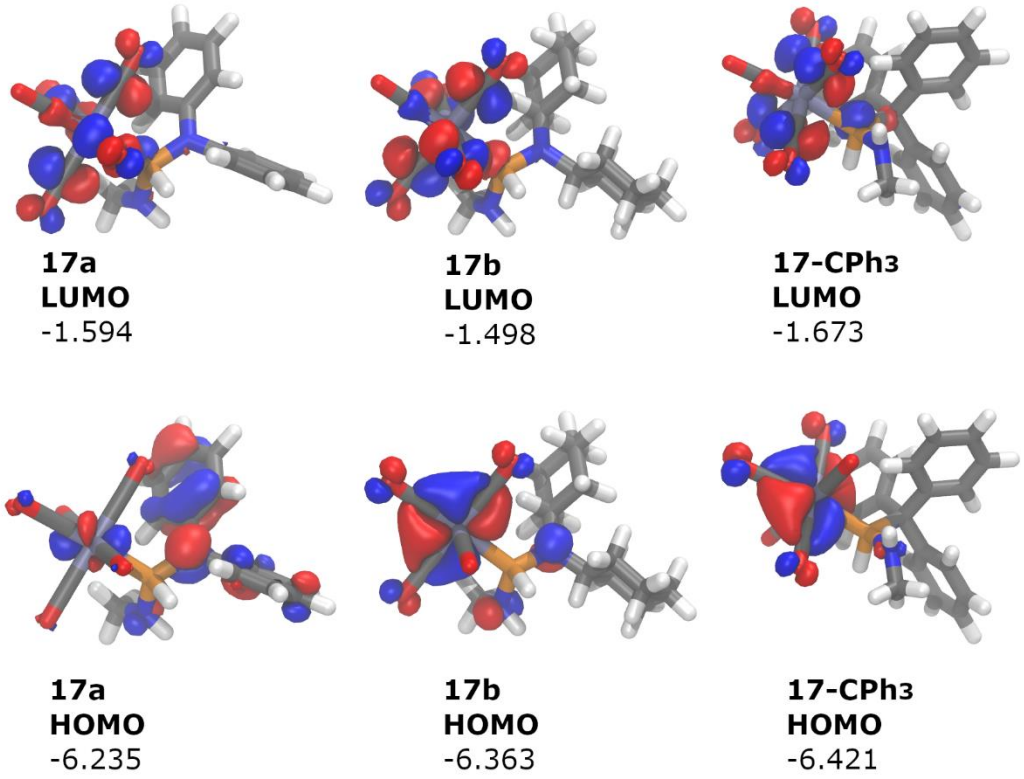

Figure 3.3.9 *Calculated HOMO and LUMO frontier orbitals of complex* ***17a,b*** *and for comparison* ***17-CPh₃*** *at the TPSS-D3/CPCM(THF)/def2-TZVP//PW6B95-D3/CPCM(THF)/def2-QZVP level of theory (a = ±0.04); energy values are given in eV.*

Tungsten complexes **17a,b** and **17-CPh₃** are displayed in figure 3.3.9 to visualize the differences regarding frontier orbital contributions. Surprisingly visible differences not only occur between amino- and trityl-substitution but also between NPh_2 (**a**) and NCy_2 (**b**). Again, the Ph rings contribute strongly towards the HOMO in addition to the nitrogen atom (s. **14a**, figure 3.3.6), with only little localization at the $W(CO)_5$ moiety. This again stands in strong contrast to **17b** and **17-CPh₃** with their HOMOs being largely $W(CO)_5$ centred. For **17b** also some involvement from the two nitrogen atoms can be seen, most probably with their lone pairs. The HOMO LUMO energy gaps are rather large yet very similar for all three cases with 4.64, 4.87 and 4.57 eV for **17a,b** and **17-CPh₃**, respectively.

3.4 Generation and trapping reactions of *P*-amino substituted terminal phosphinidene complexes

When remembering the fact, that a Li/Cl phosphinidenoid complex is formally an addition product of LiCl and a terminal phosphinidene complex,[112] the discussed destabilization of the P-Cl bond(s) due to the amino substitution seems to present an interesting and promising starting point for the synthesis of *P*-amino substituted terminal phosphinidene complexes. Moreover, it is known from the literature that amino substitution is stabilizing low-valent species such as phosphinidene complexes due to the π-donation from the N lone-pair towards the vacant orbital of the low-coordinate and -valent phosphorus center.[49,50]

As it was established before (see chapter 3.2), that *P*-amino substituted Li/Cl phosphinidenoid complexes **5a,b** are not only thermally more labile but also in need of higher amount of stabilization through two equivalents of 12-crown-4. Taking the pronounced ^{31}P NMR downfield shift into account, *e.g.*, compared to CPh_3-substitution, it may provide already some evidence that *P*-amino substitution starts to blur the line between Li/Cl phosphinidenoid and phosphinidene complexes in general.

As the first step of all reactions described beforehand was the addition of ^{t}BuLi to achieve the Li/Cl exchange forming the corresponding Li/Cl phosphinidenoid complex **5a,b**. So the idea was now to react complexes **2a,b** with ^{t}BuLi in an (apolar or) low-polar solvent such as toluene without 12-crown-4 in order to force the Li cation into close vicinity of the phosphorus and chlorine atoms, *i.e.* to avoid formation of separated ion pairs. Therefore, a loss of LiCl should be much more favoured, thus forming the terminal phosphinidene complexes **22a,b** (scheme 3.4.1).

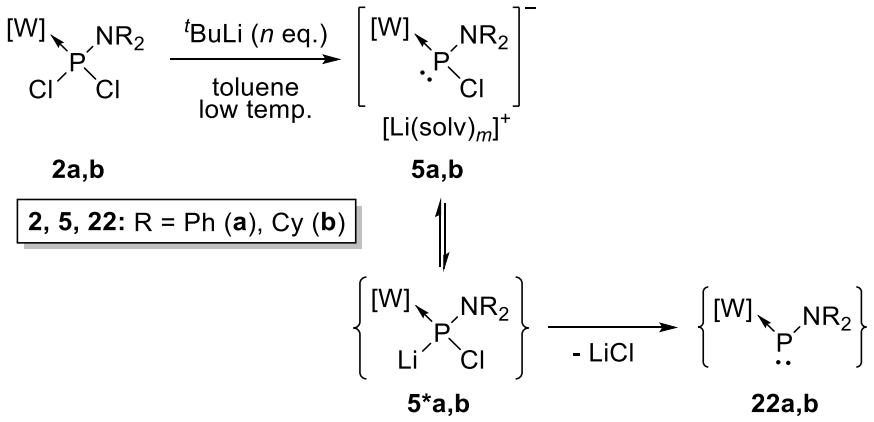

Scheme 3.4.1 *Plan to generate transient terminal phosphinidene complexes **16a,b**.*

The first parameter to investigate was the temperature of the reaction. This was first investigated using complex **2a** with a solvent having a lower polarity than Et_2O and THF which were formerly used. The

addition of ^{t}BuLi was done either at room temperature or at -80 °C in toluene, but this resulted in very little differences in the obtained NMR spectrum of the reaction mixture (Figure 3.4.1). So, the reaction was repeated at lower temperature (-120 °C) in ^{n}pentane, of course due to the temperature toluene was naturally eliminated as a possible solvent (m.p. (toluene) -95 °C).

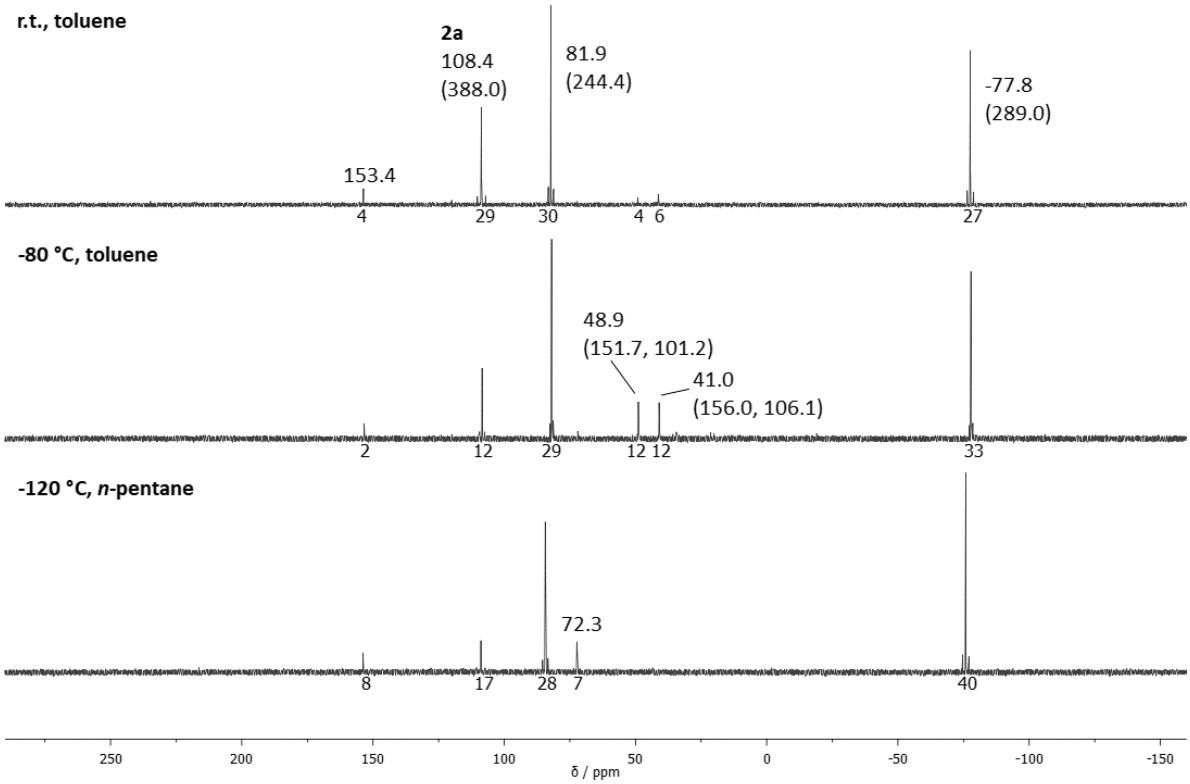

Figure 3.4.1 *$^{31}P\{^{1}H\}$ NMR spectra of the reaction mixtures of **2a** with ^{t}BuLi in weakly polar solvents, with the addition of ^{t}BuLi at different temperatures. (Given values in ppm with the $^{1}J_{W,P}$ coupling constant in Hz in brackets. Integration values are given in % below the baseline).*

Surprisingly, it appeared that the temperature had little impact on the outcome of the reaction. Not only are the same signals visible, they also appear in very similar ratios of the reaction mixture, giving evidence for a very fast reaction. In all cases some starting material **2a** remained unreacted (12 (-80 °C) to 29 % (r.t.)) with main products visible at 81.9 (~30 %) and -77.8 ppm (27 (r.t.) to 40 % (-120 °C). The rather small $^{1}J_{W,P}$ coupling constants (in comparison with complexes **2**) indicate alkyl/H substit-uents at the P centre, possibly even without the amino-substituent. For a better overview of the pro-duct spectrum, the ^{31}P NMR spectrum of the reaction done at -80 °C is displayed in figure 3.4.2.

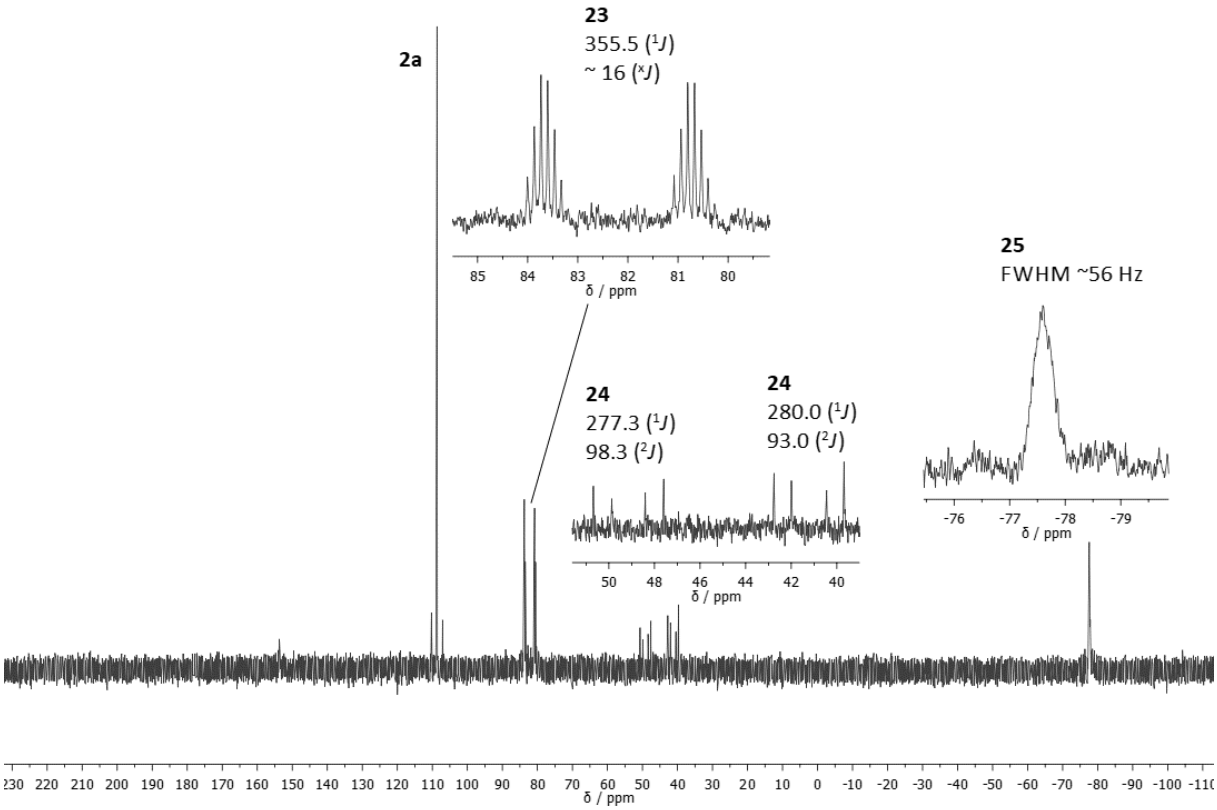

Figure 3.4.2 *^{31}P NMR spectrum of the reaction mixture of **2a** with ^{t}BuLi in toluene at r.t. (done at -80 °C). (Given values in ppm with $^{x}J_{P,H}$ coupling constants given in Hz with x in brackets).*

The first aspect to mention is that a reaction with the solvent is out of the question, since the control reaction in C_6D_6 displayed the same outcome. This leaves the added ^{t}BuLi also as a possible hydride source, and its further reacted species ^{t}BuCl and ^{i}Butene, as formal HCl source and possible cycloaddition educt, respectively. The signal at 81.9 ppm shows a $^{1}J_{P,H}$ = 355.5 Hz with further splitting, usually seen for *P*-^{t}Bu substitution, and could belong to compound **23** (figure 3.4.3).[68] The two signals at 48.9 and 41.0 ppm could be assigned to two stereoisomers of the symmetrical diphosphane complex **24** due to their characteristic two P-W and two P-H couplings. Further confirmation could be obtained through simulations of one of the signals with *gNMR* (figure 3.4.3)

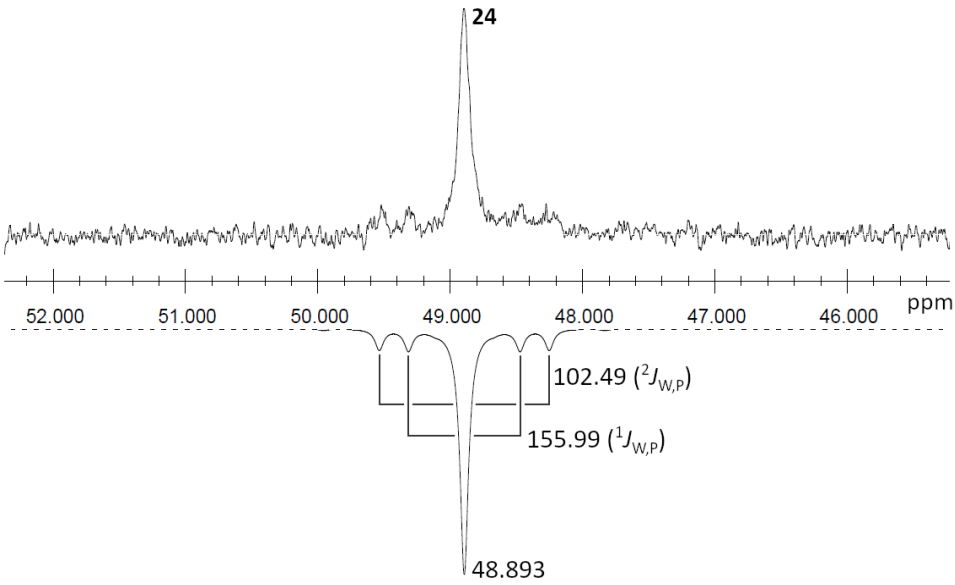

Figure 3.4.3 *Experimental $^{31}P\{^1H\}$ NMR spectrum of **24** (top) and simulated spectrum (bottom) (simulated line width 9.17).*

Resulting from rather bad signal-to-noise ratio only the coupling constants for the ABX system could be simulated.

Surprisingly, the high-field shifted signal at -77.8 ppm displayed no $^1J_{P,H}$ coupling, yet some smaller couplings leading to the strong signal broadening of FWHM ~ 56 Hz. The highfield shift paired with the rather normal $^1J_{W,P}$ coupling can be tentatively assigned to *P*-amino phosphirane complex **25** as the reaction product of a *P*-amino phosphinidene with *iso*-butene, especially as **28** has related NMR parameters (figure 3.4.4).

Phosphirane complexes, in general, are known for a long time and usually formed via [2+1]-cycloaddition of a transient phosphinidene complex with alkenes, a reaction unknown for Li/Cl phosphinidenoid chemistry so far. Unfortunately, the reaction is very fast and takes place in a temperature window not accessible via VT-NMR studies. Yet, when comparing the ^{31}P NMR data with the literature some very similar compounds could be found (figure 3.4.4).

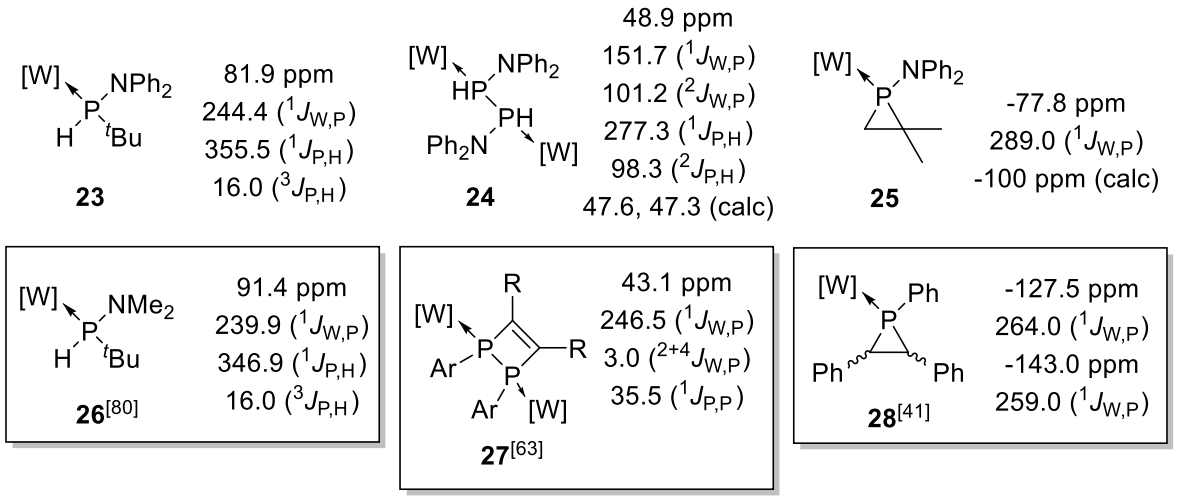

Figure 3.4.4 *Possible products of the reaction of phosphinidene complex **22a** in the reaction mixture, along with their calculated shifts (TPSS-D3/GIAO def2-QZVP) and literature known related compounds. (^{31}P NMR shifts are given in ppm with coupling constants in Hz for the element couple in brackets.)*

It can be seen in figure 3.4.4, that the side-products match very well with known compounds and calculated shifts, especially compounds **23** and **26**. It can also be seen that it is quite common to find couplings of symmetrical diphosphane complexes in higher order spectra (*e.g.* for **27**), due to the existence of an overlap of three different spin systems A_2, ABX and AA'XX', simulations also show that A_2 and ABX spin systems are dominating.[63]

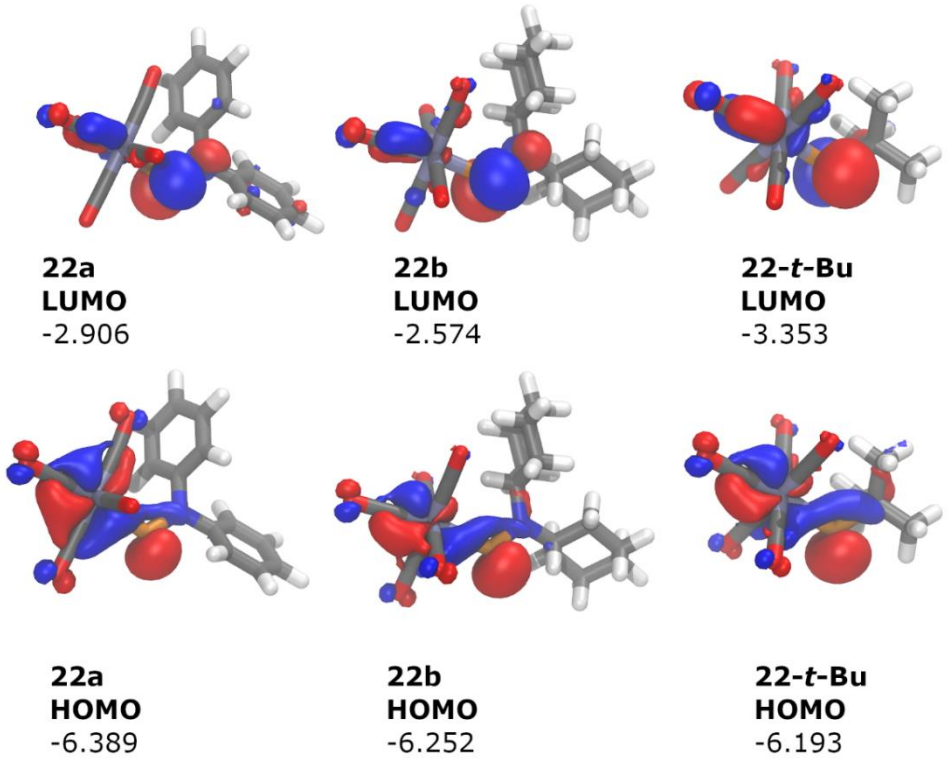

Figure 3.4.5 *Calculated HOMO and LUMO frontier orbitals of complex* ***22a,b*** *and for comparison* ***22-^{t}Bu*** *at the TPSS-D3/CPCM(THF)/def2-TZVP//PW6B95-D3/CPCM(THF)/def2-QZVP level of theory (a = ±0.04); energy values are given in eV.*

As expected for electrophilic terminal phosphinidene complexes (**XII**, figure 1.3.1), the HOMO and LUMO in all cases are strongly P located, due to the still accessible P-lone pair. Yet, the HOMO frontier orbitals also show strong contributions from the $W(CO)_5$-centre along the W-P-R bonds, most likely due to possible partial P-W double bond character. Yet another important fact is that the LUMO frontier orbitals are mostly P-located with smaller contributions from the $W(CO)_5$ group, as well as the N atoms, which was expected due to the stabilizing π(N)-donation towards the vacant P-orbital (**22a,b**). The HOMO LUMO energy gaps appear to be smaller (30 % by average) than for the corresponding phosphinidenoid/phosphanide complexes (figure 3.1.7) with 3.48, 3.68 and 2.84 eV for **22a,b** and **22-^{t}Bu**, respectively, which is the result of rather energetically low-lying LUMO frontier orbitals. It was reported, that due to small HOMO-LUMO gaps the paramagnetic contribution to ^{31}P NMR shifts is increased, resulting in a larger low-field shifts.[114] This could be shown with a correlation between ^{31}P NMR shift and frequency for π-π* electron excitation (via UV-vis absorption).[114]

To get proof for the existence of the transient terminal phosphinidene complexes **22a,b**, trapping reactions were done using weakly polar alkynes and unpolar alkenes such as tolane, 1-pentene and 1-hexene (scheme 3.4.2).

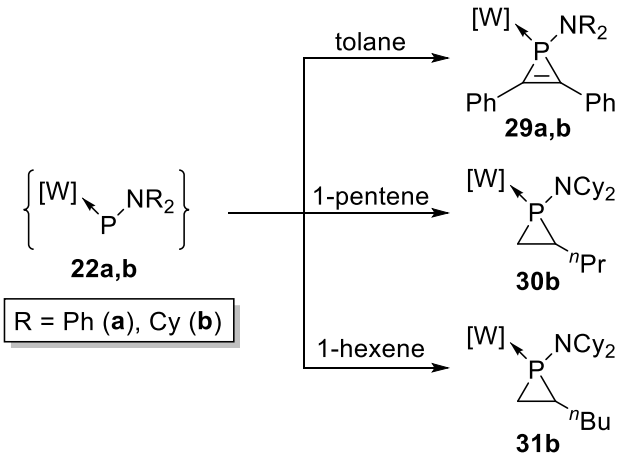

Scheme 3.4.2 *Reaction of complexes* ***22a,b*** *with 1-pentene and 1-hexene.*

Firstly, the two reactions of the assumed intermediate **22a** with tolane were investigated, in which an excess of tolane (3-5 eq.) was added after and/or before the addition of ^{t}BuLi at room temperature (figure 3.4.6).

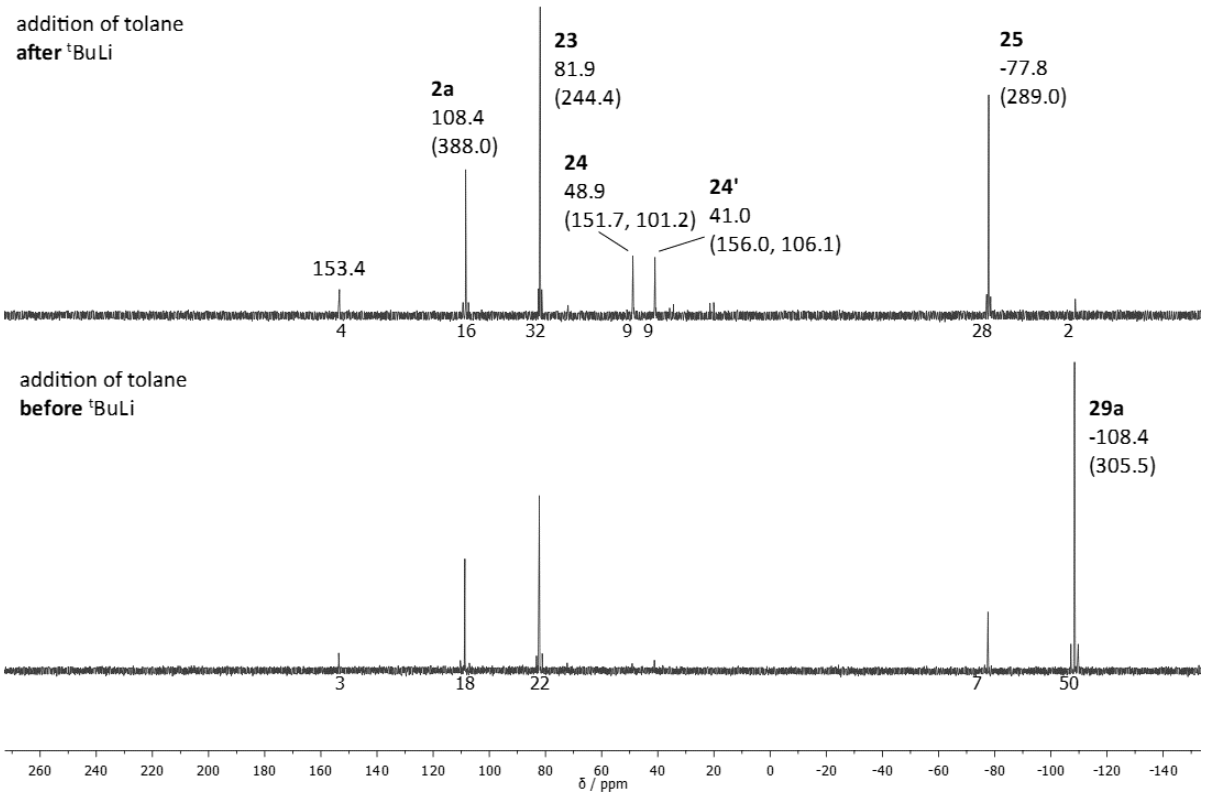

Figure 3.4.6 *$^{31}P\{^{1}H\}$ NMR of the reaction mixture with the addition of tolane done after (top) and before (bottom) the addition of ^{t}BuLi. (Given values in ppm with $^{1}J_{W,P}$ coupling constants in Hz given in brackets. Integration values are given in % below the baseline).*

The outcome was striking as there was a significant difference depending on the sequence in which the reagents were applied: in the top spectrum, a small new signal at -108.4 ppm (2 %; $^{1}J_{W,P}$ = 305.5 Hz) fits very well with the expected 1*H*-phosphirene complex **29a**, especially when compared to literature-known derivatives **32a-d** (figure 3.4.7).[39]

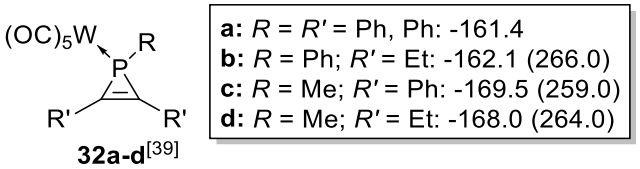

Figure 3.4.7 *Examples for literature known 1H-phosphirene tungsten complexes* ***32a-d,*** *^{31}P NMR shifts are given in ppm with the corresponding $^{1}J_{W,P}$ coupling constant in Hz in brackets.*

But when tolane was added before ^{t}BuLi, much more of the desired complex **29a** was formed. This also clearly reveals that the exchange and follow-up reactions must be very fast so that adding tolane 5 min after the ^{t}BuLi addition has almost no effect; this, again, gives evidence for a very reactive intermediate. The nature of complex **29a** could be further supported by mass spectroscopy ([M]$^{+}$ 701.1) but, unfortunately, not fully characterized as separation of **29** from the excess of tolane failed.

Investigating the possibility of the existence of a transient phosphinidene complex **22** further, calculations were done regarding its (phosphinidene) chloride affinity. Yet, for a better representation of the actual direction of the observed reaction, here the energetically equivalent loss of chloride from phosphinidenoid complexes **5**$^{-}$ is displayed (scheme 3.4.3). This was computed for several substituents quantifying the relative stabilization between the substituents. Many different substituents with several metal centres were calculated (appendix table 7.3). ΔG values are obtained via single-point calculation at the PW6B95-D3/ CPCM(THF)/def2-QZVP level with zero-point-energy (ZPE), thermal and entropic corrections at the TPSS-D3/CPCM(THF)/def2-TZVP level. Again, the combination of the functionals/basisset should be sufficient to yielding good computational results (figure 3.2.12). Even though a continuum solvent model was applied, strong solvent stabilization was not taken into account, *e.g.* introduction of explicit solvent molecules.

More calculations regarding terminal phosphinidene complex adducts were reported by Espinosa and Streubel, recently, using comparable combinations of functional and basisset (similar margin of error)[115] yielding reasonable results.[112]

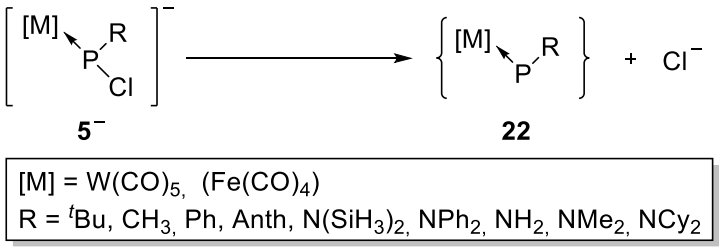

Scheme 3.4.3 *Calculated formal chloride loss from anionic complexes* ***5*** *forming complexes* ***22****.*

The computed data is given in table 3.4.1. The MBO values of the P-M and P-R bonds were taken as a measure for the stabilization of the corresponding metal centre and substituent.

Table 3.4.1 *Free enthalpy values for the chloride abstraction for Fe, W with different P-N/C substituents.*

Phosphanide complexes **5**$^-$ ($W(CO)_5$)			Phosphinidene complexes **22** ($W(CO)_5$)			
R	**MBO (P-R)**	**MBO (P-M)**	**R**	**MBO (P-R)**	**MBO (P-M)**	**ΔG / kcal mol^{-1}**
CH_3	0,981	0,760	CH_3	1,017	1,342	29,61
^{t}Bu	1,009	0,684	^{t}Bu	0,989	1,277	30,99
Ph	1,012	0,727	Ph	1,088	1,221	28,35
Anth	0,898	0,731	Anth	1,161	1,146	25,79
NH_2	1,174	0,747	NH_2	1,397	1,081	15,27
NMe_2	1,259	0,746	NMe_2	1,532	1,016	12,67
NPh_2	1,119	0,695	NPh_2	1,380	1,056	17,48
NCy_2	1,338	0,709	NCy_2	1,565	0,979	10,75
$N(SiH_3)_2$	0,992	0,701	$N(SiH_3)_2$	1,312	1,119	22,77

What can be seen in table 3.4.1 is that *P*-amino substitution has a strong stabilizing effect thus lowering the energetic difference of the two sides of the reaction (scheme 3.4.3). The backbonding of the N

centres plays an important role, due to increased π-donation towards the P-centre, meaning the existence of aromatic systems at nitrogen are counter-productive with a more pronounced delocalization of the N lone pair. This is visible in the energetic difference of 6.73 kcal/mol between the NPh_2 and NCy_2 substitution (for $W(CO)_5$ complexes). For alkyl/aryl substitution in general aryl substitution is better, of course due to a better electron donation with its delocalization, *e.g.*, difference of 5.20 kcal/mol between ^{t}Bu and Anth substitution for $W(CO)_5$ complexes. Rather interesting is the fact, that the metal centre only seems to make a difference in case of P-substitution with low electron donation ability. For example, in case of NCy_2 both values are nearly identical for W and Fe with 10.75 and 10.68 kcal/mol, respectively, yet for CH_3 there is a significant difference of 7.58 kcal/mol. Furthermore, this can be seen at the P-M bond, for the anionic complexes **5**$^-$ the average MBO value for Fe (0.604) is 16 % less than the average value for W (0.722), but in case of the neutral phosphinidene complexes **22** the value is 4 % higher (average MBOs, Fe 1.186, W 1.137) with significant differences in case of the alkyl substitution, *e.g.* 1.519 (Fe, CH_3) and 1.342 (W, CH_3). Surprisingly, in case of $W(CO)_5$ complexes a linear relation between the MBO(P-R) of the phosphinidene complexes **22** and the free enthalpy ΔG was found and plotted against in figure 3.4.8.

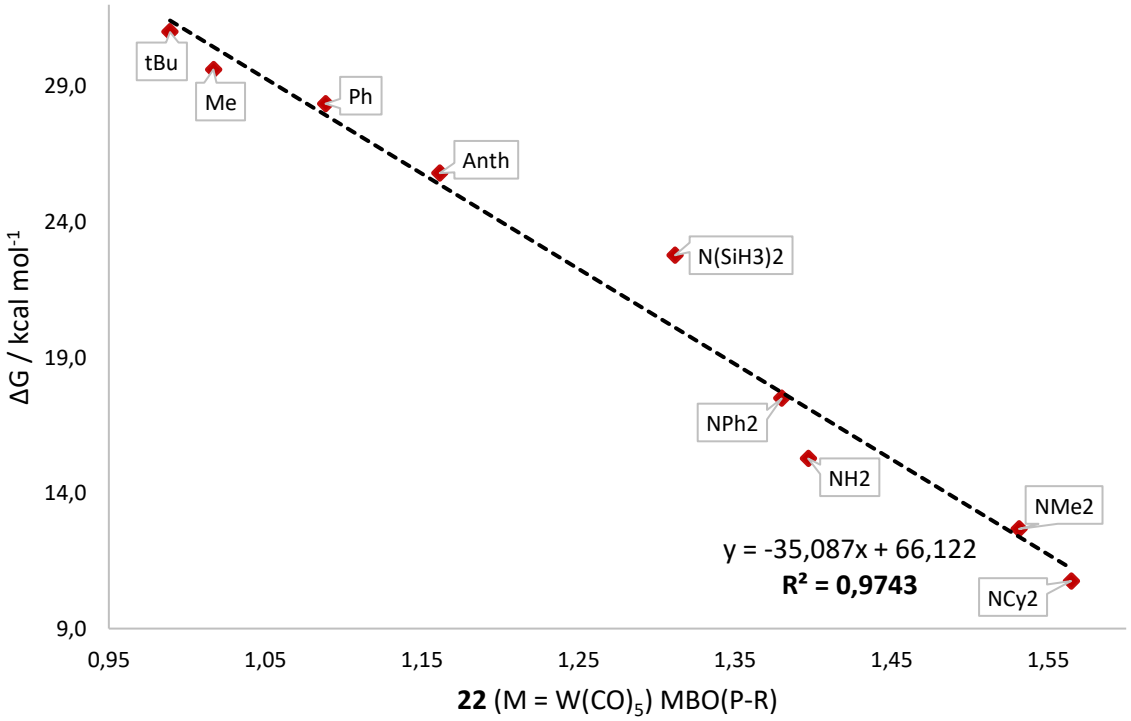

Figure 3.4.8 *MBO(P-R) of complexes* ***22*** *(M = W(CO)$_6$) plotted against the corresponding free enthalpy of their chloride abstractions (scheme 3.4.3).*

The R value of 0.9743 shows a very good linear relation in the graph regarding the stabilization effect going from alkyl → aryl → (aryl)amino → (alkyl)amino for the chloride abstraction. The HOMO and LUMO of **22a,b** and **22-^{t}Bu** (M = $W(CO)_5$) are displayed in figure 3.4.5 to observe a possible difference resulting from the varying substitution.

With these results in hand it can be seen that the NCy_2 substituent is much better suited for this kind of chemistry than NPh_2, while the metal centre seems to have a lesser impact. Therefore, the following reactions were performed using tungsten complex **2b** as starting material, due to its strong advantage of visible and indicative W,P couplings. In this case, the first factor to be investigated was the temperature, since the formed intermediate **22b** should be more stable than **22a**. Two reactions were done reacting complex **2b** with ^{t}BuLi at r.t. and -80 °C in toluene (figure 3.4.9).

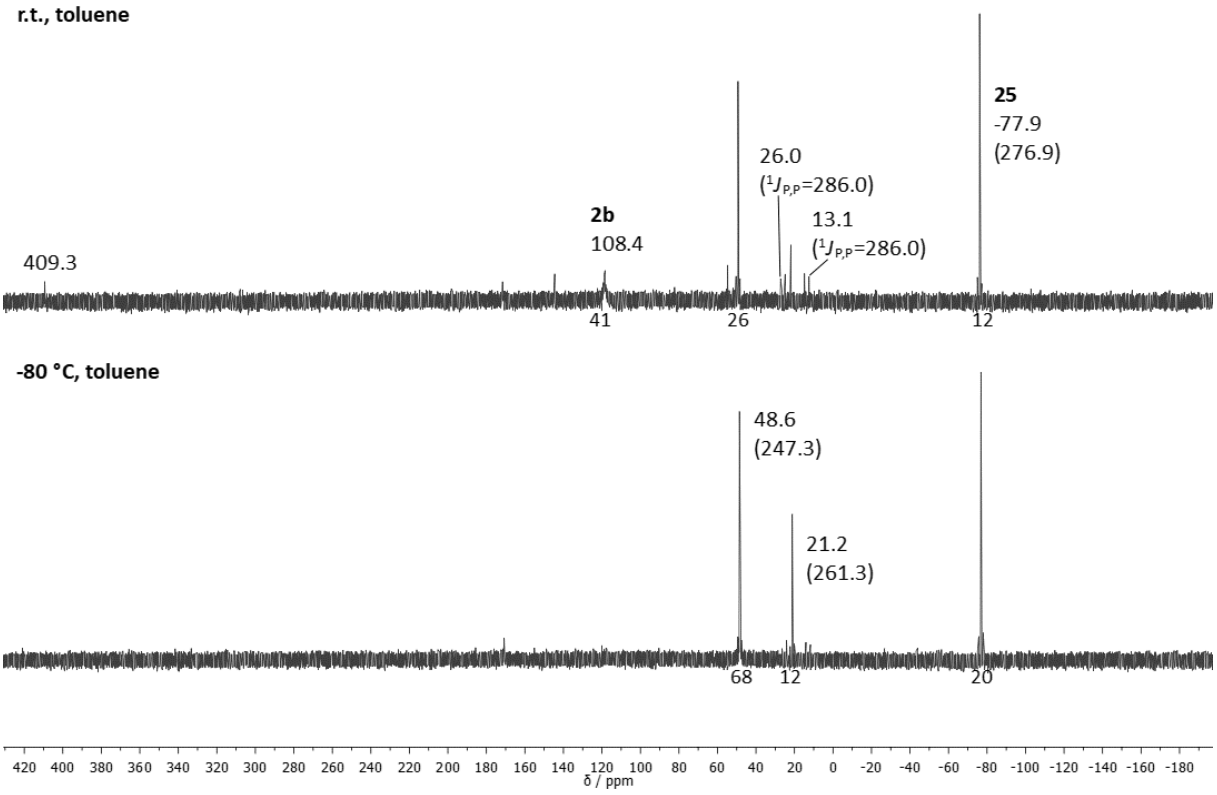

Figure 3.4.9 *$^{31}P\{^{1}H\}$ NMR of the reaction mixture with ^{t}BuLi at room temperature (top) and -80 °C (bottom). (Given values in ppm with $^{1}J_{W,P}$ coupling constants in Hz given in brackets, if not stated otherwise, with selected integration values in % below the baseline).*

It is visible that due to a higher stability of the intermediately formed moiety the temperature makes a difference here. The reaction mixture at room temperature shows several signals which were not

observed beforehand (compared to NPh_2, figure 3.4.1), while the reaction at -80 °C shows a similar outcome as already discussed possible products with P-NCy_2 were formed (compared to NPh_2, figure 3.4.3). Unfortunately, due to strong signal broadening paired with low resolution in the ^{31}P NMR spectrum no statements regarding P-H couplings can be made, besides that the signal at -77.9 ppm shows no $^{1}J_{P,H}$ coupling, possibly being the NCy_2 derivative of the assumed phosphirane complex **25** (figure 3.4.4).

In the next step, complex **2b** was reacted with an excess of tolane, 1-pentene and 1-hexene following the here established (preliminary) protocol (toluene, -80 °C). One exception was made regarding the amount of added ^{t}BuLi, since often some starting material was left in the reaction mixture, 2 eq. of ^{t}BuLi were used (figure 3.4.10).

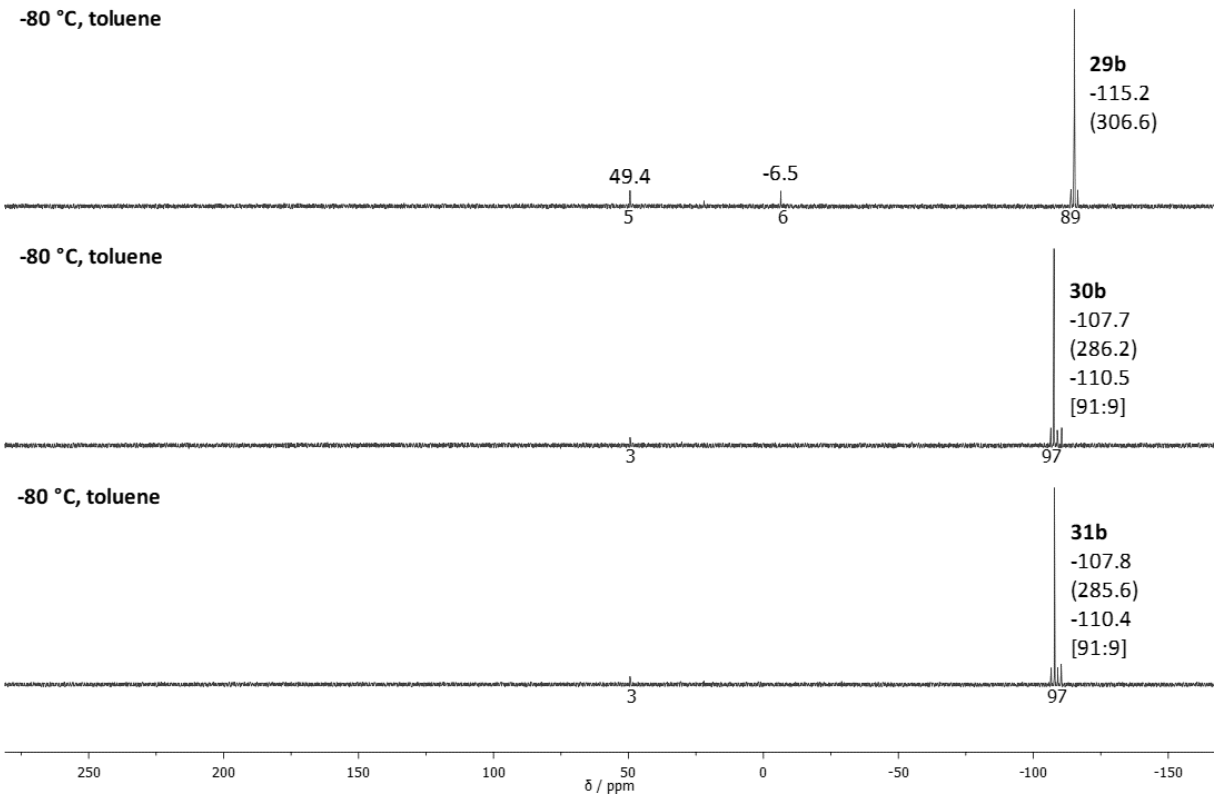

Figure 3.4.10 *$^{31}P\{^{1}H\}$ NMR of the reaction mixtures with tolane (top), 1-pentene (middle) and 1-hexene (bottom) at -80 °C in toluene. (Given values in ppm with $^{1}J_{W,P}$ coupling constants in Hz and isomeric ratios given in curved and square brackets, respectively, with the integration values in % below the baseline).*

It is immediately apparent that the derivative with the *P*-NCy_2 substitution shows a higher selectivity than the *P*-NPh_2 derivative in the [2+1] cycloaddition reactions, *i.e.*, with tolane 89 % and with 1-pentene and 1-hexene 97 % product formation was observed. The signals of the products **29b**, **30b**, and **31b** can be seen in the ^{31}P NMR spectra at high field. While the 1*H*-phosphirene complex **29b** displays a signal at -115.2 ppm ($^{1}J_{W,P}$ = 306.6 Hz), the phosphirane complexes **30b, 31b** have very similar shifts due to their very small structural differences (**30b:** -107.7 ppm ($^{1}J_{W,P}$ = 286.2) and **30b':** -110.5 ppm; **31b**: -107.8 ppm ($^{1}J_{W,P}$ = 285.6 Hz) and **31b':** -110.4 ppm), and both are formed as stereoisomers with an isomeric ratio of 91:9. Complex **29b** could not be separated from the excess of tolane due to its high solubility in polar as well as unpolar solvents and high boiling point, but complexes **30b, 30b** were isolated and characterized. It was also attempted to observe any intermediate prior to the formation of complex **30b** and, hence, VT-NMR studies were performed in toluene (figure 3.4.11).

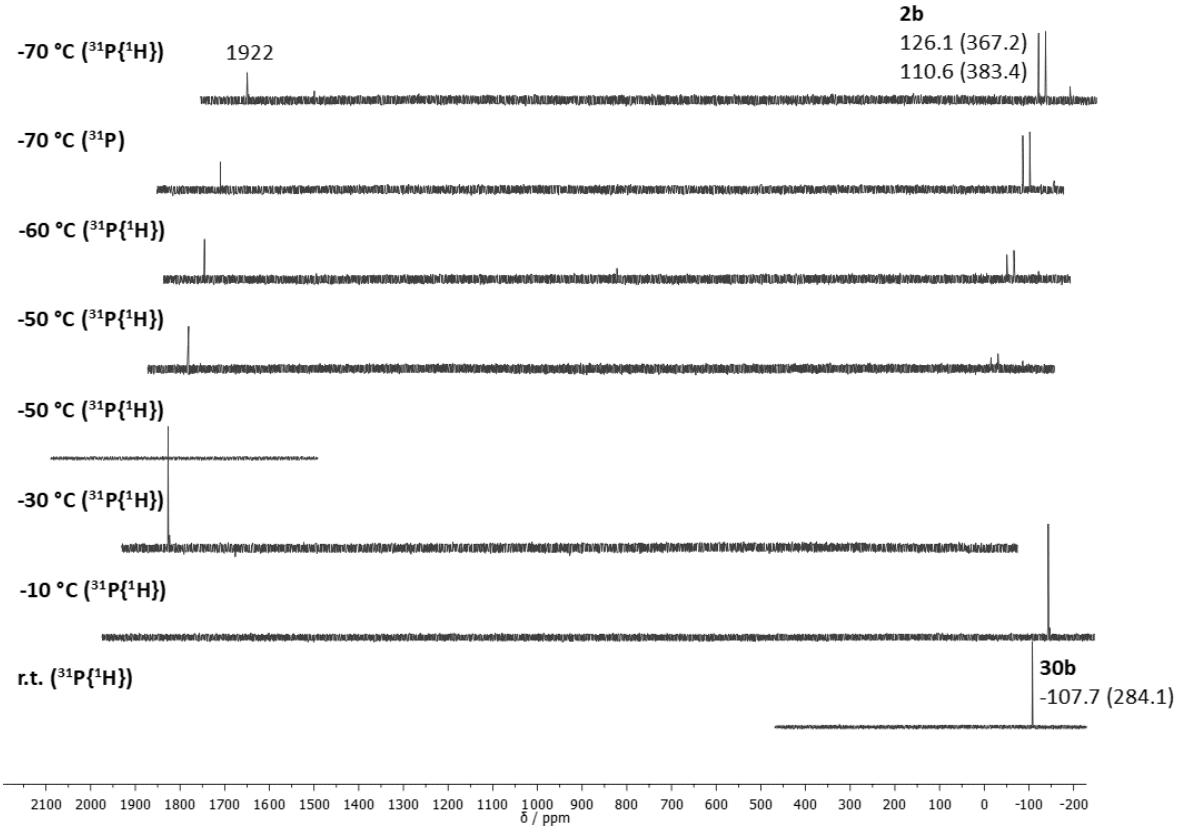

Figure 3.4.11 *^{31}P and $^{31}P\{^{1}H\}$ NMR of the reaction mixture with 1-pentene at variable temperature. (Given values in ppm with the $^{1}J_{W,P}$ coupling constants in Hz in brackets).*

This VT-NMR experiment revealed that the reaction is very fast and already taking place at very low temperature (< -70 °C). The first ^{31}P NMR measurement shows complex **2b** as its two atropisomers at

low temperature (126.1 ($^1J_{W,P}$ = 367.2 Hz) and 110.6 ($^1J_{W,P}$ = 383.4 Hz) ppm), along with a signal very far in the low field at 1922 ppm with no P-H coupling. Unfortunately, it became clear during further measurements that it was not the expected terminal phosphinidene complex **22b**, appearing at low field, but complex **30b** "folded" back into the ^{31}P NMR spectrum due to analogue measurement of the low-field region, a phenomenon caused by the *Aliasing effect*.[116] Digital measurement of the specific shift region (figure 3.4.11, -50 °C (bottom)) showed the lack of a signal in this region.

Complexes **30b, 31b** appeared to be unstable at room temperature (after 12 h) forming several side products in the range of 0 – 150 ppm. It was already reported that phosphirane complexes can inhabit a low stability, while 1*H*-phosphirene complexes appear to be thermodynamically more stable.[49] In one special case from *Niecke* a 1*H*-phosphirene was formed from the corresponding TMS-substituted phosphirane through intramolecular H_2 elimination (*P*-^{t}Bu: 20 °C, P-Ph: 60 °C).[117] Yet also more stable *P*-amino substituted phosphirane complexes are known since the early 80s.[118] Nevertheless, they also form the more stable 1*H*-phosphirene complexes at 90 °C in the presence of alkynes.[118]

Here, one idea was to investigate the so called *substrate hopping*, which is known and reported for phosphirane complexes, formally having a transient terminal electrophilic phosphinidene complex hop from one substrate to another forming the thermodynamically more stable complex, releasing the alkene on the way.[50,118] Such reactions were also reported for phosphiranium salts reacting with acetylene derivatives under formation of the corresponding phosphirenium salts.[119] To test this, **2b** was reacted with 1-pentene following the protocol and measured via ^{31}P{^{1}H} NMR spectroscopy to make sure the corresponding phosphirane complex **30b** was formed (figure 3.4.12). Afterwards an excess (3-5 eq.) of tolane was added and the reaction mixture was stirred for 4 days at room temperature.

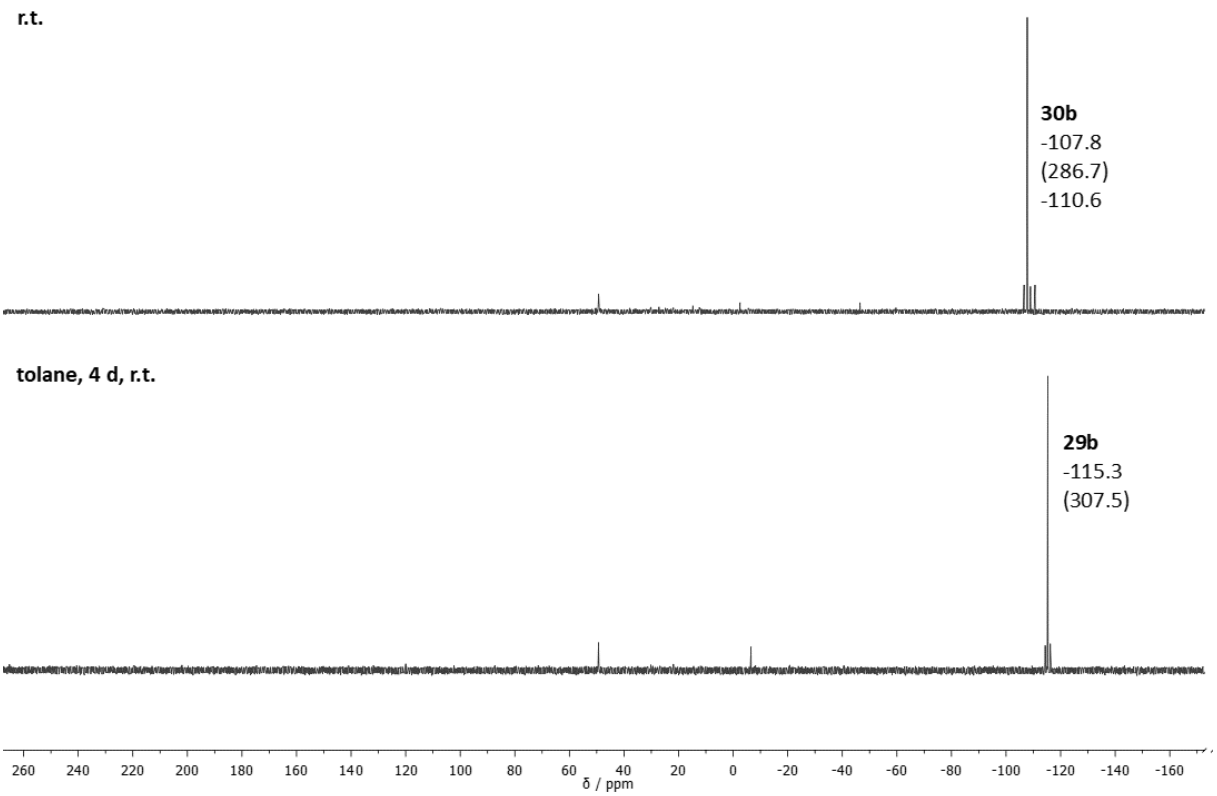

Figure 3.4.12 *$^{31}P\{^{1}H\}$ NMR of the reaction mixtures with 1-pentene at r.t. (top, after filtration with SiO_2 with the reaction mixture at -20 °C) and after 4 days stirring with tolane at r.t. (bottom) in toluene. (Given values in ppm with the $^{1}J_{W,P}$ coupling constants in Hz in brackets).*

It can be seen that, indeed, the thermodynamically more stable 1*H*-phosphirene complex **29b** (-115.3 ppm and $^{1}J_{W,P}$ = 307.5 Hz) was selectively formed from complex **30b** (-107.8 ppm and $^{1}J_{W,P}$ = 286.7 Hz; -110.6 ppm) and tolane. This further underlines the possibility of a transient existence of the terminal electrophilic phosphinidene complex [$W(CO)_5(PNCy_2)$].

To get further support for the existence of this transient electrophilic phosphinidene complex, and to separate a possible nucleophilic attack from a concerted (electrophilic) [2+1]-cycloaddition, more calculations were done by *Qu* for **2a** and ^{t}BuLi regarding its reactivity in different solvents (figure 3.4.13).[109]

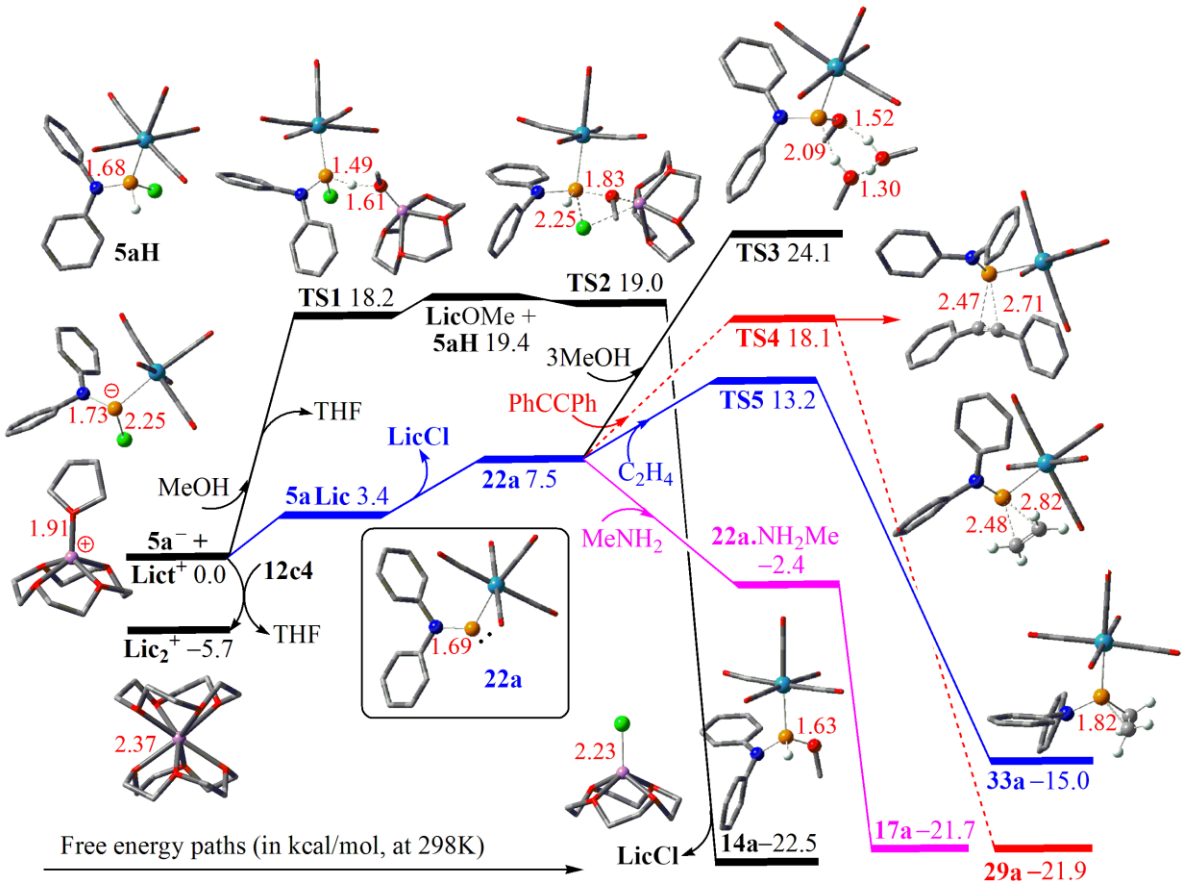

Figure 3.4.13 *Free energy reaction paths (in kcal/mol, at 298 K) at the TPSS-D3/COSMO-RS(THF)/def2-TZVP level of theory for several reaction pathways regarding phosphinidenoid complex* ***5a*** *and phosphinidene complex* ***22a*** *with methanol, tolane, ethene and methylamine. Crucial P, Cl, Li, W, O, C and H atoms are high-lighted as orange, green, violet, cyan, red, grey and white, respectively. Important bond distances are given in Å and highlighted in red. Hydrogen atoms are omitted for clarity.*

To unveil the dichotomy of *P*-amino substituted Li/Cl phosphinidenoid complex **5a** and the terminal phosphinidene complex **22a**, in-depth DFT calculations were done (figure 3.4.13). Calculated were both possibilities, while for the Li/Cl phosphinidenoid complex **5a** the reaction mechanism with MeOH was calculated, the reaction mechanism for the phosphinidene complex **22a** was calculated for its reaction with MeOH, tolane, ethene and methylamine.

The reaction of the Li/Cl phosphinidenoid complex **5a** starts with the two separated ions, the phosphanide complex **5a**$^-$ and a THF stabilized Li(12-c-4) (**Lict**$^+$) which then reacts with MeOH via a **Lic**-O-H-**2a**$^-$ transition state (**TS1**) with a rather high barrier of 18.2 kcal/mol forming **5aH** and **Lic**OMe. TS2 then occurs via a concerted substitution of chloride with methoxy at the phosphorus centre forming the corresponding alkoxyphosphane complex **14a** with -41.5 kcal/mol (overall -22.5 kcal/mol). The

other reaction path starts with the formation of the contact ion pair **Lic5a** followed by an **LicCl** elimination forming phosphinidene complex **22a** with 10.9 kcal/mol. From here the four different reactions display free energy reaction barriers depending on the nucleophilicity of the substrates with MeOH < PhCCPh < C_2H_4 < NH_2Me. Since MeOH is least feasible in this case it displays the highest barrier with 13.2 kcal/mol (24.1 kcal/mol overall) showing that in this case the reaction with phosphinidenoid is energetically favoured by 5.1 kcal/mol (**TS3** vs. **TS2**). **TS3** shows a methanol assisted concerted reaction, matching the already calculated OH-insertion mechanism for $[Fe(CO)_4P(Cl)Me]^-$ using water for a similar H-transfer step.[81] The computed [2+1]-cycloadditions with tolane and ethene show rather small free energetic barriers of 10.6 and 5.7 kcal/mol (18.1 and 13.2 kcal/mol overall), respectively. Both of them appear to react via an - for an electrophilic phosphinidene complex expected – concerted ring closing mechanism with rather symmetrical transition states regarding the P-C(olefine) distances **TS4** (9 %), **TS5** (13 %). From there the corresponding 1*H*-phosphirene **29a** and phosphirane complexes **33a** are formed with strong energetic driving forces of 40.0 and 28.2 kcal/mol, respectively. It can also be seen again that the reaction to the 1*H*-phosphirene complex **29a** appears to be 6.9 kcal/mol energetically more favoured than to the phosphirane complex **33a**. Surprising is the completely barrierless reaction with $MeNH_2$ – maybe due to its strong nucleophilicity – which already forms a rather stable, intermediate N-to-P adduct **22a.NH_2Me** (-9.9 kcal/mol), followed by the barrierless formation of the (final) 1,1-addition product **16a**. It is to mention, that for most Li/Cl phosphinidenoid complexes studied before there was no difference in reactivity regarding MeOH and $MeNH_2$ which is now surprising taking the computed significant differences for complex **22a** into account.

3.5 Synthesis and properties of phosphaquinomethane complexes

As described in the introduction, quinoidal compounds (*cf.* figure 1.5.1) attracted a lot of interest over decades for a variety of reasons.[83] In 2014 a thorough theoretical study of neutral group 6B (Cr, Mo, W) pentacarbonyl complexes [$M(CO_5)L$], possessing various P-ligands such as phosphanes, phospha-alkenes and phosphaquinomethanes, was reported.[94] The focus was then on the spin density distribution and charge localization of formed radicals and radical anions/cations, which was derived from the bond dissociation energies (BDE) for the different bond cleavages. The conclusion was that phosphaquinomethane ligands have the most "non-innocent" character of the complexes studied and therefore represent the most promising starting point regarding redox chemistry and catalysis. Yet, even at this point very little was known about phosphaquinomethanes **LXI** and even less about their complexes. The first synthesized phosphaquinomethane complex containing a *P*-$CH(SiMe_3)_2$ substitution was not thoroughly investigated in 2010 as the focus was on the transient *P*-chloro phosphanyl complexes **LV** (scheme 1.5.2). Also, the mechanism of the final product formation remained not understood, and a transient dearomatized phosphane complex **LXII**, representing the product of the initial radical hetero-coupling step in the reaction cascade, was just postulated.

This was the starting point for the investigation presented hereafter. First, the synthesis of new phosphaquinomethane complexes was attempted targeting derivatives containing *P*-NPh_2 and *P*-CPh_3 substituents. Furthermore, the focus was on the elucidation of the reaction mechanism and to study the electronic and redox properties of such complexes.

The reason that complexes **LXII** were not observed and/or studied in more detail could be that they were thermally labile, since there should be a strong inherent driving force for re-aromatization which could happen intra- or intermolecular, especially in a polar solvent like THF with Lewis acidic cations like Li^+ around. So, the idea was to remove the THF from the reaction mixture at low temperature (-50 °C) which of course would hamper a possible upscaling, due to the rather high boiling point of THF (66 °C) itself. The already discussed thermal stability difference between the derivatives with *P*-CPh_3 and *P*-NPh_2 groups led also to different protocols for this reaction, *i.e.*, two equivalents of 12-crown-4 were used and added before ^{t}BuLi, whereas the *P*-CPh_3 substituted Li/Cl phosphinidenoid complex doesn't need 12-crown-4 for stabilization.[60] The reactions were done at -80 and -100 °C for complexes **2a,3a** and **2c,4c**, respectively (scheme 3.5.1).

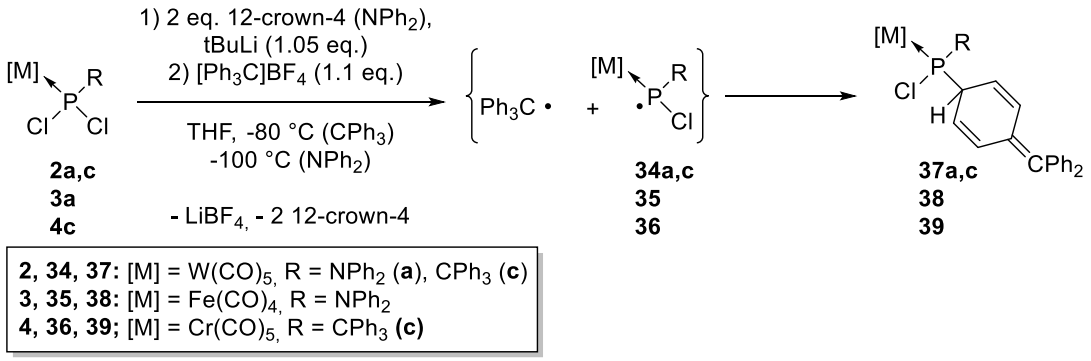

Scheme 3.5.1 *One electron oxidation reactions of the corresponding Li/Cl phosphinidenoid complexes forming the transient phosphanyl complex/trityl radical pair yielding complexes* ***34-36****.*

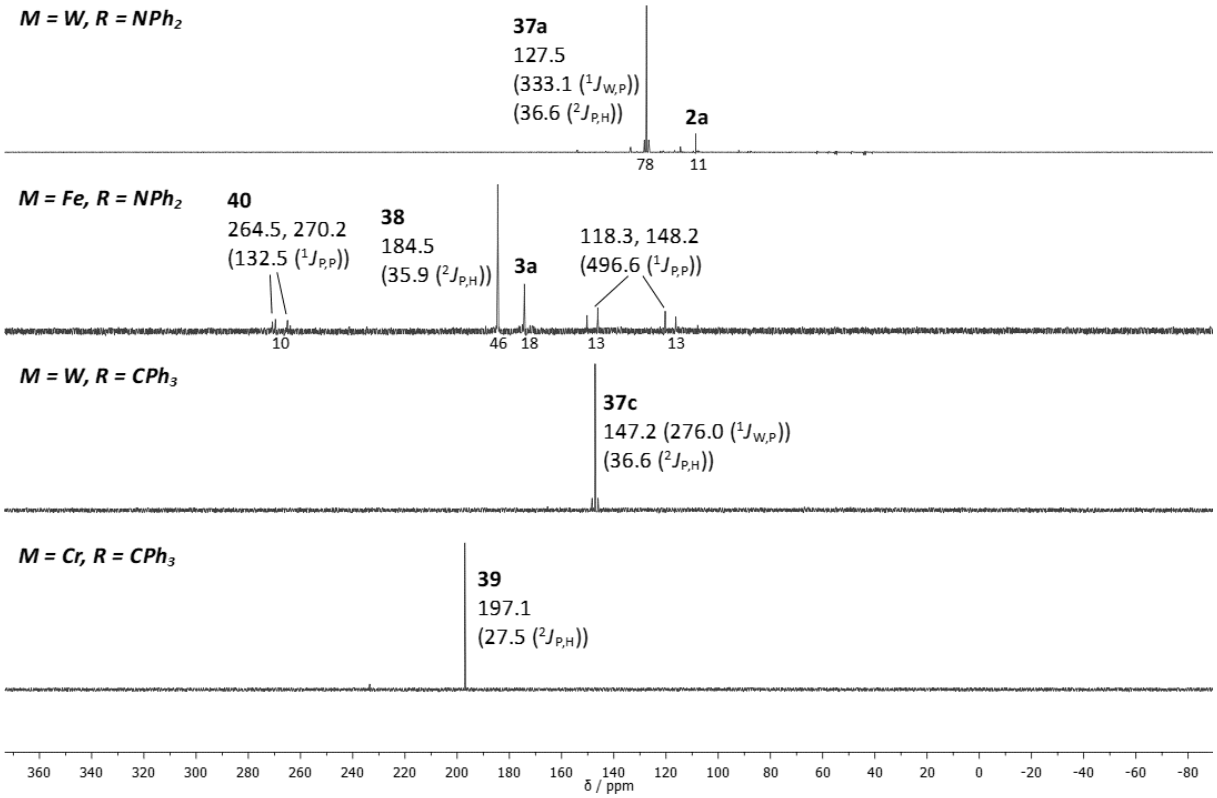

Figure 3.5.1 *$^{31}P\{^{1}H\}$ NMR spectra of complexes* ***37-39*** *in solution (****37a, 38:*** *C_6D_6;* ***37c, 39****: toluene). (Given values in ppm with coupling constants in Hz given in brackets, with the corresponding $^{x}J_{P,H}$ couplings taken from the ^{31}P NMR spectra with selected integration values in % below the baseline).*

Very selective reactions can be seen in case of *P*-CPh_3 substitution (**37c, 39**) with nearly 100 % selectivity. In case of *P*-NPh_2 substitution some unreacted starting material (**2a, 3a**) remained with some minor side products for **37a** and some major problems in case of **38**. Two different side products can be seen there, one being a strongly low-field shifted asymmetric P-P system with very similar P-atoms at 264.5 and 270.2 ppm with a rather small $^{x}J_{P,P}$ coupling of 132.5 Hz. The other is the same

asymmetric diphosphane (complex) already visible in figure 3.2.5 as a side-product of the "self-condensation reaction" of **3a**. The ^{31}P NMR shifts of the main products are in the expected region 100 – 200 ppm (**37a:** 127.5 ppm, **38:** 184.5 ppm, **27c:** 147.2 ppm, **39:** 197.1 ppm) with the Fe (**38**) and Cr (**39**) complexes being more low-field shifted than the corresponding W (**37a,c**) complexes (Δδ ~ 50-60 ppm). The structurally important $^{2}J_{P,H}$ coupling constants were observed for all complexes in the range of 27 – 37 Hz (**37a:** 36.6 Hz, **38:** 35.9 Hz, **37c:** 36.6 Hz, **39:** 27.5 Hz) with W-P coupling constants fitting the substitution pattern, e.g., with $^{1}J_{W,P}$ = 333.1 Hz for NPh_2 (**37a**) and $^{1}J_{W,P}$ = 276.0 Hz for CPh_3 (**37c**). The corresponding proton signals could also be found in the ^{1}H NMR spectra at 4.45, 4.70, and 4.66 ppm for **37a,c** and **39**, respectively. The obtained IR spectra showed the expected absorptions due to CO stretch vibration (table 3.5.1).

Table 3.5.1 *Measured IR frequencies for complexes **37-39**.*

Complex	IR (CO bands, exp) / cm^{-1}
37a	1923, 2075
37c	2070, 2060, 1984, 1918
39	1926, 1989, 2063

A possible side-product in this region could be complex **40** (figure 3.5.2), when comparing the values with the literature.

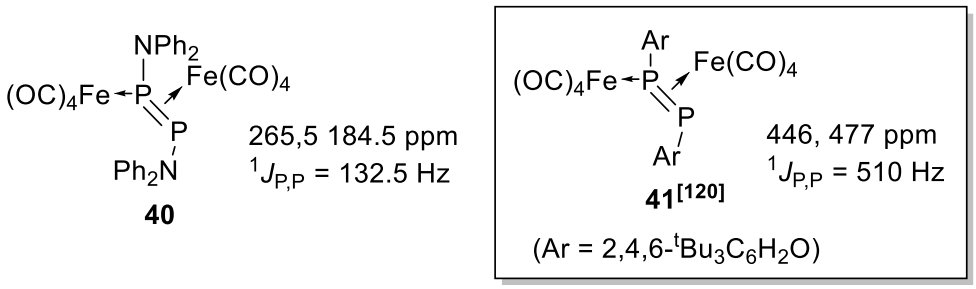

Figure 3.5.2 *Proposed structure for **40**.*

From here the work-up methods were very limited due to sensitivity (thermally and chemically) of complexes **37-39** regarding the 1,5-H shift, so the products were just extracted with cold toluene and washed at low temperature. Nevertheless, compounds **37c** and **39** could be obtained as clean products in 42 and 52 % yields and were fully characterized, while **37a** was obtained as a rather crude product with a 12 % yield.

The next step was to examine the reaction towards either the re-aromatized complexes **LXIV** concerning a potential a 1,5-H shift or towards the phosphaquinomethane complexes **LXIII** via formal

HCl elimination . For this the complexes **37-39** were reacted with a rather weak base (NEt_3) and a strong base (KHMDS) at low temperatures (scheme 3.5.2).

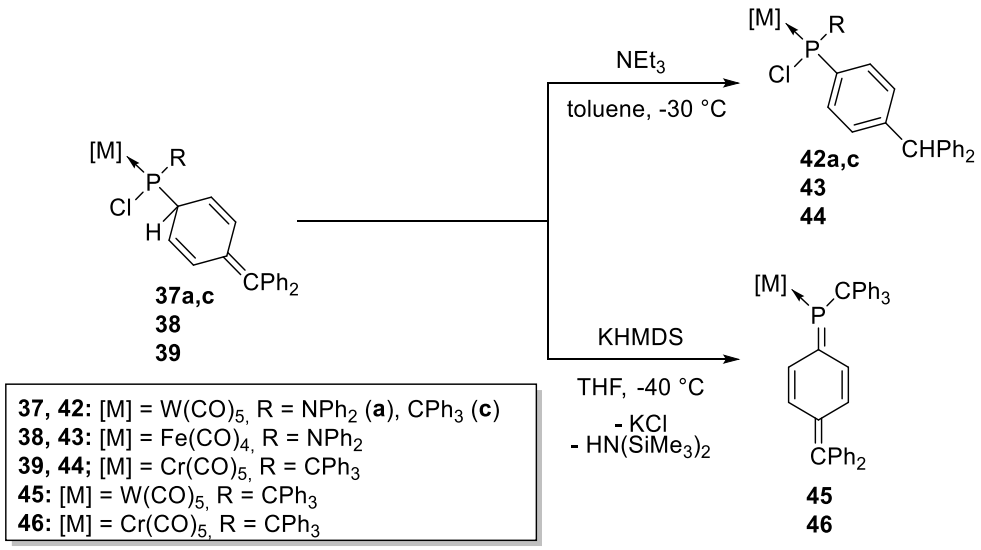

Scheme 3.5.2 *Base-dependant follow-up reactions of precursor complexes **37-39** undergoing 1,5-H shift or formal HCl elimination with weak and strong N-bases, respectively.*

Firstly, the reactions with NEt_3 in toluene were performed for all four derivatives and are displayed in figure 3.5.3.

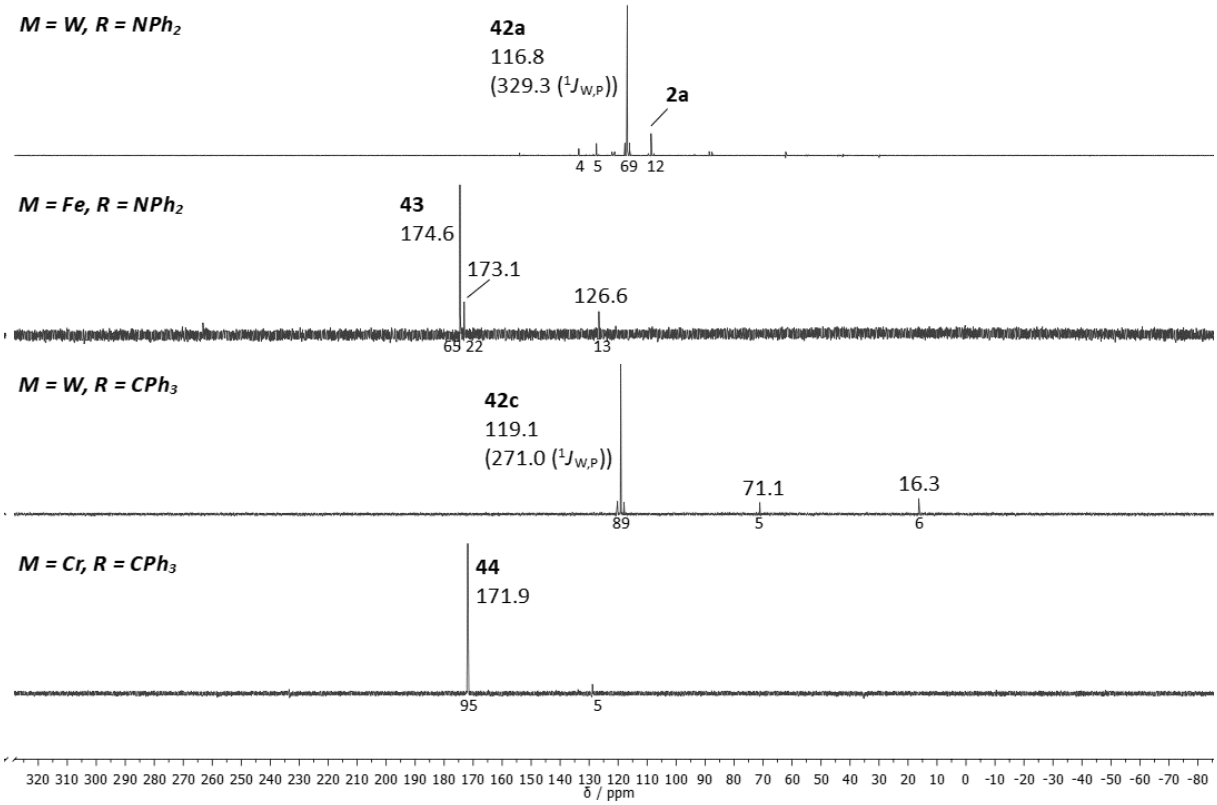

Figure 3.5.3 *$^{31}P\{^{1}H\}$ NMR spectra of the reaction mixtures of **37-39** with NEt_3. (Given values in ppm with coupling constants in Hz given in brackets with selected integration values in % underneath the baseline).*

In all cases NEt_3 promoted selectively the 1,5-H shift to furnish complexes **42-44** together with some minor side-products, the nature of which was not further investigated. While the W-P coupling appears to be not affected and, in general, a small high-field shift occurred with 10-11 ppm for **42a**, **43** (compared to **37a**, **38**) and 26-28 ppm for **42c**, **44** (compared to **37c**, **39**), respectively. Complexes **42c, 43** and **44** could further be purified via column chromatography at low temperature to be obtained in 43, <5 and 20 % yields, respectively, and were further characterized. Two column chromatographies were needed for the purification of **43** diminishing its yield. Moreover, single crystals could be obtained for **42c, 44** and measured via X-ray diffraction (figure 3.5.4-3.5.5).

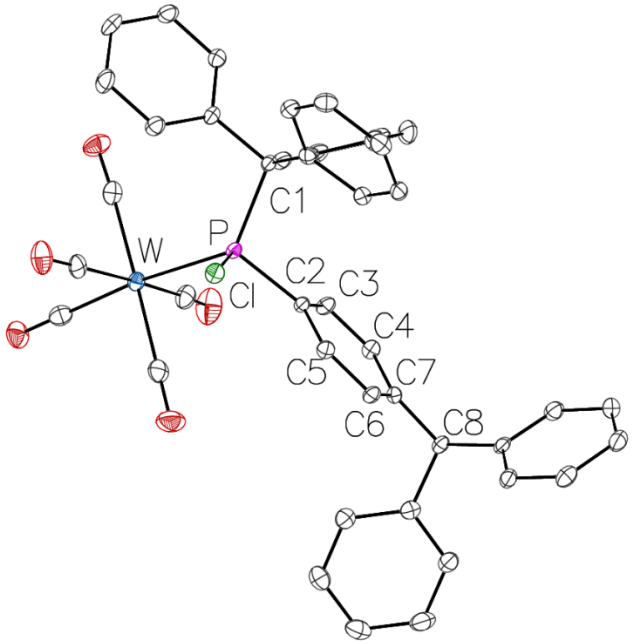

Figure 3.5.4. *Molecular structure of* ***42c*** *in the solid state. The ellipsoids were set to 50 % possibility and hydrogen atoms have been omitted for clarity. Bond lengths in Å and angles in °: P-W 2.5241(5), P-C1 1.9533(5), P-C2 1.8357(18), C2-C3 1.396(3), C3-C4 1.389(3), C4-C7 1.394(3), C7-C8 1.522(2), Σ(<C2) 359.6,* ***Σ****(<C7) 360.0.*

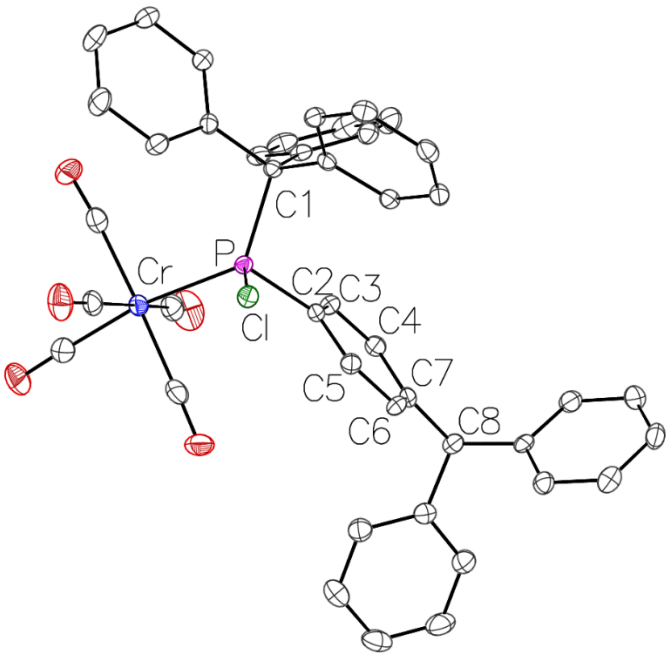

Figure 3.5.5. *Molecular structure of* ***44*** *in the solid state. The ellipsoids were set to 50 % possibility and hydrogen atoms have been omitted for clarity. Bond lengths in Å and angles in °: P-Cr 2.3910(5), P-C1 1.9549(17), P-C2 1.8445(15), C2-C3 1.400(2), C3-C4 1.387(2), C4-C7 1.385(2), C7-C8 1.524(2), Σ(<C2) 359.3,* ***Σ****(<C7) 360.0.*

The obtained bond lengths and angles are in the expected range. Both obtained solid state structures prove the re-aromatized ring with equal bond lengths of the central ring atoms ~1.4 Å and planar geometry at the two opposite *para*-C ring atoms.

When complexes **37-39** were treated with KHMDS in THF at low temperature, only signals of complexes **45** and **46** could be obtained (figure 3.5.6).

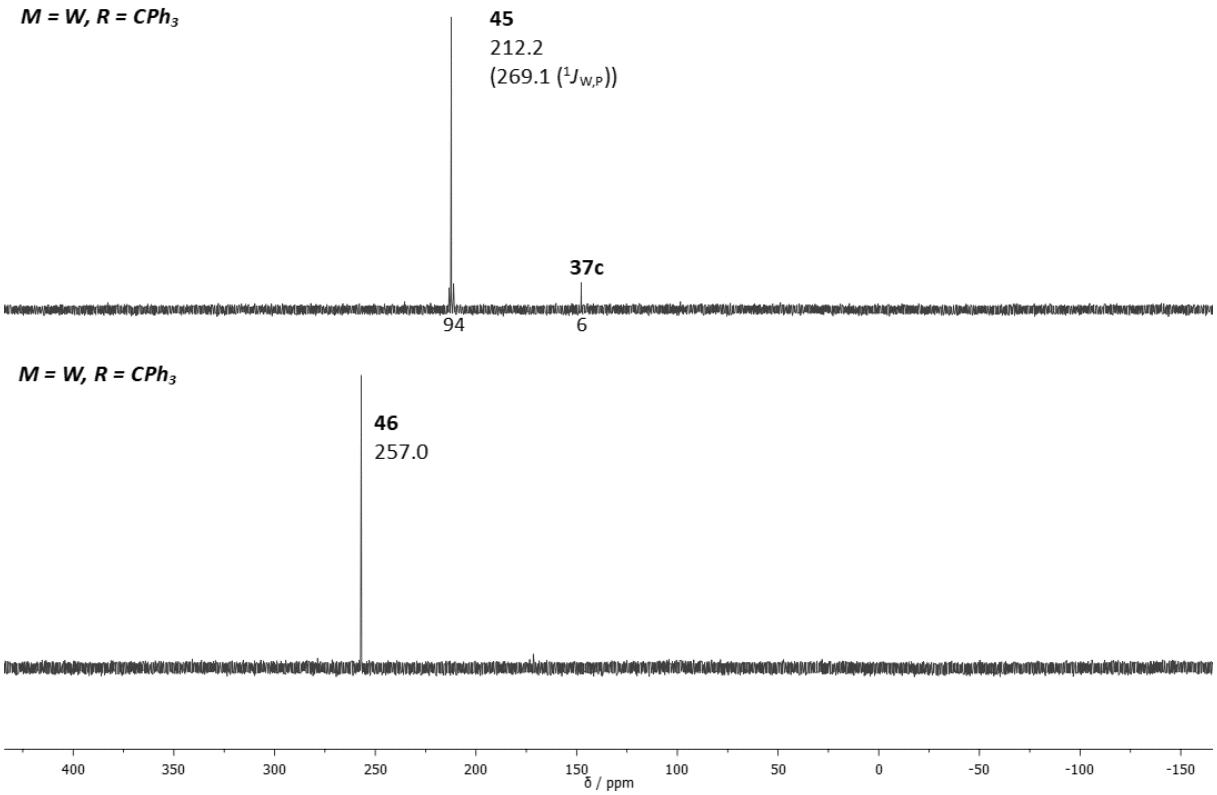

Figure 3.5.6 *$^{31}P\{^{1}H\}$ NMR spectra of the reaction mixtures for complexes **36** and **37** in toluene. (Given values in ppm with coupling constants in Hz given in brackets with selected integration values in % below the baseline).*

Complexes **45** and **46** were selectively formed with signals in low-field at 212.2 and 257.0 ppm, respectively, which fits the region of complexes **LIX** with 246-262 ppm, reported beforehand.[84] Complex **45** could be further purified via filtration (inside the glovebox) and obtained with a 73 % yield and further characterized. In the other cases (**37a, 38**) an unselective reaction could be observed with no signal fitting for a corresponding *P*-amino substituted phosphaquinomethane complex, even with different bases utilized in case of **37a** (NEt_3, KHMDS) and **38** (NEt_3, KHMDS, ^{n}BuLi, LDA). Only possible indication was a short-lived strong violet colour during the course of the reaction; which may hint at an *in-situ* formed phosphaquinomethane complex.

The full detailed mechanism was then computed by *Qu* at the TPSS-D3/COSMO-RS(THF)/def2-QZVP//TPSS-D3/COSMO(THF)/def2-TZVP level of theory to better understand the formation of complexes **42c, 45** (figure 3.5.7).[121]

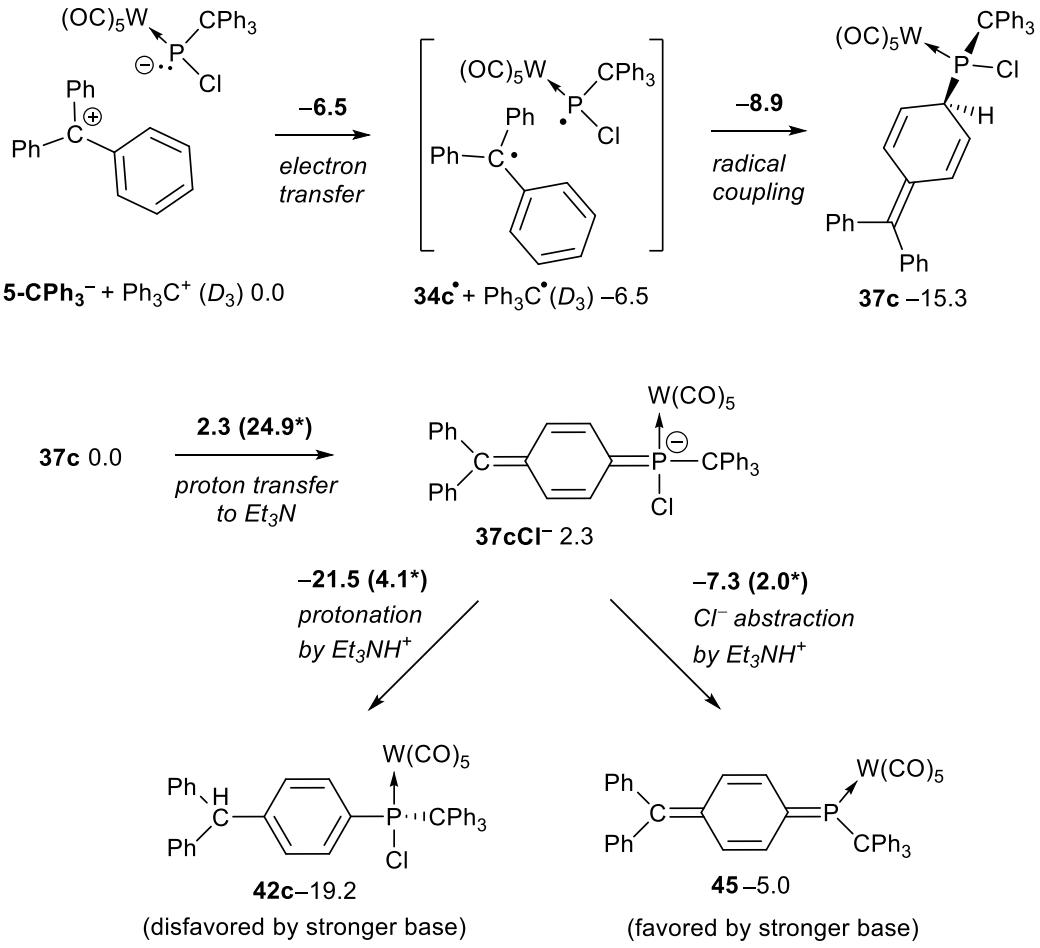

Figure 3.5.7 *DFT computed reaction free energy paths (in kcal/mol) for the formation of various complexes **37c**, **42c** and **45**. For each reaction step, the free energy change ΔG (and barrier ΔG* in parentheses) are shown above the arrows.*

Dissolved in THF, complex **5-CPh$_3$** exists as an ion pair of **5-CPh$_3^-$** and Li(thf)$_4^+$. The single electron transfer (SET) reaction with CPh_3^+ is 6.5 kcal/mol exergonic forming the corresponding radical pair **34c$^\bullet$** + $^\bullet CPh_3$, which should exist for rather short time in the solvent cage. The followed selective P,C-coupling in *para*-position appears to be 8.9 kcal/mol exergonic, which was surprising when looking at the spin density distribution of CPh_3 with 0.59*e*, 0.11*e* and 0.12*e* at *ortho*-, *meta*- and *para*-positions of the phenyl rings, respectively (0.68*e* at P)[82]. Yet, the C,P-coupling at the central and *ortho*-carbons appear to be reversible with a neutral free energy. It should be mentioned at this point, that direct P,C-coupling of **5-CPh$_3^-$** and CPh_3^+ are almost barrierless and may compete with the SET pathway, although

yielding the same coupled complex **37c**. The next step was the proton abstraction from the former *para*-C going over a high free energy barrier of 24.9 kcal/mol forming complex **37cCl⁻** (2.3 kcal/mol endergonic). The importance of the base shows itself for the next two feasible and competing reaction channels with small free energy barriers of 2-4 kcal/mol. One being the (reversible) chloride abstraction forming complex **45** being 5.0 kcal/mol exergonic and kinetically slightly favoured, the other being the protonation of **37cCl⁻** at the CPh_2 site which is thermodynamically strongly favoured by 14.2 kcal/mol due to the formation of the aromatic ring system. The protonation appears to be the crucial step, since it also becomes 11.4 kcal/mol more endergonic when using a strong base like $(SiMe_3)_2N^-$ (from KHMDS), even though the initial proton abstraction gets 30.5 kcal/mol more exergonic, since KHMDS appears to be 32.8 kcal/mol or 24.0 pKb units more basic than Et_3N.

With this background information, it should be mentioned that a crucial factor for the in 2010 reported synthesis might be the different routes for obtained Li/Cl phosphinidenoid complexes (scheme 1.4.1), since the previously used route, starting from the chlorophosphane instead of the dichlorophosphane complexes, yielded reaction mixtures containing diisopropylamine which immediately promoted the follow-up reactions (1,5H-shift/HCl elimination).[82]

The experimentally obtained UV/vis absorption spectra of complex **45** possesses three major absorption bands at 238.0, 336.0 and 563.0 nm (5.21, 3.69 and 2.20 eV, respectively), with the absorption of 563.0 nm (visible spectrum, yellow) resulting in the dark blue violet appearance of complex **36** (figure 3.5.8). TD-DFT (PBE0/def2-TZVPD) calculations by *Qu* clearly indicate the first band corresponding to the electronic π→π* type HOMO–LUMO transition (computed excitation at 2.02 eV with a large oscillator strength of 0.94) within the phosphaquinomethane motif. The second band is most likely due to a *metal-to-ligand* charge-transfer excitation.

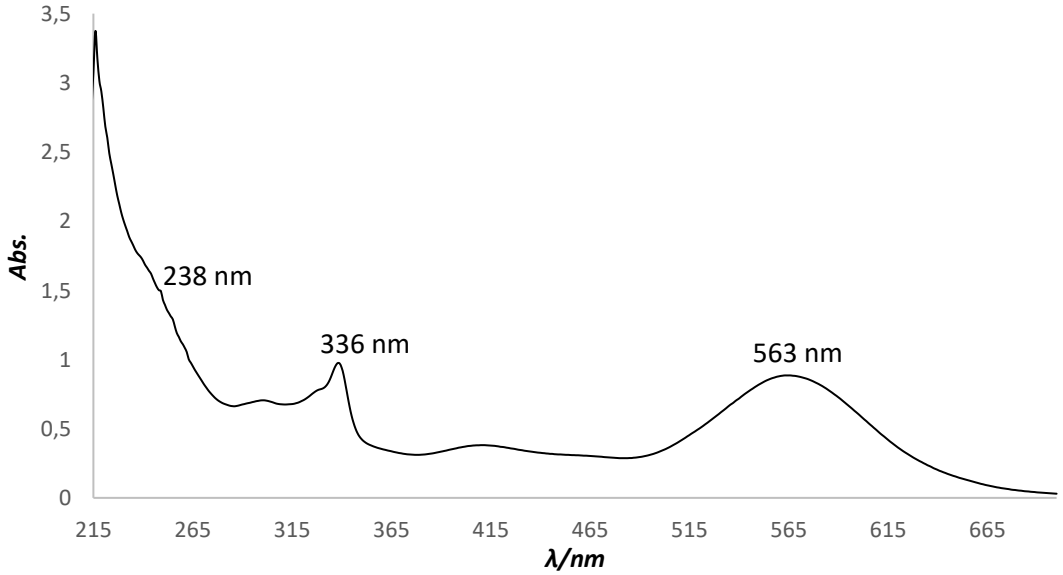

Figure 3.5.8 *UV/vis spectrum of* ***45*** *in THF solution.*

To investigate the quest of "innocence" of the phosphaquinomethane $W(CO)_5$ complexes, cyclo voltammetric experiments were performed in THF (figure 3.5.9) and MeCN (figure 3.5.10).

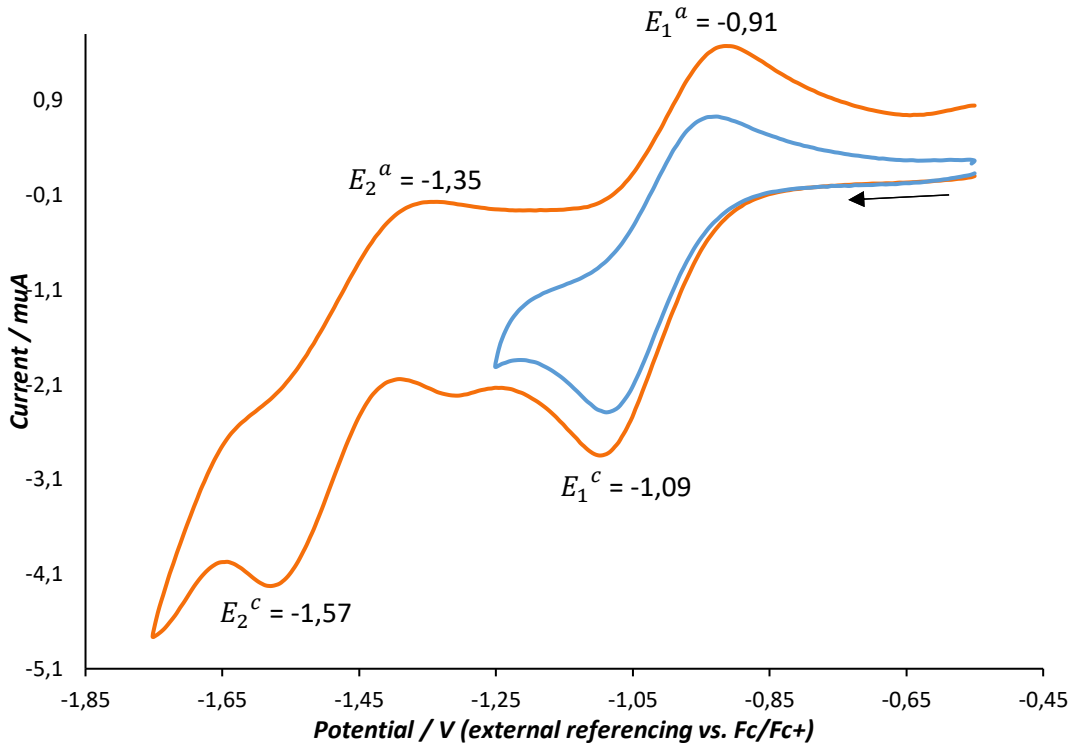

Figure 3.5.9 *Cyclic voltammograms on solutions of* ***45*** *in THF with potential values given in V and the scan direction indicated shown with an arrow (2 mmol/L of* ***45****, 0.2 mol/L n-Bu_4NPF_6, 50 mV/s (orange), 100 mV/s (blue)).*

The general appearance of the curves is very similar to that of the earlier reported free phosphaquinomethane by *Yoshifuji* as the cyclic voltammetric measurements also revealed a two-wave-stepwise reduction, typical for quinoidal systems.[84,86] The first reduction takes place at -1.09 V with its oxidation return wave at -0.91 V yielding a midpoint potential of E_m = -1.00 V (vs. $Cp_2Fe^{0/+}$) (-1.83 V for **LXI**)[86] for the -1/0 process with a rather large peak difference $\Delta E_p^c - \Delta E_p^a$ of 0.18 V. The next reduction process -2/-1 can be seen at -1.57 V with a separation of ΔE = 0.48 V to the -1/0 process and a rather small return wave at -1.35 V yielding a midpoint at E_m = -1.46 V (vs. $Cp_2Fe^{0/+}$) with a large peak difference of 0.22 V. The inequivalent shape as well as the large peak separation for the -2/-1 process shows a rather irreversible (or at best quasi-reversible) second process, most likely accompanied with a structural change. Reversible or irreversible (irr) processes happening during CV can either be purely electronical (E) or followed by chemical processes (C). Overall, the mechanism here is best described as EE_{irr} or EEC_{irr}, if the second reduction is followed by some sort of chemical reaction (*e.g.* loss of CO). Nevertheless, the results give clear evidence for the stabilizing effect of the $W(CO)_5$ group towards reduction showing significantly greater (chemical) reversibility compared to **LXI** even when the latter

was measured at 195 K.[86] Complex **37** was also measured and a slightly higher E_m = -1.36 V (vs. $Cp_2Fe^{0/+}$) was determined.

The isolated -1/0 process in MeCN was measured over different scan rates 20 – 1500 mV/s and are displayed in figure 3.5.10.

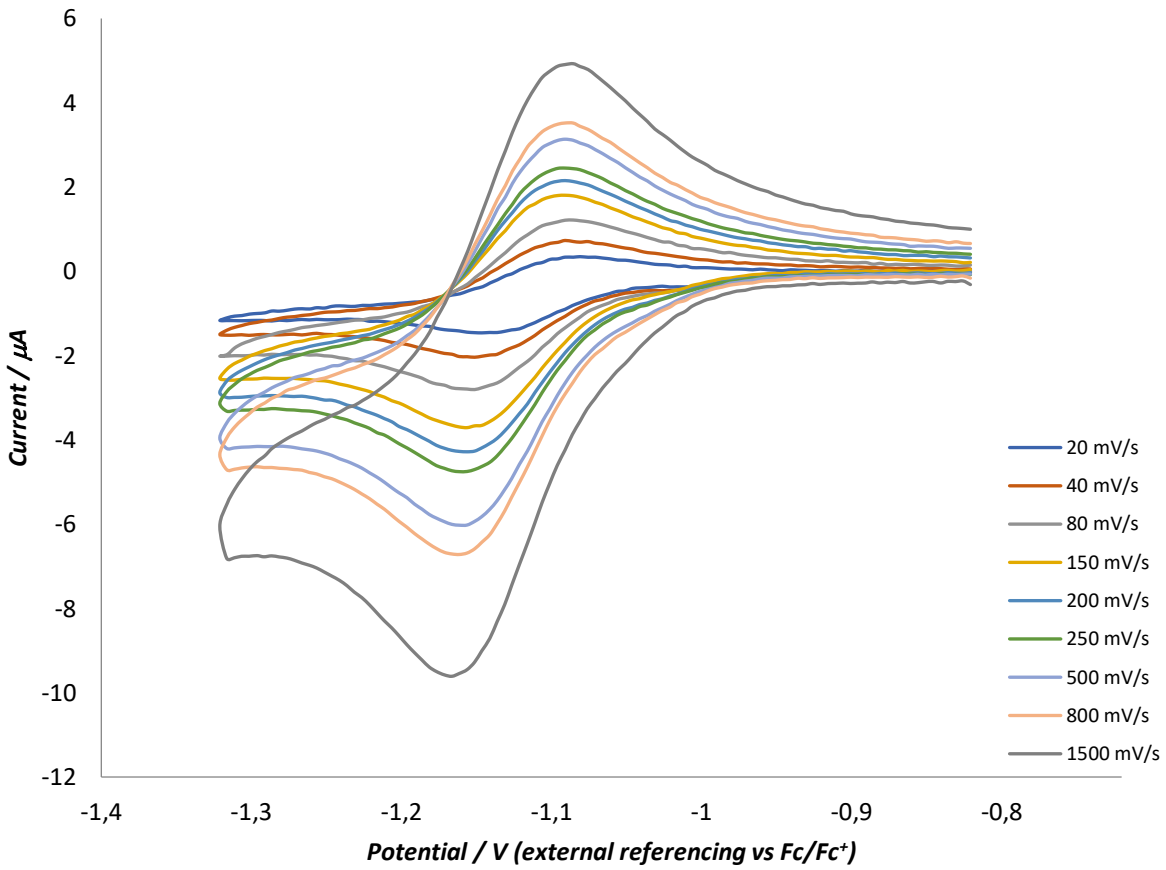

Figure 3.5.10 *Cyclic voltammograms on solutions of* ***45*** *in MeCN (2 mmol/L of* ***45****, 0.1 mol/L n-Bu_4NPF_6).*

It can be seen, that for the measurements in MeCN, which is in most cases an electrochemically more suitable solvent, the peak difference is only 0.079 V and appears to be invariant over all measured scan rates from 20 – 1500 mV/s, which is indicative of reversible processes.

It is important to keep in mind that the flux is the sum of migration (movement of particles due to electrical fields), convection (movement of particles due to forced movement of solution) and diffusion (movement of particles due to concentration gradients). The use of high electrolyte concentrations reduces migration effects, while a quiescent solution removes the influence of convection. The remaining term of diffusion is influenced by the concentration gradient near the electrodes surface, which itself is affected by how fast the species can diffuse through solution. The concentration of the species at the surface is set by the *Nernst* equation[122] and increases with the

scan rate. The *Randles-Sevčik* equation[123] (formula 3.5.1) describes a root-one-half dependence of the current *I* with the scan rate *v* which, if plotted against each other, displays a linear behaviour and shows the existence of a truly reversible one electron redox process (figure 3.5.11).

$$i_p = 0.4463nFAC\left(\frac{nFvD}{RT}\right)^{\frac{1}{2}}$$

Formula 3.5.1 *One description of the Randles-Sevčik equation. (i_p / A = current maximum, n = average number of electrons = 0.78, F = Faraday constant = 96485.33 C mol^{-1}, A = electrode area = 0.126 cm^2, C = concentration = 0.002 mol/mL, D / cm^{2}s^{-1} = diffusion coefficient, v / s = scan rate, R = gas constant = 8.314462 J K^{-1}mol^{-1}, T = 298 K).*

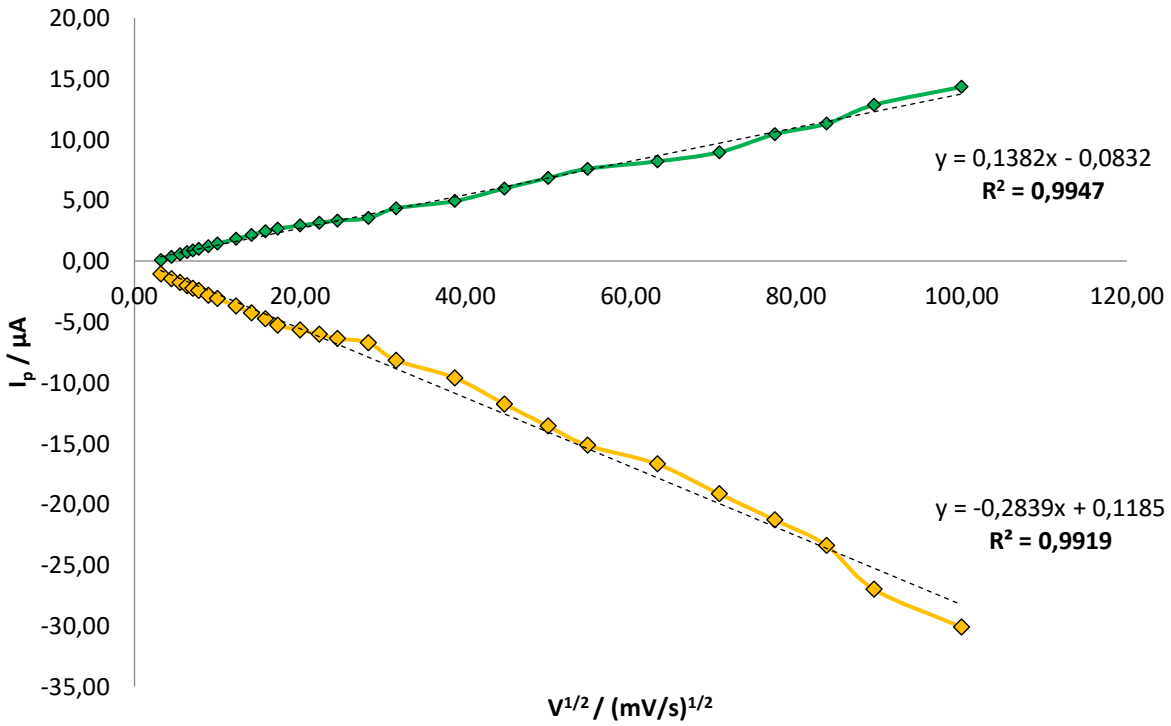

Figure 3.5.11. *Plotted Randles- Sevčik equation for the reductive (bottom) and oxidative (top) process of **45** in MeCN solution (figure 3.5.11).*

It can be seen, that for both processes a very linear plot for $i_p \sim v^{1/2}$ could be obtained with $R^2 = 0.9947$ and $R^2 = 0.9919$ for the oxidative and reductive processes, respectively. This indeed proves the existence of a diffusion controlled reversible one-electron process for this case. Moreover, from this the corresponding diffusion constants *D* could be calculated with 8.812×10^{-6} and 3.719×10^{-5} cm^2/s for oxidation and reduction, respectively.

The formation of a radical anion could further be seen from a chemical reduction in THF using KC_8 as reductant (scheme 3.5.3).

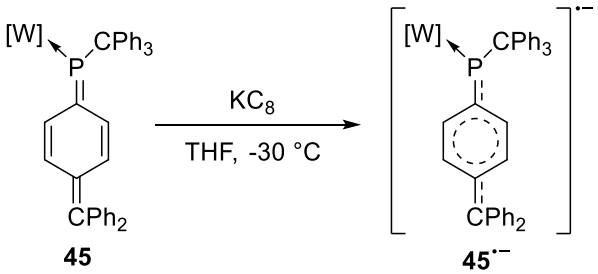

Scheme 3.5.3 *Chemical reduction of* ***45*** *using KC_8 at low temperature in the glove box.*

The reaction solution immediately underwent a colour change from dark purple to dark red with no visible ^{31}P NMR signal (*WIDE* measurement). (Cw-)EPR measurements displayed a signal with a g value of 2.0029 (figure 3.5.12), which appeared to be very close to a "free" electron ($g_e \approx 2.00$ for pure spin magnetism)[124] or a CPh_3-radical (*Gomberg* radical: $g = 2.0026$),[125] which is structurally similar to the "bottom" part of the **45** radical anion. The missing visible coupling with the P-atom indicates a strong localization of the radical at the carbon chromophore of the complex (**45**). It was indicated before by EPR spectra and DFT calculations that the electron spin density can mainly reside on carbon atoms rather than on phosphorus in such species.[126]

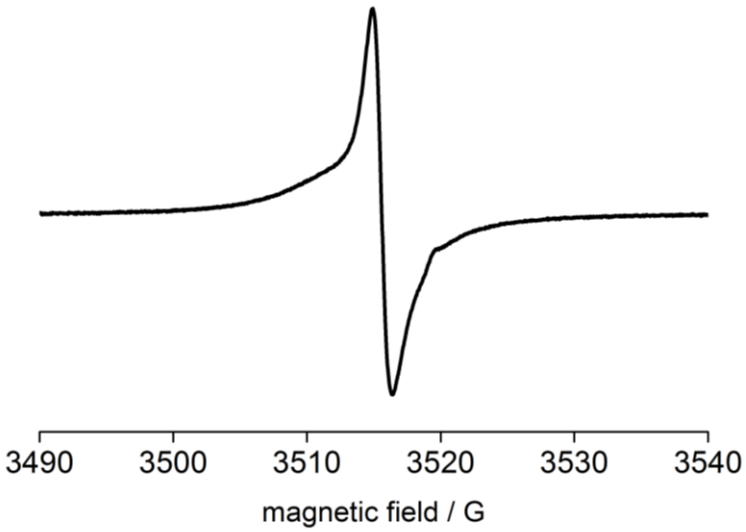

Figure 3.5.12 *(Cw-)EPR measurement of the reaction solution (scheme 3.5.3) at room temperature (g = 2.0029) with ~0.4 mol/L.*

For further insights, theoretical studies on phosphaquinomethane pentacarbonyl tungsten complex **45** were done, focusing on relevant redox properties for differently charged (redox) states and on the

nature of the additional P substituent. Two phosphaquinomethanes bearing model Me and NH_2 substituents at P were computed either as free ligands (**47**) and as metal complexes using the $W(CO)_5$ fragment (**48**) (figure 3.5.13).

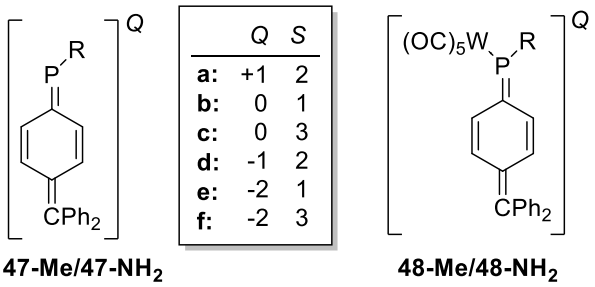

	Q	S
a:	+1	2
b:	0	1
c:	0	3
d:	-1	2
e:	-2	1
f:	-2	3

Figure 3.5.13 *Computed phosphaquinomethane model systems as free ligand* ***47-Me/47-NH₂*** *and metal complex* ***48-Me/48-NH₂****.*

Each of these six different situations were computed with charges varying from +1 to -2 and considering the two possible spin states – singlet and triplet (*S* = 1, 3) – for neutral and dianionic species to get insight into possible diradical properties favoured by rearomatization of the ring. The structures were optimized and computed at the B3LYP-D3/COSMO(THF)/def2-TZVP level representing a robust and often used hybrid functional.[105] Herein, the focus was on the bond lengths, the bond orders (MBO), the *Löwdin* charges at relevant parts of the molecules and HOMO-LUMO gaps (table 3.5.2).

Table 3.5.2 *Computed electronic and structural (Å) parameters of the model compounds* ***47-Me/47-NH₂*** *and* ***48-Me/48-NH₂.***

Q / S		d(C-C_{ring})	d(P-C_{ring})	MBO(C-C_{ring})	MBO(P-C_{ring})	MBO (PW)	MBO(PR)	E_{HOMO}/eV	E_{LUMO}/eV	$\lvert\Delta E_{HOMO/LUMO}\rvert$/eV
+1 / 2	**47a-Me**	1.429	1.774	1.125	1.290	-	1.057	-6.43	-4.32	2.11
	47a-NH_2	1.424	1.752	1.157	1.299	-	1.346	-5.88	-3.90	1.98
	48a-Me	1.423	1.751	1.152	1.224	1.021	0.987	-5.93	-4.19	1.74
	48a-NH_2	1.424	1.744	1.157	1.191	0.998	1.270	-5.75	-3.83	1.92
0 / 1	**47b-Me**	1.383	1.719	1.393	1.655	-	1.052	-5.03	-2.66	2.37
	47b-NH_2	1.383	1.709	1.412	1.607	-	1.160	-4.62	-2.24	2.38
	48b-Me	1.385	1.708	1.381	1.473	0.795	0.958	-4.98	-2.84	2.14
	48b-NH_2	1.382	1.696	1.414	1.434	0.813	1.124	-4.75	-2.49	2.26
0 / 3	**47c-Me**	1.471	1.809	0.974	1.175	-	1.064	-4.43	-0.80	3.63
	47c-NH_2	1.468	1.809	0.987	1.169	-	1.181	-4.18	-0.77	3.41
	48c-Me	1.465	1.796	0.994	1.059	0.895	0.972	-6.18	-3.46	2.72
	48c-NH_2	1.462	1.803	1.008	0.924	0.771	1.167	-4.51	-1.63	2.88
-1 / 2	**47d-Me**	1.427	1.773	1.186	1.455	-	1.081	-3.37	-1.41	1.96
	47d-NH_2	1.427	1.766	1.196	1.443	-	1.014	-3.18	-1.24	1.94
	48d-Me	1.445	1.814	1.083	1.044	0.670	0.976	-4.19	-1.99	2.20
	48d-NH_2	1.445	1.812	1.087	1.009	0.646	1.030	-4.21	-1.98	2.23
-2 / 1	**47e-Me**	1.488	1.813	0.889	1.365	-	1.110	-1.92	1.01	2.93
	47e-NH_2	1.488	1.818	0.893	1.324	-	0.957	-1.89	1.03	2.92
	48e-Me	1.472	1.830	0.981	0.960	0.671	0.971	-2.20	-0.11	2.09
	48e-NH_2	1.469	1.823	0.998	0.963	0.676	1.015	-2.18	-0.12	2.06
-2 / 3	**47f-Me**	1.442	1.788	1.121	1.444	-	1.095	-0.15	1.05	1.20
	47f-NH_2	1.442	1.790	1.124	1.399	-	0.977	-0.14	1.09	1.23
	48f-Me	1.442	1.781	1.120	1.235	0.358	0.983	-1.01	0.26	1.27
	48f-NH_2	1.441	1.778	1.120	1.179	0.331	1.009	-1.10	0.32	1.42

It is apparent that it is very important to calculate closed-shell systems (**b, e**) in a singlet as well as a triplet state since it has a strong influence on the structural and electronic properties. It can be seen that system **b** displays the shortest C-C_{ring}/P-C_{ring} bonds with an average of 1.383 and 1.708 Å, respectively. It also fits with the obtained highest double bond character according to the MBO values (1.655 (**47b-Me**), 1.607 (**47b-NH_2**), 1.473 (**48b-Me**) and 1.434 (**48b-NH_2**)). The result is a strong deviation towards **c** displaying significant bi-radical character with MBO values smaller by ~0.4 or 29.2 % and 29.8 % (by average) for C-C_{ring} and P-C_{ring} bonds, respectively. The double negatively charged singlet system (**e**) has in total the longest C-C_{ring}/P-C_{ring} bonds, indicating the at least partial occupation of the π*(C-C)- and π*(P-C)-orbitals (*vide infra*) and therefore less double bond character which will

also result in a more aromatic ring. The MBO values for the P-W and P-R bonds strongly correlate with the charge of the system (not so much with the spin system) which is of course the result of the stabilization effects of these substituents (figure 3.5.14). For example, the MBO for the P-W bond decreases with increasing negative charge of the system from 1.021 (**48a-Me**) and 0.998 (**48a-NH_2**) to 0.358 and 0.331, respectively. This indicates a localization of the charge at the metal centre with partial occupation of the σ*(P-W) orbital. The same behaviour can be seen for NH_2 substitution starting from MBO for the P-N bond of 1.346 (**47a-NH_2**) and 1.270 (**48a-NH_2**), due to the +M-effect of the N towards the positively charged system, decreasing to 0.983 and 1.009, respectively.

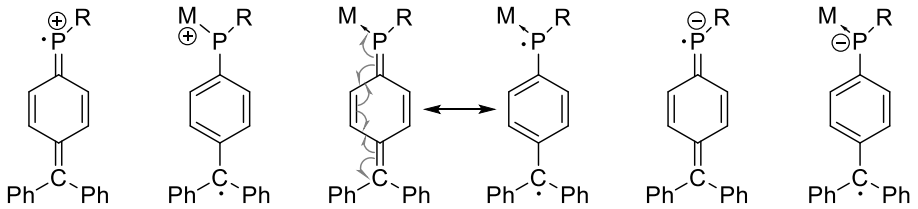

Figure 3.5.14 *Aromatization of the phosphaquinomethane moiety on changing the electronic state of neutral compounds **1**-**2** from singlet (**b**) to triplet (**c**) and most likely description of the one-electron oxidation (**a**) and reduction (**d**) products (R = Me, NH_2; M = LP, $W(CO)_5$).*

The size of the HOMO-LUMO gap changes significantly depending on charge and spin state of the system. The complexes **48** show smaller gaps than the corresponding free systems for the neutral (**b**, **c**), the cationic (**a**) and closed-shell anionic (**e**) systems which is the opposite for the open-shell anionic systems (**d-f**). The largest differences can be seen for the systems **c-Me, e-Me/NH_2** and **f-Me/NH_2** with ~ 1 eV.

When looking at the q^L(P) it becomes apparent that the $W(CO)_5$ group is electron withdrawing with a large part of the negative charge then locating at the metal centre. The result is a significantly higher q^L(P) value for all complexes (**48**) by 0.2 - 0.3.

Table 3.5.3. *Computed electronic parameters of the model compounds* ***47-Me/47-NH₂*** *and* ***48-Me/48-NH₂.***

Q / S		q^L(P)	$spin^L$(P)	q^L(5-C)	$spin^L$(5-C)	q^L ($PW(CO)_5$)	$spin^L$ ($PW(CO)_5$)	q^L(PR)	$spin^L$(PR)
+1 / 2	**47a-Me**	0.609	0.572	0.067	0.093	-	-	0.503	0.624
	47a-NH₂	0.615	0.235	0.037	0.214	-	-	0.773	0.341
	48a-Me	0.775	0.243	0.049	0.154	0.609	0.469	0.758	0.267
	48a-NH₂	0.738	0.127	0.029	0.248	0.569	0.203	0.941	0.181
0 / 1	**47b-Me**	0.436	-	-0.016	-	-	-	0.276	-
	47b-NH₂	0.446	-	-0.043	-	-	-	0.481	-
	48b-Me	0.697	-	-0.013	-	0,234	-	0,634	-
	48b-NH₂	0.659	-	-0.036	-	0,240	-	0,759	-
0 / 3	**47c-Me**	0.461	0.753	-0.006	0.399	-	-	0.304	0.820
	47c-NH₂	0.348	0.664	-0.007	0.396	-	-	0.353	0.838
	48c-Me	0.688	0.572	-0.006	0.393	0,270	0.808	0.614	0.630
	48c-NH₂	0.594	0.561	-0.006	0.388	0.125	0.733	0.681	0.721
-1 / 2	**47d-Me**	0.165	0.359	-0.082	0.203	-	-	-0.069	0.391
	47d-NH₂	0.167	0.441	-0.100	0.153	-	-	0.050	0.506
	48d-Me	0.398	0.052	-0.026	0.344	-0.349	0.081	0.218	0.057
	48d-NH₂	0.350	0.051	-0.026	0.343	-0.435	0.082	0.269	0.053
-2 / 1	**47e-Me**	-0.094	-	-0.148	-	-	-	-0.389	-
	47e-NH₂	0.164	-	-0.148	-	-	-	-0.354	-
	48e-Me	0.380	-	-0.145	-	-0.469	-	0.185	-
	48e-NH₂	0.343	-	-0.144	-	-0.561	-	0.246	-
-2 / 3	**47f-Me**	0.029	0.187	-0.077	0.296	-	-	-0.237	0.205
	47f-NH₂	-0.038	0.188	-0.078	0.294	-	-	-0.205	0.197
	48f-Me	0.346	0.228	-0.050	0.291	-1.040	1.015	0.135	0.247
	48f-NH₂	0.284	0.236	-0.052	0.285	-1.098	1.020	0.166	0.256

A similar behaviour can be seen when looking at the spin distribution (figure 3.5.15), first at the cationic system (**a**). It is obvious that an amino substituent stabilizes the same amount as the $W(CO)_5$ group (with *P*-Me) ($spin^L$(P): 0.235 **47a-NH₂,** 0.243 **48a-Me**). For **47a-Me** the spin density can be mainly found at the P with 0.572 (or PR 0.624). In general, the spin density at the $PW(CO)_5$ moiety increases going from cationic (**a**) 0.469 (**48a-Me**) and 0.203 (**48a-NH₂**) to the anionic system (**f**) with 1.015 and 1.020, respectively.

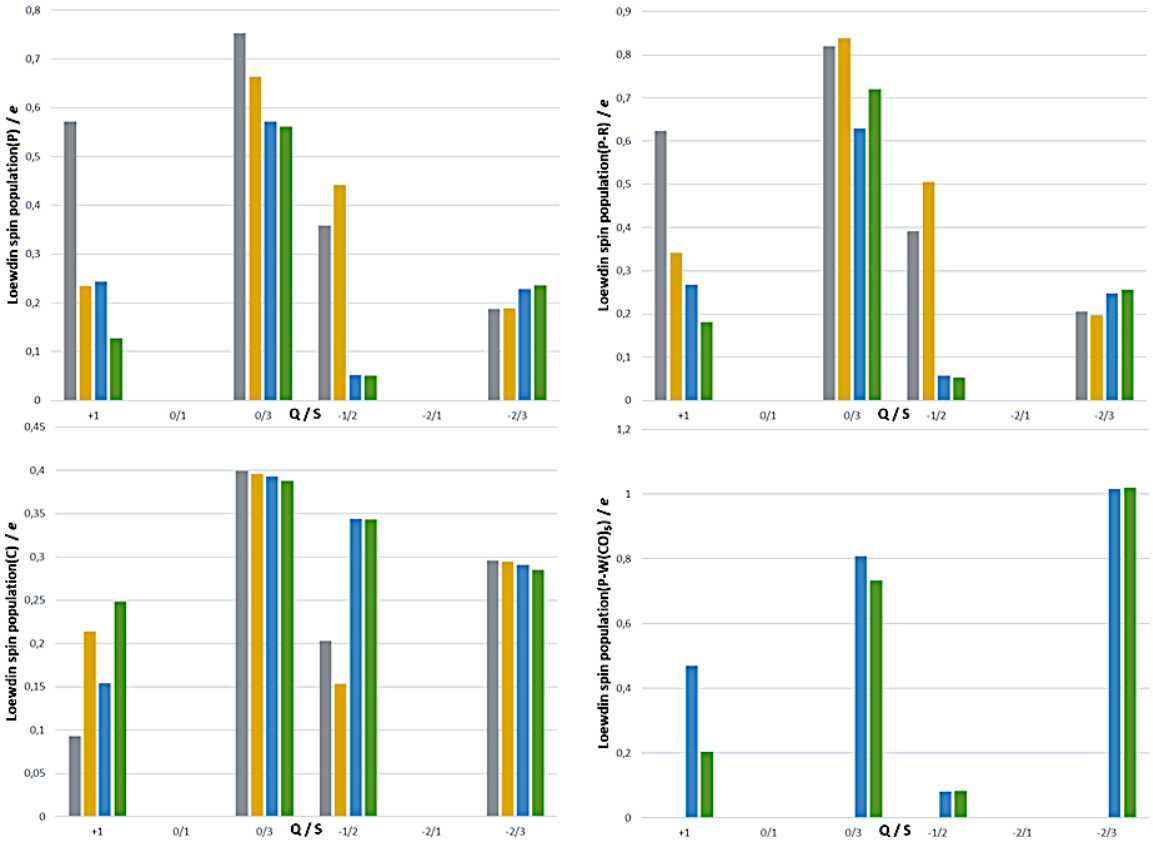

Figure 3.5.15 *Computed spin charge populations for P (top left), P-R (top right), C(CPh$_2$) (bottom left) and P-W(CO)$_5$ (bottom right) plotted against all charged states for complexes* ***47a,b*** *(grey, yellow) and* ***48a,b*** *(blue, green).*

One particular surprising finding is the properties of the radical anion (**d**). It shows the by far smallest spin^L(P) of 0.052 (**Me**) and 0.051 (**NH$_2$**) as well as spin^L(PW(CO)$_5$) of 0.081 (**Me**) and 0.082 (**NH$_2$**). The complexes for (**d**) also show a significantly higher spin^L(5-C) of 0.344 (**Me**) and 0.343 (**NH$_2$**) as the free systems with 0.203 and 0.153, respectively. The charge completely remains at the PW(CO)$_5$ moiety which can be seen when comparing the values q^L(PW(CO)$_5$) -0.349 (**48d-Me**) and -0.435 (**48d-NH$_2$**) to the singlet dianion (**e**) which should have a complete charge separation between the PW(CO)$_5$ moiety and the C chromophore q^L(PW(CO)$_5$) -0.469 (**48e-Me**) and -0.561 (**48e-NH$_2$**), respectively. The result is a strongly delocalized radical at the carbon chromophore with very little spin density at the PW(CO)$_5$ moiety. Therefore, complexes **48** are best described as distonic radical anions (DRAs), a term introduced in 1984[127] for ions with a separation of charge and radical sites, representing another class of radical anions (conventional vs distonic). Distonic ions (anionic or cationic) in general show large differences in stability and reactivity compared to the corresponding conventional radical ion and have been studied until today.[128] The strong radical delocalization for complexes **48** should also result in the lowest change of the structure of the ligand, which should strongly contribute to the reversibility

of the one-electron reduction. It also gives more strong evidence for the non-innocence of such phosphaquinomethane ligands in group 6 metal complexes regarding one-electron-reduction.

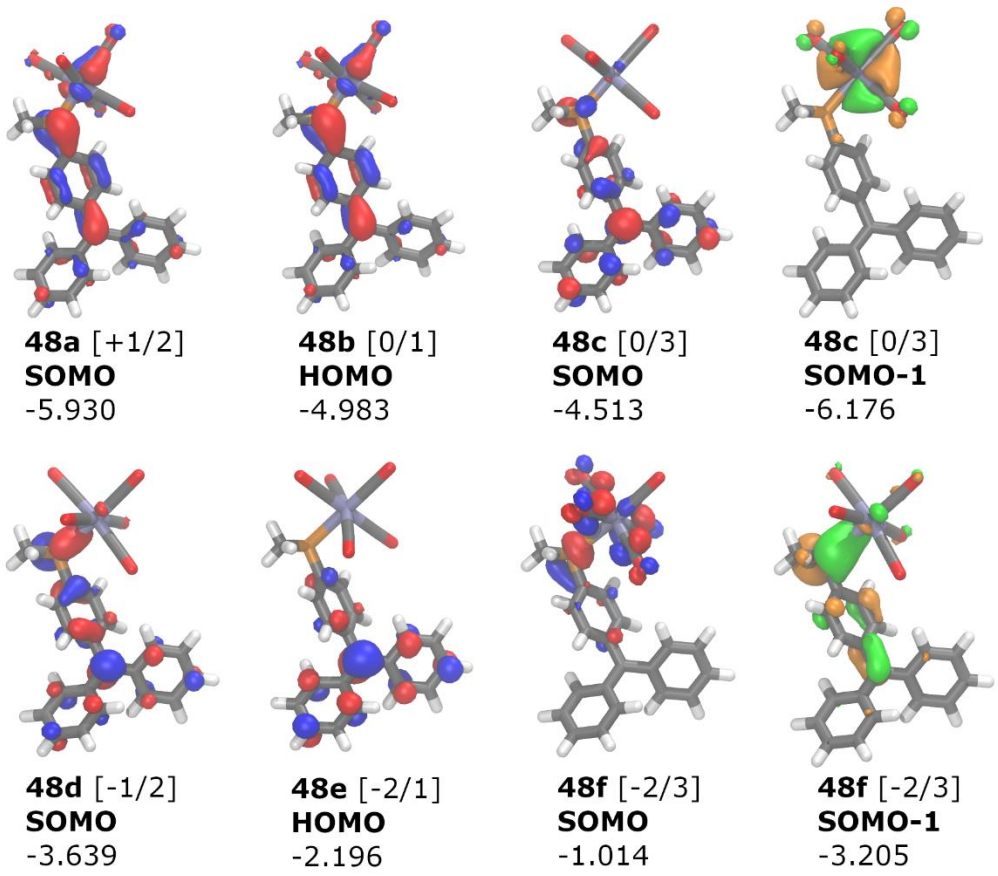

Figure 3.5.16 *HOMO and SOMO frontier orbitals of* ***48a-f-Me*** *with the charge (Q) and spin state (S) given in square brackets and energy values in eV.*

To quantify the aromaticity *nucleus independent chemical shift* (NICS) calculations[129] were done using GIAO B3LYP/def2-TZVPPD on the beforehand optimized structures (table 3.5.4). The TZVPPD basis sets inherit additional polarization (P) and diffuse functions (D) necessary for NICS calculations, similar to the often used 6-311+G* basis sets.[129] For these calculation a dummy atom is placed 1 Å above/under the ring and a NMR calculation is performed. The obtained isotropic shielding of the atom functions as a measurement of the ring-current as one model of aromaticity and is usually compared to benzene. Signs of the computed values are reversed corresponding to the NMR chemical shift convention with negative NICS shifts denote aromaticity, while positive NICS shifts describe antiaromaticity.

Table 3.5.4 *NICS(1) values for compounds* ***47-48*** *(benzene: -13.45).*

	+1/2 (**a**)	0/1 (**b**)	0/3 (**c**)	-1/2 (**d**)	-2/1 (**e**)	-2/3 (**f**)
47-Me	-6,42	-2,20	-7,60	-3,63	-4,81	-4,09
47-NH_2	-5,66	-1,63	-7,36	-3,34	-4,64	-4,11
48-Me	-5,87	-2,48	-7,43	-5,93	-6,38	-3,02
48-NH_2	-5,53	-1,73	-7,40	-5,92	-6,11	-3,45

The NICS(1) values display a similar behaviour regarding aromaticity as was indicated by the MBO (table 3.5.2) and spin distribution values (table 3.5.3). The biggest difference is presented for the radical anions regarding free ligands and complexes going from -3.63 (**47-Me**) and -3.34 (**47-NH_2**) to -5.93 (**48-Me**) and -5.92 (**48-NH_2**), respectively. Interesting is also the strong aromaticity in case of the neutral triplet state (**c**) showing a strong radical separation accompanied by the rearomatization of the central ring.

Since the aromaticity of the middle ring is a strong indicator for delocalization in addition to NICS also *Harmonic Oscillator Measure of Aromaticity* (HOMA) values were calculated using optimized geometries at the B3LYP-D3/COSMO(THF)/def2-TZVP level for the middle rings of all spin systems.[130,131] For this model the index of aromaticity is defined as a normalized function of variance of bond lengths inside the ring of the molecule (formula 3.5.3). R_{opt} was reported with 1.388 Å (for C-C), estimated from the corresponding double and single bonds and their deformation and compression energy, respectively.[130,131]

$$HOMA = 1 - \frac{\alpha}{n}\sum\left[R_{opt} - R_i\right]^2$$

Formula 3.5.3 *Formula for calculation of the HOMA index (with n = 6, being the number of bonds taken into summation and α = 257.7 $Å^{-2}$, an empirical constant fixed for HOMA = 1 for a perfect aromatic structure).*[131]

With this and the distances taken from the optimized structures the corresponding values were calculated, listed in table 3.5.5 for all compounds **47-48**.

Table 3.5.5 *Calculated HOMA values for compounds* ***47-48****.*

	+1/2 (**a**)	0/1 (**b**)	0/3 (**c**)	-1/2 (**d**)	-2/1 (**e**)	-2/3 (**f**)
47-Me	0,819	0,366	0,949	0,743	0,915	0,801
47-NH_2	0,781	0,354	0,952	0,738	0,932	0,815
48-Me	0,791	0,419	0,953	0,901	0,944	0,816
48-NH_2	0,798	0,361	0,956	0,907	0,938	0,819

There are a few things worth mentioning looking at the HOMA values, *e.g.* that all of the charged states display quite aromatic structures with +1/2 (**a**) showing the lowest (0.797) and -2/1 (**e**) the highest value (0.932). Also, a large discrepancy can be seen for the neutral spin states, whereas the singlet state (**b**) displays the expected quinoidal structure with a low average HOMA value of 0.374, the triplet state (**c**) yields an average value of 0.952 emphasizing the formation of the aromatic ring-structure as a 1,6-bi-radical, which in reality is better described as the combination of CPh_2- and (M)PR-centred radicals, respectively (figure 3.5.17). Inside each group of spin states there are small differences for the free ligands **47** and their complexes **39** (**a:** 0.78 %, **b:** 8.4 %, **c:** 0.43 %, **e:** 1.87 % and **f:** and 1.12 %) with the exception of the radical anion (**d**). As observed for the spin distributions there is also here a strong impact of the $W(CO)_5$ group visible increasing the HOMA value by 22.0 % somehow enhancing the aromaticity of the middle ring. This will result in a thermodynamically more stable molecule, which also displays the stabilizing effect of the $W(CO)_5$ group on the radical anion formation (as seen for the CV measurements).

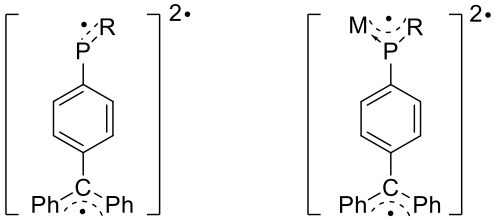

47c
(S = 3)

48c
(S = 3)

Figure 3.5.17 *Display of the radical localization for computed model compounds* ***47c*** *and* ***48c****.*

4. Summary

In this PhD Thesis results from the investigation on the synthesis of *P*-amino substituted Li/Cl phosphinidenoid complexes with a particular focus on their reactivity in polar and apolar solvents is presented. In particular, their use in the synthesis of phosphaquinomethane complexes was investigated experimentally and theoretically, and the obtained products studied via cyclic voltammetry to examine their redox properties with a special emphasis on the quest of a non-innocent character.

In chapter 3.1 six dichloro(diorganoamino)phosphane complexes (**2-4**) were synthesized, fully characterized and solid-state structures of **2a, 3b** and **4a** obtained. All complexes were theoretically investigated at the TPSS-D3/CPCM(THF)/def2-TZVP//PW6B95-D3/CPCM(THF)/def2-QZVP level regarding their structural (bond lengths, angles) and bonding parameters (MBOs). The data show a slight P-Cl bond elongation compared to the P-alkyl derivative **2-CPh$_3$**. MBOs for P-N bonds of 1.21 (*P*-NPh$_2$) and 1.35 (*P*-NCy$_2$) reveal some degree of π-donation from the N to the P atom which is in agreement with the observation of planar N environments in the solid state. Furthermore, the latter seems to be the reason for a partial destabilization of the P-Cl bonds.

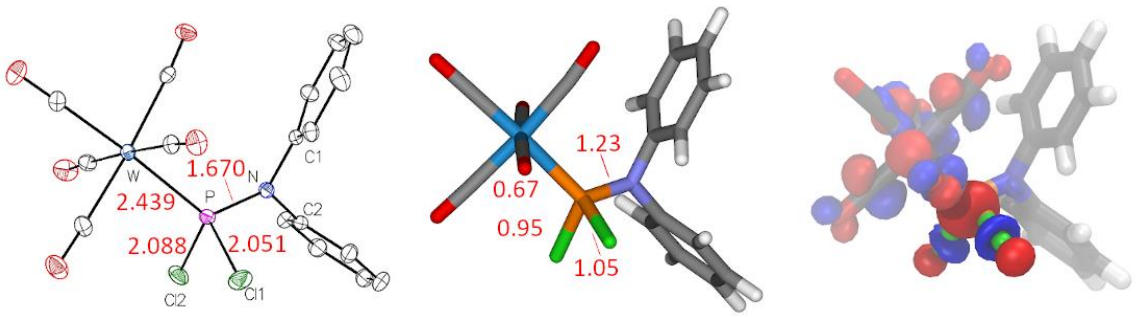

Figure 4.1 *Measured solid state structure (with bond lengths in Å), computed structure (with MBO values), as well as the LUMO frontier orbital for* ***2a****.*

In chapter 3.2, the experiments for the generation of *P*-amino substituted Li/Cl phosphinidenoid complexes **5-7** are described (scheme 4.1). These intermediates appeared to be thermally very labile which was shown in VT-NMR experiments, with the exception of **7a** displaying a signal in the very low-field region at 425.6 ppm. In-depth state of the art DFT calculations (TPSS-D3/COSMO(THF)/def2-TZVP//PW6B95-D3/COSMO-RS(THF)/def2-QZVP) were done in collaboration with Qu regarding possible solvated structures for complex **5a** and the conditions for its formation. The calculations postulated the most stable phosphinidenoid complex **5a** as separated ion pairs as **5a**$^-$ with [Li(12-crown-4)$_2$]$^+$. The situation changes if 12-crown-4 is absent and, for the first time, a possible equilibrium

between phosphinidenoid complex **5a** and the electrophilic terminal phosphinidene complex **22a** was revealed (figure 4.2). The latter possesses a rather small free energy reaction barrier of 3.3 kcal/mol.

In chapter 3.3 trapping reactions of the *in-situ* generated Li/Cl phosphinidenoid complexes **5-7** are described, using typical well-established trapping reagents MeOH and $MeNH_2$. Yet, due to the thermal instability of the reactive intermediates the existing protocol had to be altered, *i.e.*, lower temperatures and 2 eq. of 12-crown-4 were necessary to obtain a higher selectivity regarding formal EH-insertion reactions (Scheme 4.1). All complexes, except for **17b**, could be assigned in the ^{31}P NMR spectrum due to a characteristic coupling pattern. Complexes **15a, 18a,b** and **19a** could then be isolated, purified and fully characterized. Again, all complexes **14-19** were theoretically investigated regarding their bond orders (MBO), HOMO-LUMO gaps and partial charges, and the structures of complexes **15a, 18a** and **19a** were confirmed via single crystal X-ray diffraction analysis (figure 4.3). For all *P*-NPh_2 (**a**) compounds a remarkable localization of the HOMO towards the NPh_2-group could be seen, again emphasising the influence of the amino-substitution on these complexes.

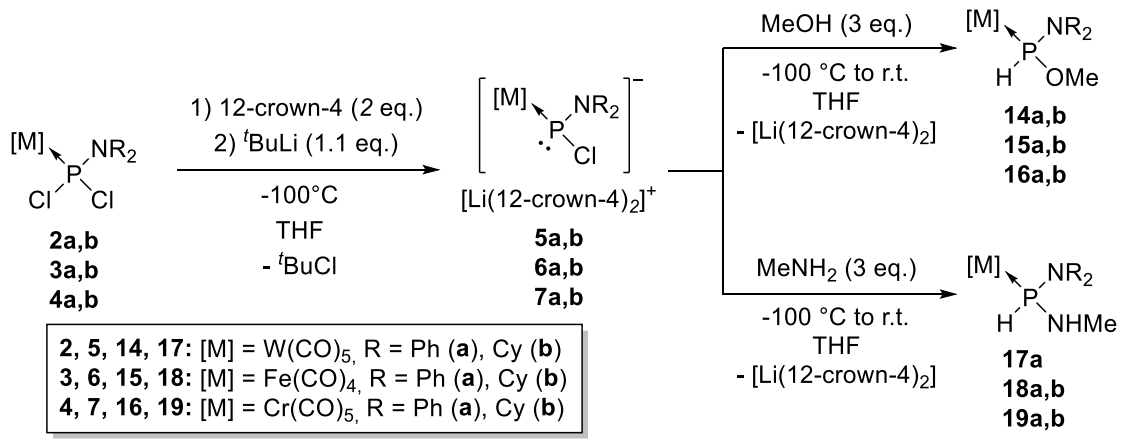

Scheme 4.1 Li/Cl phosphinidenoid complexes **5-7** generation and applied trapping reactions towards the corresponding alkoxyphosphane **14-16** and aminophosphane complexes **17-19**.

In chapter 3.4, the formation and reactivity of complexes **2a,b** in less polar solvents (toluene) was investigated with the quest to yield postulated reactive phosphinidene complexes as intermediates **22a,b** (scheme 4.2, also see figure 4.2). One crucial aspect of the trapping reactions was the addition of the olefin before *tert*-butyllithium. In case of tolane the reactions were not fully selective, but complexes **29a,b** were observed and identified by ^{31}P NMR spectroscopy and mass spectrometry.

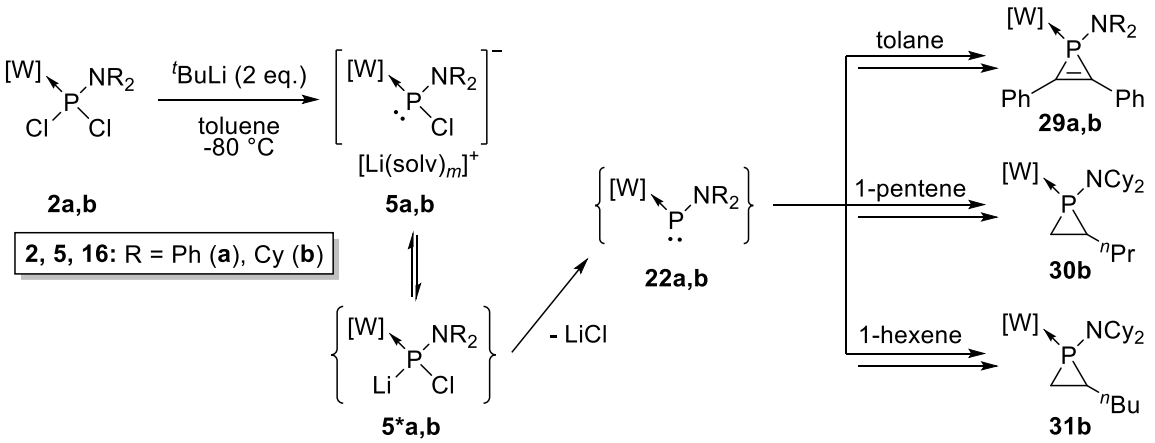

Scheme 4.2 *Generation and trapping of electrophilic phosphinidene complexes* ***22a,b****.*

Therefore, further very detailed calculations (TPSS-D3/CPCM(THF)/def2-TZVP//PW6B95-D3/CPCM(THF)/def2-QZVP) were performed regarding the chloride leaving ability from the anion of the phosphinidenoid complexes $\mathbf{5^-}$ to yield the corresponding phosphinidene complexes **22** (scheme 4.3).

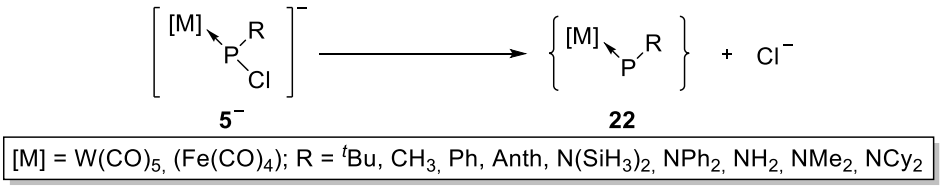

Scheme 4.3 *Computed formal chloride loss from complexes* $\boldsymbol{5^-}$ *forming complexes* ***22****.*

Therefore, complexes with various P-substituents (aryl, alkyl, amino) were calculated for tungsten and iron, thus leading, finally, to a very linear relation (R = 0.97) between the MBO(P-R) of complexes **22** and the relative free energy difference forming these (alkyl < aryl < (aryl)amino < (alkyl)amino). This shows that for the $W(CO)_5$ complexes **22** the stabilization of the phosphorus is mainly dependent on the substituent R – with the MBO(P-R) as a direct measure for the R→P electronic stabilization.

The stabilizing effect of the N-electron-lone-pair donation into the then empty P 3*p* orbital of **22a** was also seen for the computed solvated structures increasing the Wiberg bond index of the P-N bond from 1.09 ($\mathbf{5a^-}$) to 1.32 (**22a**) (figure 4.2).

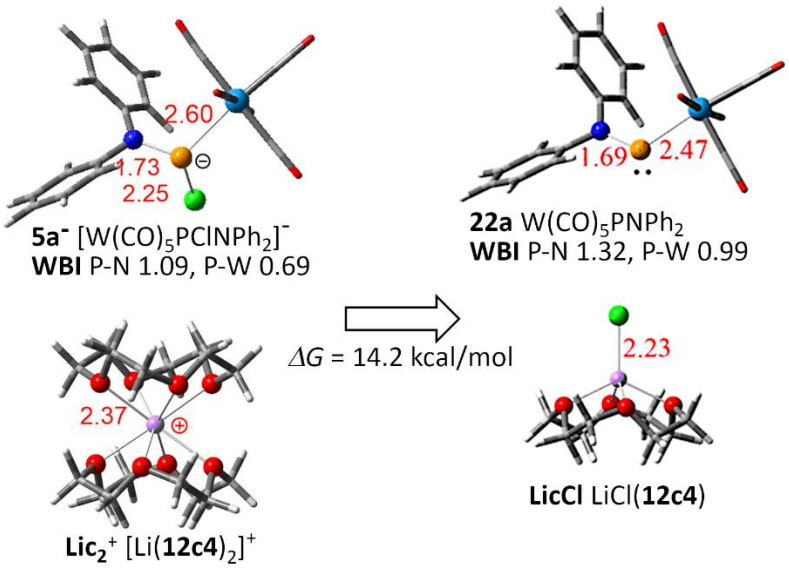

Figure 4.2 *Selected computed solution structure for complex* ***5a*** *(with bond lengths given in Å) as well as reaction free energies for different solvated structures (in kcal/mol).*

Trapping reactions, using **2b** (as starting material) for the intermediate and 1-pentene and 1-hexene showed a selective formation of the corresponding phosphirane complexes **30, 31** (scheme 4.2) which were isolated and fully characterized. VT-^{31}P NMR experiments (-70 °C to r.t.) revealed no observable intermediate. With complexes **30, 31**, being not stable in solution at ambient temperature for a longer time, additionally a so-called *hopping* reaction was observed if tolane was added. For example, the thermodynamically more stable complex **29b** was selectively formed from phosphirane complex **30b** (Scheme 4.4).

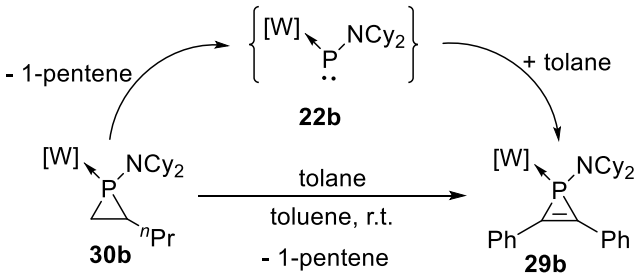

Scheme 4.4 *Observed "hopping" reaction of the transient phosphinidene complex* ***22b****.*

Very detailed calculations were performed by *Qu* to provide more insights into the intermediate conversions, including the crucial transition states for the reaction of complexes **5a** and **22a** with MeOH, tolane and ethene (Figure 4.4, here the TS for the $MeNH_2$ reaction is not shown).

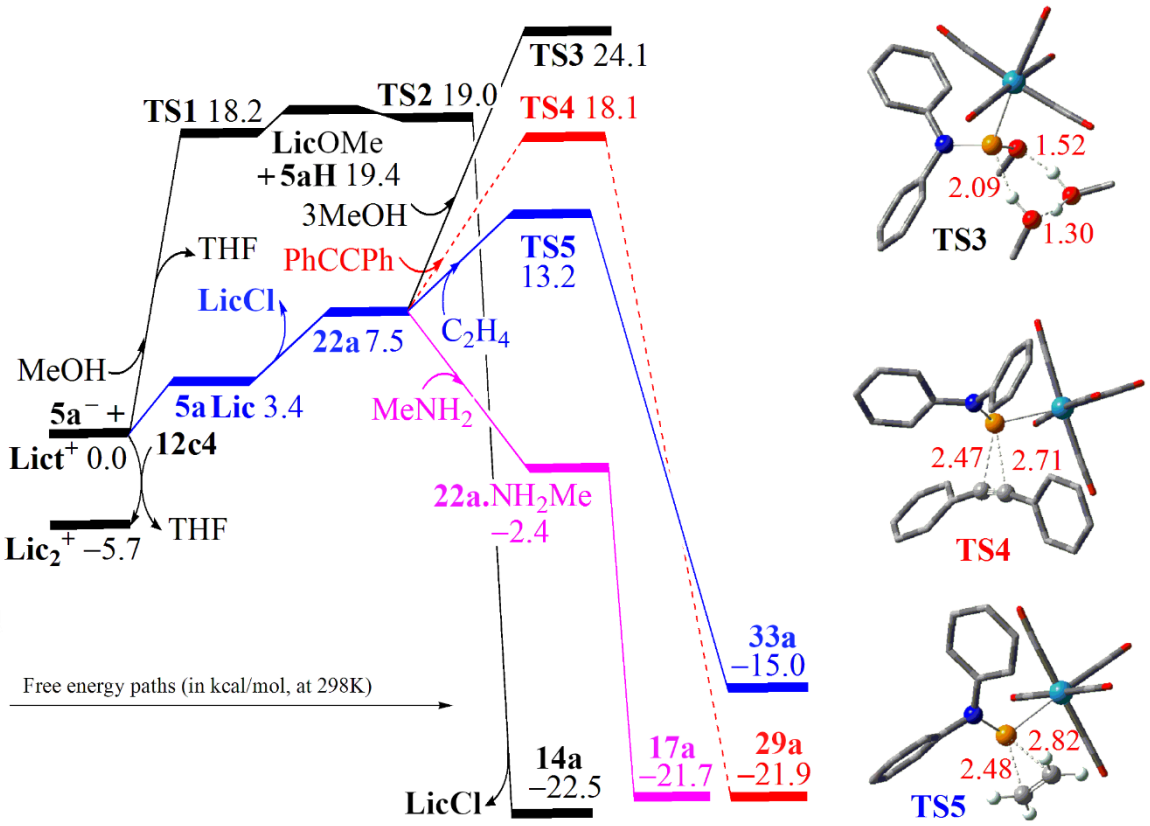

Figure 4.4 *Free energy reaction paths for several reaction pathways regarding phosphinidenoid complex* ***5a*** *and phosphinidene complex* ***22a****.*

The effect of the nucleophilicity of the reagent can be seen at the free energy level of the transition states: 24.1 kcal/mol (**TS3**, MeOH) > 18.1 kcal/mol (**TS4**, Ph_2C_2) > 13.2 kcal/mol (**TS5**, C_2H_4) > ~ 0 kcal/mol (NH_2Me). All of the investigations unveil the dichotomy of terminal phosphinidene and phosphinidenoid complexes, and this clearly underlines the influence of the solvent on the cation and, hence, on the relative stability of Li/Cl phosphinidenoid complexes.

In chapter 3.5, the synthesis of phosphaquinomethanes was investigated with focus on the beforehand only postulated intermediacy of de-aromatized complexes **37-39** (Scheme 4.5). To study the redox innocence of phosphaquinomethane ligands (in complexes **45, 46**) was another focus. Experimentally of particular importance is that the reaction of the transiently formed radical pair was stopped and the solvent removed at -50 °C, thus yielding complexes **37-39**. Complexes **37a** was obtained as crude product, while **38** and **39** could be isolated and fully characterized.

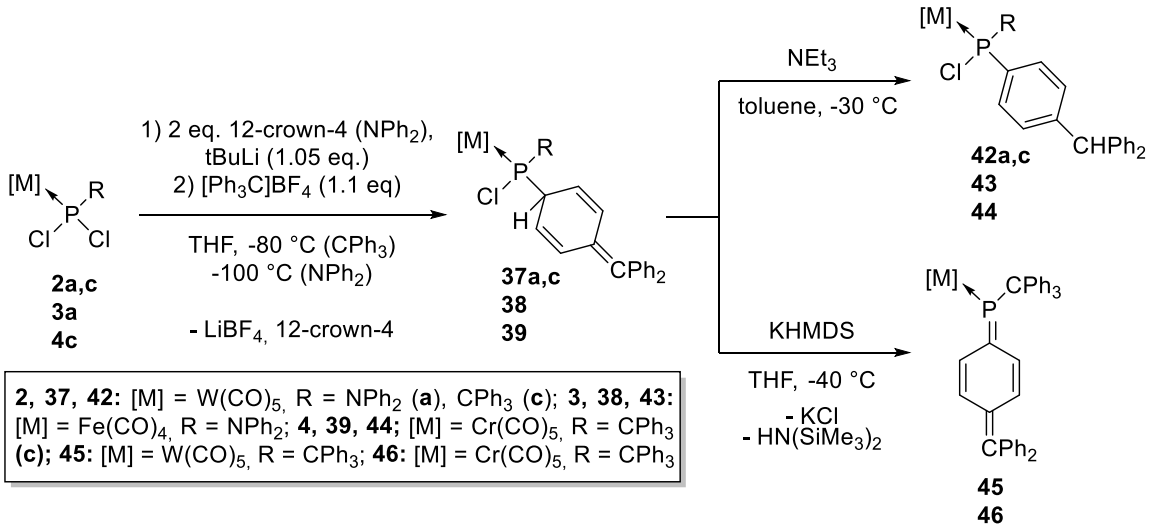

Scheme 4.5 *Reaction sequence, starting with the formation of* ***37-39*** *and their controlled reaction to complexes* ***42-44*** *(via 1,5H-shift) and* ***45, 46*** *(via HCl elimination).*

An important finding was that the addition of a comparatively weak base such as Et_3N (or DBU) can initiate a 1,5H-shift, thus selectively forming complexes **42-44** which were isolated, characterized and the structure of **42c, 44** confirmed via X-ray diffraction analysis. When complexes **37-39** were treated with a strong base such as KHMDS the HCl elimination took place, and complexes **45** and **46** were formed, of which **45** was isolated and fully characterized. Furthermore, **45** could be chemically reduced and to a radical anion which was measured by EPR spectroscopy.

For complexes **45**, **46** CV experiments were conducted, *e.g.* **45** (in THF) revealed the expected two-wave-stepwise reduction, with the first reduction taking place at (E_m = -1.00 V vs. $Cp_2Fe^{0/+}$). The second reduction takes place at E_m = -1.46 V (vs. $Cp_2Fe^{0/+}$) with an inequivalent shape displaying an irreversible (at best quasi-reversible) process. Further experiments revealed an invariant peak difference over all measured scan rates. Using the *Randles-Sevčik* equation a linear behaviour for the oxidative and reductive part of the -1/0 process could be plotted with $I_p \sim v^{1/2}$, giving proof for the existence of a diffusion controlled reversible one-electron process for oxidation and reduction, respectively.

Computational studies (B3LYP-D3/COSMO(thf)/def2-TZVP) were done for six different charge/spin states of model ligands **47** and their complexes **48**, revealing an interesting behaviour for the radical anion **48d-Me**: by comparison to all other complexes and especially its free ligand **47d-Me**, it displayed a significant increase in delocalized spin density of the C-chromophore (figure 4.8) which was further supported by calculated HOMA values showing also a strong increase in aromaticity for the complexed phosphaquinomethanes as radical anions.

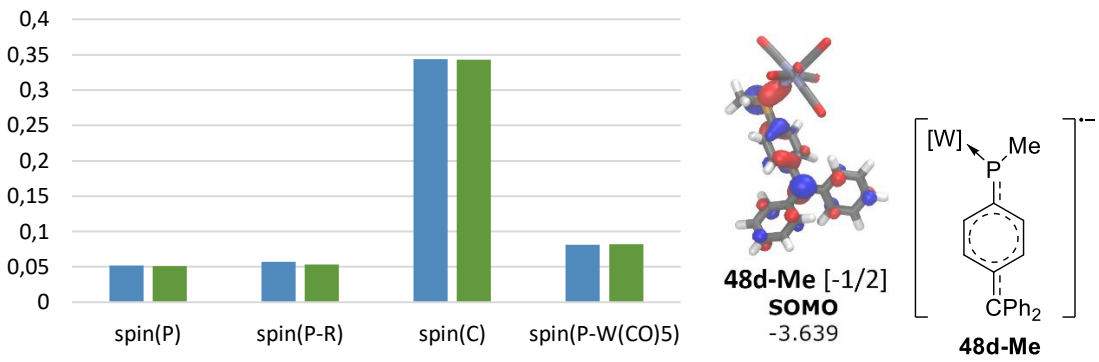

Figure 4.8 *Computed spin charge polulation (left) and SOMO frontier orbital (right) for model complex* ***48d-Me****.*

The CV measurements in combination with the calculations demonstrate a strong non-innocent character of these phosphaquinomethane ligands, especially regarding a one-electron reduction, and a strong stabilization effect of the radical anion by the $W(CO)_5$ group was revealed.

The increase of aromaticity at the central ring resulting from such stabilization was further backed by NICS (GIAO B3LYP/def2-TZVPPD) and HOMA calculations showing also the strongest increase for the radical anion (**d**) going from free ligands **47** to the corresponding complexes **48**.

5. Experimental section

5.1 General working techniques

All syntheses, if not stated otherwise, were carried out under inert gas atmosphere (Argon) using *Schlenk* technique, which means the reactions were done without contact with air and moisture. Valves and joints were greased with silicon grease OKS® 1112, before heating the glass flask with a heatgun (> 400 °C) or a *Bunsen* burner under vacuum (5 x 10^{-2} mbar). To obtain the vacuum a rotary vane pump RZ6 (*Vacuubrand*) was used. The used Argon (ARCAL Prime, Company *Air Liquide*) had a purity of > 99.998 %. This was run through BTS catalyst (Company *BASF*) heated to 110 °C removing traces of oxygen though highly disperse copper. Before this the argon was dried with glas towers containing silica gel and SICAPENT® (Company *Merck*) with Calcium chloride (anhydrous). For additional work under inertgas two glove boxes UNILab LMF (Company *MBraun*) were used. The atmosphere was purified through BTS catalyst, mol siev X13 and activated carbon, which yields oxygen and water values under 0.1 ppm. To evacuate the chamber a rotary vane pump RV12 (Company *Edwards*) was used. The used solvents were dried using standard methods. For this the solvents were stored under Argon atmosphere over a drying agent and were freshly distilled and collected the same day as used. For drying of triethylamine, tetrahydrofurane, *n*-pentane, toluene, diethylether and petroleum ether (65/40) freshly pressed sodium wire was used. Dichloromethane was drying utilizing calcium hydride. Solvents for very sensitive compounds were recondensed in a closed system after drying over-night with calcium hydride or potassium and degassing (freezing before defreezing under vacuum). The solvents were bought from *Fischer* and *VWR*.

For all reactions and steps (if not stated otherwise) magnetic stirrers with Teflon stirring bars were used. For reactions at higher temperatures paraffine oil bathes were used, while ethanol nitrogen and petroleum ether (65/40) nitrogen were used for temperatures >-100 and <-100 °C, respectively. Work-up via column chromatography was done either at room temperature or -20 °C utilizing a built-in cooling mantle which was cooled with a cryostat filled with technical ethanol. For solid phases either silica (0.063 - 0.2 mm, pH 6.5 – 7.5, Company *Merck*) or aluminium oxide (active, neutral, Company *Merck*) were used. The UV radiations were done using a mercury lamp (medium pressure; broadband emission >190 nm; Company *Heraeus*).

The glassware was cleaned with an isopropanol/potassium hydroxide bath, which was mainly used for removal of grease. For this the glassware was kept for several days inside the bath, before rinsed with water and kept for one day in a water/soap bath with added hydrochloric acid (35 %, technical) for re-protonation of the glass. Afterwards, the glassware was rinsed with water and acetone before drying at 120 °C in the oven for some days.

5.2 Methods and devices

5.2.1 NMR spectroscopy

The measurements were mainly done by the central department for analytic by the university of Bonn. The NMR measurements (*nuclear magnetic resonance*) were done with the following devices: *Avance I 300 MHz* (Oxford magnet), *Avance I 400 MHz* (Oxford magnet), *Avance I 500 MHz* (Oxford magnet), *Avance III HD Ascend* 500 MHz und *Ascend 700 MHz Cryo.* The Avance I 300 MHz is used for the variable temperature measurements (VT-NMR) in a temperature window of -80 to 100 °C. The following NMR-active cores were measured (with their standard references in brackets): ^{1}H (1 % $SiMe_4$ in $CDCl_3$), ^{7}Li (10.74 mol L^{-1} LiCl in D_2O), ^{13}C (1 % $SiMe_4$ in $CDCl_3$), ^{29}Si (1 % $SiMe_4$ in $CDCl_3$) and ^{31}P (85 % H_3PO_4). As deuterated solvents for the measurements C_6D_6, $CDCl_3$ and THF-d_8 were used and if not stated the NMR data was taken from the reaction mixture. The deuterated solvents were dried over molsieve or potassium if necessary and stored in a Schlenk under argon or in the glovebox. The chemical shifts (δ) are given in *parts per million* (ppm) and the coupling constants ($^{n}J_{X,Y}$) in Hertz (Hz), high-field shifted signals are given with a negative sign. With *n* being the number of bonds between the atoms of X and Y. For the NMR signals a signal multiplicity (s = singlet, d = doublet, t = triplet, q = quartet, quin = quintet, hex = sextet, sept = septet, m = multiplet, br = broad) is given as well as the integration of the signals in percent (in case of ^{1}H-NMR spectra it gives the number of equivalent atoms). The measurements were conducted at room temperature if not stated otherwise and edited using *MestReNova* 8.01.

5.2.2 Mass spectrometry

The measurements were done by the central department for analytic by the university of Bonn with devices of the type *MAT 95 XL* (Company *Thermo Finnigan*). The probes were ionised (EI) with 70 meV and measured/detected at various temperatures. In case of more sensitive probes the method LIFDI was utilized with a *MAT 90* sector field device (Company *Thermo Finnigan*) which was equipped with a LIFDI ion source (Company *Linden CMS*). The selected MS signals used for the characterizations refer to the isotopomer with the highest relative abundance. Stated are always the mass/charge ratio and relative intensities.

5.2.3 Elemental analysis

The measurements were done by the central department for analytic by the university of Bonn. Elemental analysis data was measured with a gas chromatograph *Vario EL* (Company *Elementa*).

5.2.4 Infrared spectroscopy

IR measurements were done using either a *Nicolet 380* with *SMART iTR diamond ATR* unit (Company *Thermo*) or a *Alpha diamond ATR FTIR* (Company *Bruker*), which was kept in the glovebox for measuring sensitive compounds. The here given absorptions values are only for selected regions and the data is given in reciprocal wavenumbers (cm^{-1}). The intensity of the corresponding absorption band is categorized and given as weak (w), medium (m), strong (s) or very strong (vs). The handling and analysis of the spectra was done using the programs *Omnic* (Company *Fischer*) and *Opus* (Company *Bruker*).

5.2.5 Single crystal X-ray diffraction analysis

The measurements were done by the central department for crystallography by the university of Bonn. The crystallographic data was obtained with the following devices: *Nonius-KappaCCD*, *X8-KappaApex II* or *D8-Venture* (Company *Bruker*) as well as the diffractometer *STOE IPDS-2T* (Company *Stoe*). It was done with Mo-Kα radiation (λ = 0.71073 Å) at a temperature of 100 or 123 K. Solving and refinement of the measured data as well as preparation of the pictures and graphics was done with the following programs: *ShelxS-97, ShelxL-97, ShelxS-2014, ShelxL-2014* and *ShelxT-2014* as well as *Olex*[132] and *OlexSys*. All here displayed structures a had their ellipsoids set to 50 % possibility. All for the discussion irrelevant hydrogen atoms and solvent molecules have been omitted for sake of clarity. The obtained crystal structures were categorized according to an in-house code: A = solving and refinement without any (known) errors (excellent structure); B = only marginal problems during refinement (very good structure); C = small problems during refinement (good structure); D = problems during refinement (moderate structure); E = not for precise discussion, only structural motive confirmed; 1 = found structure was identical with the beforehand guessed one; 2 = found structure was close, yet not identical; 3 = found structure contained proposed structural motives, yet was structurally different. All measured crystal data can be found in the appendix.

5.2.6 Melting point determination

Melting point determination was done with glass capillaries (Ø = 0.1 mm) melted shut on one side and sealed with grease on the other side using a device from the company *Büchi*. All values are uncorrected.

5.2.7 UV/vis spectroscopy

UV/vis-spectra were measured using a *UV-1650PC* spectrometer (Company *Shimadzu*) with wavelengths from λ = 190 – 900 nm. For this in the oven pre-dried cuvettes made of fused quartz with a diameter of 1 cm were used.

5.2.8 Cyclic voltammetry

The cyclic voltammetry experiments were done in the glovebox under inert gas using a potentiostat and galvanostat system from *Pine Research* with *WaveNow*® over scan rates of 20 – 1500 mV s^{-1}. Ceramic Patterned Electrodes (CPE) with working surfaces of Pt or Au were used (obtained from the company *Pine Research*) in a glass vial cell with a special PTFE insert at the bottom for small solvent volumes. The solvents were all further dried, degassed and recondensed in a closed system before usage. Depending on the solvent a different electrolyte concentration was prepared, for DCM, THF and acetonitrile with 0.4, 0.2 and 0.1 mol/L, respectively. The used electrolyte was *n*-Bu_4NPF_6, which was also dried (vacuum for 24 h at 80 °C) before usage and kept in the glovebox under inert gas. Potentials are quoted versus the operative formal potential E^0_{Fc/Fc^+} for the Cp_2Fe redox couple – abbreviated as Fc/Fc^+ - which was used as an external or internal standard, measured in the same solvent at the very same day E^0_{Fc/Fc^+} (CH_3CN): 0,440 V, E^0_{Fc/Fc^+} (THF): 0,550 V). The software for data collection and handling was *Aftermath*.

5.2.9 Electron paramagnetic resonance

All continuous wave (Cw-)EPR measurements were performed at X-band frequencies (~9.4GHz) on an EMX micro spectrometer (*Bruker BioSpin*, Rheinstetten, Germany) at room temperature using an ER4122SHQ resonator. A modulation amplitude of 1.0 G was employed alongside a microwave power of 55.14 mW corresponding to an attenuation of 5.0 dB.

5.2.10 Theoretical calculations

The quantum chemical calculations were done with ORCA 3.0.3 and ORCA 4.0.2[133] and only sets of calculations for the same program version were compared with each other. Used were a pure density functional PBE, which – as a GGA (*generalized gradient approximation*) – uses functions of the electron density gradient.[134] The *meta*-GGA TPSS functional uses the kinetic energy density.[135] Two global hybrid functionals were also use, B3LYP[136] and PW6B95[139], which are calculated from different parts of wavefunction and density functional theory. B3LYP is based on the *Becke* exchange (B)[137] with *Lee-Yang-Parr* correlation (LYP)[138], while PW6B95[139] is based on PW exchange[140] and B95 correlation[141] (with additional SOS-PT2 correlation).[142] Used were always the *Kohn-Sham* orbitals[143] – *closed-shell* (RKS) or open-shell (UKS) – of *Ahlrichs* basis sets[144] (def2-(T/Q)TZVP(P), *triple-ζ* (T) or *quadruple-ζ* (Q) with extra polarization if needed (P)) in combination with the *effective core potential* (ECP)[144] for nucleus heavier elements (ECP-46 for W: Cs-La). Used as well was the resolution-of-identity (RI)[145] as the efficient RIJCOSX (exchange integrals through semi-numeric integration)[146] or RI-JK[147] algorithm. Since semi-local density functionals and conventional hybrid functionals (with non-local *Fock*

exchange) can't correctly compute the $-C_6/R^6$ dependency of the dispersion energy with the inter-molecular distance R, the semi-empiric DFT-D3[148] (H-Pu) dispersion correction was used (s_6 $s_{r,6}$ and s_8 parametrised for the functionals). For better results, especially in case of ionic systems, were the ORCA implemented *polarizable continuum models* used as solvent corrections COSMO[149] (ORCA 3.0.3) and CPCM[150] (ORCA 4.0.2) for THF (permittivity constant ε = 7.58 with diameter R_{solv} = 3.18 Å). For definitive ground-states as well as *zero-point-energy* (ZPE) corrections numerical frequency calculations were performed and checked for imaginary frequencies (< -50 cm^{-1}). Also, for magnetic shielding values (for ^{31}P NMR calculations) the *Gauge Including Atomic Orbital method* (GIAO)[151] was used, which includes all electrons and with it relativistic core effects. The computed isotropic shielding values were then referenced with a structurally similar computed compound [$\delta(^{31}P) = \sigma_{ref} - \sigma_{calc} + \delta_{ref}(^{31}P)$].

5.3 Chemicals used

Chemical	Company
Acetone (technical)	Julius Hoesch
Aluminium oxide	Merck
tert-Butyllithium in *n*-hexane (1.7 M)	Sigma Aldrich
Benzene-d_6	Deutero
Chloroform-d_1	Deutero
Chromium hexacarbonyl	ABCR
Dicyclohexylamino	Merck
Diethylether	VWR
Diiron nonacarbonyl	ABCR
Diphenylamine	Aldrich
1-Hexene	Sigma Aldrich
Methylamine (2 M in THF)	Acros
Diphenylethine (tolane)	Fluka
Potassium hexamethyldisilazide	Sigma Aldrich
12-crown-4	Acros
Methanol	Alfa Aesar
1-Pentene	Sigma Aldrich
n-Pentane	VWR
Petroleum ether (65/40)	Julius Hoesch
Phosphorus trichloride	Acros

Silica gel	Merck
Tetrahydrofurane	Fischer
Tetrahydrofurane-d_8	Deutero
Triethylamine	Acros
Toluene	VWR
Triphenylcarbenium tetrafluoroborate	Alfa Aesar
Tungsten hexacarbonyl	ABCR

5.4 Waste disposal

All chemicals used were properly discarded, based on the *Gefahrstoffverordnung* (GefStoffV). Solids, solid phases and all with chemicals contaminated materials (gloves, papers, filters etc.) were thrown into the corresponding drum for operating resources. Solvents, as well as organic and inorganic wastes were collected in black, correspondingly labelled canisters. Remaining reactive compounds or their residues were neutralized/quenched before discarded. All properly collected wastes were then disposed of by the *Abteilung 4.2 Arbeits- und Umweltschutz* of the university of Bonn.

5.5 Syntheses and characterizations

For all new compounds full characterization with NMR, IR, MS, EA and melting point was done, if possible. X-ray diffraction analysis was done if suitable single crystals could be obtained. For intensely coloured compounds also UV/Vis measurements were conducted.

Dichloro(diphenyl)aminophosphane **1a**,[97] Dichloro(dicyclohexyl)aminophosphane **1b**[98] and [Pentacarbonyl{dichloro(triphenylmethyl)phosphane-*k*P}tungsten(0)] **2c**[60] were synthesized according to literature.[99] Dichloro(triphenylmethyl)phosphane was kindly provided by the work group.

5.5.1 Synthesis of [pentacarbonyl{dichloro(diorganylamino)phosphane-κP}metal(0)] complexes (2,4)

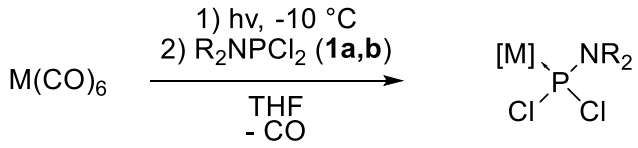

2: [M] = $W(CO)_5$, R = Ph (**a**), Cy (**b**)
4: [M] = $Cr(CO)_5$, R = Ph (**a**), Cy (**b**)

2a,b
4a,b

General Synthesis:

The metal hexacarbonyl was dissolved in THF in a UV-glas reactor. The clear, colorless solution (sometimes white suspension) was irradiated using a medium pressure mercury lamp (broadband emission >190 nm) for 60 – 70 min at 0 – 10 °C until the color was golden/yellow and the $M(CO)_5(thf)$[99] complex was formed. To this solution the dichloro(diorganylamino)phosphane **1a,b** was added, and the solution stirred at room temperatur for 3 h. Afterwards the THF was removed *in vacuo* (5 x 10^{-2} mbar).

5.5.1.1 [Pentacarbonyl{dichloro(diphenylamino)phosphane-κP}tungsten(0)] (2a)

Used reagents and solvents:

Chemicals	***M* / g mol^{-1}**	***n* / mmol**	***m* / mg**	***V* / mL**
Tungsten hexacarbonyl	351.90	1.14	400	
Dichloro(diphenyl)aminophosphane	270.09	1.14	307	
THF	72.11			100
Toluene	92.14			50
n-Pentane	72.15			5

Purification:

To the residue, obtained as yellow oil, toluene was added, the solution then filtered through a solid phase (Ø = 1.5 cm, h = 2 cm SiO_2, r.t., toluene) and, subsequently, the solvent removed *in vacuo* (5 x 10^{-2} mbar). The obtained yellow oil was washed with *n*-pentane at -40 °C (2 times 2.5 mL) and the product **2a** was obtained as a yellow powder.

Reaction cipher: PJ-151 (10m3a030.17, 10p5a021.17)

Molecular formula: $C_{17}H_{10}Cl_2NO_5PW$

Yield: 338 mg (0.57 mmol, 50 %)

Melting point 172 °C

Molar mass: 593.98 g/mol

MS (EI, 70 eV, ^{184}W) m/z (%) = 592.9 (34) $[M]^{+\bullet}$, 557.9 (20) $[M\text{-}Cl]^+$, 269.0 (6) $[M\text{-}W(CO)_5]^+$, 234.0 (100) $[M\text{-}Cl\text{-}W(CO)_5]^+$, 168.0 (26) $[NPh_2]^+$, 77.0 (12) $[C_6H_5]^+$.

IR (ATR diamond; selected bands): $\tilde{\nu}$ / cm^{-1} = 3061 (w, *ν*(CH)), 2081 (s, *ν*(CO)), 1997 (m, *ν*(CO)), 1980 (w, *ν*(CO)), 1931 (vs, *ν*(CO)).

Elemental analysis	calculated	C 34.38	H 1.70	N 2.36
	found	C 37.07	H 2.15	N 2.24

X-ray diffraction analysis A1 (GSTR546, GXray5065g)

^{1}H NMR (500.1 MHz, 298 K, C_6D_6): δ / ppm = 6.90 (m, 1 H, *para*-H), 6.97 (t, $^3J_{H,H}$ = 7.8 Hz, 2 H, *meta*-H), 7.26 (d, $^3J_{H,H}$ = 7.8 Hz, 2 H, *ortho*-H).

^{13}C{^{1}H} NMR (125.8 MHz, 298K, C_6D_6): δ / ppm = 128.5 (d, $^5J_{P,C}$ = 1.4 Hz, *para*-C), 129.5 (d, $^3J_{P,C}$ = 6.1 Hz, *ortho*-C), 129.9 (s, *meta*-C), 144.1 ($^2J_{P,C}$ = 5.1 Hz, C_{quart}), 195.2 (d_{sat}, $^1J_{W,C}$ = 127.7 Hz, $^2J_{P,C}$ = 8.3 Hz, *cis*-CO), 197.9 (d, $^1J_{W,C}$ = 141.2 Hz, $^2J_{P,C}$ = 53.2 Hz, *trans*-CO).

^{31}P NMR (121.5 MHz, 298 K, C_6D_6): δ / ppm = 108.6 (s_{sat}, $^1J_{W,P}$ = 388.7 Hz).

5.5.1.2 [Pentacarbonyl{dichloro(dicyclohexylamino)phosphane-κP}tungsten(0)] (2b)

Used reagents and solvents:

Chemicals	***M* / g mol^{-1}**	***n* / mmol**	***m* / g**	***V* / mL**
Tungsten hexacarbonyl	351.90	4.3	1.5	
Dichloro(dicyclohexyl)aminophosphane	282.19	4.3	1.2	
THF	72.11			100
ET_2O	74.12			200
n-Pentane	72.15			5

Purification:

The obtained yellow oil was filtered through a solid phase (Ø = 3 cm, h = 2 cm Al_2O_3, r.t., Et_2O) and the solvent was removed *in vacuo* (5 x 10^{-2} mbar). The remaining tungsten hexacarbonyl was removed via sublimation (50 °C, 5 x 10^{-2} mbar, 6 h) and the remaining solid was washed with *n*-pentane (2 times 2.5 mL) at -30 °C. The product was obtained as a beige powder.

Reaction cipher: PJ-229 (48p5a012.18)

Molecular formula: $C_{17}H_{22}Cl_2NO_5PW$

Yield: 1.2 g (2.0 mmol, 46 %)

Melting point 99 °C

Molar mass: 606.08 g/mol

MS (EI, 70 eV, ^{184}W) m/z (%) = 605.0 (0.8) $[M]^{+\bullet}$, 570.0 (2.2) $[M\text{-}Cl]^+$, 486.1 (2) $[M\text{-}Cl\text{-}3CO]^+$, 465.0 (3.8) $[M\text{-}5CO]^+$, 281.1 (0.4) $[M\text{-}W(CO)_5]^+$, 246.1 (100) $[ClPN(Cy)_2]^+$, 83.1 (20) $[C_6H_{11}]^+$.

IR (ATR diamond): $\tilde{\nu}$ / cm^{-1} = 2933 (m, *v*(CH)), 2857 (m, *v*(CH)), 2080 (s, *v*(CO)), 1970 (s, *v*(CO)), 1948 (s, *v*(CO)), 1912 (vs, *v*(CO)).

Elemental analysis	calculated	C 33.69	H 3.66	N 2.31
	found	C 35.26	H 4.08	N 2.44

^{1}H NMR (400.1 MHz, 298 K, C_6D_6): δ / ppm = 0.83 (qt, $J_{H,H}$ = 13.0 Hz, $J_{H,H}$ = 3.5 Hz, 1H, NCH(CH_2)(CH_2)(CH_2)), 1.15 (qt, $J_{H,H}$ = 13.2 Hz, $J_{H,H}$ = 3.6 Hz, 2H, NCH(CH_2)(CH_2)), 1.41 (dt, $J_{H,H}$ = 13.6 Hz, $J_{H,H}$ = 3.2 Hz, 1H, NCH(CH_2)(CH_2)), 1.50 – 1.62 (m, 4H, NCH(CH_2), NCH(CH_2)(CH_2)), 1.67 – 1.77 (m, 2H, NCH(CH_2)(CH_2)), 3.89 (br. d, $^2J_{P,H}$ = 11.0 Hz, 1H, NC*H*).

^{13}C{^{1}H} NMR (100.6 MHz, 298 K, C_6D_6): δ / ppm = 25.4 (s, NCH(CH_2(*C*H_2)), 26.8 (s, NCH(CH_2)(*C*H_2)), 33.9 (d, $^3J_{P,C}$ = 5.6 Hz, NCH(*C*H_2)), 62.8 (d, $^2J_{P,C}$ = 9.8 Hz, N*C*H), 196.1 ppm (d_{sat}, $^1J_{W,C}$ = 135.9 Hz, $^2J_{P,C}$ = 8.6 Hz, *cis*-CO), 198.6 ppm (d, $^2J_{P,C}$ = 50.7 Hz, *trans*-CO).

^{31}P{^{1}H} NMR (162.0 MHz, 298 K, C_6D_6): δ / ppm = 118.4 (br. s).

^{31}P{^{1}H} NMR (162.0 MHz, 239 K, C_6D_6) = 110.8 (s_{sat}, $^1J_{W,P}$ = 379.6 Hz), 126.7 (s_{sat}, $^1J_{W,P}$ = 368.2 Hz) (38:62).

5.5.1.3 [Pentacarbonyl{dichloro(diphenylamino)phosphane-κP}chromium(0)] (4a)

Used reagents and solvents:

Chemicals	*M* / g mol^{-1}	*n* / mmol	*m* / g	*V* / mL
Chromium hexacarbonyl	220.06	6.82	1.5	
dichloro(diphenyl)aminophosphane	270.09	6.66	1.8	
THF	72.11			100
Et_2O	74.12			100
Toluene	92.14			100

Purification:

To the residue, obtained as yellow oil, Et_2O was added, the solution then filtered through a solid phase (Ø = 3 cm, h = 4 cm SiO_2, r.t., Et_2O) and, subsequently, the solvent removed *in vacuo* (5 x 10^{-2} mbar). The remaining chromium hexacarbonyl was removed via sublimation (50 °C, 5 x 10^{-2} mbar, 6 h) and the remaining solid dissolved in toluene and filtered through a solid phase (Ø = 3 cm, h = 3 cm SiO_2, r.t., toluene). The solvent was removed *in vacuo* (5 x 10^{-2} mbar) and the product obtained as a slightly green powder.

Reaction cipher: PJ-250 (03m3a013.19, 03p5a053.19)

Molecular formula: $C_{17}H_{10}Cl_2CrNO_5P$

Yield: 1.2 g (3.12 mmol, 47 %)

Melting point 105 °C

Molar mass: 385.03 g/mol

MS (EI, 70 eV, ^{52}Cr) m/z (%) = 462.9 (4) $[M]^{+\bullet}$, 432.9 (0.5) $[M\text{-}CO]^+$, 425.9 (3) $[M\text{-}Cl]^+$, 404.9 (5) $[M\text{-}2CO]^+$, 348.9 (2) $[M\text{-}4CO]^+$, 320.9 (40) $[M\text{-}5CO]^+$, 269.0 (30) $[M\text{-}Cr(CO)_5]^+$, 234.0 (53) $[M\text{-}Cr(CO)_5\text{-}Cl]^+$, 199.0 (82) $[PNPh_2]^+$, 168.0 (100) $[NPh_2]^+$.

IR (ATR diamond): *v* / cm^{-1} = 3040 (w, *v*(CH)), 2079 (s, *v*(CO)), 2005 (m, *v*(CO)), 1986 (w, *v*(CO)), 1932 (vs, *v*(CO)).

Elemental analysis	calculated	C 44.18	H 2.18	N 3.03
	found	C 44.78	H 2.27	N 3.00

X-ray diffraction analysis A1 (GSTR663, GXray5925f)

^{1}H NMR (500.1 MHz, 298 K, THF-d_8): δ / ppm = 7.31 - 7.37 (m, 1 H, *para*-H), 7.39 - 7.46 (m, 2 H, *meta*-H), 7.56 - 7.62 (m, 2 H, *ortho*-H).

$^{13}C\{^{1}H\}$ NMR (125.8 MHz, 298 K, THF-d_8): δ / ppm = 129.4 (d, $^{5}J_{P,C}$ = 1.56 Hz, *para*-C), 130.2 (d, $^{3}J_{P,C}$ = 5.9 Hz, *ortho*-C), 130.7 (d, $^{4}J_{P,C}$ = 0.6 Hz, *meta*-C), 145.1 ($^{2}J_{P,C}$ = 4.5 Hz, C_{quart}), 214.3 (d, $^{2}J_{P,C}$ = 16.3 Hz, *cis*-CO), 220.0 (d, $^{2}J_{P,C}$ = 1.8 Hz, *trans*-CO).

^{31}P NMR (121.5 MHz, 298 K, THF-d_8): δ / ppm = 177.6 (s).

5.5.1.4 [Pentacarbonyl{dichloro(dicyclohexylamino)phosphane-κP}chromium(0)] (4b)

Used reagents and solvents:

Chemicals	*M* / g mol^{-1}	*n* / mmol	*m* / g	*V* / mL
Chromium hexacarbonyl	220.06	18.2	4.0	
Dichloro(dicyclohexyl)aminophosphane	282.19	13.1	3.7	
THF	72.11			270
Toluene	92.14			320

Purification:

The remaining unreacted chromium hexacarbonyl was removed via sublimation (50 °C, 5 x 10^{-2} mbar, 5 h). Afterwards the remaining solid was filtered through a solid phase (Ø = 3 cm, h = 4 cm SiO_2, r.t., toluene) and the solvent was removed *in vacuo* (5 x 10^{-2} mbar). The product was obtained as a yellow powder.

Reaction cipher: PJ-274 (20p5a023.19)

Molecular formula: $C_{17}H_{22}Cl_2CrNO_5P$

Yield: 2.5 g (5.27 mmol, 40 %)

Melting point 80 °C

Molar mass: 474.23 g/mol

MS (EI, 70 eV, ^{184}W) m/z (%) = 473.0 (3) $[M]^{+\bullet}$, 438.0 (4) $[M\text{-}Cl]^{+}$, 281.1 (12) $[M\text{-}Cr(CO)_5]^{+}$, 246.1 (100) $[M\text{-}Cl\text{-}Cr(CO)_5]^{+}$, 211.2 (50) $[PNCy_2]^{+}$, 180.2 (15) $[NCy_2]^{+}$, 83.0 (18) $[Cy]^{+}$.

IR (ATR diamond): *v* / cm^{-1} = 2931 (w, *v*(CH)), 2074 (s, *v*(CO)), 1993 (w, *v*(CO)), 1920 (vs, *v*(CO)).

Elemental analysis	calculated	C 43.06	H 4.68	N 2.95
	found	C 43.64	H 4.70	N 2.71

^{1}H NMR (500.1 MHz, 298 K, C_6D_6): δ / ppm = 0.83 (qt, $J_{H,H}$ = 13.2 HZ, $J_{H,H}$ = 3.7 Hz, 1H, NCH(CH_2)(CH_2)(CH_2)), 1.15 (qt, $J_{H,H}$ = 13.1 Hz, $J_{H,H}$ = 3.5 Hz, 2H, NCH(CH_2)(CH_2)), 1.41 (dt, $J_{H,H}$ = 13.6 Hz, $J_{H,H}$ = 3.2 Hz, 1H, NCH(CH_2)(CH_2)), 1.51 – 1.68 (m, 4H, NCH(CH_2), NCH(CH_2)(CH_2)), 1.69 – 1.77 (m, 2H, NCH(CH_2)(CH_2)), 3.89 (br. s, 1H, NC*H*).

$^{13}C\{^{1}H\}$ NMR (125.8 MHz, 298 K, C_6D_6): δ / ppm = 25.4 (s, NCH(CH_2(CH_2)), 26.8 (s, NCH(CH_2)(CH_2)), 33.6 (s, NCH(CH_2)), 62.7 (d, $^{2}J_{P,C}$ = 7.6 Hz, N*C*H), 214.5 ppm (d_{sat}, $^{2}J_{P,C}$ = 16.0 Hz, *cis*-CO), 220.1 ppm (s, *trans*-CO).

^{31}P NMR (202.5 MHz, 298 K, C_6D_6): δ / ppm = 184.2 (br. s).

5.5.2 Synthesis of [tetracarbonyl{dichloro(diorganylamino)-phosphane-κP}iron(0)] complexes (3)

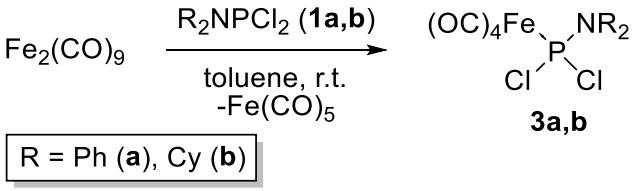

General synthesis:

The diiron nonacarbonyl was dissolved in toluene to obtain a dark green solution before the dichloro-(diorganylamino)phosphane was added and the reaction mixture was stirred at r.t. for 6 h (**Ph**) /4 d (**Cy**). The solvent and all volatiles were then removed *in vacuo* (5 x 10^{-2} mbar).

5.5.2.1 [Tetracarbonyl{dichloro(diphenylamino)phosphane-κP}iron(0)] (3a)

Used reagents and solvents:

Chemicals	***M* / g mol^{-1}**	***n* / mmol**	***m* / g**	***V* / mL**
Diiron nonacarbonyl	363.78	11.0	4.0	
Dichloro(diphenyl)aminophosphane	270.09	22.1	6.0	
Toluene	92.14			200
Et_2O	74.12			500

Purification:

The obtained brown red oil was filtered through a solid phase (Ø = 5 cm, h = 30 cm Al_2O_3, r.t., Et_2O). The solvent was removed *in vacuo* (5 x 10-2 mbar) and the product obtained as a red oil.

Reaction cipher: TK-10 (17p5a027.17)

Molecular formula: $C_{16}H_{10}Cl_2NO_4Fe$

Yield: 3.49 g (7.97 mmol, 36 %)

Molar mass: 360.87 g/mol

MS (EI, 70 eV, ^{56}Fe) m/z (%) = 436.9 (0.25) $[M]^{+\bullet}$, 408.9 (5) $[M\text{-}CO]^+$, 401.9 (1) $[M\text{-}Cl]^+$, 380.9 (2) $[M\text{-}2CO]^+$, 352.9 (8) $[M\text{-}3CO]^+$, 324.9 (20) $[M\text{-}4CO]^+$ $[M\text{-}Cl\text{-}Ph]^+$, 269.0 (3) $[M\text{-}Fe(CO)_4]^+$, 234.0 (22) $[M\text{-}Fe(CO)_4\text{-}Cl]^+$, 199 (100), $[M\text{-}Fe(CO)_4\text{-}2Cl]^+$, 168 (30) $[NPh_2]^+$, 122 (49) $[M\text{-}Fe(CO)_4\text{-}2Cl\text{-}Ph]^+$, 111.9 (2), $[Fe(CO)_2]^+$, 83.9 (2) $[Fe(CO)]^+$, 77.0 (20) $[Ph]^+$.

IR (ATR diamond): $\tilde{\nu}$ / cm^{-1} = 2067 (vs, ν(CO)), 1946 (m, ν(CO)).

Elemental analysis	calculated	C 43.88	H 2.30	N 3.20
	found	C 44.38	H 2.52	N 3.32

^{1}H NMR (500.1 MHz, 298 K, C_6D_6): δ / ppm = 6.49 – 7.67 (br. m, 10 H, *ortho*-/*meta*-/*para*-H)

^{13}C{^{1}H} NMR (125.8 MHz, 298 K, C_6D_6: δ / ppm = 128.5 (s, *para*-C), 129.5 (d, $^3J_{P,C}$ = 5.9 Hz, *ortho*-C), 129.9 (s, *meta*-C), 144.3 (d, $^2J_{P,C}$ = 4.3 Hz, *ipso*-C), 212.3 (d, $^2J_{P,C}$ = 13.2 Hz, *C*O).

^{31}P NMR (202.5 MHz, 298 K, C_6D_6): δ / ppm = 172.9 (s).

5.5.2.2 [Tetracarbonyl{dichloro(dicyclohexylamino)phosphane-κP}iron(0)] (3b)

Used reagents and solvents:

Chemicals	***M* / g mol^{-1}**	***n* / mmol**	***m* / mg**	***V* / mL**
Diiron nonacarbonyl	363.78	1.37	500	
Dichloro(dicyclohexyl)aminophosphane	282.19	2.73	770	
Toluene	92.14			35
Et_2O	74.12			250
PE(40/65)				6

Purification:

The obtained brown green solid was filtered through a solid phase (Ø = 2 cm, h = 26 cm Al_2O_3, r.t., Et_2O). The solvent was removed *in vacuo* (5 x 10^{-2} mbar) and afterwards washed with PE(40/65) (3 times 2 mL) . The product was obtained as a yellow solid.

Reaction cipher: TK-41 (29p5a010.17)

Molecular formula: $C_{16}H_{22}Cl_2FeNO_4P$

Yield: 347 mg (0.77 mmol, 56 %)

Melting point 96 °C

Molar mass: 450.07 g/mol

MS (EI, 70 eV, ^{56}Fe) m/z (%) = 499.0 (0.4) $[M]^{+\bullet}$, 421.0 (3.3) $[M\text{-}CO]^+$, 414.0 (0.4) $[M\text{-}Cl]^+$, 365.0 (5) $[M\text{-}3CO]^+$, 337.0 (7) $[M\text{-}4CO]^+$, 281.1 (9) $[M\text{-}Fe(CO)_4]^+$, 246.1 (100) $[M\text{-}Fe(CO)_4\text{-}Cl]^+$, 211.2 (56) $[M\text{-}Fe(CO)_4\text{-}2Cl]^+$, 83.1 (9) $[M\text{-}C_6H_{11}\text{-}4CO]^+$.

IR (ATR diamond): $\tilde{\nu}$ / cm^{-1} = 2930 (s, ν(CH)), 2850 (m, ν(CH)), 2080 (s, ν(CO)), 1985 (vs, ν(CO)), 1951 (vs, ν(CO)).

Elemental analysis	calculated	C 42.70	H 4.93	N 3.11
	found	C 42.97	H 5.01	N 3.04

X-ray diffraction analysis B1 (GSTR584, GXray5294f)

^{1}H NMR (500.1 MHz, 298 K, C_6D_6): δ / ppm = 0.85 (br. s, NCH(CH_2)(CH_2)(CH_2), 1 H), 1.13 (br. s, NCH(CH_2)(CH_2), 2 H), 1.41 (br. s, NCH(CH_2)(CH_2)(CH_2), 1 H), 1.57 (br. s, NCH(CH_2), NCH(CH_2)(CH_2), 4 H), 1.75 (br. s, NCH(CH_2), 2 H), 4.08 (br. s, NC*H*).

^{13}C{^{1}H} NMR (202.5 MHz, 298 K, C_6D_6): δ / ppm = 25.6 (s, NCH(CH_2)(CH_2)(*C*H_2)), 27.0 (s, NCH(CH_2)(*C*H_2)), 34.1 (s, NCH(*C*H_2)), 62.9 (d, $^{2}J_{P,C}$ = 6.9 Hz, N*C*H), 212.2 (d, $^{2}J_{P,C}$ = 16.2 Hz, *C*O).

^{31}P NMR (202.5 MHz, 298 K, C_6D_6): δ / ppm = 181.8 (s).

5.5.3 Synthesis of [pentacarbonyl{methoxy(diorganylamino)phosphane-κP}metal(0)] (14,16) and [tetracarbonyl{methoxy(diorganylamino)phosphane-κP}iron(0)] (15)

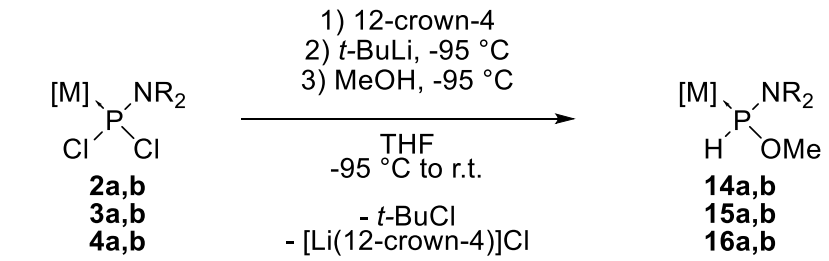

2, 14: [M] = $W(CO)_5$, R = Ph (**a**), Cy (**b**)
3, 15: [M] = $Fe(CO)_4$, R = Ph (**a**), Cy (**b**)
4, 16: [M] = $Cr(CO)_5$, R = Ph (**a**), Cy (**b**)

The dichloro(diorganylamino)phosphane-κP-pentacarbonylmetal(0) (**2,4**) or dichloro(diorganylamino)phosphane-κP-tetracarbonyliron(0) (**3**) was dissolved in THF before 12-crown-4 was added and the solution was cooled down to -95 °C. The *tert*-butyllithium was slowly added before methanol was added after 5 min. The solution was stirred for 2 h while slowly warming up to ambient temperature. Afterwards the solvent was removed *in vacuo* (5 x 10^{-2} mbar).

5.5.3.1 [Pentacarbonyl{methoxy(diphenylamino)phosphane-κP}tungsten(0)] (14a)

Used reagents and solvents:

Chemicals	*M* / g mol^{-1}	*n* / mmol	*m* / mg	*V* / mL
Dichloro(diphenylamino)phosphane-κP-pentacarbonyltungsten(0)	593.98	0.20	118	
12-crown-4	176.21	0.40		0.064
tert-Butyllithium (1.7 M in *n*-hexane)	64.05	0.22		0.13
Methanol	32.04	1.26		0.05
THF	72.11			4

Purification:

The desired product was extracted using Et_2O (2 times with 2.5 mL) and the Et_2O was removed in vacuo (5 x 10-2 mbar). The product **14a** was obtained as a yellow-orange oil (crude product).

Reaction cipher: PJ-431 (27m3a041.20)

Molecular formula: $C_{18}H_{14}NO_6PW$

Yield of the raw product): 60 mg (0.11 mmol, 54 %)

Molar mass: 555.12 g/mol

MS (EI, 70 eV, ^{184}W) m/z (%) = 555.0 (50) $[M]^{+\bullet}$, 527.0 (28) $[M\text{-}CO]^+$, 471 (100) $[M\text{-}3CO]^+$, 333.0 (20) $[W(CO)_5]^+$, 168.1 (50) $[NPh_2]^+$.

IR (ATR diamond): *v* / cm^{-1} = 1908 (vs, *v*(CO)), 2075 (s, *v*(CO)), 2661 (m, *v*(PH)).

Elemental analysis	calculated	C 38.95	H 2.54	N 2.52
	found	C 42.47	H 4.17	N 2.09

^{1}H NMR (300.1 MHz, 298 K, C_6D_6): δ / ppm = 2.99 ($^3J_{P,H}$ = 11.8 Hz, C*H*$_3$, 3H), 6.90-6.94 (m, Ph, 4H), 6.94-6.97 (m, Ph, 4H), 6.97-6.99 (m, Ph, 2H), 7.90 ($^1J_{P,H}$ = 383.3 Hz, P*H*, 1H).

^{13}C{^{1}H} NMR (75.7 MHz, 298 K, C_6D_6): δ / ppm = 59.0 (d, $^2J_{P,C}$ = 14.3 Hz, O*C*H$_3$), 125.8 (s, Ph), 125.9 (s, Ph), 129.8 (s, Ph), 147.9 (d, $^2J_{P,C}$ = 2.7 Hz, *quart*-C), 195.8 (d, $^2J_{P,C}$ = 8.3 Hz, *cis*-CO), 198.8 (d_{sat}, $^1J_{W,P}$ = 82.6 Hz $^2J_{P,C}$ = 31.2 Hz, *trans*-CO).

^{31}P NMR (121.5 MHz, 298 K, C_6D_6): δ / ppm = 112.5 (dq_{sat}, $^1J_{W,P}$ = 315.6 Hz, $^1J_{P,H}$ = 383.3 Hz, $^3J_{P,H}$ = 11.8 Hz).

5.5.3.2 [Pentacarbonyl{(dicyclohexylamino)methoxyphosphane-κP}tungsten(0)] (14b)

Used reagents and solvents:

Chemicals	*M* / g mol^{-1}	*n* / mmol	*m* / mg	*V* / mL
Dichloro(dicyclohexylamino)phosphane-κP-pentacarbonyltungsten(0)	606.08	0.1	61	
12-crown-4	176.21	0.20		0.032
tert-Butyllithium (1.7 M in *n*-hexane)	64.05	0.12		0.07
Methanol	32.04	0.74		0.03
THF	72.11			2

Reaction cipher: PJ-237 (42m3b021.18)

Molecular formula: $C_{18}H_{26}NO_6PW$

Content in solution (^{31}P NMR integration of reaction mixture): 24 %

Molar mass: 567.22 g/mol

^{31}P NMR (121.5 MHz, 298 K, THF): δ / ppm = 87.8 (dq_{sat}, $^1J_{W,P}$ = 302.6 Hz , $^1J_{P,H}$ = 387.7 Hz, $^3J_{P,H}$ = 13.5 Hz).

5.5.3.3 [Tetracarbonyl{methoxy(diphenylamino)phosphane-κP}iron(0)] (15a)

Used reagents and solvents:

Chemicals	*M* / g mol^{-1}	*n* / mmol	*m* / mg	*V* / mL
Dichloro(diphenylamino)phosphane-κP-tetracarbonyliron(0)	437.98	0.91	397	
12-crown-4	176.21	1.81		0.29
tert-Butyllithium (1.7 M in *n*-hexane)	64.05	1.09		0.64
Methanol	32.04	2.72		0.11
THF	72.11			20
ET_2O	74.12			30
PE(40/65)				2

Purification:

The obtained red brown oil was extracted with Et_2O. The solvent was removed *in vacuo* before washing with PE(40/65) at -40 °C to obtain the product as a red oil.

Reaction cipher: TK-15 (19m3a041.17)

Molecular formula: $C_{17}H_{14}FeNO_5P$

Yield: 18 mg (0.05 mmol, 5 %)

Molar mass: 399.12 g/mol

MS (EI, 70 eV, ^{56}Fe) m/z (%) = 399.0 (1.2) $[M]^{+\bullet}$, 371.0 (30) $[M\text{-}CO]^+$, 315.0 (99) $[M\text{-}3CO]^+$, 287.0 (100) $[M\text{-}4CO]^+$, 230.1 (25) $[M\text{-}Fe(CO)_4\text{-}H]^+$.

IR (ATR diamond): $\tilde{\nu}$ / cm^{-1} = 2054 (vs, ν(CO)), 1291 (m, ν(CO)).

X-ray diffraction analysis E1 (GSTR577, Gxray5170)

^{1}H NMR (300.1 MHz, 298 K, C_6D_6): δ / ppm = 7.76 (d, $^1J_{P,H}$ = 433.0 Hz, 1 H, PH), 3.0 (d, $^3J_{P,H}$ = 13.2 Hz, 3 H, CH_3).

^{13}C{^{1}H} NMR (75.5 MHz, 298 K, C_6D_6): δ / ppm = 57.5 (d, $^2J_{P,C}$ = 13.31 Hz, *C*H_3), 126.2 (s, *para*-C), 126.5 (d, $^2J_{P,C}$ = 3.3 Hz, *ortho*-C), 129.8 (s, *meta*-C), 146.7 ppm (C_{quart}), 213.1 (d, $^2J_{P,C}$ = 21.8 Hz, *C*O).

^{31}P NMR (121.5 MHz, 298 K, C_6D_6): δ / ppm = 162.3 (dq, $^1J_{P,H}$ = 432.5 Hz, $^3J_{P,H}$ = 13.2 Hz).

5.5.3.4 [Tetracarbonyl{(dicyclohexylamino)methoxyphosphane-κP}iron(0)] (15b)

Used reagents and solvents:

Chemicals	*M* / g mol^{-1}	*n* / mmol	*m* / mg	*V* / mL
Dichloro(dicyclohexylamino)phosphane-κP-tetracarbonyliron(0)	450.07	0.90	403	
12-crown-4	176.21	1.79		0.29
tert-Butyllithium (1.7 M in *n*-hexane)	64.05	0.94		0.55
Methanol	32.04	2.71		0.11
THF	72.11			20

Reaction cipher: TK-52 (29m3b037.17)

Molecular formula: $C_{17}H_{26}NO_5PFe$

Content in solution (^{31}P NMR integration of reaction mixture): 45 %

Molar mass: 411.22 g/mol

^{31}P NMR (121.5 MHz, 298 K, THF): δ / ppm = 137.9 (dq, $^1J_{P,H}$ = 442.6 Hz, $^3J_{P,H}$ = 14.5 Hz).

5.5.3.5 [Pentacarbonyl{methoxy(diphenylamino)phosphane-*κ*P}chromium(0)] (16a)

Used reagents and solvents:

Chemicals	***M* / g mol^{-1}**	***n* / mmol**	***m* / mg**	***V* / mL**
Dichloro(diphenylamino)phosphane-*κ*P-pentacarbonylchromium(0)	462.14	0.1	46	
12-crown-4	176.21	0.20		0.032
tert-Butyllithium (1.7 M in *n*-hexane)	64.05	0.12		0.07
Methanol	32.04	0.74		0.3
THF	72.11			2.5

Reaction cipher: PJ-254 (04p5a028.19)

Molecular formula: $C_{18}H_{14}NO_6PCr$

Content in solution (^{31}P NMR integration of reaction mixture): 88 %

Molar mass: 423.28 g/mol

^{31}P NMR (121.5 MHz, 298 K, THF): δ / ppm = 204.3 (dq, $^{1}J_{P,H}$ = 373.4 Hz, $^{3}J_{P,H}$ = 12.3 Hz).

5.5.3.6 [Pentacarbonyl{(dicyclohexylamino)methoxyphosphane-*κ*P}chromium(0)] (16b)

Used reagents and solvents:

Chemicals	***M* / g mol^{-1}**	***n* / mmol**	***m* / mg**	***V* / mL**
Dichloro(dicyclohexylamino)phosphane-*κ*P-pentacarbonylchromium(0)	474.23	0.1	47	
12-crown-4	176.21	0.20		0.032
tert-Butyllithium (1.7 M in *n*-hexane)	64.05	0.12		0.07
Methanol	32.04	0.25		0.01
THF	72.11			3

Reaction cipher: PJ-275 (18m3a014.19)

Molecular formula: $C_{18}H_{26}NO_6PCr$

Content in solution (^{31}P NMR integration of reaction mixture): 38 %

Molar mass: 435.38 g/mol

^{31}P{^{1}H} NMR (121.5 MHz, 298 K, THF): δ / ppm = 135.3 (s).

^{31}P NMR (121.5 MHz, 298 K, THF): δ / ppm = 135.3 (dq, $^{1}J_{P,H}$ = 371.8 Hz, $^{3}J_{P,H}$ = 13.2 Hz).

5.5.4 Synthesis of [pentacarbonyl{methylamino(diorganylamino)-phosphane-*κ*P}metal(0)] (17,19) and [tetracarbonyl{methyl-amino(diorganylamino)phosphane-*κ*P}iron(0)] (18)

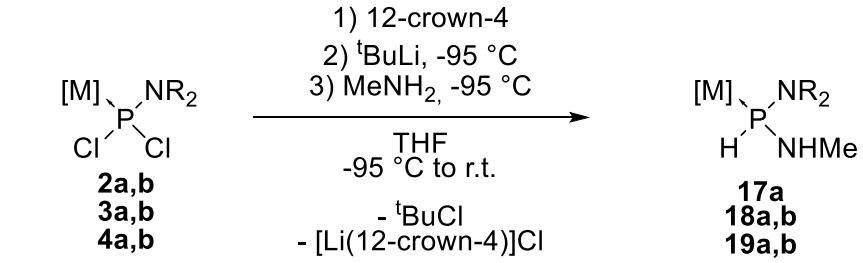

2, 17: [M] = $W(CO)_5$, R = Ph (**a**), Cy (**b**)
3, 18: [M] = $Fe(CO)_4$, R = Ph (**a**), Cy (**b**)
4, 19: [M] = $Cr(CO)_5$, R = Ph (**a**), Cy (**b**)

General synthesis:

The dichloro(diorganylamino)phosphane-*κ*P-pentacarbonylmetal(0) (**2,4**) or dichloro(diorganyl-amino)phosphane-*κ*P-tetracarbonyliron(0) was dissolved in THF und 12-crown-4 was added. The solution was cooled down to -95 °C and *tert*-butyllithium was slowly added. The methylamine was added after 5 min at -95 °C before the solution was stirred for 2.5 h while warming up to ambient temperature. Afterwards the solvent was removed in vacuo (5 x 10^{-2} mbar).

5.5.4.1 [Pentacarbonyl{methylamino(diphenylamino)phosphane-*κ*P}tungsten(0)] (17a)

Used reagents and solvents:

Chemicals	***M* / g mol^{-1}**	***n* / mmol**	***m* / mg**	***V* / mL**
Dichloro(diphenylamino)phosphane-*κ*P-pentacarbonyltungsten(0)	592.92	0.2	118	
12-crown-4	176.21	0.4		0.064
tert-Butyllithium (1.7 M in *n*-hexane)	64.05	0.22		0.013
Methylamine (2 M in THF)	31.06	1.0		0.5
THF	72.11			4
Et_2O	74.12			10

Purification:

The desired product was filtered through solid phase (Ø = 1 cm, h = 3 cm SiO_2, r.t.) and the Et_2O was removed in vacuo (5 x 10^{-2} mbar). The product was obtained as an orange oil (crude product).

Reaction cipher: PJ-432 (29m3a047.20)

Molecular formula: $C_{18}H_{15}N_2O_5PW$

Yield of the raw product: 65 mg (0.12 mmol, 59 %)

Molar mass: 554.14 g/mol

MS (EI, 70 eV, ^{184}W) m/z (%) = 554.0 (9) $[M]^{+\bullet}$, 526.0 (1) $[M\text{-}CO]^+$, 470.0 (3) $[M\text{-}3CO]^+$, 414.0 (2) $[M\text{-}5CO]^+$, 229.1 (6) $[M\text{-}W(CO)_5\text{-}H]^+$, 168.1 (25) $[NPh_2]^+$.

IR (ATR diamond): $\tilde{\nu}$ / cm^{-1} = 1901.2 (vs, ν(CO)), 1982.3 (m, ν(CO)), 2071.6 (s, ν(CO)), 2861.2 (m, ν(PH)), 3320.3 (w ν(NH)).

Elemental analysis	calculated	C 39.01	H 2.73	N 5.06
	found	C 42.64	H 4.74	N 4.37

^{1}H NMR (300.1 MHz, 298 K, C_6D_6): δ / ppm = 2.04 ($^3J_{P,H}$ = 11.1 Hz, C*H*$_3$, 3H), 6.79-6.85 (m, Ph), 6.87-6.98 (m, Ph), 7.4 ($^1J_{P,H}$ = 407.0 Hz, $^3J_{H,H}$ = 8.5 Hz, P*H*, 1H).

^{13}C{^{1}H} NMR (75.6 MHz, 298 K, C_6D_6): δ / ppm = 26.9 (d, $^3J_{P,C}$ = 1.7 Hz, NCH_2CH_3), 33.6 (d, $^2J_{P,C}$ = 10.5 Hz, NCH_2), 124.7 (s, Ph), 125.3 (d, $^3J_{P,C}$ = 4.0 Hz, Ph), 129.3 (s, Ph), 148.0 (d, $^2J_{P,C}$ = 3.0 Hz, *quart.*-C), 195.9 (d, $^2J_{P,C}$ = 7.7 Hz, *cis*-CO), 198.5 (d, $^2J_{P,C}$ = 26.1, *trans*-CO).

^{31}P NMR (121.5 MHz, 298 K, C_6D_6): δ / ppm = 67.6 (ddq_{sat}, $^1J_{W,P}$ = 281.3 Hz, $^1J_{P,H}$ = 407.0 Hz, $^2J_{P,H}$ = 22.1 Hz, $^3J_{P,H}$ = 11.1 Hz).

5.5.4.2 [Tetracarbonyl{methylamino(diphenylamino)phosphane-κP}iron(0)] (18a)

Used reagents and solvents:

Chemicals	***M* / g mol^{-1}**	***n* / mmol**	***m* / mg**	***V* / mL**
Dichloro(diphenylamino)phosphane-κP-tetracarbonyliron(0)	437.98	0.46	203	
12-crown-4	176.21	0.94		0.15
tert-Butyllithium (1.7 M in *n*-hexane)	64.05	0.56		0.33
Methylamine (2 M in THF)	31.06	1.4		0.7
THF	72.11			10
ET_2O	74.12			30
PE(40/65)				0.5

Purification:

The obtained brown oil was filtered through solid phase (Ø = 2 cm, h = 1 cm Al_2O_3, r.t., Et_2O) and the solvent was removed *in vacuo* (5 x 10^{-2} mbar). After washing with PE(40/65) at -30 °C the product was obtained as a beige solid.

Reaction cipher: TK-11 (17m3c038.17)

Molecular formula: $C_{17}H_{15}FeN_2O_4P$

Yield: 54 mg (0.14 mmol, 29 %)

Melting point 93 °C

Molar mass: 398.14 g/mol

MS (EI, 70 eV, ^{56}Fe) m/z (%) = 398.0 (0.3) $[M]^{+\bullet}$, 370.0 (8) $[M\text{-}CO]^+$, 368.0 (0.5) $[M\text{-}HNMe]^+$, 314.0 (24) $[M\text{-}3CO]^+$, 286.0 (28) $[M\text{-}4CO]^+$.

IR (ATR diamond): $\tilde{\nu}$ / cm^{-1} = 3411 (s, *v*(NH)), 2368 (m, *v*(PH)), 2051 (vs, *v*(CO)), 1975 (vs, *v*(CO)), 1913 (m, *v*(CO)).

Elemental analysis	calculated	C 51.29	H 3.80	N 7.04
	found	C 47.78	H 3.61	N 6.54

X-ray diffraction analysis AA1 (GSTR566, Gxraymo_5159f)

^{1}H NMR (300.1 MHz, 298 K, C_6D_6): δ / ppm = 1.98 ppm (m, $^3J_{P,H}$ = 12.1 Hz, 4 H, CH_3, NH), 6.89 – 6.95 ppm (m, 2 H, *para*-H), 6.99 – 7.03 (br. s, 4 H, *meta*-H), 7.04 ppm (d, $^4J_{P,H}$ = 1.5 Hz, 4 H, *ortho*-H), 7.44 ppm (dd, $^1J_{P,H}$ = 442.6 Hz, $^3J_{H,H}$ = 6.0 Hz, 1 H, P*H*).

^{13}C{^{1}H} NMR (75.5 MHz, 298 K, C_6D_6): δ / ppm = 32.6 ppm (d, $^2J_{P,C}$ = 10.8, *C*H_3), 125.6 ppm (d, $^5J_{P,C}$ = 0.9 Hz, *para*-C), 126.6 ppm (d, $^3J_{P,C}$ = 3.0 Hz, *ortho*-C), 129.7 ppm (s, *meta*-C), 147.1 ppm (d, $^2J_{P,C}$ = 2.8 Hz, C_{quart}), 213.6 ppm (d, $^2J_{P,C}$ = 21.8 Hz, *C*O).

^{31}P NMR (121.5 MHz, 298 K, C_6D_6): δ / ppm = 117.1 ppm (ddq, $^1J_{P,H}$ = 442.7 Hz, $^2J_{P,H}$ = 21.3 Hz, $^3J_{P,H}$ = 11.7 Hz).

5.5.4.3 [Tetracarbonyl{(dicyclohexylamino)methylaminophosphane-κP}iron(0)] (18b)

Used reagents and solvents:

Chemicals	*M* / g mol^{-1}	*n* / mmol	*m* / mg	*V* / mL
[Tetracarbonyl{dichloro(dicyclohexylamino)-phosphane-κP}iron(0)]	450.07	0.89	400	
12-crown-4	176.21	1.75		0.28
tert-Butyllithium (1.7 M in *n*-hexane)	64.05	0.94		0.55
Methylamine (2 M in THF)	31.06	2.66		1.3
THF	72.11			20
ET_2O	74.12			60
PE(40/65)				60

Purification:

The obtained brown solid was filtered through solid phase (Ø = 3 cm, h = 3.5 cm Al_2O_3, r.t., Et_2O/PE(40/65)). Afterwards the solvent was removed *in vacuo* (5 x 10^{-2} mbar) and the product obtained as a beige solid.

Reaction cipher: TK-50 (31m3a041.17, 31m3a047.17)

Molecular formula: $C_{17}H_{27}FeN_2O_4P$

Yield: 30 mg (0.07 mmol, 8 %)

Melting point 117 °C

Molar mass: 410.23 g/mol

MS (EI, 70 eV, ^{56}Fe) m/z (%) = 410.1 (0.5) $[M]^{+\bullet}$, 382.2 (1.9) $[M\text{-}CO]^+$, 354.2 (0.8) $[M\text{-}Cl]^+$, 326.2 (10) $[M\text{-}3CO]^+$, 298.2 (4) $[M\text{-}4CO]^+$, 181.3 (12) $[Cy_2NH]^+$, 152.2 (2) $[Cy_2NH\text{-}C_2H_5]^+$, 138.2 (100) $[Cy_2NH\text{-}C_2H_5\text{-}CH_3]^+$.

IR (ATR diamond): *ν* / cm^{-1} = 3438 (m, *ν*(NH)), 3419 (m, *ν*(NH), 2929 (s, *ν*(CH)), 2854 (m, *ν*(CH)), 2362 (w, *ν*(PH)), 2039 (s, *ν*(CO)), 1934 (m, *ν*(CO)), 1895 (vs, *ν*(CO)).

Elemental analysis	calculated	C 49.77	H 6.63	N 6.83
	found	C 50.54	H 7.04	N 5.92

X-ray diffraction analysis AA1 (GSTR566, GXraymo_5159f)

^{1}H NMR (500.1 MHz, 298 K, C_6D_6): δ / ppm = 0.71 – 2.15 ppm (m, 33 H), 2.98 ppm (br. s, 2 H, NC*H*) 7.16 ppm (d, $^1J_{P,H}$ = 413.5 Hz, 1 H, P*H*).

^{13}C{^{1}H} NMR (125.8 MHz, 298 K, C_6D_6): δ / ppm = 25.6 (s, NCH(CH_2)(CH_2)(*C*H_2)), 26.6 (s, NCH(CH_2)(*C*H_2)), 26.8 (s, NCH(CH_2)(*C*H_2)), 31.2 (d, N*C*H_3), 33.3 (s, NCH(*C*H_2)), 34.0 (d, $^3J_{P,C}$ = 1.9 Hz, NCH(*C*H_2)), 62.9 (d, $^2J_{P,C}$ = 6.9 Hz, N*C*H), 212.2 (d, $^2J_{P,C}$ = 16.2 Hz, *C*O).

^{31}P NMR (121.5 MHz, 298 K, C_6D_6): δ / ppm = 86.7 ppm (d, $^{1}J_{P,H}$ = 431.32 Hz).

5.5.4.4 [Pentacarbonyl{methylamino(diphenylamino)phosphane-κP}chromium(0)] (19a)

Used reagents and solvents:

Chemicals	*M* / g mol^{-1}	*n* / mmol	*m* / mg	*V* / mL
Dichloro(diphenylamino)phosphane-κP-pentacarbonylchromium(0)	462.14	1	462	
12-crown-4	176.21	2		0.32
tert-Butyllithium (1.7 M in *n*-hexan)	64.05	1.05		0.62
Methylamine (2 M in THF)	31.06	5		2.5
THF	72.11			25
Et_2O	74.12			120
PE				60
DCM	84.93			60

Purification:

The desired product was extracted using Et_2O (4 times with 25 mL) and the Et_2O was removed *in vacuo* (5 x 10^{-2} mbar) to obtain a yellow oil. The residue was separated via column chromatography (Ø = 3 cm, h = 4 cm SiO_2, -20 °C) and three fractions were collected (60 mL PE (1), 120 mL Et_2O (2), 60 mL DCM (3)). The solvents were evaporated *in vacuo* (5 x 10^{-2} mbar) and the product obtained from fraction 2 as a yellow oil.

Reaction cipher: PJ-253 (25m3b038.19)

Molecular formula: $C_{18}H_{15}N_2O_5PCr$

Yield: 120 mg (0.28 mmol, 28 %)

Molar mass: 422.30 g/mol

MS (Lifdi, ^{52}Cr) m/z (%) = 422.1 (100) $[M]^+$.

IR (ATR diamond): *v* / cm^{-1} = 3427 (w, *v*(NH)), 2929 (w, *v*(PH)), 2065 (s, *v*(CO)), 1986 (m, *v*(CO)), 1904 (vs, *v*(CO)).

Elemental analysis	calculated	C 51.20	H 3.58	N 6.63
	found	C 50.45	H 4.32	N 5.88

X-ray diffraction analysis A1 (GSTR683, GXray_5996h)

^{1}H NMR (300.1 MHz, 298 K, C_6D_6): δ / ppm = 2.01 ($^{3}J_{P,H}$ = 12.0 Hz, C*H*$_3$, 3H), 6.8-7.1 (m, Ph, 12H), 7.1 ($^{1}J_{P,H}$ = 402.0 Hz, P*H*, 1H).

$^{13}C\{^{1}H\}$ NMR (75.5 MHz, 298 K, C_6D_6): δ / ppm = 33.9 (d, $^{2}J_{P,C}$ = 11.7 Hz, N*C*H$_3$), 125.0 (s, Ph), 125.5 (d, $^{3}J_{P,C}$ = 3.6 Hz, Ph), 129.7 (s, Ph), 148.4 (d, $^{2}J_{P,C}$ = 2.7 Hz, *quart.*-C), 216.3 (d, $^{2}J_{P,C}$ = 15.7 Hz, *cis*-CO), 220.5 (d, $^{2}J_{P,C}$ = 7.2 Hz, *trans*-CO).

^{31}P NMR (121.5 MHz, 298 K, C6D6): δ / ppm = 119.1 (ddq, $^{1}J_{P,H}$ = 402.0 Hz, $^{2}J_{P,H}$ = 24.5 Hz, $^{3}J_{P,H}$ = 12.0 Hz).

5.5.4.5 [Pentacarbonyl{(dicyclohexylamino)methylaminophosphane-κP}chromium(0)] (19b)

Used reagents and solvents:

Chemicals	*M* / g mol^{-1}	*n* / mmol	*m* / mg	*V* / mL
Dichloro(dicyclohexylamino)phosphane-κP-pentacarbonylchromium(0)	474.23	0.1	47	
12-crown-4	176.21	0.2		0.032
tert-Butyllithium (1.7 M in *n*-hexane)	64.05	0.12		0.07
Methylamine (2 M in THF)	31.06	0.6		0.3
THF	72.11			3

Reaction cipher: PJ-276 (18m3a012.19)

Molecular formula: $C_{18}H_{27}N_2O_5PCr$

Content in solution (^{31}P NMR integration of reaction mixture): 42 %

Molar mass: 434.39 g/mol

^{31}P NMR (121.5 MHz, 298 K, THF): δ / ppm = 81.3 (ddq$_{sat}$, $^{1}J_{P,H}$ = 374.6 Hz, $^{2}J_{P,H}$ = 21.5 Hz, $^{3}J_{P,H}$ = 11.5 Hz).

5.5.5 Syntheses of [pentacarbonyl{(diorganylamino)-2,3-diphenyl-1*H*-phosphirene-*κ*P}tungsten(0)] (29) and [pentacarbonyl-{(diorganylamino)-2-*n*-propyl/butyl-phosphirane-*κ*P}tungsten(0)] (30-31)

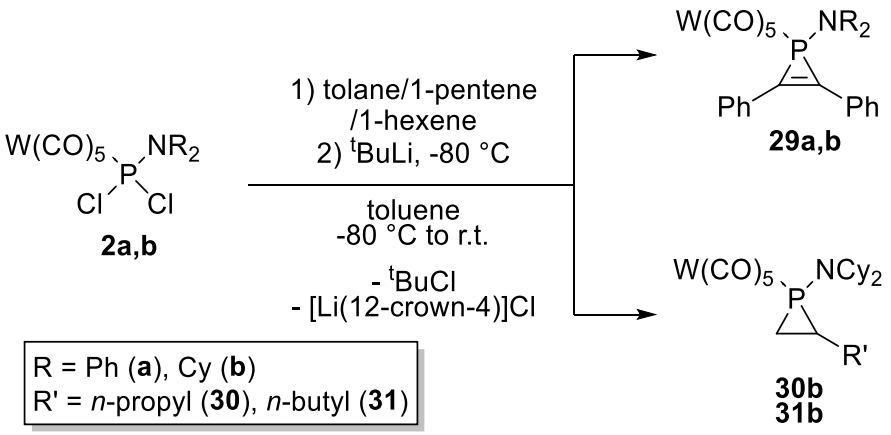

General synthesis:

The [pentacarbonyl{dichloro(diorganylamino)phosphane-*κ*P}tungsten(0)] **2** was dissolved in toluene and an excess of the trapping reagent was added. The solution was cooled down to -80 °C and t-butyllithium was added. The solution was kept in the cooling bath while warming up to 0 °C before the toluene was evaporated.

5.5.5.1 [Pentacarbonyl{(diphenylamino)-2,3-diphenyl-1*H*-phosphirene-*κ*P}tungsten(0)] (29a)

Used reagents and chemicals:

Chemicals	*M* / g mol^{-1}	*n* / mmol	*m* / mg	*V* / mL
[Pentacarbonyl{dichloro(diphenylamino)-phosphane-*κ*P}tungsten(0)]	593.98	0.6	0.356	
tert-Butyllithium (1.7 M in *n*-hexane)	64.05	0.63		0.37
Tolane	178.23	5.61	0.105	
Toluene	92.14			12

Reaction cipher: PJ-372 (29m3a024.19)

Molecular formula: $C_{31}H_{20}NO_5PW$

Content in solution (^{31}P NMR integration of reaction mixture): 31 %

Molar mass: 701.32 g/mol

MS (EI, 70 eV, ^{184}W) m/z (%) = 701.1 (10) $[M]^+$, 617.1 (8) $[M\text{-}3CO]^+$, 533.0 (7) $[M\text{-}NPh_2]^+$, 505.0 (3) $[M\text{-}NPh_2\text{-}CO]^+$, 477.0 (4) $[M\text{-}NPh_2\text{-}2CO]^+$, 449.0 (22) $[M\text{-}NPh_2\text{-}3CO]^+$, 393.0 (13) $[M\text{-}NPh_2\text{-}5CO]^+$, 209.1 (30) $[M\text{-}NPh_2\text{-}W(CO)_5]^+$, 178.1 (70) $[C_2Ph_2]^+$, 168.1 (50) $[NPh_2]^+$.

^{31}P NMR (121.5 MHz, 298 K, THF): δ / ppm = -108.3 (s_{sat}, $^1J_{W,P}$ = 305.3 Hz)

5.5.5.2 [Pentacarbonyl{(dicyclohexylamino)-2,3-diphenyl-1*H*-phosphirene-*κ*P}tungsten(0)] (29b)

Used reagents and solvents:

Chemicals	*M* / g mol^{-1}	*n* / mmol	*m* / mg	*V* / mL
[Pentacarbonyl{dichloro(diphenylamino)-phosphane-*κ*P}tungsten(0)]	606.08	0.1	61	
tert-Butyllithium (1.7 M in ^{n}Hexan)	64.05	0.2		0.13
Tolane	178.23	0.5	90	
Toluene	92.14			2
n-Pentane	72.15			6

Purification:

The product was extracted using *n*-pentane (2 x 3 mL). After evaporation of *n*-pentane *in vacuo* (5 x 10^{-2} mbar) the product was obtained as an orange oil (quickly crystallizing due to remaining tolane; crude product).

Reaction cipher: PJ-414 (11m3a028.20)

Molecular formula: $C_{31}H_{32}NO_5PW$

Yield: 45 mg (0.06 mmol, 64 %)

Molar mass: 713.41 g/mol

MS (EI, 70 eV, ^{184}W) m/z (%) = 713.1 (0.1) $[M]^{+\bullet}$, 535.0 (28) $[M\text{-}Ph_2C_2]^+$, 507 (53) $[M\text{-}Ph_2C_2\text{-}CO]^+$, 178 (100) $[Ph_2C_2]^+$.

^{1}H NMR (300.1 MHz, 298 K, C_6D_6): δ / ppm = 0.64-0.80 (Cy, 2H), 0.89-0.98 (Cy, 2H), 1.10-1.20 (Cy, 4H), 1.51-1.61 (Cy, 4H), 1.62-1.72 (Cy, 4H), 3.12-3.29 ($^3J_{P,H}$ = 15.3 Hz, NC*H*, 2H), 6.94 – 7.05 (m, Ph), 7.47 – 7.54 (m, Ph), 7.84 – 7.89 (m, Ph).

^{13}C{^{1}H} NMR (75.8 MHz, 298 K, C_6D_6): δ / ppm = 25.7 (Cy), 27.0 (Cy), 34.5 (d, $^3J_{P,C}$ = 3.2 Hz, NCH*C*H$_2$), 58.0 (d, $^2J_{P,C}$ = 6.7 Hz, N*C*H), 129.5 (Ph), 129.8 (d, $^2J_{P,C}$ = 4.4 Hz, PCC_{Ph}), 130.5 (Ph), 146.2 (d, $^1J_{P,C}$ = 16.8 Hz, P*C*), 197.5 (d, $^2J_{P,C}$ = 9.1 Hz, *cis*-CO), 199.3 (d, $^2J_{P,C}$ = 33.9 Hz, *trans*-CO).

^{31}P NMR (121.5 MHz, 298 K, C_6D_6): δ / ppm = -115.3 (t_{sat}, $^1J_{W,P}$ = 306.1 Hz, $^2J_{P,H}$ = 15.6 Hz).

5.5.5.3 [Pentacarbonyl{(dicyclohexylamino)-2-*n*-propylphosphirane-*κ*P}tungsten(0)] (30b)

Used reagents and solvents:

Chemicals	*M* / g mol^{-1}	*n* / mmol	*m* / mg	*V* / mL
[Pentacarbonyl{dichloro(dicyclohexylamino)-phosphane-*κ*P}tungsten(0)]	606.08	0.2	122	
tert-Butyllithium (1.7 M in *n*-hexane)	64.05	0.4		0.23
1-Pentene	70.13	1.9	130	
Toluene	92.14			4
n-Pentane	72.15			20

Purification:

The product was extracted using *n*-pentane (4 x 5 mL) and the solvent was removed *in vacuo* (5 x 10^{-2} mbar). The product was obtained as a red oil.

Reaction cipher: PJ-416 (11m3a020.20, 11c5a033.20)

Molecular formula: $C_{22}H_{32}NO_5PW$

Yield: 89 mg (0.147 mmol, 74%)

Molar Mass: 605.31 g/mol

IR (ATR Diamant): *ν* / cm^{-1} = 1904.7 (vs), 1978.7 (m), 2068.1 (s), 2854.9 (m), 2929.8 (s).

MS (EI, 70 eV, ^{184}W) m/z (%) = 507.0 (1.2) $[M\text{-}CO\text{-}C_5H_{10}]^+$, 323.9 (5) $[W(CO)_5]^+$, 295.9 (1) $[W(CO)_4]^+$, 267.9 (4) $[W(CO)_3]^+$, 239.9 (3) $[W(CO)_2]^+$.

Elemental analysis calculated C 43.65 H 5.33 N 2.31

found C 41.85 H 5.09 N 2.48

^{1}H NMR (500.1 MHz, 298 K, C_6D_6): δ / ppm = 0.53 (td, $^3J_{H,H}$ = 8.4 Hz, $^2J_{P,H}$ = 6.8 Hz, 1H, PC*H*), 0.93 (t, $^3J_{H,H}$ = 7.2 Hz, 3H, C*H*$_3$), 1.03-1.13 (m, 4H, NCHC*H*$_2$), 1.13-1.22 (m, 4H, NCHC*H*$_2$), 1.24-1.34 (m, 4H, NCHCH$_2$CH$_2$C*H*$_2$), 1.35-1.46 (m, 6H, NCHCH$_2$C*H*$_2$), 1.41-1.44 (m, $^3J_{P,H}$ = 3.8 Hz, 2H, CHC*H*$_2$), 1.53-1.56 (m, 2H, CHCH$_2$C*H*$_2$), 1.64-1.67 (m, 2H, PC*H*$_2$), 1.84-1.92 (m, 2H, NCHCH$_2$C*H*$_2$), 2.67-2.77 (m, 2H, NC*H*).

^{13}C{^{1}H} NMR (125.8 MHz, 298 K, C_6D_6): δ / ppm = 14.0 (s, *C*H$_3$), 23.0 (d, $^3J_{P,C}$ = 6.7 Hz, CH$_2$*C*H$_2$CH$_3$), 23.4 (d, $^1J_{P,C}$ = 17.5 Hz, P*C*H), 26.8 (d, $^3J_{P,C}$ = 7.1 Hz, NCH*C*H$_2$), 31.7 (d, $^1J_{P,C}$ = 21.1 Hz, P*C*H$_2$), 33.6 (d, $^4J_{P,C}$ = 3.3 Hz, NCHCH$_2$*C*H$_2$), 34.0 ($^2J_{P,C}$ = 3.4 Hz, *C*H$_2$CH$_2$CH$_3$), 35.3 (d, $^5J_{P,C}$ = 1.5 Hz, NCHCH$_2$CH$_2$*C*H$_2$), 60.3 (d, $^2J_{P,C}$ = 3.9 Hz, N*C*H), 197.7 (d_{sat}, $^2J_{P,C}$ = 8.8 Hz, $^1J_{W,C}$ = 126.8 Hz, *cis*-CO), 198.9 (d, $^2J_{P,C}$ = 32.0 Hz, *trans*-CO).

^{31}P{^{1}H} NMR (202.5 MHz, 298 K, C_6D_6): δ / ppm = -108.1 (s_{sat}, $^1J_{W,P}$ = 287.0 Hz), -111.1 (s_{sat}, $^1J_{W,P}$ = 281.8 Hz) [83:17].

^{31}P NMR (202.5 MHz, 298 K, C_6D_6): δ / ppm = -108.1 (br. s_{sat}, $^1J_{W,P}$ = 287.0, FWHM ~54 Hz), -111.1 (br. s FWHM ~49).

5.5.5.4 [Pentacarbonyl{2-*n*-butyl(dicyclohexylamino)phosphirane-*κ*P}tungsten(0)] (31b)

Used reagents and solvents:

Chemicals	*M* / g mol^{-1}	*n* / mmol	*m* / mg	*V* / mL
[Pentacarbonyl{dichloro(dicyclohexylamino)-phosphane-*κ*P}tungsten(0)]	606.08	0.2	122	
tert-Butyllithium (1.7 M in *n*-hexane)	64.05	0.4		0.23
1-Hexene	84.16	1.5	130	
Toluene	92.14			4
Et_2O	74.12			20

Purification:

The residue was filtered through solid phase (Ø = 2 cm, h = 1.5 cm SiO_2, r.t., Et_2O). The solvent was evaporated *in vacuo* (5 x 10^{-2} mbar) and the product obtained as an orange oil.

Reaction cipher: PJ-417 (16m3a026.20)

Molecular formula: $C_{23}H_{34}NO_5PW$

Yield: 72 mg (0.116 mmol, 58%)

Molar mass: 619.34 g/mol

IR (ATR diamond): *v* / cm^{-1} = 2929 (m, *v*(CH)), 2855 (m, *v*(CH)), 2068 (s, *v*(CO)), 1978 (s, *v*(CO)), 1904 (vs, *v*(CO)).

MS (EI, 70 eV, ^{184}W) m/z (%) = 536.1 (3) $[M\text{-}Cy]^+$, 508.1 (2) $[M\text{-}Cy\text{-}CO]^+$, 354.9 (1) $[W(CO)_5\text{-}P]^+$, 295.2 (2) $[M\text{-}W(CO)_5]^+$, 267.9 (4) $[W(CO)_3]^+$, 239.9 (2) $[W(CO)_2]^+$, 212.2 (4) $[M\text{-}W(CO)_5\text{-}Cy]^+$, 84.1 (17) $[C_6H_{12}]^+$, 56.1 (45) $[C_4H_8]^+$.

Elemental analysis	calculated	C 44.60	H 5.53	N 2.26
	found	C 42.48	H 4.75	N 2.85

^{1}H NMR (300.1 MHz, 298 K, C_6D_6): δ / ppm = 0.53 (m, $^3J_{H,H}$ = 7.7 Hz, $^2J_{P,H}$ = 7.6 Hz, 1H, PC*H*), 0.92 (t, $^3J_{H,H}$ = 7.2 Hz, 3H, CH_3), 1.07-1.26 (m, xH, NCHCH_2), 1.23-1.39 (m, 2H, $CHCH_2CH_2CH_2$), 1.34-1.53 (m, $NCHCH_2CH_2CH_2$), 1.40-1.52 (m, 6H, $NCHCH_2CH_2$), 1.48-1.58 (m, 2H, CHCH_2), 1.55-1.70 (m, 2H, $CHCH_2CH_2$), 1.57-1.72 (m, 2H, PCH_2), 1.60-1.73 (m, xH, NCHCH_2), 1.84-1.95 (m, 2H, $NCHCH_2CH_2$), 2.64-2.81 (m, 2H, NC*H*).

$^{13}C\{^1H\}$ NMR (75.5 MHz, 298 K, C_6D_6): δ / ppm = 14.2 (s, *C*H_3), 22.8 (s, CH_2*C*H_2CH_3), 22.8 (s, P*C*H), 25.9 (s, $CHCH_2$*C*H_2), 25.9 (s, CH*C*H_2), 26.8 (d, $^3J_{P,C}$ = 4.1 Hz, NCH*C*H_2), 31.6 (d, $^4J_{P,C}$ = 3.3 Hz, $NCHCH_2$*C*H_2), 32.0 (d, $^1J_{P,C}$ = 14.0 Hz, P*C*H_2), 33.6 ($^4J_{P,C}$ = 3.5 Hz, NCH_2CH_2*C*H_2), 35.3 (d, $^5J_{P,C}$ = 1.8 Hz, $NCHCH_2CH_2$*C*H_2), 60.4 (d, $^2J_{P,C}$ = 4.1 Hz, N*C*H), 197.8 (d_{sat}, $^2J_{P,C}$ = 8.9 Hz), 198.9 (d, $^2J_{P,C}$ = 32.0 Hz, *trans*-CO).

$^{31}P\{^1H\}$ NMR (121.5 MHz, 298 K, C_6D_6): δ / ppm = -108.3 (s_{sat}, $^1J_{W,P}$ = 285.9 Hz), -110.9 (s_{sat}, $^1J_{W,P}$ = 281.9 Hz) [80:20].

^{31}P NMR (121.5 MHz, 298 K, C_6D_6): δ / ppm = -107.8 (br. s_{sat}, $^1J_{W,P}$ = 285.9, FWHM ~51 Hz), -110.4 (br. s, FWHM ~37 Hz).

5.5.6 Synthesis of [Pentacarbonyl-{1-chloro-2-hydro-1-organyl-6-diphenyl-*p*-phosphaquinodimethane-*κ*P}metal(0)] (37,39) and [Tetracarbonyl-{1-chloro-2-hydro-1-organyl-6-diphenyl-*p*-phosphaquinodimethane-*κ*P}iron(0)] (38)

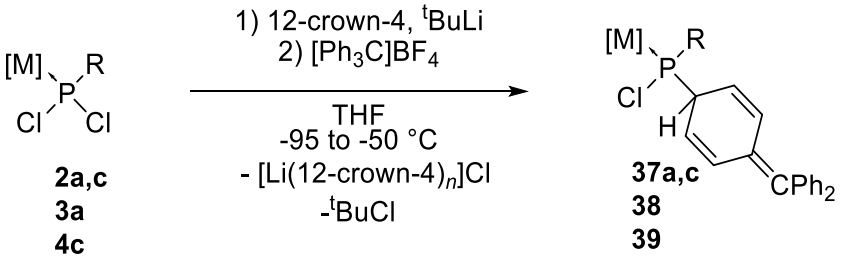

2, 37: [M] = $W(CO)_5$, R = NPh_2 (**a**), CPh_3 (**c**)
3, 38: [M] = $Fe(CO)_4$, R = NPh_2
4, 39; [M] = $Cr(CO)_5$, R = CPh_3 **(c)**

General synthesis:

The [Pentacarbonyl{dichloro(organyl)phosphane-*κ*P}metal(0)] (**2,4**) or [Tetracarbonyl{dichloro-(organyl)phosphane-*κ*P}iron(0)] (**3**) was dissolved in THF and 12-crown-4 was added (R = **NPh_2**, **NCy_2**). The *tert*-butyllithium was added at -80 (**2c,4**) or -95 (**2a,3a**) °C and after 10 - 30 min the triphenylcarbenium tetrafluoroborate was added. The solution was stirred while warming up to -50 °C and the solvent was removed *in vacuo* (2 x 10^{-2} mbar) at -50 °C.

5.5.6.4 [Pentacarbonyl-{1-chloro-2-hydro-1-diphenylamino-6-diphenyl-*p*-phosphaquinodimethane-*κ*P}tungsten(0)] (37a)

Used reagents and solvents:

Chemicals	*M* / g mol^{-1}	*n* / mmol	*m* / mg	*V* / mL
[Pentacarbonyl{dichloro(diphenylamino)-phosphane-*κ*P}tungsten(0)]	593.98	0.2	118	
tert-Butyllithium (1.7 M in *n*-hexane)	64.05	0.21		0.12
12-crown-4	176.21	0.22		0.064
Triphenylcarbenium tetrafluoroborate	330.10	0.22	73	
THF	72.11			2.5
Toluene	92.14			10

Purification:

The product was extracted using toluene (2 x 5 mL) to obtain a clear yellow solution. The solvent was evaporated *in vacuo* (5 x 10^{-2} mbar) and the crude product obtained as a yellow oil.

Reaction cipher: PJ-433 (38p5a035.20)

Molecular formula: $C_{36}H_{25}ClNO_5PW$

Yield: 20 mg (0.02 mmol, 25 %)

Molar mass: 801.86 g/mol

MS (EI, 70 eV, 184W) m/z (%) = 766.0 (0.03) $[M\text{-}Cl]^+$, 688.0 (0.07) $[M\text{-}Cl\text{-}Ph\text{-}H]^+$, 661.1 (0.05) $[M\text{-}Cl\text{-}Ph\text{-}CO]^+$, 523.0 (0.04) $[M\text{-}Cl\text{-}C_{19}H_{15}]^+$, 243.1 (100) $[C_{19}H_{15}]^+$, 165.1 (85) $[C_{13}H_9]^+$, 77.0 (10) $[Ph]^+$.

IR (ATR diamond): *ν* / cm^{-1} = 2075 (s, *ν*(CO)), 1923 (vs, *ν*(CO)).

^{1}H NMR (500.1 MHz, 298 K, C_6D_6): δ / ppm = 4.45 (dm, $^2J_{P,H}$ = 36.7 Hz, P-C*H*, 1H), 5.82 (m, $^3J_{H,H}$ = 10.5 Hz, P-CH-C*H*, 1H), 5.98 (m, $^3J_{H,H}$ = 10.4 Hz, P-CH-C*H*, 1H), 7.21 (m, $^3J_{H,H}$ = 10.7 Hz, P-CH-CH=C*H*, 1H), 7.23 (m, $^3J_{H,H}$ = 10.7 Hz, P-CH-CH=C*H*, 1H), 6.9-7.5 (m, Ph, 20H).

^{13}C{^{1}H} NMR (125.8 MHz, 298 K, C_6D_6): δ / ppm = 52.7 (d, $^1J_{P,C}$ = 24.6 Hz, P-*C*H), 122.2 (m, P-CH-*C*H), 123.5 (s, P-CH-*C*H), 127.3 (s, Ph), 127.8-130.1 (m, Ph), 129.2 (d, $^xJ_{P,C}$ = 5.7 Hz, Ph), 130.8 (m, Ph), 132.7 (d, $^3J_{P,C}$ = 14.4 Hz, P-CH-CH=*C*H), 133.7 (d, $^3J_{P,C}$ = 14.3 Hz, P-CH-CH=*C*H), 141.7 (d, $^2J_{P,C}$ = 5.6 Hz, *ipso*-Ph), 142.0 (d, $^2J_{P,C}$ = 5.5 Hz, *ipso*-Ph), 141.9 (s, *ipso*-Ph), 142.1 (s, P-C-C=C-C=*C*), 142.3 (s, *ipso*-Ph), 144.0 (d, $^4J_{P,C}$ = 5.1, Hz, P-C-C=C-*C*), 196.1 (d_{Sat}, $^2J_{P,C}$ = 7.7 Hz, $^1J_{W,C}$ = 126.6, *cis*-CO), 198.3 (d, $^2J_{P,C}$ = 40.8 Hz, *trans*-CO).

^{31}P NMR (202.5 MHz, 298 K, C_6D_6): δ / ppm = 127.5 (d_{sat}, $^1J_{W,P}$ = 333.0 Hz, $^2J_{P,H}$ = 36.6 Hz).

5.5.6.2 [Pentacarbonyl-{2-hydro-1-chloro-1-triphenylmethyl-6-diphenyl-*p*-phosphaquinodimethan-*κ*P}tungsten(0)] (37c)

Used reagents and solvents:

Chemicals	*M* / g mol^{-1}	*n* / mmol	*m* / mg	*V* / mL
[Pentacarbonyl{dichloro(triphenylmethyl)phosphane-*κ*P}tungsten(0)]	669.09	0.5	334	
tert-Butyllithium (1.7 M in *n*-hexane)	64.05	0.53		0.31
Triphenylcarbenium tetrafluoroborate	330.10	0.52	173	
THF	72.11			4.5
Toluene	92.14			40

Purification:

The product was extracted using cold toluene (4 x 10 mL) and the solvent was removed *in vacuo* (5 x 10^{-2} mbar). The product was obtained as a grey powder.

Reaction cipher: PJ-335 (46m3a020), VN-847, JMV-524

Molecular formula: $C_{43}H_{30}ClO_5PW$

Yield: 184 mg (0.21 mmol, 42 %)

Melting point 159 – 161 °C

Molar mass: 876.97 g/mol

MS (Lifdi, ^{184}W) m/z (%) = $[M\text{-}CHPh_3]^+$ (30), $[CHPh_3]^+$ (100).

IR (ATR diamond): *v* / cm^{-1} = 3053 (b, *v*(CH_2)), 2070 (b, *v*(CO)), 2060 (s, *v*(CO)), 1984 (s, *v*(CO)), 1918 (s, *v*(CO)).

Elemental analysis calculated C 59.37 H 3.59

found C 58.89 H 3.45

^{1}H NMR (300.1 MHz, 298 K, C_6D_6) δ / ppm = 4.7 (m, $^2J_{P,H}$ = 29.1 Hz, P-C*H*, 1H), 5.0 (m, P-CH-C*H*, 1H), 6.1 (m, P-CH-C*H*, 1H), 6.7 (m, P-CH-CH=C*H*, 1H), 7.0 (m, P-CH-CH=C*H*, 1H), 6.8-7.8 (m, Ph, 25H).

^{13}C{^{1}H} NMR (75.7 MHz, 298 K, C_6D_6): δ / ppm = 54.9 (d, $^1J_{P,C}$ = 1.2 Hz, P-*C*H), 70.4 (d, $^1J_{P,C}$ = 12.2 Hz, *C*Ph_3), 124.4 (s, P-CH-CH), 126.2 (d, $^2J_{P,C}$ = 3.3 Hz, P-CH-CH), 127-131 (s, Ph), 132.1 (d, $^2J_{P,C}$ = 12.3 Hz, P-CH-CH=CH), 132.5 (d, $^2J_{P,C}$ = 11.3 Hz, P-CH-CH=CH), 140.1 (d, $^2J_{P,C}$ = 4.2 Hz, *ipso*-Ph), 141.3 (d, $^2J_{P,C}$ = 5.3 Hz, *ipso*-Ph), 141.4 (d, $^2J_{P,C}$ = 5.2 Hz, *ipso*-Ph), 141.9 (s, *ipso*-Ph), 142.1 (s, P-C=C-C=C), 142.3 (s, *ipso*-Ph), 143.3 (d, $^xJ_{P,C}$ = 1.1, Hz, P-C=C-C=C), 196.8 (d_{Sat}, $^2J_{P,C}$ = 6.0 Hz, $^1J_{W,C}$ = 128.2, *cis*-CO), 198.5 (d, $^2J_{P,C}$ = 37.2 Hz, *trans*-CO).

^{31}P NMR (121.5 MHz, 298 K, C_6D_6): δ / ppm = 147.8 (d_{sat}, $^1J_{W,P}$ = 275.8 Hz, $^2J_{P,H}$ = 29.1 Hz).

5.5.6.3 [Tetracarbony{2-hydro-1-chloro-1-diphenylamino-6-diphenyl-*p*-phosphaquinodimethane-*κ*P}iron(0)] (38)

Used reagents and solvents:

Chemicals	*M* / g mol^{-1}	*n* / mmol	*m* / mg	*V* / mL
[Tetracarbonyl{dichloro(diphenylamino)-phosphane-*κ*P}iron(0)]	437.98	1.71	750	
tert-Butyllithium (1.7 M in *n*-hexane)	64.05	1.80		1.06
12-crown-4	176.21	3.43		0.55
Triphenylcarbenium tetrafluoroborate	330.10	1.71	565	
THF	72.11			18
Toluene	92.14			30

Purification:

The product was extracted using toluene (6 x 5 mL). The solvent was evaporated in vacuo (5 x 10^{-2} mbar) to obtain a crude product.

Reaction cipher: TK-37 (28m3a019.17)

Molecular formula: $C_{35}H_{25}ClFeNO_4P$

Content in solution (^{31}P NMR integration of reaction mixture): 100 % (bad signal/noise ratio)

Molar mass: 645.86 g/mol

^{31}P NMR (121.5 MHz, 298 K, THF): δ / ppm = 183.6 (d, $^{2}J_{P,H}$ = 35.9 Hz)

5.5.6.4 [Pentacarbonyl{2-hydro-1-chloro-1-triphenylmethyl-6-diphenyl-*p*-phosphaquinodimethane-*κ*P}chromium(0)] (39)

Used reagents and solvents:

Chemicals	*M* / g mol^{-1}	*n* / mmol	*m* / mg	*V* / mL
[Pentacarbonyl{dichloro(triphenylmethyl)phosphane-*κ*P}chromium(0)]	537.25	0.3	161	
tert-Butyllithium (1.7 M in *n*-hexane)	64.05	0.32		0.18
Triphenylcarbenium tetrafluoroborate	330.10	0.3	99	
THF	72.11			4.5
Toluene	92.14			15

Purification:

The product was extracted using cold toluene (3 x 5 mL) and the solvent was removed *in vacuo* (5 x 10^{-2} mbar). After scratching in liquid Argon, the product was obtained as a green powder.

Reaction cipher: PJ-196 (05p5a020.18)

Molecular formula: $C_{43}H_{30}ClCrO_5P$

Yield: 83 mg (0.11 mmol, 37%)

Melting point 115 °C

Molar mass: 745.13 g/mol

MS (EI, 70 eV, ^{56}Cr) m/z (%) = 243.1 (100) $[CPh_3]^+$, 77.0 (38) $[Ph]^+$.

IR (ATR Diamant): ν / cm^{-1} = 2063.7 (m, ν(CO)), 1989.2 (w, ν(CO)), 1926.4 (vs, ν(CO)).

Elemental analysis	calculated	C 69.31	H 4.06
	found	C 67.47	H 4.54

^{1}H NMR (500.1 MHz, 298 K, C_6D_6): δ / ppm = 4.66 (d, $^2J_{P,H}$ = 27.6 Hz, 1 H, P-C*H*), 5.05 (m, 1 H, P-CH-C*H*), 6.19 (m, 1 H, P-CH-C*H*), 6.74 (m, 1 H, P-CH-C*H*), 6.91 - 7.13 (m, 20 H, Ph), 7.14 - 7.21 (m, 10 H, Ph), 7.28 - 7.33 (m, 7 H, Ph), 7.73 - 7.77 (m , 2 H, Ph).

^{13}C{^{1}H} NMR (125.8 MHz, 298 K, C_6D_6): δ / ppm = 55.7 (d, $^2J_{P,C}$ = 5.8 Hz, P-*C*H), 72.3 (d, $^1J_{P,C}$ = 16.9 Hz, *C*Ph_3), 124.9 (s), 126.7 (d, $^xJ_{P,C}$ = 2.8 Hz, P-Ar), 128.4 (s), 128.8 (s), 130.8 (s), 130.9 (d, $^xJ_{P,C}$ = 3.6 Hz, P-Ar), 131.2 (d, $^xJ_{P,C}$ = 4.9 Hz, P-Ar), 132.9 (d, $^xJ_{P,C}$ = 8.0 Hz, P-Ar), 140.9 (d, $^xJ_{P,C}$ = 4.4 Hz, *ipso*-C), 141.7 (d, $^xJ_{P,C}$ = 5.1 Hz, *ipso*-C), 141.8 (d, $^xJ_{P,C}$ = 4.9 Hz, *ipso*-C), 142.4 (s, *ipso*-C, Ph), 142.5 (s, *ipso*-C, Ph), 143.5 (s, *ipso*-C, Ph), 215.6 (d, $^2J_{P,C}$ = 10.3 Hz, *cis*-CO), 221.5 (s, *trans*-CO).

^{31}P NMR (202.5 MHz, 298 K, C_6D_6): δ / ppm = 197.0 ($^2J_{P,H}$ = 27.7 Hz)

5.5.7 Synthesis of [pentacarbonyl-{chloro(organyl)-*p*-(diphenylmethyl)phenylphosphane-*κ*P}metall(0)] (42,44) and [tetracarbonyl-{chloro(organyl)-*p*-(diphenylmethyl)phenylphosphane-*κ*P}metall(0)] (43)

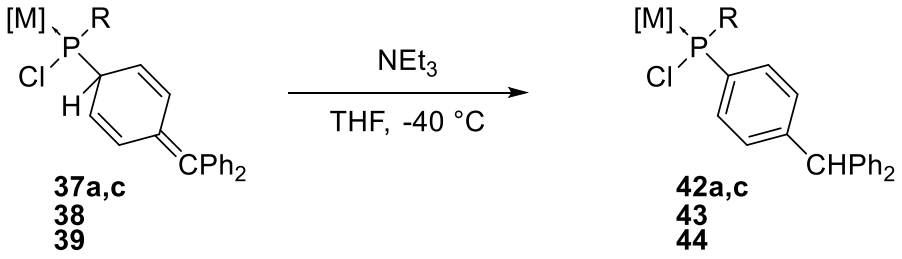

37a,c
38
39

42a,c
43
44

37, 42: [M] = $W(CO)_5$, R = NPh_2 (**a**), CPh_3 (**c**)
38, 43: [M] = $Fe(CO)_4$, R = NPh_2
39, 44; [M] = $Cr(CO)_5$, R = CPh_3 **(c)**

General syntheses:

Complexes **37-39** were dissolved in THF or toluene and NEt_3 was added at -40 °C. The solution was stirred for at least 2 h while warming up to ambient temperatures, before removing the solvent in vacuo (5 x 10^{-2} mbar).

5.5.7.1 [Pentacarbonyl{chloro(diphenylamino)-*p*-(diphenylmethyl)phenylphosphane-*κ*P}tungsten(0)] (42a)

Used reagents and solvents:

Chemicals	*M* / g mol^{-1}	*n* / mmol	*m* / mg	*V* / mL
{Pentacarbonyl-(1-chloro-1-diphenylamino-6-diphenyl-2-hydro-*p*-phosphaquinodimethane-*κ*P)tungsten(0)}	801.86	0.02	15	
Triethylamine	101.19	0.71		0.1
Toluene	92.14			2

Reaction cipher: PJ-434 (38p5a041.20)

Molecular formula: $C_{36}H_{25}ClNO_5PW$

Yield: <5 %

Molar mass: 801.86 g/mol

MS (EI, 70 eV, ^{184}W) m/z (%) = 801.1 (0.2) $[M]^{+\bullet}$, 243.1 (45) $[CPh_3]^+$, 168.1 (78) $[NPh_2]^+$, 77.0 (25) $[Ph]^+$.

IR (ATR diamond): 2076 (s, *ν*(CO)), 1921 (vs, *ν*(CO)).

^{1}H NMR (500.1 MHz, 298 K, C_6D_6): δ / ppm = 5.3 (s, C*H*Ph_2, 1H), 6.80-7.13 (m, P-Aryl, CPh_2, NPh_2, 17H), 7.29 (m, N-Ph, 5H), 7.64 (m, $^{3}J_{P,C}$ = 11.4 Hz, P-C-C*H*, 2H).

^{13}C{^{1}H} NMR (125.8 MHz, 298 K, C_6D_6): δ / ppm = 56.2 (s, *C*HPh_2), 123.5 (s, Ph), 126.9 (d, $^{x}J_{P,C}$ = 2.3 Hz, N-Ph), 127.3 (s, Ph), 127.8-130.1 (m, Ar), 128.6 (d, $^{1}J_{P,C}$ = 21.1 Hz, P-C), 129.0 (d, $^{x}J_{P,C}$ = 6.2 Hz, P-Ar), 129.6 (d, $^{x}J_{P,C}$ = 2.6 Hz, N-Ph), 129.8 (d, $^{x}J_{P,C}$ = 2.0 Hz, N-Ph), 129.9 (d, $^{x}J_{P,C}$ = 3.26 Hz, P-Ar), 130.9 (s, Ar), 131.0 (s, Ar), 143.5 (d, $^{2}J_{P,C}$ = 6.1 Hz, *ipso*-Ph), 143.7 (s, *ipso*-Ph), 144.0 (d, $^{2}J_{P,C}$ = 5.06 Hz, *ipso*-Ph), 144.4 (s, *ipso*-Ph), 147.8 (d, $^{4}J_{P,C}$ = 1.6 Hz, P-Ar), 147.8 (s, *ipso*-Ph), 195.9 (d_{sat}, $^{2}J_{P,C}$ = 7.7 Hz, $^{1}J_{W,C}$ = 127.1, *cis*-CO), 198.7 (d, $^{2}J_{P,C}$ = 38.6 Hz, *trans*-CO).

^{31}P NMR (202.5 MHz, 298 K, C_6D_6): δ / ppm = 116.8 (t_{sat}, $^{1}J_{W,P}$ = 328.9 Hz, $^{3}J_{P,H}$ = 11.5 Hz).

5.5.7.2 [Pentacarbonyl{chloro(triphenylmethyl)-*p*-(diphenylmethyl)phenylphosphane-*κ*P}tungsten(0)] (42c)

Used reagents and solvents:

Chemicals	*M* / g mol^{-1}	*n* / mmol	*m* / mg	*V* / mL
{Pentacarbonyl[1-chloro-1-triphenylmethyl-6-diphenyl-2-hydro-*p*-phosphaquinodimethane-*κ*P)]tungsten(0)}	876.97	0.47	412	
Triethylamine	101.19	2.2		0.3
Toluene	92.14			45
Et_2O	74.12			4

Purification:

After the extraction of complex **42c** with toluene, NEt_3 was added at -30 °C and kept stirring over night while warming up to ambient temperature. The solvent was removed *in vacuo* (5 x 10^{-2} mbar) and the obtained blue-violet solid was washed with Et_2O (2 x 2 mL). The product was obtained as a beige powder.

Reaction cipher: PJ-145 (04p5a002.17)

Molecular formula: $C_{43}H_{30}ClO_5PW$

Yield: 310 mg (0.35 mmol, 43%)

Melting point 150 °C

Molar mass: 876.97 g/mol

MS (EI, 70 eV, ^{184}W) m/z (%) = 764.1 (0.007) [M-Ph-Cl]$^{+}$, 680.1 (0.02) [M-Ph-Cl-3CO]$^{+}$, 633.0 (0.04) [M-CPh_3]$^{+}$, 492.0 (0.2) [M-Cl-Ph-CPh_3-CO]$^{+}$, 458.0 (0.1) [M-Cl-CPh_3-5CO]$^{+}$, 243.1 (100) [CPh_3]$^{+}$.

IR (ATR diamond): $\tilde{\nu}$ / cm^{-1} = 3058.3 (w, ν(CH)), 2072.7 (s, ν(CO)), 1988.2 (w, ν(CO)), 1907.2 (vs, ν(CO)).

Elemental analysis	calculated	C 58.89	H 4.25
	found	C 59.70	H 3.72

X-ray diffraction analysis BC1 (GSTR547, GXray5066f)

^{1}H NMR (500.1 MHz, 298 K, $CDCl_3$): δ / ppm = 5.71 (s, 1 H, $CHPh_2$), 6.81-6.85 (m, 2 H, Ph), 7.09 - 7.15 (m, 4 H, P-Ar), 7.16 - 7.25 (m, 5 H, Ph), 7.26 - 7.32 (m, 2 H, Ph), 7.32 - 7.43 (m, 5 H, Ph), 7.44 - 7.54 (m, 9 H, Ph), 7.55 - 7.62 (m, 5 H, Ph), 7.77 - 7.83 (m, 2 H, Ph), 7.83 - 7.88 (m, 2 H, Ph).

^{13}C{^{1}H} NMR (125.8 MHz, 298 K, $CDCl_3$): δ / ppm = 56.4 (*C*HPh_2), 70.3 ($^{1}J_{P,C}$ = 4.5 Hz, *C*Ph_3), 126.7 ($^{X}J_{P,C}$ = 2.0 Hz, CPh_3), 127.4 (CPh_3), 127.7 (CPh_3), 128.3 (CPh_3), 128.6 ($CHPh_2$), 128.7 (CPh_3), 128.9 ($^{X}J_{P,C}$ = 9.2 Hz, P-Ar), 129.5 ($CHPh_2$), 131.0 ($^{X}J_{P,C}$ = 2.2 Hz, CPh_3), 131.2 ($^{X}J_{P,C}$ = 11.7 Hz, P-Ar), 131.8 ($^{X}J_{P,C}$ = 7.4 Hz, CPh_3), 136.1 ($^{1}J_{P,C}$ = 17.2 Hz, P-C), 139.2 ($^{2}J_{P,C}$ = 5.9 Hz, *ipso*-C, CPh_3), 139.8 ($^{2}J_{P,C}$ = 5.6 Hz, *ipso*-C, CPh_3), 143.2 (*ipso*-C, $CHPh_2$), 143.3 (*ipso*-C, $CHPh_2$), 143.6 ($^{2}J_{P,C}$ = 8.9 Hz, *ipso*-C, CPh_3), 146.7 ($^{4}J_{P,C}$ = 1.4 Hz, P-Ar), 196.9 ($^{2}J_{P,C}$ = 6.3 Hz, $^{1}J_{W,C}$ = 128.2 Hz, *cis*-CO), 199.3 ($^{2}J_{P,C}$ = 34.5 Hz, $^{1}J_{W,C}$ = 143.7 Hz, *trans*-CO).

^{31}P NMR (202.5 MHz, 298 K, $CDCl_3$): δ / ppm = 118.8 ($^{1}J_{W,P}$ = 271.0 Hz).

5.5.7.3 [Tetracarbonyl{chloro(diphenylamino)-*p*-(diphenylmethyl)phenylphosphane-*κ*P}iron(0)] (43)

Used reagents and solvents:

Chemicals	***M* / g mol^{-1}**	***n* / mmol**	***m* / mg**	***V* / mL**
{Tetracarbonyl-(1-chloro-1-diphenylamino-6-diphenyl-2-hydro-*p*-phosphaquinodimethane-*κ*P)]iron(0)}	645.86	0.47	0.3	
Triethylamine	101.19	4.6		0.64
THF	72.11			40
Toluene	92.14			
PE(40/65)				
Et_2O	74.12			

Purification:

The obtained brown residue was purified with a column chromatography (Ø = 3 cm, h = 11 cm SiO_2, -38 °C, toluene/PE) and the following fractions were collected:

1. Toluene/PE (1:10), 200 mL
2. Toluene/PE (1:5), 200 mL
3. Toluene/PE (1:2), 200 mL

4. Toluene/PE (1:1), 350 mL (product)

Fraction 4 was containing the desired product. After evaporation of the solvent in vacuo (5 x 10^{-2} mbar) the residue was purified again through column chromatography (Ø = 1 cm, h = 7.5 cm Al_2O_3, -20 °C, Et_2O/PE) and the following fractions were collected

1. Et_2O/PE (1:10), 75 mL
2. Et_2O/PE (1:5), 75 mL (product)
3. Et_2O/PE (1:5), 75 mL (product)
4. Et_2O/PE (1:1), 75 mL

Fractions 2 and 3 were containing the product. After evaporation of the solvents *in vacuo* (5 x 10^{-2} mbar) and the product was obtained as an orange solid.

Reaction cipher: TK-53 (30m3a053.17, 34p5a012.17)

Molecular formula: $C_{35}H_{25}ClFeNO_4P$

Yield: 15 mg (0.02 mmol, 5 %)

Molar mass: 645.86 g/mol

MS (Lifdi, ^{56}Fe) m/z (%) = 644.9 (100) $[M-H]^+$.

IR (ATR diamond): $\tilde{\nu}$ / cm^{-1} = 3060 (w, *ν*(CH)), 2960 (m, *ν*(CH, Ph)), 2924 (m, *ν*(CH, Ph)), 2853 (m, *ν*(CH, Ph)), 2057 (vs, *ν*(CO)), 1984 (vs, *ν*(CO)), 1932 (vs, *ν*(CO)).

^{1}H NMR (300.1 MHz, 298 K, C_6D_6): δ / ppm = 5.20 (s, 1H, C*H*), 6.75 – 6.97 (m, 14 H, Ph), 7.00 – 7.12 (m, 9 H, Ph), 7.23 – 7.33 (m, 5 H, Ph), 7.74 (m ,3 H, Ph).

^{13}C{^{1}H} NMR (125.8 MHz, 298 K, C_6D_6): δ / ppm = 56.7 (s, *C*HPh_2), 126.9 (d), 127.4 (s), 128.7 (d), 129.3 (d), 129.4 (s), 129.5 (d, $^3J_{P,C}$ = 12.4 Hz, *meta*-PPh), 129.8 (d, $^nJ_{P,C}$ = 3.3 Hz, *ortho*-$CHPh_2$), 132.0 ppm (d, $^3J_{P,C}$ = 13.6 Hz, *ortho*-C, P-Ph), 135.5 (d, $^1J_{P,C}$ = 63.1 Hz, PC_{quart}), 143.3 (d, $^2J_{P,C}$ = 5.8 Hz, NC_{quart}), 145.6 (s, *ipso*-$CHPh_2$), 148.3 (d, $^4J_{P,C}$ = 2.4 Hz, *para*-PPh), 212.9 (d, $^2J_{P,C}$ = 18.6 Hz, *C*O).

^{31}P NMR (121.5 MHz, 298 K, C_6D_6): δ / ppm = 174.4 (s).

5.5.7.4 [Pentacarbonyl{chloro(triphenylmethyl)-*p*-(diphenylmethyl)phenyl-phosphan-*κ*P}chromium(0)] (44)

Used reagents and chemicals:

Chemicals	*M* / g mol^{-1}	*n* / mmol	*m* / mg	*V* / mL
{Pentacarbonyl[1-chloro-1-triphenylmethyl-6-diphenyl-2-hydro-*p*-phosphaquinodimethane-*κ*P)]chromium(0)}	745.13	0.2	149	
Triethylamine	101.19	0.57		0.08
Toluene	92.14			5
Et_2O	74.12			50

Purification:

The reaction was done with the extracted crude product from the synthesis of **39** in toluene. The NEt_3 was added at -30 °C and the reaction was stirred overnight while warming to ambient temperature. The solvent was removed *in vacuo* (5 x 10^{-2} mbar) and the residue filtered through solid phase (Ø = 1 cm, h = 15 cm Al_2O_3, r.t., Et_2O). The product was obtained as a yellow solid.

Reaction cipher: PJ-195 (05p5a012.18)

Molecular formula: $C_{43}H_{30}ClCrO_5P$

Yield: 30 mg (0.04 mmol, 20%)

Melting point 169 °C

Molar mass: 745.13 g/mol

MS (Lifdi, ^{184}W) m/z (%) = 744.0 (7) $[M-H]^+$, 243.1 (100) $[CPh_3]^+$.

IR (ATR diamond): *v* / cm^{-1} = 2064.6 (m, *v*(CO)), 1991.1 (s, *v*(CO)), 1916.3 (vs, *v*(CO)).

Elemental analysis calculated C 69.31 H 4.06

found C 68.10 H 4.07

X-ray diffraction analysis A1 (GSTR609, GXray5535)

^{1}H NMR (500.1 MHz, 298 K, C_6D_6): δ / ppm = 5.25 (s, $CHPh_2$, 1 H), 6.79 - 6.82 (m, 2 H, Ph), 6.86 - 6.90 (m, 4 H, Ph), 6.91 - 6.95(m, 5 H, Ph), 6.98 - 7.03 (m, 4 H, Ph), 7.04 - 7.07 (m, 4 H, Ph), 7.07 - 7.10 (m, 4 H, Ph), 7.20 - 7.25 (m, 2 H, Ph), 7.72 - 7.76 (m, 2 H, Ph), 7.76 - 7.80 (m, 2 H, Ph).

^{13}C{^{1}H} NMR (125.8 MHz, 298 K, C_6D_6): δ / ppm = 56.6 ($CHPh_2$), 72.4 (d, $^1J_{P,C}$ = 9.4, CPh_3), 126.9 (Ph), 127.6 (Ph), 128.4 (Ph), 128.7 (Ph), 128.8 (Ph), 128.9 (Ph), 129.4 (d, $^xJ_{P,C}$ = 8.2 Hz, P-Ar), 129.7 (Ph), 129.8 (Ph), 131.2 (Ph), 131.3 (d, $^xJ_{P,C}$ = 8.9, P-Ar), 131.9 (d, $^xJ_{P,C}$ =6.0 Hz, P-Ar), 132.0 (d, $^xJ_{P,C}$ = 7.8 Hz, P-Ar), 136.7 (d, $^2J_{P,C}$ = 10.5 Hz, *ipso*-C, CPh_3), 139.9 (d, $^2J_{P,C}$ = 6.2 Hz, *ipso*-C, CPh_3), 140.8 (d, $^2J_{P,C}$ = 5.4 Hz, *ipso*-

C, CPh_3), 143.4 (*ipso*-C, $CHPh_2$), 143.6 (*ipso*-C, $CHPh_2$), 147.2 (d, $^{x}J_{P,C}$ = 1.5 Hz, *ipso*-C, P-Ar), 215.5 (d, $^{2}J_{P,C}$ = 11.0 Hz, *cis*-CO), 221.3 (d, $^{2}J_{P,C}$ = 1.2 Hz, *trans*-CO).

^{31}P NMR (202.5 MHz, 298 K, C_6D_6): δ / ppm = 171.8 (s).

5.5.8 Synthesis of [Pentacarbonyl{1-triphenylmethyl-6-diphenylmethyl-*p*-phosphaquinodimethane-*κ*P}metal(0)] complexes (45,46)

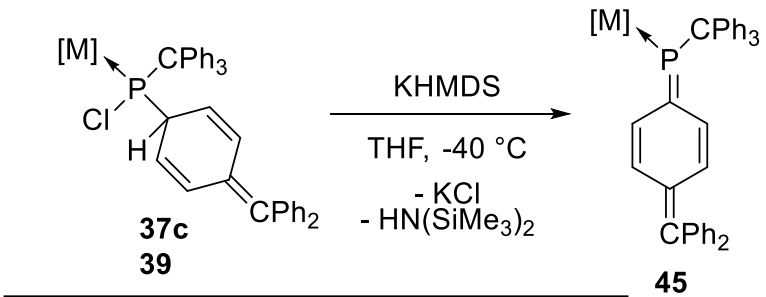

37c
39

45
46

37c, 39: [M] = $W(CO)_5$; **31, 37:** [M] = $Cr(CO)_5$

General Synthesis:

{Pentacarbonyl-(2-hydro-1-chloro-1-triphenylmethyl-6-diphenyl-*p*-phosphaquinomethane)metal(0)} and KHMDS were separately dissolved in equal amounts of THF and cooled down to -40°C before the KHMDS (in THF) was slowly added. The solution immediately changes its colour to dark violet and after 1 h the solvent was removed *in vacuo* (5 x 10^{-2} mbar).

5.5.8.4 [Pentacarbonyl{1-triphenylmethyl-6-diphenylmethyl-*p*-phosphaquinodimethane-*κ*P}tungsten(0)] (45)

Used reagents and solvents:

Chemicals	***M* / g mol^{-1}**	***n* / mmol**	***m* / mg**	***V* / mL**
[Pentacarbonyl{chloro(triphenylmethyl)-*p*-(diphenylmethyl)phenyl-phosphane-*κ*P}tungsten(0)]		0.18	158	
KHMDS		0.18	36	
THF	72.11			2+1
Et_2O	92.14			5

Purification:

The residue was dissolved in Et_2O and filtered over silanized SiO_2 (h= 1 cm, Ø = 0.5 cm, r.t., syringe) in the glovebox. After evaporation of the solvent in vacuo (5 x 10^{-2} mbar) a dark violet solid was obtained.

Reaction cipher: PJ-225 (27m3a028.18)), VN-839 (36m3a018.15), JMV- 522 (12p5a017.16)

Molecular formula: $C_{43}H_{29}O_5PW$

Yield: 110 mg (0.13 mmol, 73%)

Melting point 146 – 148 °C

Molar mass: 850.51 g/mol

IR (ATR diamond): ν / cm^{-1} = ν(CO): 2962 (b, $\nu(CH_2)$), 2065 (b, ν(CO)), 1985 (s, ν(CO)), 1913 (b, ν(CO)).

Elemental analysis	calculated	C 61.45	H 3.48
	found	C 62.80	H 4.64

^{1}H NMR (300.1 MHz, 298 K, $CDCl_3$): δ / ppm = 6.0 (dd, $^3J_{P,H}$ = 3.5 Hz, $^3J_{H,H}$ = 10.2 Hz, P=C-C*H*, 2H), 6.5 (d, $^3J_{H,H}$ = 10.2 Hz, P=C-CH=C*H*, 2H), 6.9-7.6 (m, Ph, 25H).

^{13}C{^{1}H} NMR (100.6 MHz, 298 K, $CDCl_3$): δ / ppm = 69.7 (s, CPh_3), 126-134 (Ph), 128.4 (s, P=C-C=C), 129.0 (s, P=C-C=C), 130.2 (s, P=C-C=C), 137.5 (s, P=C-C=C), 141.8 (d, $^4J_{P,C}$ = 17.8 Hz, P=C-C=C-C=C), 144.6 (d, $^5J_{P,C}$ = 3.9 Hz, P=C-C=C-C=C), 166.8 (d, $^1J_{P,C}$ = 36.2 Hz, P=C), 195.8 (d_{Sat}, $^2J_{P,C}$ = 13.2 Hz, $^1J_{W,C}$ = 126.9, *cis*-CO), 199.8 (d, $^2J_{P,C}$ = 34.4 Hz, $^1J_{W,C}$ = 145.7, *trans*-CO).

^{31}P NMR (202.5 MHz, 298 K, $CDCl_3$): δ / ppm = 212.9 (s_{sat}, $^1J_{W,P}$ = 270.3 Hz).

UV-vis (Et_2O): λ_{max} (abs., ε / L mol^{-1} cm^{-1}) = 238.0 (0.682, 56833); 336.0 (0.114, 9500); 563 (0.092, 7667)

5.5.8.2 [Pentacarbonyl-{1-triphenylmethyl-6-diphenylmethyl-*p*-phosphaquinodimethane-*κ*P}chromium(0)] (46)

Used reagents and solvents:

Chemicals	***M* / g mol^{-1}**	***n* / mmol**	***m* / mg**	***V* / mL**
{Pentacarbonyl-(2-hydro-1-chloro-1-triphenylmethyl-6 diphenyl-p-phosphaquinomethane)chromium(0)}	745.13	0.06	45	
KHMDS	199.48	0.06	12	
THF	72.11			5

Reaction cipher: PJ-218 (21m3b051.18)

Molecular formula: $C_{43}H_{29}O_5CrP$

Molar Mass: 708.67 g/mol

^{31}P NMR (202.5 MHz, 298 K, THF): δ / ppm = 257.0

6. References

[1] E. Wiberg, A. F. Holleman, N. Wiberg, *Lehrbuch der Anorganischen Chemie*, 102. Aufl., Walter de Gruyter, Berlin, **2007**.

[2] M. E. Weeks, *J. Chem. Educ.* **1932**, *9*, 11–21.

[3] E. Riedel, *Anorganische Chemie*, 6. Aufl., Walter de Gruyter, Berlin, **2004**.

[4] J. A. Osborn, F. H. Jardine, J. F. Young, G. Wilkinson, *J. Chem. Soc. A 1966, 1711–1732.*

[5] (a) P. Schwab, M. B. France, J. W. Ziller, R. H. Grubbs, *Angew. Chem. Int. Ed. Engl.* **1995**, *34*, 2039–2041; (b) P. Schwab, R. H. Grubbs, J. W. Ziller, *J. Am. Chem. Soc.* **1996**, *118*, 100–110; (c) M. Scholl, S. Ding, C. W. Lee, R. H. Grubbs, *Org. Lett*. **1999**, *1*, 953–956.

[6] (a) F. Mathey, *Angew. Chem. Int. Ed*. **1987**, *26*, 275-370; (b) K. Lammertsma, *Top. Curr. Chem.* **2003**, *237*, 95-119.

[7] F. Mathey, N. H. T. Huy, A. Marinetti, *Helv. Chim. Acta.* **2001**, *84*, 2938-2957.

[8] (a) A. H. Cowley, A. R. Barron, *Acc. Chem. Res.* **1988**, *21*, 81-87; (b) A. H. Cowley, *Acc. Chem. Res.* **1979**, *12*, 98-104; H. Aktaş, J. C. Slootweg, K. Lammertsma, *Angew. Chem. Int. Ed.* **2010**, *49*, 2102-2113; (c) J. C. Slootweg, K. Lammertsma in *Science of Synthesis, Vol. 42* (Eds: B. M. Trost, F. Mathey), Thieme, Stuttgart **2009**, pp. 15-36.

[9] M. T. Nguyen, A. V. Keer, L. G. Vanquickenborne, *J. Org. Chem.* **1996**, *61*, 7077.

[10] (a) S. Creve, K. Pierloot, M. T. Nguyen, L. G. Vanquickenborne, *Eur. J. Inorg. Chem.* **1999**, 107-115; (b) S. Grigoleit, A. Alijah, A. B. Rozhenko, R. Streubel, W. W. Schoeller, *J. Organomet. Chem.* **2002**, *643-644*, 223-230; (c) Z. Benkö, R. Streubel, L. Nyulászi, *Dalton Trans.* **2006**, 4321-4327.

[11] (a) E. O. Fischer, A. Maasböl, *Angew. Chem.* **1964**, *76*, 645; (b) A. J. Arduengo III, R. L. Harlow, M. Kline, *J. Am. Chem. Soc.* **1991**, *113*, 361-363; (c) A. Igau, H. Grützmacher, A. Baceiredo, G. Bertrand, *J. Am. Chem. Soc.* **1988**, *110*, 6463-6466; (d) A. Igau, A. Baceiredo, G. Trinquier, G. Bertrand, *Angew. Chem*. **1989**, *101*, 617-618; (e) G. Bertrand, *Carbene Chemistry*, Marcel Dekker, New York, **2002**; (f) D. Bourissou, O. Guerret, F. P. Gabbaï, G. Bertrand, *Chem. Rev*. **2000**, *100*, 39-92; (g) F. E. Hahn, M. C. Jahnke, *Angew. Chem. Int. Ed.* **2008**, *47*, 3122-3172.

[12] (a) W. A. Nugent, B. L. Haymore, *Coord. Chem. Rev*. **1980**, *31*, 123-175; (b) J. K. Brask, T. Chivers, *Angew. Chem. Int. Ed.* **2001**, *40*, 3960-3976; (c) P. R. Sharp, *J. Chem. Soc. Dalton Trans.* **2000**, 2647-2657; (d) D. E. Wigley, *Prog. Inorg. Chem*. **1994**, *42*, 239-482; (e) L. H. Gade, P. Mountford, *Coord. Chem. Rev*. **2001**, *216-217*, 65-97; (f) F. Dielmann, O. Back, M. Henry-Ellinger, P. Jerabek, G. Frenking, G. Bertrand, *Science* **2012**, *337*, 1526.

[13] (a) X. Li, S. I. Weissmann, T.-S. Lin, P. P. Gaspar, A. H. Cowley, A. I. Smirnov, *J. Am. Chem. Soc.* **1994**, *116*, 7899-7900; (b) G. Bucher, M. L. G. Borst, A. W. Ehlers, K. Lammertsma, S. Ceola, M. Huber, D. Grote, W. Sander, *Angew. Chem. Int. Ed.* **2005**, *44*, 3289-3293; (c) J. Glatthaar, G. Maier, *Angew. Chem.*

Int. Ed. **2004**, *43*, 1294-1296; (d) J. J. Harrison, B. E. Williamson, *J. Phys. Chem. A*, **2005** *109*, 1343-1347; (e) A. Mardyukov, F. Keul, P. R. Schreiner, *Angew. Chem. Int. Ed.* **2020**, *59*, 1-6.

[14] L. Liu, D. A. Ruiz, D. Munz, G. Bertrand, *Chem.* **2016**, *1*, 147-153.

[15] M. M. Hansmann, R. Jazzar, G. Bertrand, *J. Am. Chem. Soc*. **2016**, *138*, 8356-8359.

[16] (a) E. Niecke, R. Streubel, M. Nieger, D. Stalke, *Angew. Chem. Int. Ed. Engl.* **1989**, *28*, 1673-1674; (b) R. Streubel, E. Niecke, P. Paetzold, *Chem. Ber.* **1991**, *124*, 765–767; (c) E. Niecke, R. Streubel, M. Nieger, *Angew. Chem. Int. Ed. Engl.* **1991**, *30*, 90-91; (d) R. Streubel, E. Niecke, M. Nieger, *Phosphorus, Sulfur, Silicon Relat. Elem.* **1992**, *65*, 115–118.

[17] I. Kalinina, F. Mathey, *Organometallics* **2006**, *25*, 5031-5034.

[18] T. Krachko, M. Bispinghoff, A. M. Tondreau, D. Stein, M. Backer, A. W. Ehlers, J. C. Slootweg, H. Grützmacher, *Angew. Chem. Int. Ed.* **2017**, *56*, 7948-7951.

[19] (a) K. M. Szkop, M. B. Geeson, D. W. Stephan, C. C. Cummins, *Chem. Sci.* **2019**, *10*, 3627; (b) W. J. Transue, A. Velian, M. Nava, C. García-Iriepa, M. Temprado, C. C. Cummings, *J. Am. Chem. Soc.* **2017**, *139*, 10822-10831; (c) M. B. Geeson, W. J. Transue, C. C. Cummins, *J. Am. Chem. Soc.* **2019**, *141*, 13336-13340.

[20] A. Velian, C. C. Cummins, *J. Am. Chem. Soc.* **2012**, *134*, 13978-13981.

[21] L. D. Quin, A. S. Ionkin, R. Kalgutkar, G. Keglevich, *Phosphorus, Sulfur, Silicon Relat. Elem.* **1996**, *109*, 433-436.

[22] K. M. Szkop, M. B. Geeson, D. W. Stephan, C. C. Cummins, *Chem. Sci.* **2019**, *10*, 3627-3631.

[23] (a) I. M. Riddlestone, A. Kraft, J. Schaefer, I. Krossing, *Angew. Chem. Int. Ed.* **2018**, *57*, 13982-14024; (b) S. H. Strauss, *Chem. Rev.* **1993**, *93*, 927-942.

[24] A. W. Ehlers, E. J. Baerends, K. Lammertsma, *J. Am. Chem. Soc.* **2002**, *124*, 2831-2838.

[25] (a) G. te Velde, E. J. Baerends, *J. Comput. Phys.* **1992**, *99*, 84; (b) F. M. Bickelhaupt, N. J. R. van Eikema Hommes, C. Fonseca Guerra, E. J. Baerends, *Organometallics* **1996**, *15*, 2923.

[26] (a) P. B. Hitchcock, M. F. Lappert, W.-P. Leung, *J. Chem. Soc. Chem. Commun.* **1987**, 1282-1283; (b) R. Bohra, P. B. Hitchcock, M. F. Lappert, W.-P. Leung, *Polyhedron* **1989**, *8*, 1884.

[27] J. B. Bonanno, P. T. Wolczanski, E. B. Lobkovsky, *J. Am. Chem. Soc*. **1994**, *116*, 11159-11160.

[28] E. Niecke, J. Hein, M. Nieger, *Organometallics* **1989**, *8*, 2290-2291.

[29] R. Melenkivitz, D. J. Mindiola, G. L. Hillhouse, *J. Am. Chem. Soc*. **2002**, *124*, 3846 – 3847.

[30] A. H. Cowley, B. Pellerin, J. L. Atwood, S. G. Bott, *J. Am. Chem. Soc*. **1990**, *112*, 6734 – 6735.

[31] A. T. Termaten, T. Nijbacker, M. Schakel, M. Lutz, A. L. Spek, K. Lammertsma, *Chem. Eur. J.* **2003**, *9*, 2200-2208.

[32] A. T. Termaten, H. Aktas, M. Schakel, A.W. Ehlers, M. Lutz, A. L. Spek, K. Lammertsma, *Organometallics* **2003**, *22*, 1827-1834.

[33] T. L. Breen, D. W. Stephan, *J. Am. Chem. Soc.* **1995**, *117*, 11914-11921.

[34] T. L. Breen, D. W. Stephan, *J. Am. Chem. Soc.* **1996**, *118*, 4204-4205.

[35] T. L. Breen, D. W. Stephan, *Organometallics* **1996**, *15*, 4223-4227.

[36] R. Waterman, G. L. Hillhouse, *J. Am. Chem. Soc.* **2003**, *125*, 13350-13351.

[37] (a) B. T. Sterenberg, A. J. Carty, *Organometallics* **2001**, 617-618; (b) B. T. Sterenberg, K. A. Udachin, A. J. Carty, *Organometallics* **2001**, *20*, 2657-2659; (c) B. T. Sterenberg, K. A. Udachin, A. J. Carty, *Organometallics* **2001**, *20*, 4463-4465; (d) J. Sánchez-Nieves, A. E. Allen, K. A. Udachin, A. J. Carty*, J. Am. Chem. Soc.* **2003**, *125*. 2404-2405; (e) T. W. Graham, R. P.-Y. Cariou, J. Sánchez-Nieves, A. E. Allen, K. A. Udachin, R. Regragui, A. J. Carty, *Organometallics* **2005**, *24*, 2023-2026.

[38] B. T. Sterenberg, K. A. Udachin, A. J. Carty, *Organometallics* **2003**, *22*, 3927-3932.

[39] A. Marinetti, F. Mathey, J. Fischer, A. Mitschler, *J. Am. Chem. Soc*. **1982**, *104*, 4484-4485. 28a

[40] (a) A. Marinetti, F. Mathey, J. Fischer, A. Mitschler*, J. Chem. Soc. Chem. Commun*. **1982**, 667-668; (b) A. Marinetti, C. Charrier, F. Mathey, J. Fischer, *Organometallics* **1985**, *4*, 2134-2138.

[41] A. Marinetti, F. Mathey, *Organometallics* **1984**, *3*, 456-461.

[42] K. Lammertsma, A. W. Ehlers, M. L. McKee, *J. Am. Chem. Soc.* **2003**, *125*, 14750–14759.

[43] R. Streubel, A. Kusenberg, J. Jeske, P. G. Jones, *Angew. Chem. Int. Ed.* **1994**, *33*, 80-82.

[44] M. L. G. Borst, R. E. Bulo, C. W. Winkel, D. J. Gibney, A. W. Ehlers, M. Schakel, M. Lutz, A. L. Spek, K. Lammertsma, *J. Am. Chem. Soc.* **2005**, *127*, 5800-5801.

[45] H. Jansen, J. C. Slootweg, A. W. Ehlers, K. Lammertsma, *Organometallics* **2010**, *29*, 6653-6659.

[46] (a) G. Märkl, W. Burger, *Tetrahedron Lett.* **1983**, *24*, 2545; (b) S. Yasuike, T. Kiharada, T. Tsuchiya, J. Kurita, *J. Bull. Chem. Pharm.* **2003**, *51*, 1283.

[47] A. H. Cowley, R. L. Geerts, C. M. Nunn, *J. Am. Chem. Soc.* **1987**, *109*, 6523.

[48] (a) R. B. King, F. J.Wu, E. M. Holt, *J. Am. Chem. Soc*. **1987**, *109*, 7764-7775; (b) R. B. King, G. S. Chorghade, *J. Organomet. Chem*. **1988**, *341*, 407-414; (c) R. A. Bartlett, H. V. Rasika Dias, K. M. Flynn, M. M. Olmstead, P. P. Power, *J. Am. Chem. Soc*. **1987**, 104, 5699-5703; (d) J. Borm, G. Huttner, O. Orama*, J. Organomet. Chem.* **1986**, *306*, 29.

[49] J. B. M. Wit, G. T. van Eijkel, F. J. J. de Kanter, M. Schakel, A. W. Ehlers, M. Lutz, A. L. Spek, K. Lammertsma, *Angew. Chem. Int. Ed.* **1999**, *38*, 2596-2599.

[50] J. B. M. Wit, G. B. de Jong, M. Schakel, M. Lutz, A. W. Ehlers, J. C. Slootweg, K. Lammertsma, *Organometallics* **2016**, *35*, 1170-1176.

[51] G. Boche, J. C. Lohrenz, *Chem. Rev.* **2001**, *101*, 697–756.

[52] (a) A. Kawachi, K. Tamao, *BCSJ* **1997**, *70*, 945–955; (b) M. A. Weidenbruch, *Angew. Chem. Int. Ed.* **2006**, *45*, 4241–4242.

[53] (a) M. Yoshifuji, I. Shima, N. Inamoto, K. Hirotsu, T. Higuchi, *J. Am. Chem. Soc.* **1981**, *103*, 4587–4589; (b) M. Yoshifuji, *J. Chem. Soc., Dalton Trans.* **1998, 3343–3350.**

[54] H. Lang, G. Mohr, O. Scheidsteger, G. Huttner, *Chem. Ber.* **1985**, *118*, 574–596.

[55] R. Streubel, *Phosphiniden-Transferreaktionen: Untersuchung zur Reaktivität von Halogen(silyl)-phosphanen,* Dissertation, University of Bonn, **1990**.

[56] A. Özbolat, G. von Frantzius, J. M. Pérez, M. Nieger, R. Streubel, *Angew. Chem. Int. Ed.* **2007**, *46*, 9327.

[57] R. Streubel, A. W. Kyri, L. Duan, G. Schnakenburg, *Dalton Trans.* **2014**, *43*, 2088.

[58] R. Streubel, A. Özbolat-Schön, G. von Frantzius, H. Lee, G. Schnakenburg, D. Gudat, *Inorg. Chem.* **2013**, *52*, 3313–3325.

[59] A. Özbolat, G. von Frantzius, W. Hoffbauer, R. Streubel, *Dalton Trans.* **2008**, 2674–2676

[60] V. Nesterov, G. Schnakenburg, A. Espinosa, R. Streubel, *Inorg. Chem.* **2012**, *51*, 12343–12349.

[61] M. Bode, J. Daniels, R. Streubel, *Organometallics* **2009**, *28*, 4636–4638.

[62] A. Özbolat, G. von Frantzius, E. Ionescu, S. Schneider, M. Nieger, P. G. Jones, R. Streubel, *Organometallics* **2007**, *26*, 4021–4024.

[63] (a) A. Schmer, A. Bauza, G. Schnakenburg, A. Frontera, R. Streubel, **2020**, *submitted*; (b) A. Schmer, *Von neuen Li/Cl-Phosphinidenoid-Komplexen zu neuartigen funktionellen Phosphanyliden-Phosphoran-Komplexen*, Dissertation, University of Bonn, **2020**.

[64] (a) N. F. Ramsey, *Phys. Rev.* **1950**, *77*, 567; (b) N. F. Ramsey, *Phys. Rev.* **1950**, *78*, 699-703; (c) N. F. Ramsey, *Phys. Rev.* **1951**, *83*, 540-541; (d) N. F. Ramsey, *Phys. Rev.* **1952**, *86*, 243-246; (e) N. F. Ramsey, *Phys. Rev.* **1953**, *91*, 303-307; (f) P. Pyykkö, *Theor. Che. Acc.* **2000**, *103*, 214-216; (g) J. A. Pople, *Discuss. Faraday Soc.* **1962**, *34*, 7–14.

[65] C. M. Widdifield, R. W. Schurko, *Concepts in Magnetic Resonance Part A* **2009**, *34*, 91–123.

[66] (a) J. M. Pérez, M. Klein, A. W. Kyri, G. Schnakenburg, R. Streubel, *Organometallics* **2011**, *30*, 5636-5640; (b) C. Albrecht, M. Bodo, J. M. Pérez, J. Daniels, G. Schnakenburg, R. Streubel, *Dalton Trans.* **2011**, *40*, 2654; (c) R. Streubel, M. Klein, G. Schnakenburg, *Organometallics* **2012**, *31*, 4711-4715; (d) R. Streubel, E. Schneider, G. Schnakenburg, *Organometallics* **2012**, *31*, 4707-4710; (e) R. Streubel, P. Junker, A. W. Kyri, G. Schnakenburg, *Organometallics* **2017**, *36*, 2952-2955.

[67] J. Faßbender, N. Künemund, A. Espinosa Ferao, G. Schnakenburg, R. Streubel, *Organometallics* **2018**, *37*, 1331-1336.

[68] J. Faßbender, *Untersuchungen zu Synthese und Eigenschaften P-tert-Butyl-substituierter Oxaphosphirankomplexe*, Dissertation, University of Bonn, **2018**.

[69] L. Abdrakhmanova, G. Schnakenburg, A. Espinosa, R. Streubel, *Eur. J. Inorg. Chem.* **2013,** *42*, 10510.

[70] (a) J. M. Villalba Franco, A. Espinosa Ferao, G. Schnakenburg, R. Streubel, *Chem. Commun.* **2013**, *49*, 9648; (b) R. Streubel, J. M. Villalba Franco, G. Schnakenburg, A. Espinosa Ferao, *Chem. Commun.* **2012**, *48*, 5986-5988.

[71] (a) J. M. Villalba Franco, *Studies on the Synthesis of Strained Azaphosphiridene Complexes and their Reactivity towards Small Molecules*, University of Bonn, **2015**; (b) J. M. Villalba Franco, T.

Sasamori, G. Schnakenburg, A. Espinosa Ferao, R. Streubel, *Chem. Commun.* **2015**, *51*, 3878; (c) J. M. Villalba Franco, A. Espinosa Ferao, R. Streubel, *Chem. Commun.* **2013**, *49*, 9648-9650; (d) J. M. Villalba Franco, G. Schnakenburg, A. Espinosa Ferao, R. Streubel, *Dalton Trans.* **2016,** *45*, 13951.

[72] (a) A. W. Kyri, V. Nesterov, G. Schnakenburg, R. Streubel, *Angew. Chem., Int. Ed.* **2014**, *53*, 10809−10812; (b) A. W. Kyri, F. Gleim, A. Garcia Alcaraz, G. Schnakenburg, A. Espinosa Ferao, R. Streubel, *Chem. Commun.* **2018**, *54*, 7123.

[73] A. W. Kyri, G. Schnakenburg, R. Streubel, *Organometallics* **2016**, *35*, 563-568.

[74] A. W. Kyri, F. Gleim, D. Becker, G. Schnakenburg, A. Espinosa Ferao, R. Streubel, *Chem. Commun.* **2019**, *55*, 1615.

[75] A. Espinosa Ferao, R. Streubel, *Inorg. Chem.* **2020**, *59*, 3110-3117.

[76] P. K. Majhi, A. W. Kyri, A. Schmer, G. Schnakenburg, R. Streubel, *Chem. Eur. J*. **2016**, *22*, 15413–15419.

[77] R. Streubel, A. Schmer, A. W. Kyri, G. Schnakenburg, *Organometallics* **2017**, *36*, 1488–1495.

[78] A. Schmer, T. Terschüren, G. Schnakenburg, A. Espinosa Ferao, R. Streubel *Eur. J. Inorg. Chem.* **2019**, 1604-1611.

[79] R. Streubel, T. Terschüren, P. Junker, A. Schmer, *manuscript in preparation*.

[80] T. Terschüren*, Investigations on the quest of selective N- versus P-deprotonation of 1,1'-bifunctional phosphane complexes*, Master Thesis, University of Bonn, **2019**.

[81] A. Schmer, N. Volk, A. Espinosa Ferao, R. Streubel, *Dalton Trans.* **2019**, *48*, 339-345.

[82] A. Özbolat-Schön, M. Bode, G. Schnakenburg, A. Anoop, M. van Gastel, F. Neese, R. Streubel, *Angew. Chem. Int. Ed.* **2010**, *49*, 6894-6898.

[83] *The Chemistry of the Quinoid Compounds*, Parts 1 and 2 (Ed.: S. Patai), Wiley, London, **1974**; *The Chemistry of the Quinoid Compounds*, Vol. 2, Parts 1 and 2 (Eds.: S. Patai, Z. Rappoport), Wiley, Chichester, **1988**.

[84] F. Murakami, S. Sasaki, M. Yoshifuji, *Angew. Chem. Int. Ed.* **1999**, *38*, 340.

[85] G. Märkl, R. Henning, K. M. Raab, *Chem. Commun.* **1996**, 2057.

[86] F. Murakami, S. Sasaki, M. Yoshifuji, *J. Am. Chem. Soc.* **2005**, *127,* 8926-8927**.**

[87] (a) R. F. Heck, J. P. Nolley, *J. Org. Chem.* **1972**, *37*, 2320–2322; (b) W. Kaim, *Coord. Chem. Rev.* **1987**, *76*, 187– 235; (c) K. E. Toccara, L. McElwee-White, *Coord. Chem. Rev.* **2000**, 206–207, 469–491; (d) H.-J. Grützmacher, *Angew. Chem. Int. Ed.* **2008**, *47*, 1814-1818; (e) H. Li, M. B. Hall, *J. Am. Chem. Soc.* **2015**, *137*, 12330-12342; (f) L. A. Berben, *Chem. Eur. J.* **2015**, *21*, 2734-2742; (g) A. R. Corcos, O. Villanueva, R. C. Walroth, S. K. Sharma, J. Bacsa, K. M. Lancaster, C. E. MacBeth, J. F. Berry, *J. Am. Chem. Soc.* **2016**, *138*, 1796-1799; (h) H. C. Wan, J.-X. Zhang, C. S. Leung, F. K. Sheong, Z. Lin, *Dalton Trans.* **2019**, *48*, 14801-14807.

[88] (a) T. J. Meyer, *Acc. Chem. Res.* **1978**, *11*, 94–100; (b) W. Kaim, *Inorg. Chem.* **1984**, *23*, 504–505.

[89] (a) A. Almenningen, A. Haaland, J. E. Nilson, *Acta Chem. Scand.* **1968**, *22*, 972; (b) A. H. Clark, A. Haaland, *Chem Commun.* **1969**, 912; (c) M. Niemeyer, P. P. Power, *Inorg. Chem.* **1997**, *36*, 4688. (d) S. T. Haubrich, P. P. Power, *J. Am. Chem. Soc.* **1998**, *120*, 2202; (e) M. Niemeyer, P.P Power, *Angew. Chem., Int. Ed.* **1998**, *37*, 1277.

[90] (a) A. Goodman, J. D. Raynor, *Adv. Inorg. Chem. Radiochem.* **1970**, *13*, 135–362; (b) C. K. Jørgensen, *Coord. Chem. Rev.* **1966**, *1*, 164–178.

[91] S. Sasaki, K. Sutoh, F. Murakami, M. Yoshifuji, *J. Am. Chem. Soc.* **2002**, *124*, 14830–14831.

[92] (a) J. K. Kochi in *Free Radicals*, Wiley, New York, **1973**; (b) C. Walling, M. S. Pearson, *Top. Phosphorus Chem.* **1966**, *3*, 1.

[93] (a) M. Regitz, O. J. Scherer, in *Multiple Bonds and Low- Coordination in Phosphorus Chemistry*, Thieme, Stuttgart, **1990**; (b) M. Klein, C. Albrecht, G. Schnakenburg, R. Streubel, *Organometallics* **2013**, *32*, 4938–4943

[94] E. B. Garner III, A. J. Arduengo III, R. Streubel, D. A. Dixon, *Dalton Trans.* **2014**, *43*, 2069-2078.

[95] M. Klein, C. Albrecht, G. Schnakenburg, R. Streubel, *Organometallics* **2013**, *32*, 4938-4943; P. K. Majhi, K. C. F. Chow, T. H. H. Hsieh, E. G. Bowes, G. Schnakenburg, P. Kennepohl, R. Streubel, D. P. Gates, *Chem. Commun.* **2016**, *52*, 998-1001.

[96] V. Nesterov, A. Özbolat-Schön, G. Schnakenburg, L. Shi, A. Cangönül, M. van Gastel, F. Neese, R. Streubel, *Chem. Asian. J.* **2012**, *7*, 1708-1712.

[97] H. Falius, M. Babin, *Z. allg. anorg. Chem.* **1976**, *420*, 65-73.

[98] R. B. King, N. D. Sadanani, *Inorg. Chem.* **1985**, *24*, 3136-3139.

[99] W. Strohmeier, F.-J. Müller, *Chem. Ber.*, **1969**, *102*, 3608-3612.

[100] H. Eyring, *Chem. Phys.* **1935**, *3*, 197-115.

[101] G. Binsch, H. Kessler, *Angew. Chem. Int. Ed. Engl.* **1980**, *19*, 411.

[102] A. G. Császár, W. D. Allen, H. F. Schaefer, *J. Chem. Phys.* **1998**, *108*, 9751.

[103] H. A. Bent, *Chem. Reviews* **1961**, *61*, 275-311.

[104] S. Kurth, J. P. Perdew, P. Blaha, *Int. J. Quant. Chem*. **1999**, *75*, 889; J. P. Perdew, A. Ruzsinszky, J. Tao, V. N. Staroverov, G. E. Scuseria, G. I. Csonka, *J. Chem. Phys.* **2005**, *123*, 062201.

[105] L. Goerigk, S. Grimme, *Phys. Chem. Chem. Phys.* **2011**, *13*, 6670-6688.

[106] H. R. G. Bender, E. Niecke, M. Nieger, H. Westermann, *Z. anorg. allg. Chem.* **1994**, *620*, 1194-1202.

[107] M. Scheer, S. Gremler, E. Herrmann, *J. Organomet. Chem.* **1991**, *414*, 337-349.

[108] H. R. G. Bender, M. Nieger, E. Niecke, *Z. Naturforsch.* **1993**, *48b*, 1742-1752.

[109] P. Junker, Z.-W. Qu, T. Kalisch, G. Schnakenburg, A. Espinosa Ferao, R. Streubel, *submitted*.

[110] P. P. Power, *Acc. Chem. Res.* **1988**, *21*, 147-553.

[111] K. Dilchert, M. Schmidt, A. Großjohann, K.-S. Feichtner, R. E. Mulvey, V. H. Gessner, *Angew. Chem. Int. Ed.* **2020**, *59*, 2-8.

[112] A. Espinosa Ferao, A. G. Alcaraz, S. Z. Noguera, R. Streubel, *Inorg. Chem.* **2020**, *59*, 12829-12841.

[113] A. Espinosa Ferao, R. Streubel, *Chem. Eur. J.* **2017**, *23*, 8632-86-43.

[114] (a) G. Huttner, *J. Organomet. Chem.* **1986**, *308*, C11-C13. (b) D. Gudat, E. Niecke, W. Sachs, *Z. anorg. allg. Chem.* **1987**, *545*, 7-23.

[115] J. A. Pople, M. Head-Gordon, K. Raghavachari, *J. Chem. Phys.* **1987,** *87*, 5968-5975.

[116] Effect occurring during signal processing causing signals to be indistinguishable.

[117] H. J. Metternich, E. Niecke, *Tetrahedron Lett.* **1991**, *32*, 6537-6538.

[118] F. Mercier, B. Deschamps, F. Mathey, *J. Am. Chem. Soc.* **1989**, *111*, 9098-9100.

[119] D. C. R. Hockless, M. A. McDonald, M. Pabel, S. B. Wild, *J. Organomet. Chem.* **1997**, *529*, 189-196.

[120] K. M. Flynn, H. Hope, B. D. Murray, M. M. Olmstead, P. P. Power, *J. Am. Chem. Soc.* **1983**, *105*, 7750-7751.

[121] P. Junker, J. M. Villalba Franco, G. Schnakenburg, V. Nesterov, R. T. Boeré, Z.-W. Qu, R. Streubel, *Dalton Trans.* **2020**, *49*, 13544-13548.

[122] (a) M. D. Archer in *Electrochemistry, Past and Present*, American Chemical Society, **1989**, pp. 115-126; (b) P. Atkins, *Physical Chemistry*, 8. Aufl., Oxford University Press, Oxford, **2007**, pp. 221-224.

[123] P. Zanello, *Inorganic Electrochemistry: Theory, Practice and Application*, The Royal Society of Chemistry, **2003**, pp. 118-123.

[124] (a) A. Landé, *Z. Physik* **1923**, 189-205. (b) A. Landé, *Z. Physik* **1921**, *5*, 231-241.

[125] J. Sinclair, D. Kivelson, *J. Am. Chem. Soc.* **1968**, *90*, 5074-5080.

[126] (a) C. Pi, Y. Wang, W. Zheng, L. Wan, H. Wu, L. Weng, L. Wu,Q. Li, P. v. Ragué Schleyer, *Angew. Chem., Int. Ed.* **2010**, *49*, 1842. (b) T. Cantat, F. Biaso, A. Momin, L. Ricard, M. Geoffroy, N. Mézailles, P. Le Floch, *Chem. Commun.* **2008**, 874.

[127] (a) B. F. Yates, W. J. Bouma, L. Radom, *J. Am. Chem. Soc.* **1984**, *106*, 5805. (b) B. F. Yates, W. J. Bouma, L. Radom, *Tetrahedron* **1986**, *42*, 6225.

[128] (a) X. Chen, L. L. Liu, S. Liu, H. Grützmacher, Z. Li, *Angew. Chem. Int. Ed.* **2020**, *59*, 2-8; (b) H. Helten, S. Fankel, O. Feier-Iova, M. Nieger, A. Espinosa Ferao, R. Streubel, *Eur. J. Inorg. Chem.* **2009**, 3226-3237; (c) H. Helten, C. Neumann, A. Espinosa, P. G. Jones, M. Nieger, R. Streubel, *Eur. J. Inorg. Chem.* **2007**, 4669-4678; (d) H. Helten, *Electrophilic Ring Bond Activation of 2H-Azaphosphirene Complexes,* Dissertation, University of Bonn, **2009**.

[129] P. v. Ragué Schleyer, C. Maerker, A. Dransfeld, H. Jiao, N. J. R. v. Eikema Hommes, *J. Am. Chem. Soc.* **1996**, *118*, 6317.

[130] (a) T. M. Krygowski, *J. Chem. Inf. Comput. Sci.*, **1993**, *33*, 70; (b) T. M. Krygowski, M. Cyrañski, *Tetrahedron*, **1996**, *52*, 1713; (c) T. M. Krygowski, M. Cyrañski, *Chem. Rev.*, **2001**, *101*, 1385; (d) T. M. Krygowski, M. Cyrañski, *Phys. Chem. Chem. Phys.*, **2004**, *6*, 249.

[131] T. M. Krygowski, M. Cyrañski, *Tetrahedron*, **1996**, *52*, 10255.

[132] O. V. Dolomanov, L. J. Bourhis, R. J. Gildea, J. A. K. Howard, H. Puschmann, *OLEX2: A complete structure solution, refinement and analysis program* (2009). *J. Appl. Cryst.*, **42**, 339-341.

[133] Neese, F. (2012) The ORCA program system, Wiley Interdiscip. Rev.: *Comput. Mol. Sci.*, 2, 73-78.

[134] J. P. Perdew, K. Burke, M. Ernzerhof, *Phys. Rev. Lett.* **1996**, *77*, 3865.

[135] J. Tao, J. P. Perdew, V. N. Staroverov and G. E. Scuseria, *Phys. Rev. Lett.*, **2003**, *91*, 146401.

[136] P. J. Stephens, F. J. Devlin, C. F. Chabalowski, M. J. Frisch, *J. Phys. Chem.* **1994**, *98*, 11623

[137] Becke, A. D. *Phys Rev A* 1988, 38, 3098.

[138] C. Lee, W. Yang, R. G. Parr, *Phys. Rev. A* **1988**, *37*, 785.

[139] (a) Y. Zhao and D. G. Truhlar, *J. Phys. Chem. A*, **2005**, *109*, 5656–5667.

[140] J. P. Perdew, in *Proceedings of the 21st Annual International Symposium on the Electronic Structure of Solids*, ed. P. Ziesche und H. Eschrig, Akademie Verlag, Berlin, **1991**, p. 11.

[141] A. D. Becke, *J. Chem. Phys.* **1996**, *104*, 1040–1046.

[142] Y. Jung, R. C. Lochan, A. D. Dutoi, M. Head-Gordon, *J. Chem. Phys*. **2004**, *121*, 9793–9802.

[143] (a) P. Hohenberg, W. Kohn, *Phys. Rev.* **1964**, *136*, 864–871. (b) W. Kohn, L. J. Sham, *Phys. Rev.* **1965**, 140, A1133–A1138.

[144] (a) F. Weigend, R. Ahlrichs, *Phys. Chem. Chem. Phys.* **2005**, 7, 3297–3305. (b) F. Weigend, M. Häser, H. Patzelt, R. Ahlrichs, *Chemical Physics Letters* **1998**, *294*, 143-152. (c) F. Weigend, R. Ahlrichs, *Phys. Chem. Chem. Phys.* **2005**, *7*, 3297-3305. (d) F. Weigend, F. Furche, R. Ahlrichs, *J. Chem. Phys.* **2003**, *119*, 12753-12762.

[145] (a) B. Metz, H. Stoll, M. Dolg, *J. Chem. Phys.* **2000**, *113*, 2563–2569. (b) K. A. Peterson, D. Figgen, E. Goll, H. Stoll, M. Dolg, *J. Chem. Phys.* **2003**, *119*, 11113–11123. (c) A. Schaefer, H. Horn, R. Ahlrichs, *J. Chem. Phys.* **1992**, *97*, 2571.

[146] C. Hättig, F. Weigend, *J. Chem. Phys.* **2000**, *113*, 5154–5161.

[147] F. Weigend, *Phys. Chem. Chem. Phys.* **2002**, *4*, 4285–4291.

[148] (a) S. Grimme, J. Antony, S. Ehrlich, H. Krieg, *J. Chem. Phys.* **2010**, *132*, 154104. (b) S. Grimme, S. Ehrlich, L. Goerigk, *J. Comput. Chem.* **2011**, *32*, 1456–1465.

[149] (a) A. Klamt and G. Schüürmann, *J. Chem. Soc., Perkin Trans. 2*, **1993**, 799-805 (b) F. Eckert and A. Klamt, *AIChE Journal* **2002**, *48*, 369-385. (c) F. Eckert and A. Klamt, COSMOtherm, Version C3.0, Release 16.01; COSMOlogic GmbH & Co. KG, Leverkusen, Germany 2015.

[150] V. Barone, M. Cossi,*J. Phys. Chem. A* **1998**, *102,* 1995.

[151] T. Ziegler, G. Schreckenbach, *J. Phys. Chem.* **1995**, *99*, 606–611.

7. Appendix

7.1 Crystal data and structure refinements

7.1.1 [Pentacarbonyl{dichloro(diphenylamino)phosphane-κP}tungsten(0)] (2a)

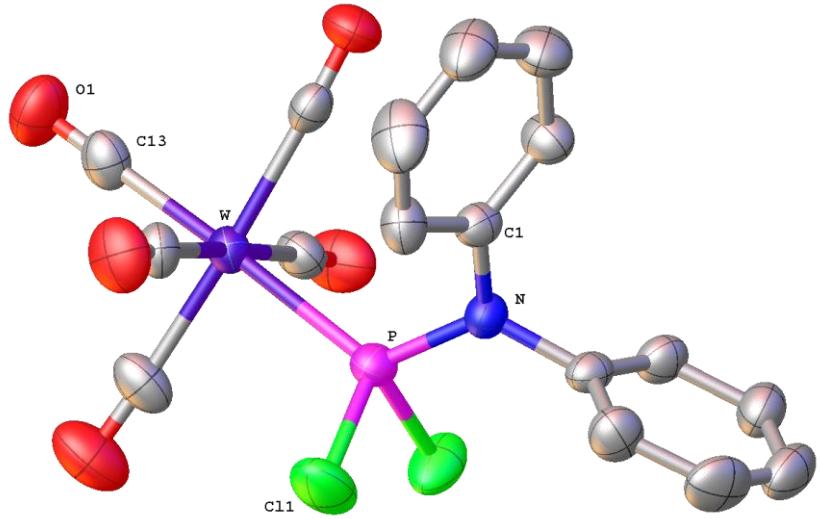

Identification code	GSTR546, PJ-151 // GXray5065g	$P_{calc}g$ / cm³	1.950
Device type	Nonius KappaCCD	μ / mm^{-1}	6.078
Moiety formula	C17 H10 Cl2 N O5 P W	F(000)	1128.0
Empirical formula	$C_{17}H_{10}NO_5PCl_2W$	Crystal size / mm	0.21 × 0.14 × 0.12
Temperature / K	123	2Θ range for data collection / °	5.95 - 55.998
Radiation	MoKα (λ = 0.71073)	T_{min}; T_{max}	0.4745; 0.7459
Crystal system	orthorhombic	Absorption correction	empirical
Space group	$P2_12_12_1$	Completeness to theta	0.998
a / Å	9.085(5)	Index ranges	-12 ≤ h ≤ 12, -17 ≤ k ≤ 17, -22 ≤ l ≤ 19
b / Å	13.306(8)	Reflections collected	29500
c / Å	16.740(11)	Independent reflections	4866 [R_{int} = 0.0499, R_{sigma} = 0.0408]
α / Å	90	Data/restraints/ Parameters	4866/12/245
β / Å	90	*Goodness-of-fit* on F^2	1.026

γ / Å	90	Final R Indices [I ≥ 2σ (I)]	R_1 = 0.0257, wR_2 = 0.0471
Volume / Å³	2024(2)	R Indices (all Data)	R_1 = 0.0318, wR_2 = 0.0490
Z	4	Largest diff. peak/hole / e Å^{-3}	0.59/-0.59

Table 7.1.1.1. *Bond lenghts for 5065g.*

Atom	Atom	Lenth/Å	Atom	Atom	Length/Å
W	P	2.4395(19)	N	C1	1.463(7)
W	C13	2.034(7)	N	C7	1.461(7)
W	C14	2.073(6)	C1	C2	1.395(8)
W	C15	2.057(7)	C1	C6	1.382(8)
W	C16	2.024(6)	C2	C3	1.392(9)
W	C17	2.064(7)	C3	C4	1.378(10)
Cl1	P	2.088(2)	C4	C5	1.379(11)
Cl2	P	2.051(3)	C5	C6	1.379(9)
P	N	1.665(5)	C7	C8	1.380(9)
O1	C13	1.136(8)	C7	C12	1.387(10)
O2	C14	1.122(7)	C8	C9	1.406(10)
O3	C15	1.144(8)	C9	C10	1.369(11)
O4	C16	1.143(8)	C10	C11	1.369(10)
O5	C17	1.139(8)	C11	C12	1.385(8)

Table 7.1.1.2. *Bond angles for 5065g.*

Atom	Atom	Atom	Angle/˚	Atom	Atom	Atom	Angle/˚
C13	W	P	176.67(19)	C7	N	C1	114.4(4)
C13	W	C14	88.7(2)	C2	C1	N	121.3(5)
C13	W	C15	91.8(2)	C6	C1	N	118.3(5)
C13	W	C17	89.8(2)	C6	C1	C2	120.4(5)
C14	W	P	93.92(15)	C3	C2	C1	118.7(6)
C15	W	P	90.17(18)	C4	C3	C2	120.7(6)
C15	W	C14	91.7(2)	C3	C4	C5	119.9(6)
C15	W	C17	177.9(3)	C6	C5	C4	120.3(6)
C16	W	P	89.6(2)	C5	C6	C1	120.0(6)
C16	W	C13	87.7(3)	C8	C7	N	119.6(6)
C16	W	C14	176.3(3)	C8	C7	C12	121.0(6)
C16	W	C15	89.5(3)	C12	C7	N	119.4(5)
C16	W	C17	89.2(3)	C7	C8	C9	118.0(7)
C17	W	P	88.18(18)	C10	C9	C8	120.9(6)
C17	W	C14	89.7(2)	C9	C10	C11	120.5(7)
Cl1	P	W	114.39(9)	C10	C11	C12	119.9(8)
Cl2	P	W	113.22(10)	C11	C12	C7	119.8(7)
Cl2	P	Cl1	97.31(11)	O1	C13	W	178.4(6)
N	P	W	122.63(16)	O2	C14	W	176.0(5)
N	P	Cl1	104.92(19)	O3	C15	W	177.1(6)

N	P	Cl2	100.70(19)	O4	C16	W	177.4(7)
C1	N	P	119.0(4)	O5	C17	W	177.8(6)
C7	N	P	124.5(3)				

7.1.2 [Tetracarbonyl{dichloro(diphenylamino)phosphane-κP}iron(0)] (3b)

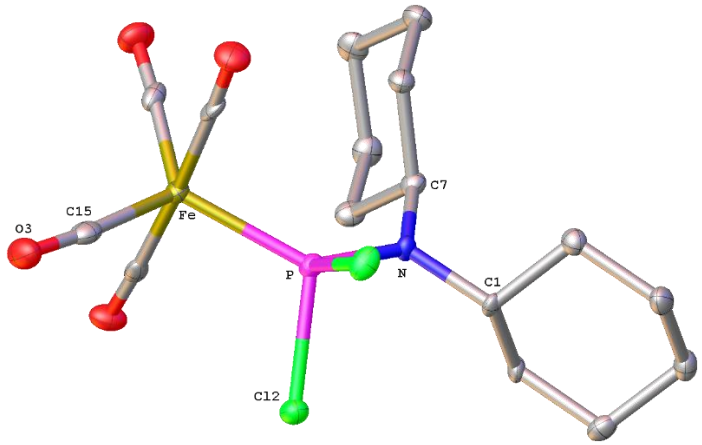

Identification code	GSTR584, TK-41 // GXray5294f	$P_{calc}g$ / cm³	1.537
Device type	Bruker X8-KappaApexII	μ / mm^{-1}	1.152
Moiety formula	C16 H22 Cl2 Fe N O4 P	F(000)	928.0
Empirical formula	$C_{16}H_{22}NO_4PCl_2Fe$	Crystal size / mm	0.11 × 0.03 × 0.02
Temperature / K	100	2Θ range for data collection / °	3.568 - 50.494
Radiation	MoKα (λ = 0.71073)	T_{min}; T_{max}	0.6471; 0.7459
Crystal system	monoklin	Absorption correction	empirisch
Space group	Cc	Completeness to theta	0.990
a / Å	6.5919(6)	Index ranges	-7 ≤ h ≤ 7, -27 ≤ k ≤ 27, -15 ≤ l ≤ 9
b / Å	22.8260(19)	Reflections collected	9237
c / Å	12.9769(10)	Independent reflections	2623 [R_{int} = 0.0597, R_{sigma} = 0.0746]
α / Å	90	Data/restraints/	2623/2/226
β / Å	94.918(3)	parameters	1.081
γ / Å	90	*Goodness-of-fit* on F^2	R_1 = 0.0366, wR_2 = 0.0555
Volume / Å³	1945.4(3)	Final R Indices [I ≥ 2σ (I)]	R_1 = 0.0665, wR_2 = 0.0664
Z	4	R Indices (all Data)	0.67/-0.79

Table 7.1.2.1. Bond lengths for 5294f.

Atom	Atom	Length/Å	Atom	Atom	Length/Å
Fe	P	2.1925(17)	N	C7	1.507(8)
Fe	C13	1.813(7)	C1	C2	1.530(8)
Fe	C14	1.786(8)	C1	C6	1.541(8)
Fe	C15	1.799(8)	C2	C3	1.537(8)
Fe	C16	1.818(7)	C3	C4	1.532(9)
Cl1	P	2.086(2)	C4	C5	1.532(9)
Cl2	P	2.103(2)	C5	C6	1.524(8)
P	N	1.638(5)	C7	C8	1.525(8)
O1	C13	1.144(8)	C7	C12	1.526(8)
O2	C14	1.157(8)	C8	C9	1.532(9)
O3	C15	1.150(8)	C9	C10	1.538(9)
O4	C16	1.142(8)	C10	C11	1.529(9)
N	C1	1.496(7)	C11	C12	1.553(9)

Table 7.1.2.2. Bond angles for 5294f.

Atom	Atom	Atom	Angle/˚	Atom	Atom	Atom	Angle/˚
C13	Fe	P	91.9(2)	N	C1	C6	111.7(5)
C13	Fe	C16	177.1(3)	C2	C1	C6	112.3(5)
C14	Fe	P	124.9(2)	C1	C2	C3	110.6(5)
C14	Fe	C13	88.1(3)	C4	C3	C2	111.1(5)
C14	Fe	C15	119.3(3)	C3	C4	C5	111.0(5)
C14	Fe	C16	89.9(3)	C6	C5	C4	110.9(5)
C15	Fe	P	115.8(2)	C5	C6	C1	109.5(5)
C15	Fe	C13	89.8(3)	N	C7	C8	112.8(5)
C15	Fe	C16	89.3(3)	N	C7	C12	112.6(5)
C16	Fe	P	91.0(2)	C8	C7	C12	112.9(5)
Cl1	P	Fe	112.22(9)	C7	C8	C9	110.0(5)
Cl1	P	Cl2	95.71(10)	C8	C9	C10	111.1(6)
Cl2	P	Fe	111.83(10)	C11	C10	C9	110.7(5)
N	P	Fe	127.7(2)	C10	C11	C12	111.0(5)
N	P	Cl1	101.6(2)	C7	C12	C11	110.2(5)
N	P	Cl2	102.8(2)	O1	C13	Fe	177.2(6)
C1	N	P	120.0(4)	O2	C14	Fe	176.9(6)
C1	N	C7	114.5(5)	O3	C15	Fe	175.5(6)
C7	N	P	125.3(4)	O4	C16	Fe	177.9(6)
N	C1	C2	111.2(5)				

7.1.3 [Pentacarbonyl{dichloro(diphenylamino)phosphane- κP}chromium(0)] (4a)

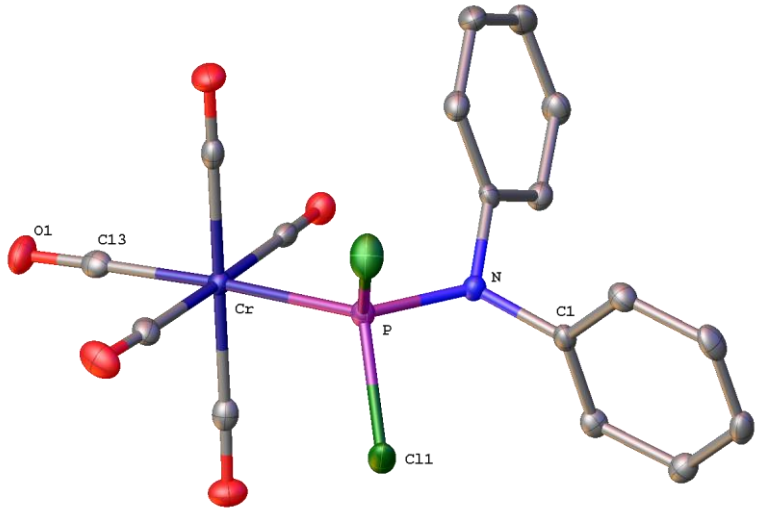

Identification code	GSTR663, PJ-259 // GXray5925f	$P_{calc}g$ / cm³	1.636
Device type	Bruker X8-KappaApexII	μ / mm^{-1}	1.008
Moiety formula	C17 H10 Cl2 Cr N O5 P	F(000)	928.0
Empirical formula	$C_{17}H_{10}NO_5PCl_2Cr$	Crystal size / mm	0.18 × 0.17 × 0.1
Temperature / K	100	2Θ range for data collection / °	4.992 - 55.99
Radiation	MoKα (λ = 0.71073)	T_{min}; T_{max}	0.5721; 0.7462
Crystal system	orthorhombisch	Absorption correction	empirisch
Space group	$P2_12_12_1$	Completeness to theta	0.998
a / Å	8.8950(4)	Index ranges	-9 ≤ h ≤ 11, -17 ≤ k ≤ 16, -21 ≤ l ≤ 17
b / Å	12.9286(5)	Reflections collected	16856
c / Å	16.3172(6)	Independent reflections	4516 [R_{int} = 0.0417, R_{sigma} = 0.0393]
α / Å	90	Data/restraints/	4516/0/244
β / Å	90	parameters	1.044
γ / Å	90	*Goodness-of-fit* on F^2	R_1 = 0.0259, wR_2 = 0.0566
Volume / Å³	1876.48(13)	Final R Indices [I ≥ 2σ (I)]	R_1 = 0.0301, wR_2 = 0.0587
Z	4	R Indices (all Data)	0.28/-0.24

Table 7.1.3.1 *Bond lengths for 5925f.*

Atom	Atom	Length/Å	Atom	Atom	Lenth/Å
Cr	P	2.2891(8)	N	C1	1.456(3)
Cr	C13	1.892(3)	N	C7	1.446(3)
Cr	C14	1.897(3)	C1	C2	1.383(4)
Cr	C15	1.915(3)	C1	C6	1.386(4)
Cr	C16	1.917(3)	C2	C3	1.395(4)
Cr	C17	1.908(3)	C3	C4	1.377(4)
Cl1	P	2.0421(10)	C4	C5	1.383(4)
Cl2	P	2.0872(10)	C5	C6	1.394(4)
P	N	1.667(2)	C7	C8	1.390(4)
O1	C13	1.140(3)	C7	C12	1.391(4)
O2	C14	1.134(4)	C8	C9	1.382(4)
O3	C15	1.133(3)	C9	C10	1.383(4)
O4	C16	1.139(3)	C10	C11	1.381(5)
O5	C17	1.140(3)	C11	C12	1.389(4)

Table 7.1.3.2 *Bond angles for 5925f.*

Atom	Atom	Atom	Angle/˚	Atom	Atom	Atom	Angle/˚
C13	Cr	P	176.52(9)	C7	N	C1	114.5(2)
C13	Cr	C14	87.58(12)	C2	C1	N	119.6(2)
C13	Cr	C15	89.52(11)	C2	C1	C6	120.9(2)
C13	Cr	C16	89.02(12)	C6	C1	N	119.4(2)
C13	Cr	C17	91.38(11)	C1	C2	C3	119.5(3)
C14	Cr	P	89.47(8)	C4	C3	C2	120.0(3)
C14	Cr	C15	89.24(12)	C3	C4	C5	120.2(2)
C14	Cr	C16	176.41(12)	C4	C5	C6	120.5(3)
C14	Cr	C17	89.25(12)	C1	C6	C5	118.9(3)
C15	Cr	P	88.60(8)	C8	C7	N	118.3(2)
C15	Cr	C16	89.57(12)	C8	C7	C12	119.9(3)
C16	Cr	P	93.89(8)	C12	C7	N	121.8(2)
C17	Cr	P	90.43(8)	C9	C8	C7	119.9(3)
C17	Cr	C15	178.21(13)	C8	C9	C10	120.3(3)
C17	Cr	C16	91.98(12)	C11	C10	C9	119.8(3)
Cl1	P	Cr	113.84(4)	C10	C11	C12	120.5(3)
Cl1	P	Cl2	96.71(4)	C11	C12	C7	119.5(3)
Cl2	P	Cr	114.45(4)	O1	C13	Cr	178.7(3)
N	P	Cr	122.73(9)	O2	C14	Cr	177.8(2)
N	P	Cl1	100.32(8)	O3	C15	Cr	178.8(3)
N	P	Cl2	104.91(9)	O4	C16	Cr	176.3(2)
C1	N	P	123.91(18)	O5	C17	Cr	177.7(3)
C7	N	P	119.07(17)				

7.1.4 [Bispentacarbonyl{1,2-bis(diphenylamino)diphosphane- $\kappa P^{1,2}$}tungsten(0)] (11)

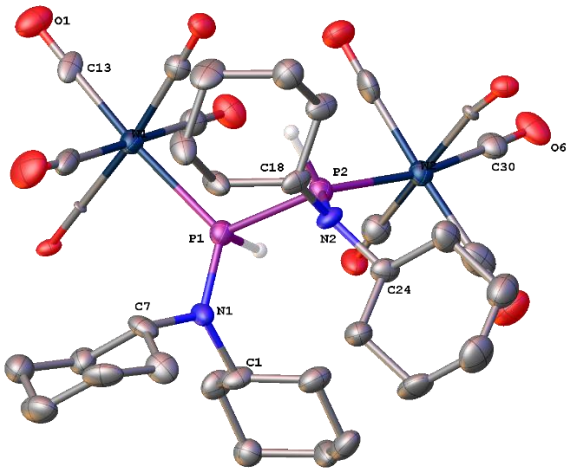

Identification code	GSTR648, PJ-237 // GXray5802	$P_{calc}g$ / cm³	1.805
Device type	Bruker APEX-II CCD	μ / mm^{-1}	5.960
Moiety formula	C34 H46 N2 O10 P2 W2	F(000)	1044.0
Empirical formula	$C_{34}H_{46}N_2O_{10}P_2W_2$	Crystal size / mm	0.1 x 0.03 x 0.03
Temperature / K	100	2Θ range for data collection / °	3.926 - 50.496
Radiation	MoKα (λ = 0.71073)	T_{min}; T_{max}	0.4373; 0.7458
Crystal system	Triklin	Absorption correction	empirisch
Space group	$P\bar{1}$	Completeness to theta	1.000
a / Å	11.5880(5)	Index ranges	-13 ≤ h ≤ 13, -14 ≤ k ≤ 14, -19 ≤ l ≤ 19
b / Å	11.8529(5)	Reflections collected	56984
c / Å	16.5434(7)	Independent reflections	7150 [R_{int} = 0.1254, R_{sigma} = 0.0544]
α / Å	78.659(4)	Data/restraints/	7150/60/458
β / Å	82.857(3)	parameters	1.078
γ / Å	62.420(4)	*Goodness-of-fit* on F^2	R_1 = 0.0843, wR_2 = 0.1979
Volume / Å³	1973.28(16)	Final R Indices [I ≥ 2σ (I)]	R_1 = 0.1039, wR_2 = 0.2174
Z	2	R Indices (all Data)	8.21/-2.62

Table 7.1.4.1 *Bond lengths for 5802.*

Atom	Atom	Length/Å	Atom	Atom	Length/Å
W1	P1	2.5115(10)	N2	C18	1.477(5)
W1	C13	1.977(4)	N2	C24	1.501(5)
W1	C14	2.017(5)	C1	C2	1.546(7)
W1	C15	1.998(4)	C1	C6	1.504(8)
W1	C16	2.011(5)	C2	C3	1.539(5)
W1	C17	2.042(5)	C3	C4	1.514(8)
W2	P2	2.5235(12)	C4	C5	1.529(8)
W2	C30	1.993(5)	C5	C6	1.503(6)
W2	C31	2.056(6)	C7	C8	1.512(7)
W2	C32	2.011(4)	C7	C12	1.509(8)
W2	C33	2.012(4)	C8	C9	1.491(8)
W2	C34	2.043(5)	C9	C10	1.558(10)
P1	P2	2.306(2)	C10	C11	1.522(8)
P1	N1	1.684(4)	C11	C12	1.544(7)
P2	N2	1.675(4)	C18	C19	1.530(7)
O1	C13	1.187(6)	C18	C23	1.540(7)
O2	C14	1.168(7)	C19	C20	1.520(6)
O3	C15	1.184(5)	C20	C21	1.546(9)
O4	C16	1.186(6)	C21	C22	1.506(8)
O5	C17	1.131(6)	C22	C23	1.559(6)
O6	C30	1.169(7)	C24	C25	1.546(8)
O7	C31	1.095(7)	C24	C29	1.498(7)
O8	C32	1.186(5)	C25	C26	1.527(7)
O9	C33	1.172(5)	C26	C27	1.492(10)
O10	C34	1.144(6)	C27	C28	1.528(10)
N1	C1	1.517(5)	C28	C29	1.511(7)
N1	C7	1.474(6)			

Table 7.1.4.2 Bond angles for 5802.

Atom	Atom	Atom	Angle/˚	Atom	Atom	Atom	Angles/˚
C13	W1	P1	170.39(15)	N1	C1	C2	110.3(4)
C13	W1	C14	91.7(2)	C6	C1	N1	113.8(4)
C13	W1	C15	87.50(16)	C6	C1	C2	111.5(4)
C13	W1	C16	87.17(19)	C3	C2	C1	108.5(4)
C13	W1	C17	86.67(18)	C4	C3	C2	110.8(5)
C14	W1	P1	97.85(13)	C3	C4	C5	110.3(4)
C14	W1	C17	88.0(2)	C6	C5	C4	111.3(4)
C15	W1	P1	91.25(9)	C5	C6	C1	111.0(5)
C15	W1	C14	92.16(18)	N1	C7	C8	114.3(4)
C15	W1	C16	86.11(18)	N1	C7	C12	112.0(4)
C15	W1	C17	174.16(14)	C12	C7	C8	110.0(4)
C16	W1	P1	83.24(12)	C9	C8	C7	113.3(4)
C16	W1	C14	178.0(2)	C8	C9	C10	110.2(4)
C16	W1	C17	93.7(2)	C11	C10	C9	110.8(5)
C17	W1	P1	94.52(12)	C10	C11	C12	110.7(4)

C30	W2	P2	170.85(13)	C7	C12	C11	111.4(4)
C30	W2	C31	85.9(2)	O1	C13	W1	179.0(5)
C30	W2	C32	87.60(19)	O2	C14	W1	176.0(4)
C30	W2	C33	87.75(18)	O3	C15	W1	176.4(3)
C30	W2	C34	89.8(2)	O4	C16	W1	179.3(4)
C31	W2	P2	94.98(15)	O5	C17	W1	178.7(4)
C32	W2	P2	83.26(14)	N2	C18	C19	113.6(4)
C32	W2	C31	92.4(2)	N2	C18	C23	111.2(4)
C32	W2	C33	85.32(19)	C19	C18	C23	110.0(3)
C32	W2	C34	177.3(2)	C20	C19	C18	111.1(4)
C33	W2	P2	90.95(11)	C19	C20	C21	112.0(5)
C33	W2	C31	173.36(18)	C22	C21	C20	108.8(4)
C33	W2	C34	93.66(19)	C21	C22	C23	113.3(5)
C34	W2	P2	99.28(16)	C18	C23	C22	109.3(4)
C34	W2	C31	88.3(2)	N2	C24	C25	111.1(4)
P2	P1	W1	114.04(5)	C29	C24	N2	114.3(4)
N1	P1	W1	123.84(15)	C29	C24	C25	111.7(4)
N1	P1	P2	112.71(16)	C26	C25	C24	109.2(4)
P1	P2	W2	113.47(5)	C27	C26	C25	112.8(5)
N2	P2	W2	124.42(15)	C26	C27	C28	111.0(5)
N2	P2	P1	112.39(18)	C29	C28	C27	110.7(4)
C1	N1	P1	122.3(3)	C24	C29	C28	112.1(5)
C7	N1	P1	120.1(2)	O6	C30	W2	178.2(4)
C7	N1	C1	117.0(4)	O7	C31	W2	176.2(4)
C18	N2	P2	122.2(3)	O8	C32	W2	177.3(5)
C18	N2	C24	117.3(3)	O9	C33	W2	169.6(3)
C24	N2	P2	119.2(3)	O10	C34	W2	178.9(5)

7.1.5 [Tetracarbonyl{methoxy(diphenylamino)phosphane-κP}iron(0)] (9a)

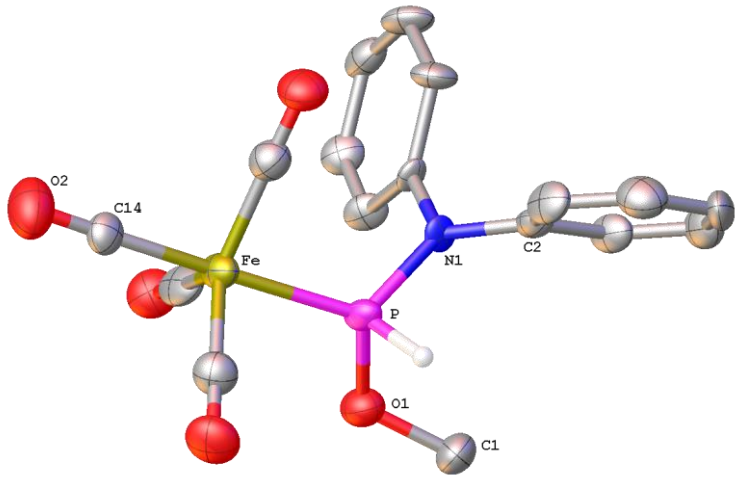

Identification code	GSTR577, TK-14 // GXray5170	Pcalcg / cm³	1.444

Device type	STOE IPDS-2T	μ / mm-1	0.934
Moiety formula	C17 H14 Fe N O5 P	F(000)	816.0
Empirical formula	$C_{17}H_{14}FeNO_5P$	Crystal size / mm	0.12 × 0.03 × 0.03
Temperature / K	123	2Θ range for data collection / °	5.528 - 55.998
Radiation	MoKα (λ = 0.71073)	Tmin; Tmax	0.0920; 0.6365
Crystal system	monoklin	Absorption correction	integration
Space group	$P2_1/c$	Completeness to theta	0.997
a / Å	7.6212(7)	Index ranges	-10 ≤ h ≤ 10, -23 ≤ k ≤ 23, -18 ≤ l ≤ 17
b / Å	17.413(2)	Reflections collected	16706
c / Å	13.8559(14)	Independent reflections	4414 [R_{int} = 0.3463, R_{sigma} = 0.3152]
α / Å	90	Data/restraints/	4414/42/230
β / Å	93.105(8)	parameters	0.928
γ / Å	90	Goodness-of-fit on F^2	R_1 = 0.1015, wR_2 = 0.2087
Volume / $Å^3$	1836.1(3)	Final R Indices [I ≥ 2σ (I)]	R_1 = 0.2568, wR_2 = 0.2973
Z	4	R Indices (all Data)	0.84/-1.08

Table 7.1.5.2 *Bond lengths for 5170.*

Atom	Atom	Length/Å	Atom	Atom	Length/Å
Fe	P	2.181(3)	N1	C8	1.450(11)
Fe	C14	1.774(10)	C2	C3	1.390(17)
Fe	C15	1.798(12)	C2	C7	1.387(12)
Fe	C16	1.798(14)	C3	C4	1.403(19)
Fe	C17	1.742(16)	C4	C5	1.404(16)
P	O1	1.620(8)	C5	C6	1.369(19)
P	N1	1.686(8)	C6	C7	1.391(19)
O1	C1	1.489(13)	C8	C9	1.430(13)
O2	C14	1.159(13)	C8	C13	1.401(16)
O3	C15	1.156(14)	C9	C10	1.412(17)
O4	C16	1.148(15)	C10	C11	1.332(18)
O5	C17	1.194(17)	C11	C12	1.399(16)
N1	C2	1.415(14)	C12	C13	1.368(15)

Table 7.1.5.3 *Bond angles for 5170.*

Atom	Atom	Atom	Angle/˚	Atom	Atom	Atom	Angle/˚
C14	Fe	P	176.7(4)	C7	C2	C3	118.9(11)

C14	Fe	C15	91.7(5)	C2	C3	C4	119.4(9)
C14	Fe	C16	90.6(5)	C3	C4	C5	121.0(13)
C15	Fe	P	87.2(4)	C6	C5	C4	118.9(12)
C16	Fe	P	87.4(3)	C5	C6	C7	120.3(10)
C16	Fe	C15	121.3(6)	C2	C7	C6	121.5(12)
C17	Fe	P	91.2(4)	C9	C8	N1	118.2(9)
C17	Fe	C14	92.0(5)	C13	C8	N1	122.8(8)
C17	Fe	C15	117.5(6)	C13	C8	C9	119.0(9)
C17	Fe	C16	121.0(6)	C10	C9	C8	117.1(11)
O1	P	Fe	111.6(3)	C11	C10	C9	122.7(10)
O1	P	N1	109.2(4)	C10	C11	C12	120.2(11)
N1	P	Fe	119.3(3)	C13	C12	C11	119.9(12)
C1	O1	P	116.7(8)	C12	C13	C8	121.0(10)
C2	N1	P	123.1(6)	O2	C14	Fe	178.8(12)
C2	N1	C8	117.7(7)	O3	C15	Fe	179.7(13)
C8	N1	P	119.2(6)	O4	C16	Fe	179.5(11)
C3	C2	N1	119.5(9)	O5	C17	Fe	177.5(10)
C7	C2	N1	121.5(11)				

7.1.6 [Tetracarbonyl{methylamino(diphenylamino)phosphane- κP}iron(0)] (12a)

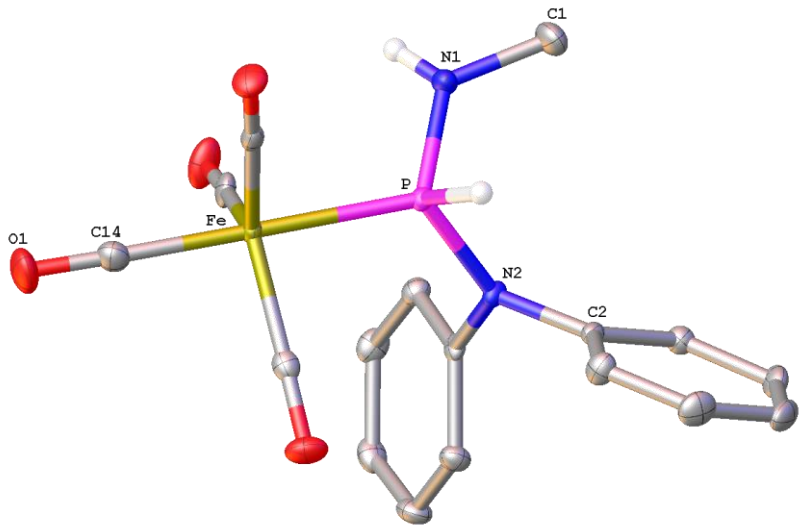

Identification code	GSTR566, TK-11 // GXraymo_5159f	$P_{calc}g$ / cm³	1.510
Device type	Bruker D8-Venture	μ / mm^{-1}	0.976
Moiety formula	C17 H15 Fe N2 O4 P	F(000)	1632.0
Empirical formula	$C_{17}H_{15}FeN_2O_4P$	Crystal size / mm	0.16 × 0.12 × 0.06
Temperature / K	100	2Θ range for data collection / °	4.676 - 55.992
Radiation	MoKα (λ = 0.71073)	T_{min}; T_{max}	0.6964; 0.7460

Crystal system	orthorhombisch	Absorption correction	empirisch
Space group	Pbca	Completeness to theta	1.000
a / Å	13.6227(10)	Index ranges	-17 ≤ h ≤ 17, -20 ≤ k ≤ 20, -21 ≤ l ≤ 21
b / Å	15.5917(13)	Reflections collected	68280
c / Å	16.4911(14)	Independent reflections	4223 [R_{int} =3D 0.0988, R_{sigma} =3D 0.0333]
α / Å	90	Data/restraints/	4223/0/233
β / Å	90	parameters	1.036
γ / Å	90	*Goodness-of-fit on* F^2	R_1 =3D 0.0313, wR_2 =3D 0.0589
Volume / Å³	1.510	Final R Indices [I ≥ 2σ (I)]	R_1 =3D 0.0530, wR_2 =3D 0.0652
Z	8	R Indices (all Data)	0.41/-0.35

Table 7.1.6.1 *Bond lengths for 5159f.*

Atom	Atom	Length/Å	Atom	Atom	Length/Å
Fe	P	2.2046(5)	N2	C8	1.436(2)
Fe	C14	1.789(2)	C2	C3	1.391(3)
Fe	C15	1.787(2)	C2	C7	1.387(2)
Fe	C16	1.7979(19)	C3	C4	1.384(3)
Fe	C17	1.7928(19)	C4	C5	1.389(3)
P	N1	1.6462(17)	C5	C6	1.379(3)
P	N2	1.6932(15)	C6	C7	1.391(3)
O1	C14	1.141(2)	C8	C9	1.383(2)
O2	C15	1.148(2)	C8	C13	1.393(2)
O3	C16	1.139(2)	C9	C10	1.388(3)
O4	C17	1.144(2)	C10	C11	1.380(3)
N1	C1	1.463(3)	C11	C12	1.385(3)
N2	C2	1.435(2)	C12	C13	1.383(3)

Table 7.1.6.2. *Bond angles for 5159f.*

Atom	Atom	Atom	Angle/˚	Atom	Atom	Atom	Angle/˚
C14	Fe	P	179.39(7)	C7	C2	C3	119.66(16)
C14	Fe	C16	92.03(9)	C4	C3	C2	120.18(17)
C14	Fe	C17	91.48(9)	C3	C4	C5	120.03(18)
C15	Fe	P	89.91(6)	C6	C5	C4	119.92(17)
C15	Fe	C14	89.49(9)	C5	C6	C7	120.29(18)
C15	Fe	C16	122.23(8)	C2	C7	C6	119.91(18)
C15	Fe	C17	121.54(8)	C9	C8	N2	121.39(16)
C16	Fe	P	88.38(6)	C9	C8	C13	119.68(16)
C17	Fe	P	88.74(6)	C13	C8	N2	118.92(15)

C17	Fe	C16	116.14(8)	C8	C9	C10	119.96(17)
N1	P	Fe	112.88(6)	C11	C10	C9	120.55(18)
N1	P	N2	110.69(8)	C10	C11	C12	119.37(17)
N2	P	Fe	117.08(5)	C13	C12	C11	120.62(18)
C1	N1	P	123.00(14)	C12	C13	C8	119.75(17)
C2	N2	P	122.85(11)	O1	C14	Fe	178.64(18)
C2	N2	C8	116.02(14)	O2	C15	Fe	177.11(17)
C8	N2	P	120.89(11)	O3	C16	Fe	178.03(18)
C3	C2	N2	118.81(16)	O4	C17	Fe	177.35(17)
C7	C2	N2	121.48(16)				

7.1.7 [Pentacarbonyl{methylamino(diphenylamino)phosphane- κP}chromium(0)] (13a)

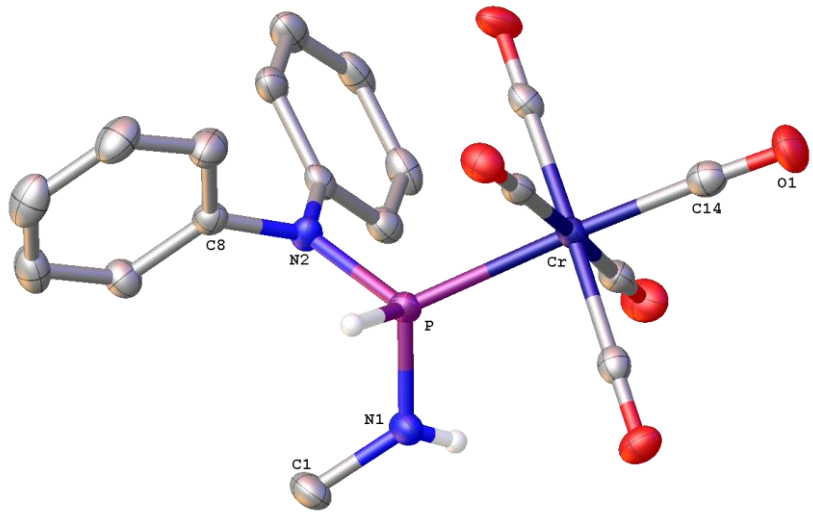

Identification code	GSTR683, PJ-251 // GXray5996h	$P_{calc}g$ / cm³	1.448
Device type	Bruker X8-KappaApexII	μ / mm^{-1}	0.704
Moiety formula	C18 H15 Cr N2 O5 P	F(000)	864.0
Empirical formula	$C_{18}H_{15}N_2O_5PCr$	Crystal size / mm	0.11 × 0.06 × 0.02
Temperature / K	100	2Θ range for data collection / °	4.422 - 51.998
Radiation	MoKα (λ = 0.71073)	T_{min}; T_{max}	0.5524; 0.7467
Crystal system	monoklin	Absorption correction	empirisch
Space group	$P2_1/n$	Completeness to theta	0.997

a / Å	11.1972(10)	Index ranges	-12 ≤ h ≤ 13, -17 ≤ k ≤ 17, -14 ≤ l ≤ 14
b / Å	14.5230(10)	Reflections collected	17061
c / Å	11.9110(10)	Independent reflections	3789 [R_{int} = 0.0736, R_{sigma} = 0.0580]
α / Å	90	Data/restraints/	3789/0/253
β / Å	90.403(6)	parameters	1.020
γ / Å	90	*Goodness-of-fit* on F^2	R_1 = 0.0404, wR_2 = 0.0833
Volume / Å³	1936.9(3)	Final R Indices [I ≥ 2σ (I)]	R_1 = 0.0650, wR_2 = 0.0962
Z	4	R Indices (all Data)	0.35/-0.50

Table 7.1.7.1. *Bond lengths for 5996h.*

Atom	Atom	Length/Å	Atom	Atom	Length/Å
Cr	P	2.3331(9)	N2	C2	1.421(3)
Cr	C14	1.876(3)	N2	C8	1.447(4)
Cr	C15	1.902(3)	C2	C3	1.388(4)
Cr	C16	1.907(3)	C2	C7	1.391(4)
Cr	C17	1.904(3)	C3	C4	1.393(4)
Cr	C18	1.891(3)	C4	C5	1.389(4)
P	N1	1.654(3)	C5	C6	1.379(5)
P	N2	1.713(2)	C6	C7	1.386(4)
O1	C14	1.148(4)	C8	C9	1.374(4)
O2	C15	1.142(4)	C8	C13	1.390(4)
O3	C16	1.140(3)	C9	C10	1.389(4)
O4	C17	1.143(3)	C10	C11	1.385(5)
O5	C18	1.148(3)	C11	C12	1.380(5)
N1	C1	1.460(4)	C12	C13	1.387(5)

Table 7.1.7.2 *Bond angles for 5996h.*

Atom	Atom	Atom	Angle/˚	Atom	Atom	Atom	Angle/˚
C14	Cr	P	175.32(9)	C3	C2	N2	120.5(2)
C14	Cr	C15	91.07(13)	C3	C2	C7	119.1(3)
C14	Cr	C16	92.26(12)	C7	C2	N2	120.3(3)
C14	Cr	C17	92.28(13)	C2	C3	C4	120.9(3)
C14	Cr	C18	89.36(12)	C5	C4	C3	119.3(3)
C15	Cr	P	91.84(9)	C6	C5	C4	120.0(3)
C15	Cr	C16	89.14(12)	C5	C6	C7	120.6(3)
C15	Cr	C17	176.34(13)	C6	C7	C2	120.0(3)
C16	Cr	P	91.44(9)	C9	C8	N2	119.5(3)

C17	Cr	P	84.91(9)	C9	C8	C13	120.1(3)
C17	Cr	C16	89.26(12)	C13	C8	N2	120.3(3)
C18	Cr	P	86.97(9)	C8	C9	C10	119.9(3)
C18	Cr	C15	90.18(12)	C11	C10	C9	120.5(3)
C18	Cr	C16	178.25(12)	C12	C11	C10	119.2(3)
C18	Cr	C17	91.33(12)	C11	C12	C13	120.7(3)
N1	P	Cr	114.55(10)	C12	C13	C8	119.6(3)
N1	P	N2	110.53(12)	O1	C14	Cr	178.0(3)
N2	P	Cr	119.57(9)	O2	C15	Cr	178.7(3)
C1	N1	P	123.1(2)	O3	C16	Cr	179.1(2)
C2	N2	P	122.04(19)	O4	C17	Cr	177.5(3)
C2	N2	C8	119.9(2)	O5	C18	Cr	179.5(3)
C8	N2	P	117.89(18)				

7.1.8 [Pentacarbonyl{chloro(triphenylmethyl)-*p*-(diphenylmethyl)phenylphosphane- *κ*P}tungsten(0)] (33c)

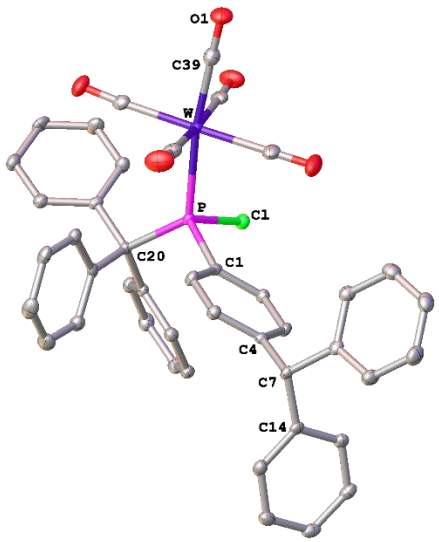

Identification code	GSTR547, PJ-145 // GXray5066f	$P_{calc}g$ / cm³	1.577
Device type	Bruker X8-KappaApexII	μ / mm^{-1}	952.0
Moiety formula	C43 H30 Cl O5 P W, C4 H10 O	F(000)	C43 H30 Cl O5 P W, C4 H10 O
Empirical formula	$C_{47}H_{40}ClO_6PW$	Crystal size / mm	0.16 × 0.14 × 0.1
Temperature / K	100	2Θ range for data collection / °	5.832 - 56
Radiation	MoKα (λ = 0.71073)	T_{min}; T_{max}	0.5693; 0.7459
Crystal system	Triklin	Absorption correction	empirisch
Space group	$P\bar{1}$	Completeness to theta	0.997

a / Å	10.9641(8)	Index ranges	$-14 \le h \le 14$, $-17 \le k \le 17$, $-18 \le l \le 18$
b / Å	13.1791(8)	Reflections collected	55667
c / Å	14.2135(10)	Independent reflections	9658 [R_{int} = 0.0320, R_{sigma} = 0.0219]
α / Å	80.151(3)	Data/restraints/	9658/1/507
β / Å	84.789(3)	parameters	1.075
γ / Å	82.795(3)	*Goodness-of-fit* on F^2	R_1 = 0.0186, wR_2 = 0.0429
Volume / Å³	2002.5(2)	Final R Indices [$I \ge 2\sigma(I)$]	R_1 = 0.0217, wR_2 = 0.0445
Z	2	R Indices (all Data)	1.15/-0.54

Tabelle 7.1.8.1 *Bond lengths for 5066f.*

Atom	Atom	Length/Å	Atom	Atom	Length/Å
W	P	2.5241(5)	C14	C19	1.391(3)
W	C39	2.009(2)	C15	C16	1.388(3)
W	C40	2.047(2)	C16	C17	1.381(3)
W	C41	2.047(2)	C17	C18	1.388(3)
W	C42	2.044(2)	C18	C19	1.391(3)
W	C43	2.052(2)	C20	C21	1.538(2)
Cl	P	2.0737(6)	C20	C27	1.541(2)
P	C1	1.8357(18)	C20	C33	1.540(3)
P	C20	1.9533(18)	C21	C22	1.403(3)
O1	C39	1.144(3)	C21	C26	1.394(3)
O2	C40	1.139(3)	C22	C23	1.388(3)
O3	C41	1.139(3)	C23	C24	1.388(3)
O4	C42	1.139(3)	C24	C25	1.384(3)
O5	C43	1.141(2)	C25	C26	1.391(3)
C1	C2	1.396(3)	C27	C28	1.396(3)
C1	C6	1.399(2)	C27	C32	1.398(3)
C2	C3	1.389(3)	C28	C29	1.382(3)
C3	C4	1.394(3)	C29	C30	1.386(3)
C4	C5	1.392(3)	C30	C31	1.382(3)
C4	C7	1.522(2)	C31	C32	1.393(3)
C5	C6	1.390(3)	C33	C34	1.403(3)
C7	C8	1.535(3)	C33	C38	1.386(3)
C7	C14	1.528(2)	C34	C35	1.390(3)
C8	C9	1.394(3)	C35	C36	1.388(3)
C8	C13	1.390(3)	C36	C37	1.377(3)
C9	C10	1.395(3)	C37	C38	1.393(3)
C10	C11	1.381(3)	O6	C45	1.424(3)

C11	C12	1.384(3)	O6	C46	1.413(3)
C12	C13	1.391(3)	C44	C45	1.495(3)
C14	C15	1.397(3)	C46	C47	1.503(3)

Table 7.1.8.2 *Bond angles for 5066f.*

Atom	**Atom**	**Atom**	**Angle/˚**	**Atom**	**Atom**	**Atom**	**Angle/˚**
C39	W	P	172.75(6)	C19	C14	C15	118.37(17)
C39	W	C40	87.90(8)	C16	C15	C14	120.49(18)
C39	W	C41	90.42(8)	C17	C16	C15	120.60(19)
C39	W	C42	87.12(8)	C16	C17	C18	119.65(18)
C39	W	C43	89.13(8)	C17	C18	C19	119.78(19)
C40	W	P	94.47(6)	C14	C19	C18	121.12(18)
C40	W	C43	90.96(8)	C21	C20	P	109.22(12)
C41	W	P	82.71(6)	C21	C20	C27	110.60(14)
C41	W	C40	90.65(9)	C21	C20	C33	113.47(15)
C41	W	C43	178.31(8)	C27	C20	P	108.12(12)
C42	W	P	90.64(6)	C33	C20	P	105.34(12)
C42	W	C40	174.84(8)	C33	C20	C27	109.84(14)
C42	W	C41	90.73(9)	C22	C21	C20	120.89(16)
C42	W	C43	87.63(8)	C26	C21	C20	121.52(16)
C43	W	P	97.67(6)	C26	C21	C22	117.60(17)
Cl	P	W	106.54(2)	C23	C22	C21	121.14(18)
C1	P	W	112.01(6)	C24	C23	C22	120.31(18)
C1	P	Cl	100.63(6)	C25	C24	C23	119.33(18)
C1	P	C20	107.32(8)	C24	C25	C26	120.37(19)
C20	P	W	125.66(6)	C25	C26	C21	121.24(18)
C20	P	Cl	101.26(6)	C28	C27	C20	120.99(16)
C2	C1	P	118.93(13)	C28	C27	C32	118.03(17)
C2	C1	C6	118.16(16)	C32	C27	C20	120.77(16)
C6	C1	P	122.53(14)	C29	C28	C27	121.08(18)
C3	C2	C1	120.88(17)	C28	C29	C30	120.50(19)
C2	C3	C4	121.11(17)	C31	C30	C29	119.31(18)
C3	C4	C7	120.32(16)	C30	C31	C32	120.48(18)
C5	C4	C3	117.90(17)	C31	C32	C27	120.59(18)
C5	C4	C7	121.75(16)	C34	C33	C20	119.40(17)
C6	C5	C4	121.43(17)	C38	C33	C20	122.56(17)
C5	C6	C1	120.49(17)	C38	C33	C34	118.00(17)
C4	C7	C8	112.41(15)	C35	C34	C33	121.07(19)
C4	C7	C14	111.55(15)	C36	C35	C34	119.94(19)
C14	C7	C8	112.86(14)	C37	C36	C35	119.40(19)
C9	C8	C7	122.04(17)	C36	C37	C38	120.8(2)
C13	C8	C7	119.68(17)	C33	C38	C37	120.78(19)
C13	C8	C9	118.22(18)	O1	C39	W	178.07(19)
C8	C9	C10	120.50(19)	O2	C40	W	176.02(19)
C11	C10	C9	120.7(2)	O3	C41	W	179.0(2)
C10	C11	C12	119.28(19)	O4	C42	W	177.12(17)
C11	C12	C13	120.2(2)	O5	C43	W	176.86(18)

C8	C13	C12	121.2(2)	C46	O6	C45	112.54(17)
C15	C14	C7	122.19(17)	O6	C45	C44	108.98(19)
C19	C14	C7	119.42(17)	O6	C46	C47	108.63(18)

7.1.9 [Pentacarbonyl{chloro(triphenylmethyl)-*p*-(diphenylmethyl)phenylphosphane- *κ*P}chromium(0)] (35)

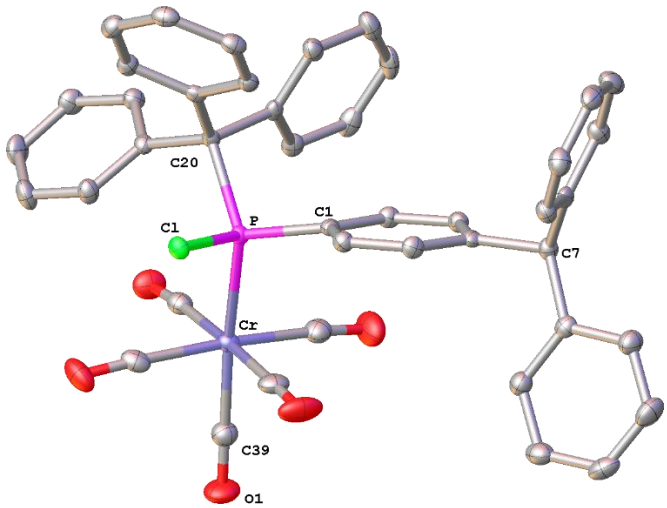

Identification code	GSTR609, PJ-195 // GXray5535	$P_{calc}g$ / cm³	1.364
Device type	STOE IPDS-2T	μ / mm^{-1}	0.444
Moiety formula	C43 H30 Cl Cr O5 P, C4 H10 O	F(000)	852.0
Empirical formula	$C_{47}H_{40}ClCrO_6P$	Crystal size / mm	0.15 × 0.09 × 0.06
Temperature / K	123	2Θ range for data collection / °	5.708 - 51.996
Radiation	MoKα (λ = 0.71073)	T_{min}; T_{max}	0.7654; 0.8508
Crystal system	triklin	Absorption correction	integration
Space group	$P\bar{1}$	Completeness to theta	0.977
a / Å	10.9642(4)	Index ranges	-13 ≤ h ≤ 13, -16 ≤ k ≤ 15, -17 ≤ l ≤ 17
b / Å	13.1023(5)	Reflections collected	14306
c / Å	14.2010(5)	Independent reflections	7669 [R_{int} = 0.0251, R_{sigma} = 0.0478]
α / Å	80.171(3)	Data/restraints/	7669/0/507
β / Å	88.218(3)	parameters	0.886
γ / Å	82.890(3)	*Goodness-of-fit on* F^2	R_1 = 0.0290, wR_2 = 0.0623

Volume / Å³	1994.56(13)	Final R Indices [I ≥ 2σ (I)]	R_1 = 0.0473, wR_2 = 0.0655
Z	2	R Indices (all Data)	0.29/-0.32

Table 7.1.9.1 *Bond lengths for 5535.*

Atom	Atom	Length/Å	Atom	Atom	Length/Å
Cr	P	2.3910(5)	C14	C19	1.391(2)
Cr	C39	1.8685(19)	C15	C16	1.386(3)
Cr	C40	1.8981(19)	C16	C17	1.385(3)
Cr	C41	1.898(2)	C17	C18	1.386(3)
Cr	C42	1.9012(18)	C18	C19	1.389(3)
Cr	C43	1.911(2)	C20	C21	1.540(2)
Cl	P	2.0726(5)	C20	C27	1.538(2)
P	C1	1.8445(15)	C20	C33	1.541(2)
P	C20	1.9549(17)	C21	C22	1.399(2)
O1	C39	1.146(2)	C21	C26	1.392(2)
O2	C40	1.143(2)	C22	C23	1.387(2)
O3	C41	1.141(2)	C23	C24	1.384(3)
O4	C42	1.143(2)	C24	C25	1.379(3)
O5	C43	1.139(2)	C25	C26	1.392(2)
C1	C2	1.400(2)	C27	C28	1.401(2)
C1	C6	1.389(2)	C27	C32	1.392(2)
C2	C3	1.387(2)	C28	C29	1.384(2)
C3	C4	1.385(2)	C29	C30	1.384(2)
C4	C5	1.395(2)	C30	C31	1.381(3)
C4	C7	1.527(2)	C31	C32	1.393(2)
C5	C6	1.390(2)	C33	C34	1.391(2)
C7	C8	1.524(2)	C33	C38	1.395(2)
C7	C14	1.532(2)	C34	C35	1.392(2)
C8	C9	1.394(2)	C35	C36	1.386(3)
C8	C13	1.392(2)	C36	C37	1.373(3)
C9	C10	1.387(3)	C37	C38	1.387(2)
C10	C11	1.376(3)	O6	C45	1.427(2)
C11	C12	1.382(3)	O6	C46	1.416(2)
C12	C13	1.385(2)	C44	C45	1.500(3)
C14	C15	1.393(2)	C46	C47	1.496(3)

Table 7.1.9.2 *Bond angles for 5535.*

Atom	Atom	Atom	Angle/˚	Atom	Atom	Atom	Angle/˚
C39	Cr	P	170.64(6)	C19	C14	C15	117.79(17)
C39	Cr	C40	87.16(8)	C16	C15	C14	121.48(17)
C39	Cr	C41	87.79(8)	C17	C16	C15	120.19(18)
C39	Cr	C42	87.01(8)	C16	C17	C18	118.92(18)
C39	Cr	C43	90.67(8)	C17	C18	C19	120.75(17)
C40	Cr	P	94.12(6)	C18	C19	C14	120.84(17)
C40	Cr	C42	173.40(8)	C21	C20	P	104.88(10)

C40	Cr	C43	90.51(8)	C21	C20	C33	109.62(13)
C41	Cr	P	82.92(5)	C27	C20	P	108.91(11)
C41	Cr	C40	91.06(8)	C27	C20	C21	114.00(12)
C41	Cr	C42	91.81(8)	C27	C20	C33	110.66(12)
C41	Cr	C43	177.75(8)	C33	C20	P	108.49(10)
C42	Cr	P	92.13(5)	C22	C21	C20	119.63(14)
C42	Cr	C43	86.47(8)	C26	C21	C20	122.30(14)
C43	Cr	P	98.59(5)	C26	C21	C22	118.06(15)
Cl	P	Cr	106.94(2)	C23	C22	C21	121.17(16)
C1	P	Cr	111.06(5)	C24	C23	C22	120.06(17)
C1	P	Cl	100.46(5)	C25	C24	C23	119.40(16)
C1	P	C20	107.05(7)	C24	C25	C26	120.86(17)
C20	P	Cr	126.90(5)	C21	C26	C25	120.39(17)
C20	P	Cl	100.83(5)	C28	C27	C20	121.21(14)
C2	C1	P	118.95(12)	C32	C27	C20	121.19(14)
C6	C1	P	122.12(12)	C32	C27	C28	117.58(15)
C6	C1	C2	118.24(14)	C29	C28	C27	121.08(15)
C3	C2	C1	120.56(16)	C28	C29	C30	120.51(16)
C4	C3	C2	121.45(15)	C31	C30	C29	119.36(16)
C3	C4	C5	117.79(14)	C30	C31	C32	120.16(16)
C3	C4	C7	120.64(14)	C27	C32	C31	121.29(16)
C5	C4	C7	121.55(15)	C34	C33	C20	120.90(14)
C6	C5	C4	121.26(16)	C34	C33	C38	117.89(15)
C1	C6	C5	120.64(15)	C38	C33	C20	121.05(15)
C4	C7	C14	113.10(13)	C33	C34	C35	121.00(16)
C8	C7	C4	111.09(13)	C36	C35	C34	120.18(17)
C8	C7	C14	112.68(14)	C37	C36	C35	119.26(16)
C9	C8	C7	119.87(15)	C36	C37	C38	120.80(16)
C13	C8	C7	121.98(15)	C37	C38	C33	120.84(17)
C13	C8	C9	118.10(16)	O1	C39	Cr	177.62(17)
C10	C9	C8	120.86(17)	O2	C40	Cr	174.83(16)
C11	C10	C9	120.40(17)	O3	C41	Cr	178.94(17)
C10	C11	C12	119.38(17)	O4	C42	Cr	175.89(15)
C11	C12	C13	120.55(17)	O5	C43	Cr	175.67(15)
C12	C13	C8	120.71(16)	C46	O6	C45	111.96(15)
C15	C14	C7	119.18(15)	O6	C45	C44	108.90(19)
C19	C14	C7	122.98(15)	O6	C46	C47	109.09(17)

7.1.10 [Octacarbonyl-{μ-[bis-(dicyclohexylamino)phosphino]}ditungsten(I)] (W-W)

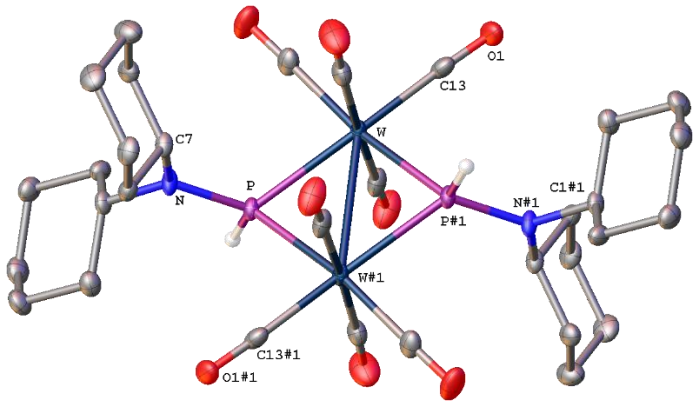

Identification code	GSTR639, PJ-234 // GXray5801f	$P_{calc}g$ / cm³	1.856
Device type	Bruker X8-KappaApexII	μ / mm^{-1}	6.459
Moiety formula	C32 H46 N2 O8 P2 W2	F(000)	988.0
Empirical formula	$C_{32}H_{46}N_2O_8P_2W_2$	Crystal size / mm	0.08 × 0.05 × 0.04
Temperature / K	100	2Θ range for data collection / °	5.556 - 56
Radiation	MoKα (λ = 0.71073)	T_{min}; T_{max}	0.5958; 0.7462
Crystal system	monoklin	Absorption correction	empirisch
Space group	$P2_1/c$	Completeness to theta	0.998
a / Å	11.5143(5)	Index ranges	-15 ≤ h ≤ 15, -12 ≤ k ≤ 12, -21 ≤ l ≤ 21
b / Å	9.5162(4)	Reflections collected	34741
c / Å	16.6078(8)	Independent reflections	4382 [R_{int} = 0.0565, R_{sigma} = 0.0315]
α / Å	90	Data/restraints/	4382/0/211
β / Å	92.4164(13)	parameters	1.029
γ / Å	90	*Goodness-of-fit* on F^2	R_1 = 0.0200, wR_2 = 0.0352
Volume / Å³	1818.14(14)	Final R Indices [I ≥ 2σ (I)]	R_1 = 0.0311, wR_2 = 0.0383
Z	2	R Indices (all Data)	0.61/-0.60

Table 7.1.10.1 *Bond lengths for 5801f.*

Atom	Atom	Length/Å	Atom	Atom	Length/Å

W	W^1	3.0681(2)	N	C7	1.470(3)
W	P^1	2.4746(8)	C1	C2	1.529(4)
W	P	2.4719(8)	C1	C6	1.530(4)
W	C13	2.012(3)	C2	C3	1.525(4)
W	C14	2.046(3)	C3	C4	1.529(4)
W	C15	2.012(3)	C4	C5	1.527(4)
W	C16	2.037(3)	C5	C6	1.527(4)
P	W^1	2.4745(8)	C7	C8	1.528(4)
P	N	1.670(2)	C7	C12	1.528(4)
O1	C13	1.142(4)	C8	C9	1.524(4)
O2	C14	1.137(4)	C9	C10	1.524(4)
O3	C15	1.145(4)	C10	C11	1.525(4)
O4	C16	1.142(4)	C11	C12	1.532(4)
N	C1	1.478(3)			

Table 7.1.10.2. *Bond angles for 5801f.*

Atom	**Atom**	**Atom**	**Angle/˚**	**Atom**	**Atom**	**Atom**	**Angle/˚**
P^1	W	W^1	51.627(18)	C1	N	P	122.69(18)
P	W	W^1	51.703(18)	C7	N	P	117.91(19)
P	W	P^1	103.33(2)	C7	N	C1	118.9(2)
C13	W	W^1	134.36(9)	N	C1	C2	111.8(2)
C13	W	P	169.52(9)	N	C1	C6	113.2(2)
C13	W	P^1	83.37(9)	C2	C1	C6	111.3(2)
C13	W	C14	87.10(12)	C3	C2	C1	110.9(2)
C13	W	C15	92.25(12)	C2	C3	C4	111.3(2)
C13	W	C16	89.66(12)	C5	C4	C3	110.5(2)
C14	W	W^1	91.12(9)	C6	C5	C4	111.2(2)
C14	W	P	84.08(9)	C5	C6	C1	111.3(2)
C14	W	P^1	97.31(9)	N	C7	C8	112.9(2)
C15	W	W^1	133.37(9)	N	C7	C12	112.6(2)
C15	W	P	82.56(9)	C8	C7	C12	111.5(2)
C15	W	P^1	168.75(9)	C9	C8	C7	110.7(2)
C15	W	C14	92.80(12)	C8	C9	C10	111.4(3)
C15	W	C16	84.97(13)	C9	C10	C11	111.3(3)
C16	W	W^1	92.83(9)	C10	C11	C12	111.4(2)
C16	W	P	98.91(8)	C7	C12	C11	110.8(3)
C16	W	P^1	84.64(9)	O1	C13	W	177.9(3)
C16	W	C14	175.99(12)	O2	C14	W	178.2(3)
W	P	W^1	76.67(2)	O3	C15	W	175.5(3)
N	P	W^1	126.60(9)	O4	C16	W	175.5(3)
N	P	W	124.65(9)				

7.1.11 [Lithium(12-crown-4)-{pentacarbonyl[(diphenylamino)phosphinito-κP]tungsten(0)}]

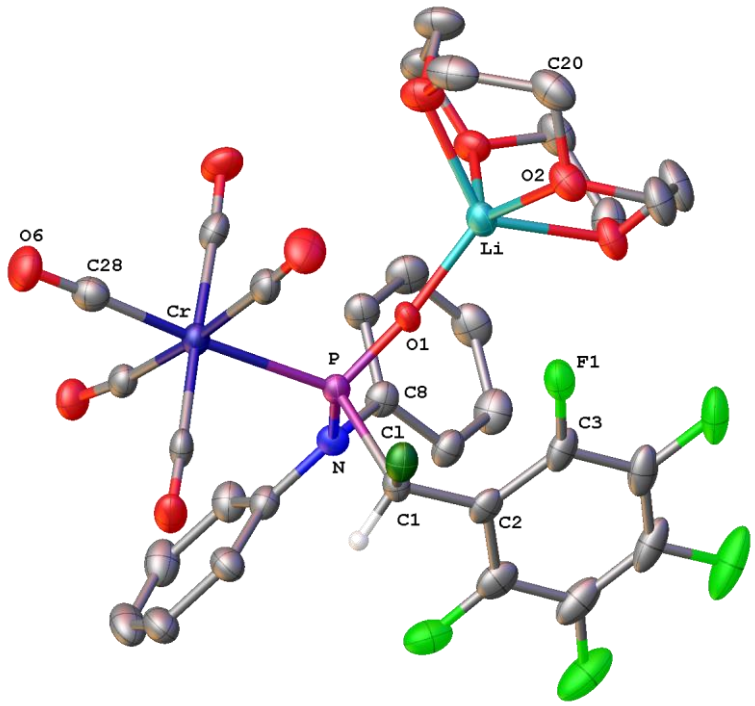

Identification code	GSTR676, PJ-267 // GXray6026f	$P_{calc}g$ / cm³	1.528
Device type	Bruker X8-KappaApexII	μ / mm^{-1}	0.532
Moiety formula	C32 H27 Cl Cr F5 Li N O10 P	F(000)	820.0
Empirical formula	$C_{32}H_{27}ClCrF_5LiNO_{10}P$	Crystal size / mm	0.22 × 0.21 × 0.16
Temperature / K	100	2Θ range for data collection / °	4.224 - 55.998
Radiation	MoKα (λ = 0.71073)	T_{min}; T_{max}	0.5476; 0.7461
Crystal system	triklin	Absorption correction	empirisch
Space group	$P\bar{1}$	Completeness to theta	0.998
a / Å	9.602(2)	Index ranges	-12 ≤ h ≤ 12, -13 ≤ k ≤ 13, -25 ≤ l ≤ 25
b / Å	10.583(2)	Reflections collected	70026
c / Å	19.040(4)	Independent reflections	8437 [R_{int} = 0.1392, R_{sigma} = 0.0798]
α / Å	101.934(6)	Data/restraints/	8437/0/469
β / Å	96.729(6)	parameters	1.088

γ / Å	109.222(6)	*Goodness-of-fit* on F^2	R_1 = 0.0875, wR_2 = 0.2268
Volume / Å³	1751.1(7)	Final R Indices [I ≥ 2σ (I)]	R_1 = 0.1384, wR_2 = 0.2643
Z	2	R Indices (all Data)	1.63/-1.05

Table 7.1.11.1 *Bond lengths for 6026f.*

Atom	Atom	Length/Å	Atom	Atom	Length/Å
Cr	P	2.3809(17)	O7	C29	1.145(8)
Cr	C28	1.866(7)	O8	C30	1.144(8)
Cr	C29	1.890(7)	O9	C31	1.142(7)
Cr	C30	1.896(7)	O10	C32	1.141(7)
Cr	C31	1.910(6)	N	C8	1.432(7)
Cr	C32	1.887(6)	N	C14	1.421(7)
Cl	C1	1.798(6)	C1	C2	1.482(8)
P	O1	1.504(4)	C2	C3	1.411(9)
P	N	1.741(5)	C2	C7	1.376(9)
P	C1	1.914(6)	C3	C4	1.386(9)
F1	C3	1.325(7)	C4	C5	1.363(11)
F2	C4	1.353(8)	C5	C6	1.371(12)
F3	C5	1.336(7)	C6	C7	1.385(10)
F4	C6	1.342(8)	C8	C9	1.401(8)
F5	C7	1.345(8)	C8	C13	1.387(8)
O1	Li	1.827(11)	C9	C10	1.394(9)
O2	C20	1.422(9)	C10	C11	1.379(10)
O2	C27	1.434(8)	C11	C12	1.380(10)
O2	Li	2.190(11)	C12	C13	1.388(9)
O3	C21	1.430(9)	C14	C15	1.419(8)
O3	C22	1.444(8)	C14	C19	1.392(9)
O3	Li	2.132(12)	C15	C16	1.390(9)
O4	C23	1.430(8)	C16	C17	1.384(11)
O4	C24	1.425(8)	C17	C18	1.372(10)
O4	Li	2.109(11)	C18	C19	1.390(9)
O5	C25	1.429(8)	C20	C21	1.513(11)
O5	C26	1.421(8)	C22	C23	1.505(10)
O5	Li	2.111(11)	C24	C25	1.514(10)
O6	C28	1.146(8)	C26	C27	1.507(10)

Table 7.1.11.2 *Bond angles for 6026f.*

Atom	Atom	Atom	Angles/˚	Atom	Atom	Atom	Angles/˚
C28	Cr	P	175.7(2)	F3	C5	C4	119.9(7)
C28	Cr	C29	90.3(3)	F3	C5	C6	120.1(7)
C28	Cr	C30	92.2(3)	C4	C5	C6	120.0(6)
C28	Cr	C31	87.3(3)	F4	C6	C5	120.8(6)
C28	Cr	C32	89.7(3)	F4	C6	C7	120.1(7)

C29	Cr	P	85.60(19)	C5	C6	C7	119.1(7)
C29	Cr	C30	87.8(3)	F5	C7	C2	119.9(6)
C29	Cr	C31	174.5(3)	F5	C7	C6	117.0(6)
C30	Cr	P	86.45(18)	C2	C7	C6	123.0(7)
C30	Cr	C31	87.4(3)	C9	C8	N	121.4(5)
C31	Cr	P	96.66(18)	C13	C8	N	119.9(5)
C32	Cr	P	91.65(17)	C13	C8	C9	118.5(6)
C32	Cr	C29	92.1(3)	C10	C9	C8	120.8(6)
C32	Cr	C30	178.1(2)	C11	C10	C9	119.2(6)
C32	Cr	C31	92.9(3)	C10	C11	C12	120.8(6)
O1	P	Cr	115.28(17)	C11	C12	C13	119.8(6)
O1	P	N	104.9(2)	C8	C13	C12	120.8(6)
O1	P	C1	103.5(2)	C15	C14	N	120.9(5)
N	P	Cr	116.32(17)	C19	C14	N	121.9(5)
N	P	C1	97.6(2)	C19	C14	C15	117.1(6)
C1	P	Cr	117.01(18)	C16	C15	C14	120.1(6)
P	O1	Li	165.9(4)	C17	C16	C15	121.3(6)
C20	O2	C27	113.9(5)	C18	C17	C16	119.2(6)
C20	O2	Li	112.0(5)	C17	C18	C19	120.5(7)
C27	O2	Li	109.8(5)	C18	C19	C14	121.8(6)
C21	O3	C22	113.5(5)	O2	C20	C21	106.5(6)
C21	O3	Li	110.0(5)	O3	C21	C20	110.9(6)
C22	O3	Li	110.5(5)	O3	C22	C23	106.0(5)
C23	O4	Li	112.0(5)	O4	C23	C22	109.5(6)
C24	O4	C23	114.4(5)	O4	C24	C25	105.3(5)
C24	O4	Li	113.8(5)	O5	C25	C24	110.5(6)
C25	O5	Li	108.3(5)	O5	C26	C27	106.7(5)
C26	O5	C25	114.0(5)	O2	C27	C26	109.5(6)
C26	O5	Li	110.8(5)	O6	C28	Cr	178.1(6)
C8	N	P	118.4(4)	O7	C29	Cr	176.7(6)
C14	N	P	123.2(4)	O8	C30	Cr	177.4(5)
C14	N	C8	115.6(5)	O9	C31	Cr	172.9(5)
Cl	C1	P	111.0(3)	O10	C32	Cr	178.4(5)
C2	C1	Cl	112.4(4)	O1	Li	O2	130.5(6)
C2	C1	P	112.6(4)	O1	Li	O3	118.0(5)
C3	C2	C1	123.0(5)	O1	Li	O4	104.5(5)
C7	C2	C1	120.3(6)	O1	Li	O5	113.2(6)
C7	C2	C3	116.5(6)	O3	Li	O2	77.8(4)
F1	C3	C2	121.0(5)	O4	Li	O2	124.9(5)
F1	C3	C4	118.5(6)	O4	Li	O3	78.3(4)
C4	C3	C2	120.4(6)	O4	Li	O5	78.8(4)
F2	C4	C3	119.3(7)	O5	Li	O2	77.8(4)
F2	C4	C5	119.6(6)	O5	Li	O3	127.5(5)
C5	C4	C3	121.0(7)				

7.2 Computational Data

Table 7.1. The TPSS-D3/def2-TZVP/CPCM(THF) optimized Cartesian coordinates (in Å). Each structure is labelled by its specific name, followed by its number of atoms, its single-point-energy and ZPE (in hartrees), and the atomic coordinates.

2a {[$W(CO)_5$]PCl_2NPh_2}
37
Energy = -2414.609913010595
ZPE = 0.22903961

P	-0,07763	-0,23318	0,32844
N	0,43189	1,07566	1,23099
C	-0,46538	1,97391	1,93583
C	-0,70016	1,76035	3,29444
C	-1,05010	3,05060	1,26760
C	-1,53480	2,63418	3,99108
H	-0,23596	0,91465	3,79136
C	-1,88612	3,91899	1,97070
H	-0,85168	3,20617	0,21254
C	-2,12918	3,71189	3,33029
H	-1,72051	2,47142	5,04854
H	-2,34515	4,75710	1,45483
H	-2,77979	4,39012	3,87447
C	1,76721	1,59545	0,98775
C	2,72578	1,47431	1,99580
C	2,06309	2,25707	-0,20602
C	3,99152	2,02661	1,80585
H	2,47500	0,95697	2,91591
C	3,33367	2,80345	-0,38947
H	1,30657	2,34287	-0,97929
C	4,29553	2,69261	0,61569
H	4,74074	1,93293	2,58618
H	3,56917	3,31443	-1,31807
H	5,28336	3,11953	0,47075
W	1,49689	-2,09314	-0,14474
C	3,15145	-0,91206	-0,52596
O	4,12429	-0,34987	-0,78308
C	1,90709	-2,06493	1,87475
O	2,12773	-2,03406	3,00786
C	2,71547	-3,69639	-0,41033
O	3,40487	-4,61513	-0,55003
C	-0,05649	-3,41700	0,14952
O	-0,90258	-4,18701	0,29756
C	1,04788	-2,03528	-2,15997
O	0,79537	-1,99513	-3,28419
Cl	-1,09521	0,55589	-1,34966
Cl	-1,74284	-0,79439	1,40991

2b {[$W(CO)_5$]PCl_2NCy_2}
49
Energy = -2421.865274930489
ZPE = 0.36768188

P	0,01080	-0,02912	0,50589
N	0,50341	1,32236	1,30973
W	1,53453	-1,86341	-0,27662
C	2,45088	-0,58879	-1,61555
O	2,96993	0,08609	-2,39534
C	2,94975	-1,53998	1,18795
O	3,74736	-1,42403	2,01568
C	2,69085	-3,37564	-0,97321
O	3,35133	-4,23595	-1,37779
C	0,62178	-3,18892	1,01638
O	0,12559	-3,94912	1,72700
C	0,11643	-2,33286	-1,70226
O	-0,66522	-2,63396	-2,49448
Cl	-1,21346	0,70827	-1,06943
Cl	-1,55223	-0,75029	1,68406
C	-0,52740	2,22810	1,91104
C	-0,55330	2,13559	3,44467
C	-0,45986	3,68480	1,43972
H	-1,48600	1,83748	1,55141
C	-1,76615	2,90434	3,98829
H	0,36410	2,56358	3,86062
H	-0,59320	1,08364	3,74372
C	-1,67106	4,45304	1,99387
H	0,46101	4,15889	1,79805
H	-0,45612	3,72375	0,34619
C	-1,74373	4,36618	3,52356
H	-1,77697	2,84846	5,08282
H	-2,68791	2,42330	3,63185
H	-1,61520	5,49880	1,67086
H	-2,58947	4,03143	1,56213
H	-2,63176	4,89504	3,88912
H	-0,86750	4,86928	3,95640
C	1,94342	1,69857	1,15709
C	2,22539	2,66677	-0,00292
C	2,58168	2,17527	2,46523
H	2,43407	0,75521	0,88955
C	3,74261	2,82184	-0,18563
H	1,78896	3,64799	0,20127
H	1,75947	2,28607	-0,91855
C	4,09547	2,35856	2,27024
H	2,14131	3,13212	2,76849

H	2,38217	1,44934	3,26000
C	4,40238	3,31234	1,10913
H	3,94337	3,51598	-1,00936
H	4,17857	1,85409	-0,46862
H	4,53725	2,73066	3,20150
H	4,55337	1,38137	2,06592
H	5,48631	3,40148	0,97213
H	4,02347	4,31513	1,35192

3a {[Fe(CO)$_4$]PCl$_2$NPh$_2$}

35

Energy = -3497.839682057685

ZPE = 0.22269393

P	-0,09930	-0,23767	0,26583
N	0,40649	1,03632	1,22945
C	-0,48808	1,92513	1,94507
C	-0,83208	1,63212	3,26525
C	-0,96483	3,07895	1,31983
C	-1,66825	2,50259	3,96460
H	-0,44679	0,73151	3,73169
C	-1,80210	3,94378	2,02500
H	-0,67921	3,29494	0,29552
C	-2,15522	3,65622	3,34557
H	-1,93747	2,27884	4,99256
H	-2,17691	4,84135	1,54213
H	-2,80673	4,33159	3,89226
C	1,75883	1,52423	1,03828
C	2,61786	1,55599	2,13839
C	2,18925	1,96314	-0,21549
C	3,91961	2,02892	1,97724
H	2,26669	1,20883	3,10498
C	3,49744	2,42269	-0,37131
H	1,50655	1,94357	-1,05928
C	4,36256	2,45802	0,72322
H	4,59099	2,05184	2,83048
H	3,83603	2,75499	-1,34801
H	5,37972	2,81786	0,60074
Cl	-1,18957	0,63830	-1,31348
Cl	-1,73640	-0,89816	1,35827
Fe	1,37542	-1,73842	-0,23171
C	3,10279	-1,29583	-0,42317
O	4,22086	-1,03158	-0,54385
C	1,64630	-1,91717	1,53910
O	1,82400	-2,02256	2,67239
C	0,78168	-3,42767	-0,35186
O	0,41497	-4,52052	-0,43127
C	1,13841	-1,49741	-2,00396
O	1,00379	-1,34481	-3,13630

3b {[Fe(CO)$_4$]PCl$_2$NCy$_2$}

47

Energy = -3505.094546379410

ZPE = 0.36125519

P	0,01238	-0,07539	0,53175
N	0,49896	1,27534	1,33952
Cl	-1,37993	0,62498	-0,90104
Cl	-1,41159	-0,91151	1,82491
C	-0,53607	2,17775	1,93163
C	-0,54297	2,14391	3,46765
C	-0,49755	3,61520	1,40077
H	-1,49304	1,75438	1,60438
C	-1,76268	2,91590	3,99185
H	0,36975	2,60284	3,85910
H	-0,56434	1,10374	3,80745
C	-1,70974	4,39162	1,94012
H	0,42371	4,11330	1,72435
H	-0,50790	3,60727	0,30632
C	-1,76362	4,35976	3,47290
H	-1,76420	2,90138	5,08777
H	-2,68064	2,40969	3,66138
H	-1,66980	5,42549	1,57863
H	-2,62858	3,94459	1,53566
H	-2,65376	4,89116	3,82963
H	-0,88866	4,88867	3,87666
C	1,94534	1,64125	1,20575
C	2,24306	2,53167	-0,00931
C	2,55931	2,20351	2,49014
H	2,43895	0,68141	1,01542
C	3,76136	2,67961	-0,18493
H	1,79316	3,52051	0,12080
H	1,79364	2,08447	-0,90377
C	4,07781	2,35478	2,30098
H	2,12720	3,18327	2,72448
H	2,34531	1,53332	3,32876
C	4,41012	3,23496	1,08943
H	3,97205	3,33118	-1,04044
H	4,19735	1,69755	-0,41476
H	4,51706	2,77477	3,21290
H	4,52199	1,35954	2,15902
H	5,49662	3,30531	0,96183
H	4,03922	4,25380	1,26985
Fe	1,44612	-1,53264	-0,23208
C	0,59144	-3,00999	-0,78682
O	0,06227	-3,97091	-1,14886
C	1,38421	-0,75242	-1,85579
O	1,37281	-0,25802	-2,89604
C	3,23008	-1,43852	-0,32975
O	4,38493	-1,39341	-0,39772
C	1,62934	-2,12864	1,45812

O	1,76792	-2,50070	2,53979

4a {[Cr(CO)$_5$]PCl$_2$NPh$_2$}

37

Energy = -3392.008827879115

ZPE = 0.23081447

P	-0,02923	-0,28327	0,32145
N	0,46926	1,03471	1,21945
C	-0,43560	1,92387	1,92693
C	-0,66589	1,70732	3,28585
C	-1,02927	2,99723	1,26128
C	-1,50554	2,57416	3,98517
H	-0,19428	0,86473	3,78104
C	-1,87018	3,85872	1,96705
H	-0,83399	3,15561	0,20602
C	-2,10919	3,64826	3,32685
H	-1,68773	2,40898	5,04288
H	-2,33617	4,69422	1,45315
H	-2,76360	4,32113	3,87316
C	1,79350	1,57608	0,96767
C	2,75400	1,48700	1,97730
C	2,07790	2,22400	-0,23630
C	4,01185	2,05273	1,77632
H	2,51131	0,98115	2,90602
C	3,34118	2,78304	-0,43127
H	1,31910	2,28759	-1,00944
C	4,30621	2,70056	0,57361
H	4,76297	1,98319	2,55735
H	3,56836	3,28248	-1,36821
H	5,28835	3,13744	0,41983
C	2,99310	-0,95485	-0,41599
O	3,99270	-0,43523	-0,65807
C	1,76581	-2,01410	1,76427
O	1,96449	-2,01047	2,90103
C	2,56864	-3,50818	-0,31774
O	3,25830	-4,42762	-0,43728
C	0,01244	-3,25728	0,08796
O	-0,82030	-4,04872	0,18439
C	1,10158	-1,95303	-1,97935
O	0,90915	-1,92120	-3,11467
Cl	-1,05871	0,50075	-1,35343
Cl	-1,69222	-0,83972	1,41088
Cr	1,44267	-2,02179	-0,10758

4b {[Cr(CO)$_5$]PCl$_2$NCy$_2$}

49

Energy = -3399.263411520244

ZPE = 0.36961929

P	0,05462	-0,05550	0,45479
N	0,53485	1,29390	1,27442
C	2,34657	-0,64809	-1,43924
O	2,88863	0,00410	-2,22134
C	2,72810	-1,49006	1,18455
O	3,49440	-1,38232	2,04154
C	2,56428	-3,20018	-0,81041
O	3,24079	-4,05766	-1,18916
C	0,61147	-3,01831	0,97737
O	0,12104	-3,78912	1,67959
C	0,19809	-2,27670	-1,54008
O	-0,55226	-2,61530	-2,34638
Cl	-1,08744	0,71020	-1,17593
Cl	-1,57293	-0,73150	1,56798
C	-0,50260	2,19202	1,88026
C	-0,53765	2,06825	3,41146
C	-0,43362	3,65810	1,43947
H	-1,45830	1,81076	1,50510
C	-1,75159	2,82667	3,96684
H	0,37924	2,48522	3,84011
H	-0,58042	1,01028	3,68820
C	-1,64908	4,41287	2,00361
H	0,48364	4,12786	1,81216
H	-0,42572	3,72055	0,34722
C	-1,72751	4,29719	3,53095
H	-1,76564	2,74902	5,06002
H	-2,67244	2,35313	3,59822
H	-1,59379	5,46458	1,70041
H	-2,56482	3,99760	1,56028
H	-2,61695	4,81888	3,90336
H	-0,85290	4,79194	3,97656
C	1,96779	1,69530	1,11588
C	2,23262	2,69069	-0,02588
C	2,60860	2,15320	2,42983
H	2,47170	0,76743	0,82540
C	3,74764	2,86139	-0,21432
H	1,79127	3,66404	0,20167
H	1,76493	2,32620	-0,94687
C	4,11944	2,35424	2,23059
H	2,16005	3,09925	2,75415
H	2,42031	1,40987	3,21111
C	4,41152	3,33213	1,08577
H	3,93733	3,57391	-1,02493
H	4,18896	1,90291	-0,51974
H	4,56319	2,71279	3,16625
H	4,58444	1,38487	2,00553
H	5,49386	3,43289	0,94421
H	4,02599	4,32703	1,34982
Cr	1,47098	-1,80321	-0,20670

2-CPh$_3$ {[W(CO)$_5$]PCl$_2$CPh$_3$}

48

Energy = -2629.744345993965

ZPE = 0.32025444

P	-1,37289	-0,51209	-0,15006
Cl	-0,14218	-2,09884	0,37595
Cl	-1,03980	0,73512	1,47551
C	-0,37606	0,36635	-1,60660
W	-3,76993	-1,24463	-0,20534
C	-0,97809	-0,23229	-2,88215
C	-1,31783	0,57753	-3,97165
C	-1,11978	-1,62239	-3,01210
C	-1,80085	0,01285	-5,15292
H	-1,19753	1,65293	-3,90484
C	-1,61876	-2,18673	-4,18399
H	-0,80645	-2,27646	-2,20438
C	-1,96410	-1,36827	-5,26030
H	-2,05410	0,65915	-5,98822
H	-1,73006	-3,26450	-4,25514
H	-2,35223	-1,80405	-6,17618
C	-0,72521	1,84912	-1,45866
C	0,24646	2,84327	-1,30828
C	-2,07486	2,23462	-1,48494
C	-0,12489	4,18196	-1,16153
H	1,29811	2,58264	-1,31492
C	-2,44866	3,56494	-1,32362
H	-2,83991	1,48264	-1,64707
C	-1,47052	4,54778	-1,15609
H	0,64670	4,93862	-1,05194
H	-3,50088	3,83292	-1,33668
H	-1,75545	5,58868	-1,03424
C	1,11952	0,06988	-1,49803
C	1,81514	-0,51642	-2,56290
C	1,84073	0,40053	-0,33874
C	3,18500	-0,77267	-2,47022
H	1,29335	-0,77243	-3,47751
C	3,20462	0,13979	-0,24271
H	1,33459	0,86712	0,49788
C	3,88561	-0,45129	-1,30927
H	3,69969	-1,22502	-3,31311
H	3,73517	0,40174	0,66819
H	4,95017	-0,65401	-1,23576
C	-4,20234	-0,65551	-2,13942
O	-4,52947	-0,34485	-3,20087
C	-3,20168	-3,09665	-0,91586
O	-2,90105	-4,13856	-1,31034
C	-5,68373	-1,89527	-0,05735
O	-6,77473	-2,26997	0,04324
C	-3,44117	-1,87654	1,72974
O	-3,27769	-2,23901	2,81300
C	-4,35448	0,60504	0,50030
O	-4,70071	1,63052	0,89990

14a {[W(CO)$_5$]P(H)(OMe)NPh$_2$}

41

Energy = -1609.906469298669

ZPE = 0.27761135

P	0,71232	-0,18393	-0,18469
N	0,84904	1,31585	0,61639
C	0,05560	1,57961	1,77155
C	-1,23684	1,04921	1,87665
C	0,58213	2,33927	2,82521
C	-1,97802	1,24434	3,04271
H	-1,66696	0,50316	1,04337
C	-0,17497	2,54840	3,97436
H	1,58309	2,75096	2,74317
C	-1,45326	1,99407	4,09498
H	-2,97504	0,81969	3,11595
H	0,24372	3,13385	4,78799
H	-2,03494	2,15267	4,99802
C	1,73347	2,34415	0,14011
C	3,08872	2,07169	-0,06741
C	1,22975	3,62507	-0,11390
C	3,93118	3,07156	-0,55725
H	3,48431	1,08801	0,16743
C	2,08022	4,62357	-0,58373
H	0,17739	3,83003	0,05838
C	3,43155	4,34883	-0,81485
H	4,98252	2,85255	-0,71926
H	1,68364	5,61538	-0,78097
H	4,09036	5,12763	-1,18717
W	0,78042	-2,31325	1,11128
C	2,82893	-2,12793	1,08568
O	3,97867	-1,99904	1,06848
C	0,74794	-1,40503	2,96880
O	0,74826	-0,95850	4,03319
C	0,90472	-4,11876	2,03386
O	0,97883	-5,15735	2,54468
C	-1,28144	-2,37443	1,12659
O	-2,43658	-2,38982	1,13907
C	0,81673	-3,25863	-0,71591
O	0,83826	-3,79774	-1,73884
H	1,75976	0,05708	-1,09686
O	-0,58250	-0,13653	-1,17550
C	-0,69981	0,97109	-2,11123
H	0,23772	1,09705	-2,66271
H	-1,50890	0,70865	-2,79245
H	-0,94266	1,88831	-1,56866

14b {[W(CO)$_5$]P(H)(OMe)NCy$_2$}

53

Energy = -1617.148619951204

ZPE = 0.41574001

P	-1,58525	0,19700	-0,01760
H	-1,39616	1,19109	-1,00330
W	-4,00608	-0,24132	0,54823
C	-3,98737	1,44033	1,73297
O	-3,97911	2,40174	2,37762
C	-4,44823	0,93770	-1,07800
O	-4,68815	1,59655	-1,99827
C	-5,98577	-0,50790	0,89304
O	-7,12185	-0,65973	1,08122
C	-3,94999	-1,89092	-0,68815
O	-3,91922	-2,81028	-1,38719
C	-3,56432	-1,47934	2,13410
O	-3,35761	-2,20888	3,00810
N	-0,48643	0,80070	1,08842
O	-0,98031	-1,13529	-0,75384
C	0,30551	-1,07622	-1,41944
H	0,40921	-2,01475	-1,96492
H	1,10644	-0,97906	-0,68199
H	0,33194	-0,23055	-2,11513
C	0,20627	2,09407	0,82143
C	0,19442	3,05925	2,01377
C	1,62732	1,95322	0,24881
H	-0,39765	2,57171	0,03933
C	0,73991	4,43163	1,58929
H	-0,82562	3,15688	2,39935
H	0,82053	2,66292	2,82245
C	2,16838	3,32790	-0,17369
H	2,29508	1,51501	0,99755
H	1,60960	1,27594	-0,61081
C	2,15070	4,31510	0,99964
H	0,06738	4,86784	0,83717
H	0,73870	5,10841	2,45169
H	3,18477	3,21913	-0,57010
H	1,54657	3,72452	-0,98909
H	2,50848	5,29936	0,67462
H	2,84062	3,96257	1,77961
C	-0,26399	-0,04001	2,29793
C	1,21890	-0,33917	2,56085
C	-0,95456	0,46943	3,57446
H	-0,73278	-1,00445	2,05019
C	1,37192	-1,35086	3,70545
H	1,68733	-0,71886	1,64659
H	1,73557	0,58865	2,83532
C	-0,78922	-0,54168	4,71928
H	-0,52307	1,42699	3,87901
H	-2,01498	0,64160	3,36686
C	0,69002	-0,84719	4,98324
H	0,91938	-2,30638	3,40489
H	2,43625	-1,54190	3,88611
H	-1,26965	-0,15127	5,62406
H	-1,30603	-1,47455	4,45991
H	0,78710	-1,59060	5,78340
H	1,19607	0,06613	5,32727

15a {[Fe(CO)$_4$]P(H)(OMe)NPh$_2$}

39

Energy = -2693.133868542427

ZPE = 0.27146662

P	0,72432	-0,26261	-0,20216
N	0,89719	1,22825	0,61039
C	0,12474	1,48023	1,78686
C	-1,21183	1,07232	1,86064
C	0,72567	2,10194	2,88854
C	-1,93251	1,25892	3,04117
H	-1,68833	0,62413	0,99444
C	-0,00722	2,30354	4,05548
H	1,76331	2,41562	2,82647
C	-1,33586	1,87541	4,14086
H	-2,96677	0,93107	3,09164
H	0,46673	2,78283	4,90739
H	-1,90036	2,02656	5,05610
C	1,72941	2,28664	0,10802
C	3,06803	2,04779	-0,21939
C	1,19308	3,57140	-0,04518
C	3,85505	3,08310	-0,72725
H	3,49800	1,06365	-0,06258
C	1,99016	4,60410	-0,53365
H	0,15599	3,75242	0,22087
C	3,32166	4,36289	-0,88524
H	4,89330	2,88859	-0,98006
H	1,56635	5,59754	-0,64979
H	3,93910	5,16843	-1,27129
H	1,80281	-0,06385	-1,08701
O	-0,53623	-0,16164	-1,23117
C	-0,57476	0,95385	-2,16325
H	0,39043	1,05292	-2,67103
H	-1,35936	0,72044	-2,88276
H	-0,81281	1,87537	-1,62620
Fe	0,67130	-2,04143	1,06344
C	2,37513	-1,64149	1,45212
O	3,46893	-1,35761	1,69561
C	0,22153	-1,89079	2,78898
O	-0,06221	-1,80610	3,90879
C	-1,05582	-2,27380	0,62558
O	-2,16935	-2,41732	0,35935
C	1,13231	-3,60359	0,32881

O	1,42897	-4,62503	-0,13312

15b {[Fe(CO)$_4$]P(H)(OMe)NCy$_2$}

51

Energy = -2700.384594624000

ZPE = 0.40990428

P	0,52488	-0,14840	-0,31220
N	0,58853	1,38710	0,32620
H	1,43399	0,03782	-1,37376
O	-0,88787	-0,37758	-1,10572
C	-1,31103	0,55307	-2,13230
H	-0,55842	0,60822	-2,92516
H	-2,24660	0,15789	-2,52913
H	-1,47251	1,54291	-1,69812
Fe	0,83898	-1,88525	1,02252
C	2,58677	-1,62204	0,73001
O	3,71305	-1,44403	0,53323
C	1,10124	-1,81572	2,78570
O	1,27451	-1,78713	3,93389
C	-0,93497	-1,89058	1,29048
O	-2,07547	-1,90035	1,48174
C	0,82420	-3,45573	0,17727
O	0,81472	-4,48854	-0,35229
C	-0,09318	1,61553	1,62245
C	0,88721	1,88560	2,77082
C	-1,15800	2,71513	1,51849
H	-0,60923	0,67388	1,85143
C	0,13199	2,04072	4,09830
H	1,45056	2,80561	2,56656
H	1,60864	1,06348	2,82680
C	-1,90131	2,87917	2,85241
H	-0,67574	3,66533	1,25087
H	-1,85790	2,46531	0,71302
C	-0,92627	3,14772	4,00635
H	0,84142	2,25324	4,90638
H	-0,35932	1,08918	4,34564
H	-2,63357	3,69098	2,77167
H	-2,46467	1,95916	3,06360
H	-1,47427	3,22769	4,95267
H	-0,42618	4,11266	3,84059
C	1,48652	2,46540	-0,17439
C	2,97252	2,08863	-0,07441
C	1,13459	2,94376	-1,58691
H	1,31177	3,30787	0,50466
C	3,86542	3,26664	-0,48766
H	3,17326	1,23577	-0,73624
H	3,19937	1,76725	0,94744
C	2,03247	4,11941	-2,00104
H	1,27049	2,11780	-2,29760
H	0,08021	3,23791	-1,62056
C	3,51844	3,75230	-1,90060
H	4,91943	2,97113	-0,43010
H	3,72428	4,09245	0,22424
H	1,78192	4,43290	-3,02115
H	1,82691	4,97561	-1,34286
H	4,14004	4,61448	-2,16966
H	3,74348	2,95421	-2,62223

16a {[Cr(CO)$_5$]P(H)(OMe)NPh$_2$}

41

Energy = -2587.305832311631

ZPE = 0.28015132

P	0,71535	-0,24052	-0,12860
N	0,84791	1,26954	0,65526
C	0,03969	1,55982	1,79359
C	-1,25748	1,04078	1,89051
C	0,55701	2,33606	2,83993
C	-2,01271	1,26176	3,04300
H	-1,68044	0,48214	1,06221
C	-0,21369	2,57126	3,97469
H	1,56174	2,73956	2,76367
C	-1,49719	2,02718	4,08851
H	-3,01380	0,84575	3,11006
H	0,19768	3,16978	4,78255
H	-2,08994	2,20653	4,98040
C	1,73883	2,28762	0,16856
C	3,09580	2,01062	-0,02080
C	1,23878	3,56406	-0,11443
C	3,94380	3,00075	-0,52090
H	3,48896	1,03165	0,23604
C	2,09462	4,55318	-0,59408
H	0,18496	3,77305	0,04344
C	3,44798	4,27339	-0,80685
H	4,99640	2,77783	-0,66873
H	1,70075	5,54142	-0,81349
H	4,11105	5,04473	-1,18705
C	2,68882	-2,04797	1,01086
O	3,83861	-1,92492	0,98279
C	0,80152	-1,41335	2,78090
O	0,82556	-0,98870	3,85343
C	0,94529	-3,90803	1,88343
O	1,03442	-4,95055	2,38028
C	-1,09181	-2,30454	1,11016
O	-2,24464	-2,35511	1,15091
C	0,81271	-3,07906	-0,63190
O	0,81904	-3,61227	-1,65757
H	1,75517	0,00180	-1,04890
O	-0,58597	-0,20316	-1,11219
C	-0,72127	0,90892	-2,03983
H	0,21212	1,05131	-2,59422

H	-1,52942	0,63990	-2,71965
H	-0,97441	1,81917	-1,49028
Cr	0,80548	-2,23031	1,06109

16b {[Cr(CO)$_5$]P(H)(OMe)NCy$_2$}

53

Energy = -2594.552717603003

ZPE = 0.41813059

P	0,82148	-0,04661	-0,00435
N	0,84298	1,47158	0,68650
H	1,93117	0,12289	-0,86095
O	-0,38983	-0,16832	-1,10898
C	-0,46495	0,82424	-2,16086
H	0,48932	0,87935	-2,69687
H	-1,25615	0,49897	-2,83698
H	-0,71327	1,80224	-1,73806
Cr	0,80113	-2,01175	1,28082
C	2,63035	-2,19902	0,83593
O	3,74808	-2,30249	0,55634
C	1,32685	-1,12810	2,87243
O	1,67824	-0,63621	3,85847
C	-1,03571	-1,71532	1,65273
O	-2,15752	-1,54403	1,87470
C	0,33480	-2,92897	-0,31226
O	0,06203	-3,51528	-1,26979
C	0,79070	-3,63650	2,20584
O	0,78122	-4,64725	2,77465
C	-0,08072	1,70211	1,82802
C	0,52519	2,50060	2,98805
C	-1,44914	2,27188	1,41099
H	-0,27804	0,69419	2,21755
C	-0,44485	2,51065	4,17967
H	0,71947	3,53340	2,67623
H	1,48149	2,05828	3,28188
C	-2,40885	2,28365	2,60967
H	-1,33102	3,29169	1,03046
H	-1,85883	1,66181	0,59810
C	-1,81596	3,07258	3,78378
H	-0,01166	3,09595	4,99899
H	-0,56798	1,48314	4,54981
H	-3,37327	2,70866	2,30795
H	-2,60006	1,24986	2,92948
H	-2,49765	3,04558	4,64218
H	-1,70478	4,12691	3,49284
C	1,67381	2,54667	0,06699
C	0,93806	3,86946	-0,18564
C	2,99137	2,77928	0,82535
H	1,94926	2,15606	-0,92081
C	1,84861	4,83731	-0,95829
H	0,65032	4,33103	0,76562
H	0,01892	3,68517	-0,75156
C	3,89261	3,74949	0,04811
H	2,78346	3,19176	1,81800
H	3,49313	1,81538	0,97015
C	3,17105	5,07643	-0,21916
H	1,32118	5,78482	-1,11839
H	2,06027	4,41570	-1,95117
H	4,82063	3,92132	0,60568
H	4,17408	3,29191	-0,91113
H	3,81293	5,74833	-0,80124
H	2,96515	5,57602	0,73813

14-CPh$_3$ {[W(CO)$_5$]P(H)(OMe)CPh$_3$}

52

Energy = -1825.032320521941

ZPE = 0.36862064

P	-1,20587	-0,51177	-0,14735
C	-0,34489	0,33937	-1,63067
W	-3,61521	-1,28558	-0,09699
C	-0,96098	-0,26997	-2,89419
C	-1,40091	0,50696	-3,96879
C	-1,01271	-1,66688	-3,00976
C	-1,89690	-0,09895	-5,12547
H	-1,35358	1,58885	-3,90895
C	-1,52318	-2,27433	-4,15402
H	-0,62410	-2,28830	-2,20623
C	-1,96960	-1,48832	-5,21901
H	-2,23219	0,52133	-5,95180
H	-1,56665	-3,35771	-4,21533
H	-2,36649	-1,95691	-6,11487
C	-0,64698	1,83521	-1,48461
C	0,36690	2,78613	-1,33969
C	-1,97994	2,27228	-1,47444
C	0,05585	4,14028	-1,18776
H	1,40568	2,47449	-1,34465
C	-2,29394	3,61876	-1,31464
H	-2,77902	1,54823	-1,59768
C	-1,27307	4,56211	-1,16993
H	0,85950	4,86352	-1,08055
H	-3,33451	3,93023	-1,30368
H	-1,51327	5,61426	-1,04681
C	1,16844	0,04881	-1,61283
C	1,85564	-0,10045	-2,82555
C	1,90651	-0,01611	-0,42223
C	3,23427	-0,31693	-2,84888
H	1,31156	-0,04753	-3,76255
C	3,28324	-0,24074	-0,44368
H	1,40918	0,12614	0,53040
C	3,95527	-0,39352	-1,65721
H	3,74102	-0,42872	-3,80341

H	3,82963	-0,29216	0,49399
H	5,02722	-0,56838	-1,67350
C	-4,12468	-0,65529	-1,99940
O	-4,50629	-0,34152	-3,04263
C	-3,02340	-3,09964	-0,87051
O	-2,70361	-4,13024	-1,28524
C	-5,51520	-1,96256	0,08705
O	-6,60150	-2,35123	0,20910
C	-3,26825	-2,04858	1,77939
O	-3,12231	-2,52712	2,82323
C	-4,17001	0,54467	0,67444
O	-4,49224	1,56685	1,10765
H	-0,30345	-1,58601	0,05014
O	-0,74231	0,54030	1,01976
C	-1,04697	0,26593	2,40701
H	-0,59927	1,08336	2,97251
H	-2,12900	0,25381	2,56229
H	-0,61043	-0,68904	2,71571

17a {[W(CO)$_5$]P(H)(NHMe)NPh$_2$}

42

Energy = -1590.021438131876

ZPE = 0.29004581

P	0,70935	0,35327	-0,55212
N	1,13210	1,25782	0,85933
C	0,33469	1,21970	2,03361
C	0,93433	1,40441	3,28927
C	-1,03996	0,96198	1,96517
C	0,17055	1,30904	4,44842
H	1,99891	1,60805	3,34873
C	-1,79451	0,84181	3,13293
H	-1,52641	0,87171	1,00017
C	-1,19552	1,01523	4,38014
H	0,64951	1,44914	5,41350
H	-2,85724	0,62992	3,05893
H	-1,78491	0,93308	5,28838
C	2,18407	2,23280	0,79026
C	1,89962	3,58406	1,02283
C	3,49070	1,83840	0,48357
C	2,91831	4,53228	0,94591
H	0,88364	3,88078	1,26612
C	4,50290	2,79500	0,39095
H	3,71296	0,78601	0,33272
C	4,22166	4,14261	0,62384
H	2,69114	5,57900	1,12741
H	5,51524	2,48160	0,15272
H	5,01258	4,88399	0,56001
W	0,15777	-2,09748	-0,20913
C	2,11657	-2,41006	-0,75822
O	3,21902	-2,58887	-1,05880
C	0,74265	-2,02443	1,76906
O	1,07665	-2,02140	2,87436
C	-0,10325	-4,09806	-0,07083
O	-0,24208	-5,24911	-0,00532
C	-1,79566	-1,83091	0,38887
O	-2,89462	-1,72546	0,73483
C	-0,42665	-2,13332	-2,18230
O	-0,75695	-2,15176	-3,29051
H	1,92950	0,58579	-1,20141
N	-0,26129	1,19403	-1,63088
H	0,11649	2,07648	-1,96772
C	-1,72572	1,13977	-1,63492
H	-2,04120	0,14115	-1,32430
H	-2,17869	1,88005	-0,96383
H	-2,08914	1,31243	-2,65137

17b {[W(CO)$_5$]P(H)(NHMe)NCy$_2$}

54

Energy = -1597.267685219134

ZPE = 0.42797539

P	1,01774	0,33392	-0,31939
N	1,15970	1,38423	0,98669
W	0,13085	-2,02441	0,07985
C	1,97055	-2,64156	-0,60471
O	3,00481	-2,98041	-0,99616
C	0,88199	-2,05786	1,99677
O	1,32063	-2,11434	3,06618
C	-0,45957	-3,94604	0,29057
O	-0,79440	-5,05276	0,40772
C	-1,71530	-1,37715	0,72221
O	-2,76835	-1,03931	1,06446
C	-0,55109	-2,03049	-1,86376
O	-0,92244	-2,05820	-2,95827
H	2,34987	0,34773	-0,77331
N	0,37526	1,04747	-1,71901
H	0,94912	1,79236	-2,10951
C	-1,06092	1,33736	-1,81429
H	-1,61815	0,49992	-1,38536
H	-1,34697	2,25236	-1,27971
H	-1,34308	1,43639	-2,86595
C	0,24372	1,26024	2,14290
C	0,94137	1,41998	3,50020
C	-1,01980	2,13670	2,05955
H	-0,10667	0,22102	2,09259
C	-0,03117	1,09866	4,64486
H	1,30200	2,44903	3,61861
H	1,81278	0,75882	3,54266
C	-1,98004	1,81144	3,21336
H	-0,75044	3,19655	2,10382
H	-1,51126	1,96577	1,09472

C	-1,28792	1,97416	4,57199
H	0,47695	1,23360	5,60691
H	-0,32373	0,04114	4,58251
H	-2,86444	2,45656	3,15116
H	-2,33217	0,77607	3,11265
H	-1,97839	1,71486	5,38343
H	-1,00485	3,02718	4,71280
C	2,11056	2,51587	0,80304
C	1,53524	3,91004	1,08569
C	3,43854	2,29630	1,54813
H	2,35529	2,50994	-0,26899
C	2,56221	4,99081	0,71197
H	1,28439	4,00578	2,14853
H	0,61163	4,05092	0,51424
C	4,45490	3,38221	1,16740
H	3,26622	2,32137	2,62901
H	3,82384	1,29976	1,30204
C	3,89294	4,78224	1,44585
H	2,15031	5,98128	0,93837
H	2,73933	4,95752	-0,37255
H	5,39015	3,22656	1,71789
H	4,69362	3,29547	0,09759
H	4,61529	5,54982	1,14343
H	3,73226	4,89894	2,52710

18a {[Fe(CO)$_4$]P(H)(NHMe)NPh$_2$}

40

Energy = -2673.244932153115

ZPE = 0.28381190

P	0,72575	0,30252	-0,57883
N	1,11859	1,23778	0,82005
C	0,31781	1,18678	1,99548
C	0,93919	1,15955	3,25265
C	-1,07703	1,13245	1,91780
C	0,16988	1,06068	4,40821
H	2,02244	1,20550	3,31296
C	-1,84274	1,00778	3,07843
H	-1,56530	1,20711	0,95185
C	-1,22430	0,97310	4,32770
H	0,66176	1,03425	5,37655
H	-2,92485	0,95448	3,00036
H	-1,81991	0,88567	5,23150
C	2,16413	2,21917	0,77456
C	1,87651	3,55396	1,08920
C	3,47022	1,85544	0,42552
C	2,88651	4,51366	1,04974
H	0,86324	3,82838	1,36736
C	4,47262	2,82486	0,36955
H	3,70347	0,81574	0,21674
C	4,18671	4,15521	0,68273
H	2,65432	5,54594	1,29635
H	5,48338	2,53280	0,09922
H	4,97119	4,90535	0,64816
H	1,96870	0,50374	-1,19320
N	-0,19300	1,13775	-1,70538
H	0,19686	2,02822	-2,00515
C	-1,64632	1,04776	-1,85945
H	-1,94300	-0,00260	-1,84964
H	-2,20230	1,58574	-1,08036
H	-1,91577	1,46800	-2,83127
Fe	0,17917	-1,79666	-0,12585
C	-1,55752	-1,47025	0,19878
O	-2,68263	-1,33763	0,42938
C	-0,27622	-2,83174	-1,50645
O	-0,57183	-3,52716	-2,38718
C	1,91429	-2,15278	-0,40575
O	3,03558	-2,37328	-0,57992
C	0,34962	-2,29869	1,57936
O	0,45718	-2,64618	2,68007

18b {[Fe(CO)$_4$]P(H)(NHMe)NCy$_2$}

52

Energy = -2680.497902054320

ZPE = 0.42168623

P	0,71691	0,28880	-0,59710
N	1,10750	1,27915	0,69871
H	1,94494	0,34947	-1,27329
N	-0,19567	1,00218	-1,83398
H	0,22591	1,84668	-2,21433
C	-1,66077	1,07531	-1,80770
H	-2,06849	0,06573	-1,71961
H	-2,05393	1,69110	-0,98747
H	-2,00113	1,49862	-2,75567
Fe	0,00284	-1,76102	-0,05837
C	-1,56378	-1,11349	0,52601
O	-2,58158	-0,73539	0,92974
C	-0,81029	-2,69779	-1,33766
O	-1,34049	-3,33025	-2,15476
C	1,62215	-2,27351	-0,62948
O	2,67184	-2,59611	-0,99399
C	0,33453	-2,42766	1,56011
O	0,54241	-2,87947	2,60989
C	0,35891	1,21711	1,96935
C	1,28032	1,00996	3,17945
C	-0,56856	2,42479	2,16792
H	-0,26604	0,32190	1,89455
C	0,45593	0,86966	4,46737
H	1,96240	1,86464	3,28132
H	1,89401	0,11776	3,01211
C	-1,37842	2,28828	3,46533

H	0,03222	3,34409	2,20819
H	-1,23699	2,51236	1,30312
C	-0,45895	2,08323	4,67614
H	1,12691	0,74233	5,32490
H	-0,15869	-0,03946	4,40414
H	-2,00822	3,17454	3,60648
H	-2,05418	1,42587	3,37664
H	-1,05588	1,95581	5,58706
H	0,15892	2,98148	4,81833
C	2,14093	2,34263	0,58272
C	3,56590	1,76882	0,60305
C	1,94769	3,26917	-0,62619
H	2,01921	2,96194	1,47938
C	4,60789	2,89687	0,61197
H	3,71480	1,14009	-0,28535
H	3,68369	1,12419	1,48015
C	2,98197	4,40419	-0,60342
H	2,08285	2,69434	-1,55363
H	0,92771	3,67024	-0,62565
C	4,41159	3,84781	-0,57592
H	5,61799	2,47103	0,59926
H	4,51177	3,46508	1,54832
H	2,83942	5,05331	-1,47518
H	2,81481	5,02330	0,28934
H	5,13641	4,66914	-0,52800
H	4,60347	3,30264	-1,51102

19a {[Cr(CO)$_5$]P(H)(NHMe)NPh$_2$}

42

Energy = -2567.419517511640

ZPE = 0.29210054

P	0,90428	-0,15831	-0,24279
N	1,00746	1,29097	0,69952
C	0,05801	1,59731	1,70826
C	-1,24674	1,09351	1,64773
C	0,43521	2,38698	2,80650
C	-2,14627	1,33476	2,68704
H	-1,56910	0,52687	0,78141
C	-0,47502	2,64508	3,82654
H	1,44438	2,78315	2,85894
C	-1,76800	2,11234	3,78090
H	-3,15041	0,92521	2,62542
H	-0,16681	3,25399	4,67194
H	-2,47142	2,30955	4,58420
C	1,94105	2,31354	0,31948
C	3,31457	2,04866	0,32242
C	1,47501	3,57730	-0,06396
C	4,21538	3,03793	-0,07549
H	3,67339	1,07691	0,64878
C	2,38066	4,56641	-0,44344
H	0,40739	3,77619	-0,05805
C	3,75281	4,29885	-0,45661
H	5,28050	2,82522	-0,07084
H	2,01298	5,54455	-0,74047
H	4,45591	5,06981	-0,75765
Cr	0,75365	-2,20535	0,93455
C	2,62084	-2,32000	0,64586
O	3,76294	-2,39595	0,48139
C	1,08876	-1,32983	2,58745
O	1,31321	-0,84187	3,60896
C	0,80721	-3,86849	1,77815
O	0,84551	-4,90582	2,29532
C	-1,10855	-2,12742	1,29204
O	-2,23571	-2,14692	1,54983
C	0,42744	-3,04065	-0,73548
O	0,23248	-3,56743	-1,74570
H	2,13911	0,04871	-0,87266
N	-0,05079	0,00262	-1,61230
H	0,22303	0,74705	-2,24942
C	-1,47169	-0,34433	-1,69026
H	-1,66617	-1,19561	-1,03521
H	-2,12672	0,48557	-1,39722
H	-1,71265	-0,64059	-2,71467

19b {[Cr(CO)$_5$]P(H)(NHMe)NCy$_2$}

54

Energy = -2574.665652311816

ZPE = 0.43023311

P	0,99820	0,27250	-0,29569
N	1,13676	1,33275	1,00497
C	1,84786	-2,50588	-0,59557
O	2,86909	-2,85797	-1,00897
C	0,90972	-1,95961	1,81663
O	1,38042	-2,03579	2,87055
C	-0,38047	-3,69879	0,28920
O	-0,72469	-4,79910	0,42436
C	-1,51521	-1,32044	0,68032
O	-2,56874	-0,99358	1,03054
C	-0,48294	-1,95442	-1,70887
O	-0,87559	-2,01452	-2,79419
H	2,33390	0,28377	-0,73860
N	0,37370	0,99756	-1,69859
H	0,96673	1,73213	-2,08030
C	-1,05372	1,32755	-1,79481
H	-1,63809	0,49769	-1,38919
H	-1,31841	2,23834	-1,24221
H	-1,32573	1,45754	-2,84569
C	0,22065	1,23548	2,16298
C	0,92187	1,40946	3,51692
C	-1,03449	2,12363	2,07127

H	-0,14000	0,20058	2,13198
C	-0,05082	1,10590	4,66612
H	1,28625	2,43864	3,62183
H	1,79027	0,74498	3,56626
C	-1,99673	1,81763	3,22872
H	-0,75474	3,18100	2,10704
H	-1,52851	1,94998	1,10847
C	-1,30254	1,98812	4,58545
H	0,45896	1,24812	5,62626
H	-0,34908	0,04920	4,61471
H	-2,87550	2,46987	3,16080
H	-2,35753	0,78433	3,13776
H	-1,99410	1,74090	5,39974
H	-1,01255	3,04055	4,71624
C	2,09215	2,45910	0,80424
C	1,52268	3,86004	1,06483
C	3,42003	2,24623	1,55127
H	2,33598	2,43689	-0,26765
C	2,55346	4,92995	0,67072
H	1,27523	3,97510	2,12650
H	0,59855	3,99533	0,49295
C	4,44031	3,32162	1,15104
H	3,24992	2,29040	2,63188
H	3,80100	1,24420	1,32129
C	3,88433	4,72843	1,40619
H	2,14596	5,92577	0,88106
H	2,72859	4,87754	-0,41337
H	5,37538	3,17169	1,70342
H	4,67782	3,21566	0,08272
H	4,60944	5,48779	1,08996
H	3,72528	4,86423	2,48545
Cr	0,17261	-1,93233	0,06960

17-CPh$_3$ {[W(CO)$_5$]P(H)(NHMe)CPh$_3$}

53

Energy = -1805.150377597356

ZPE = 0.38085598

P	-1,32397	-0,54371	-0,20585
C	-0,42265	0,40858	-1,64223
W	-3,78830	-1,22050	-0,23135
C	-0,96376	-0,18085	-2,94560
C	-1,34026	0,63620	-4,01845
C	-1,10053	-1,57093	-3,09326
C	-1,83578	0,08334	-5,19993
H	-1,25197	1,71364	-3,93125
C	-1,60845	-2,12570	-4,26690
H	-0,78861	-2,23601	-2,29343
C	-1,97938	-1,29838	-5,32757
H	-2,12006	0,73911	-6,01808
H	-1,71194	-3,20364	-4,34896
H	-2,37668	-1,72683	-6,24318
C	-0,74447	1,90239	-1,54381
C	0,19915	2,86578	-1,92629
C	-2,01722	2,34332	-1,16580
C	-0,11742	4,22492	-1,90878
H	1,18752	2,55348	-2,24681
C	-2,33742	3,70008	-1,13563
H	-2,77761	1,61414	-0,90635
C	-1,38430	4,65013	-1,50498
H	0,63033	4,95166	-2,21407
H	-3,33220	4,01016	-0,82837
H	-1,62747	5,70856	-1,48441
C	1,07101	0,14055	-1,43157
C	1,80444	-0,73119	-2,24673
C	1,73906	0,76990	-0,36665
C	3,15574	-0,98124	-1,99611
H	1,32772	-1,21308	-3,09290
C	3,08510	0,51732	-0,11283
H	1,19513	1,46562	0,26227
C	3,80188	-0,36464	-0,92504
H	3,70228	-1,65699	-2,64824
H	3,57515	1,01501	0,71951
H	4,85275	-0,55956	-0,73088
C	-4,23472	-0,39225	-2,07158
O	-4,54755	0,05954	-3,08691
C	-3,28149	-3,00248	-1,13353
O	-3,02467	-4,02384	-1,61035
C	-5,69065	-1,87717	-0,07793
O	-6,78202	-2,26341	0,02135
C	-3,34814	-2,04710	1,59799
O	-3,10196	-2,51030	2,62937
C	-4,34139	0,51700	0,72009
O	-4,68304	1,47482	1,27460
H	-0,47587	-1,66762	-0,19667
C	0,14105	-0,40613	2,16129
H	0,69023	0,39522	2,66478
H	-0,33728	-1,04324	2,91484
H	0,85433	-1,00377	1,59199
N	-0,84562	0,17045	1,23674
H	-1,57711	0,70145	1,69611

Table 7.2. The TPSS-D3/def2-TZVP/CPCM(THF) optimized Cartesian coordinates (in Å). Each structure is labelled by its specific name, followed by its number of atoms, its single-point-energy (in hartrees), and the atomic coordinates.

5^--Me {[W(CO)$_5$]PClMe}
17
Energy = -1476.018777763869
ZPE = 0.07815443

P	-1,79666	2,16612	0,76099
Cl	-1,17858	1,20235	-1,09352
C	1,10637	0,59497	4,00623
O	1,87103	0,21490	4,80663
C	1,29951	1,73946	1,25002
O	2,08574	2,03696	0,45100
C	-0,08091	3,17355	3,35966
O	-0,04433	4,25624	3,78085
C	-1,81227	0,90575	3,77886
O	-2,76145	0,71453	4,42166
C	-0,37792	-0,60038	1,77306
O	-0,51178	-1,65158	1,30135
W	-0,16935	1,26888	2,60766
C	-1,19613	3,86991	0,30698
H	-1,74055	4,23750	-0,56889
H	-1,42747	4,52089	1,15917
H	-0,12047	3,91475	0,11299

5^--*t*-bu {[W(CO)$_5$]PCl-*t*-bu}
26
Energy = -1594.031168028574
ZPE = 0.16107715

P	-1,27391	0,34190	0,93563
Cl	-1,32941	1,51235	-0,89862
C	1,19349	-3,39243	-0,24084
O	1,75151	-4,35914	-0,59344
C	1,34860	-0,47584	-0,85888
O	1,97137	0,25198	-1,51148
C	1,65889	-1,51415	1,80600
O	2,49657	-1,44901	2,61053
C	-0,95498	-2,72124	1,67709
O	-1,63927	-3,24661	2,45518
C	-1,13652	-1,99763	-1,16500
O	-1,90055	-2,17364	-2,01940
W	0,24069	-1,72568	0,34129
C	-0,38188	1,59269	2,04788
C	-0,33018	0,89528	3,42012
H	0,27293	-0,01638	3,38672
H	0,11591	1,57352	4,15911
H	-1,33652	0,62987	3,76574
C	-1,25576	2,85428	2,16376
H	-0,81033	3,54714	2,89095
H	-1,33177	3,36974	1,20142
H	-2,26709	2,60150	2,50122
C	1,02412	1,97799	1,58132
H	1,68390	1,10682	1,55734
H	0,99329	2,41227	0,57682
H	1,45829	2,72204	2,26423

5^--Ph {[W(CO)$_5$]PClPh}
24
Energy = -1667.877312903094
ZPE = 0.13058414

P	-1,45389	0,41383	0,96227
Cl	-1,60435	1,46611	-0,91817
C	1,23132	-3,24337	0,04018
O	1,91630	-4,15459	-0,22376
C	1,31187	-0,30330	-0,46086
O	1,98570	0,49472	-0,96250
C	1,10913	-1,36539	2,22162
O	1,69967	-1,21366	3,20853
C	-1,28998	-2,80422	1,48386
O	-2,08182	-3,42837	2,06087
C	-1,00139	-1,92133	-1,26114
O	-1,61267	-2,07722	-2,23414
W	0,07751	-1,66025	0,47117
C	-0,38882	1,58715	1,88907
C	-0,36385	1,40571	3,28648
C	0,37141	2,63258	1,34230
C	0,41319	2,22370	4,10248
H	-0,95684	0,60993	3,73457
C	1,14036	3,45937	2,16410
H	0,36309	2,79614	0,26939
C	1,17066	3,25947	3,54565
H	0,42056	2,05854	5,17700
H	1,72239	4,26248	1,71813
H	1,77035	3,90448	4,18190

5^--Anth {[W(CO)$_5$]PClAnth}
36
Energy = -1975.344916160436
ZPE = 0.22235319

P	-1,31622	-0,05057	1,46675
Cl	-2,15930	1,14317	-0,16618

C	1,42293	-3,12222	-0,63617
O	2,11241	-3,88494	-1,19333
C	1,15391	-0,14991	-0,59408
O	1,60840	0,79026	-1,09692
C	1,58374	-1,80058	1,88076
O	2,32508	-1,87781	2,77175
C	-0,80854	-3,22473	1,27773
O	-1,43730	-4,02536	1,83587
C	-1,10098	-1,87313	-1,22997
O	-1,86820	-1,97012	-2,09299
W	0,26708	-1,77594	0,30466
C	-0,42134	1,33294	2,29493
C	-1,18373	2,34174	3,00811
C	0,95651	1,39655	2,35300
C	-2,58268	2,35530	3,02919
C	-0,47925	3,38233	3,72924
C	1,64495	2,40047	3,08618
H	1,54114	0,66309	1,81136
C	-3,31019	3,34434	3,70570
H	-3,12320	1,57064	2,50723
C	-1,20405	4,37344	4,40453
C	0,94759	3,37549	3,74956
H	2,73158	2,39446	3,09769
C	-4,73748	3,35311	3,72075
C	-2,60386	4,38833	4,40994
H	-0,66094	5,14945	4,94071
H	1,46419	4,15884	4,29896
C	-5,42831	4,33441	4,38758
H	-5,26608	2,56525	3,18967
C	-3,35809	5,39103	5,09086
C	-4,73052	5,36543	5,08017
H	-6,51478	4,33108	4,39080
H	-2,82232	6,17659	5,61858
H	-5,29485	6,13370	5,60158

5⁻-NH₂ {[W(CO)₅]PClNH₂}

16

Energy = -1492.086131680954

ZPE = 0.06757114

P	-1,80005	2,17775	0,74041
Cl	-1,16156	1,02070	-1,12478
C	1,10085	0,61876	3,98525
O	1,86309	0,25158	4,79293
C	1,30094	1,72964	1,21953
O	2,09544	2,01397	0,42357
C	-0,09861	3,18785	3,31899
O	-0,06891	4,27077	3,73746
C	-1,81797	0,91556	3,74882
O	-2,76673	0,72503	4,39185
C	-0,37487	-0,60340	1,76580
O	-0,49964	-1,66497	1,31644
N	-1,26238	3,74898	0,41827
H	-0,27561	3,98881	0,45169
H	-1,75120	4,27048	-0,30415
W	-0,17479	1,27740	2,57631

5⁻-NMe₂ {[W(CO)₅]PClNMe₂}

22

Energy = -1570.745391823646

ZPE = 0.12286741

P	-0,22932	-0,00794	-0,08452
N	0,01343	1,07996	1,18576
C	-0,59427	2,40776	1,29382
H	0,04412	3,05384	1,90830
H	-0,70085	2,84596	0,30348
H	-1,58651	2,34700	1,76473
C	0,26651	0,49610	2,51136
H	-0,66879	0,37640	3,07846
H	0,73678	-0,48196	2,39135
H	0,93488	1,15518	3,07906
W	-0,31165	1,20732	-2,39381
C	0,92234	2,67219	-1,65775
O	1,64842	3,47855	-1,24312
C	-2,01816	2,19400	-1,79743
O	-2,98915	2,72832	-1,45834
C	-0,33796	2,06315	-4,21315
O	-0,36456	2,57690	-5,26347
C	1,35790	0,11429	-2,86598
O	2,29929	-0,51539	-3,12351
C	-1,47215	-0,36413	-3,03900
O	-2,10826	-1,25906	-3,41124
Cl	-2,43212	-0,63054	0,24872

5⁻-NPh₂ {[W(CO)₅]PClNPh₂}

36

Energy = -1954.468902360317

ZPE = 0.22589108

P	-1,25353	-0,72122	2,12654
Cl	-3,48332	-0,64468	1,73944
C	0,77432	-1,69927	-1,88383
O	1,29991	-2,04564	-2,86891
C	0,89934	0,66668	-0,32372
O	1,54136	1,62095	-0,46258
C	1,39033	-1,85166	0,96513
O	2,24697	-2,25748	1,63548
C	-1,12682	-2,90781	-0,10459
O	-1,67442	-3,93019	-0,07437
C	-1,71870	-0,28338	-1,21253
O	-2,60952	0,18724	-1,78435

W	-0,13486	-1,11112	-0,19063
N	-0,95187	0,86055	2,75033
C	-0,83268	2,05588	1,97973
C	-1,64256	2,27676	0,86125
C	0,12291	3,01686	2,34023
C	-1,48095	3,43271	0,09742
H	-2,40175	1,54538	0,61120
C	0,27314	4,17313	1,57889
H	0,74976	2,84557	3,21049
C	-0,52370	4,38563	0,44956
H	-2,11355	3,58918	-0,77223
H	1,02607	4,90454	1,86040
H	-0,39936	5,28515	-0,14659
C	-1,05316	1,02802	4,16978
C	-1,82072	2,06990	4,70940
C	-0,39747	0,14002	5,03284
C	-1,93301	2,21445	6,09185
H	-2,32900	2,75916	4,04224
C	-0,52200	0,28427	6,41432
H	0,20755	-0,65624	4,61055
C	-1,28874	1,32157	6,95217
H	-2,53679	3,02235	6,49658
H	-0,00499	-0,40930	7,07197
H	-1,37907	1,43534	8,02865

5^--NCy$_2$ {[W(CO)$_5$]PClNCy$_2$}

48

Energy = -1961.711687519924

ZPE = 0.36419006

P	-1,27201	0,54656	1,10621
Cl	-1,84742	1,57150	-0,93349
C	1,18708	-3,09939	-0,31485
O	1,77633	-4,03817	-0,68923
C	1,15980	-0,22317	-1,01451
O	1,67541	0,47925	-1,77840
C	1,59639	-1,19814	1,78906
O	2,37648	-1,09760	2,64452
C	-0,90326	-2,55034	1,66220
O	-1,54131	-3,14322	2,43095
C	-1,27659	-1,79039	-1,08775
O	-2,10733	-2,01024	-1,86580
N	-0,41143	1,75105	1,90937
W	0,19642	-1,46799	0,31327
C	-1,27061	2,64024	2,74796
C	-1,11849	2,36246	4,25419
C	-1,17588	4,14223	2,44721
H	-2,29243	2,33582	2,48525
C	-2,18303	3,13270	5,04881
H	-0,12351	2,66137	4,59989
H	-1,21425	1,28332	4,42206
C	-2,23900	4,90643	3,25269
H	-0,18364	4,52529	2,71467
H	-1,31910	4,31116	1,37509
C	-2,10673	4,63700	4,75700
H	-2,05879	2,94288	6,12197
H	-3,17985	2,76225	4,76971
H	-2,15545	5,98055	3,04717
H	-3,23718	4,59166	2,91667
H	-2,88911	5,17284	5,30856
H	-1,14029	5,02515	5,11007
C	1,00996	2,07418	1,63721
C	1,22085	3,13631	0,54009
C	1,83400	2,40539	2,88884
H	1,41333	1,14092	1,23155
C	2,71196	3,24550	0,18899
H	0,86408	4,11331	0,88079
H	0,63022	2,85665	-0,33726
C	3,32251	2,52654	2,52756
H	1,49675	3,35282	3,32682
H	1,68951	1,62338	3,64150
C	3,54989	3,57428	1,43080
H	2,85625	4,00887	-0,58544
H	3,05680	2,29250	-0,23407
H	3,90029	2,77806	3,42541
H	3,68618	1,55153	2,17491
H	4,61461	3,62591	1,17114
H	3,26230	4,56528	1,81124

5^--N(SiH$_3$)$_2$ {[W(CO)$_5$]PClN(SiH$_3$)$_2$}

22

Energy = -2073.597721301266

ZPE = 0.09831039

P	-1,37389	-0,16689	1,81777
Cl	-2,76341	0,94922	0,52158
C	1,35410	-2,65076	-0,94730
O	2,04585	-3,30182	-1,62716
C	0,60492	0,13414	-0,95344
O	0,83964	1,02129	-1,66167
C	1,71491	-1,13703	1,52696
O	2,56301	-0,96387	2,29932
C	-0,31818	-3,15064	1,34270
O	-0,59975	-4,08601	1,96867
C	-1,48203	-1,85620	-0,94793
O	-2,42475	-2,06273	-1,58966
N	-0,53896	1,16274	2,58109
W	0,17663	-1,50628	0,21626
Si	-1,18676	1,33531	4,19396
H	-0,48583	2,46731	4,85874
H	-2,64483	1,61646	4,17478
H	-0,95396	0,10828	4,99573

Si	0,51849	2,28065	1,76093
H	1,79666	1,64793	1,35958
H	-0,13280	2,82575	0,54710
H	0,81182	3,39796	2,69401

22-Me {[W(CO)$_5$]PMe}

16

Energy = -1015.569266519900

ZPE = 0.07595242

P	-1,76061	2,21800	0,94693
C	1,13291	0,51583	3,94466
O	1,89433	0,09080	4,69860
C	1,33744	1,79558	1,27459
O	2,17572	2,09174	0,54110
C	0,00230	3,22914	3,35215
O	0,10377	4,30515	3,75331
C	-1,80173	0,89086	3,82244
O	-2,69652	0,64123	4,50433
C	-0,49512	-0,54692	1,73352
O	-0,67735	-1,58758	1,27193
W	-0,20682	1,32561	2,56974
C	-1,21896	3,86886	0,32818
H	-1,42573	3,94473	-0,74551
H	-1,89107	4,58969	0,82221
H	-0,18545	4,14720	0,54355

22-*t*-bu {[W(CO)$_5$]P-*t*-bu}

25

Energy = -1133.580826442887

ZPE = 0.15938940

P	-1,17588	0,10721	1,26289
C	1,18580	-3,31266	-0,44069
O	1,73954	-4,21356	-0,90103
C	1,38848	-0,41253	-0,74871
O	2,06206	0,26954	-1,38799
C	1,62867	-1,54528	1,88377
O	2,43299	-1,49038	2,70937
C	-0,94799	-2,97169	1,53019
O	-1,59492	-3,69166	2,15493
C	-1,22373	-1,83064	-1,10062
O	-2,02608	-1,92916	-1,92240
W	0,20538	-1,67850	0,38994
C	-0,31650	1,55549	2,08584
C	-0,30065	1,09328	3,57000
H	0,39379	0,26382	3,72797
H	0,02412	1,94275	4,18527
H	-1,29631	0,79106	3,91655
C	-1,22721	2,79351	1,95320
H	-0,80872	3,61887	2,54385
H	-1,29681	3,12045	0,91039
H	-2,23752	2,58238	2,31781
C	1,09959	1,89573	1,61586
H	1,77791	1,04580	1,71971
H	1,09837	2,21280	0,56869
H	1,49722	2,72257	2,21879

22-Ph {[W(CO)$_5$]PPh}

23

Energy = -1207.432754107932

ZPE = 0.12969027

P	-1,09241	-0,18573	1,79535
C	1,17288	-3,04029	-0,86240
O	1,73327	-3,78461	-1,54418
C	0,98282	-0,09187	-0,70289
O	1,40714	0,80402	-1,29273
C	1,83106	-1,60241	1,63598
O	2,73202	-1,55275	2,35453
C	-0,62904	-3,24583	1,43691
O	-1,10715	-4,11545	2,02414
C	-1,46052	-1,76274	-0,86733
O	-2,39365	-1,82056	-1,54226
W	0,20289	-1,68254	0,36358
C	-0,24081	1,27184	2,41925
C	-1,02019	2,12721	3,24076
C	1,10418	1,63413	2,17030
C	-0,47967	3,28771	3,78455
H	-2,05445	1,85968	3,44040
C	1,64252	2,79154	2,71441
H	1,72287	0,99937	1,54697
C	0,85188	3,62057	3,52188
H	-1,08982	3,93166	4,41077
H	2,67678	3,05538	2,51455
H	1,27751	4,52578	3,94535

22-Anth {[W(CO)$_5$]PAnth}

35

Energy = -1514.905123317359

ZPE = 0.22114281

P	-1,10792	0,38623	0,90408
C	1,03840	-3,45880	-0,09921
O	1,55154	-4,46514	-0,34662
C	1,76463	-0,66329	-0,49618
O	2,66178	-0,11650	-0,97050
C	1,08174	-1,55120	2,19798
O	1,57935	-1,46693	3,23672
C	-1,41995	-2,71827	1,18931
O	-2,29351	-3,32324	1,63604

C	-0,86740	-1,63020	-1,43010
O	-1,45710	-1,61069	-2,42286
W	0,15646	-1,65483	0,36123
C	-0,31772	1,50389	2,06055
C	-1,11875	2,42102	2,86262
C	1,07168	1,67388	2,05765
C	-2,49821	2,28631	3,00505
C	-0,45638	3,49661	3,56849
C	1,70347	2,73580	2,73196
H	1,68085	0,98795	1,48035
C	-3,25837	3,17970	3,77980
H	-3,00561	1,46419	2,50512
C	-1,20667	4,38580	4,34916
C	0,95627	3,62756	3,47130
H	2,78164	2,84392	2,66555
C	-4,67068	3,04943	3,90833
C	-2,59605	4,25932	4,47155
H	-0,69377	5,18663	4,87700
H	1,43891	4,44380	4,00267
C	-5,38957	3,93570	4,67439
H	-5,16863	2,23612	3,38700
C	-3,37568	5,15588	5,26049
C	-4,73632	4,99888	5,35750
H	-6,46665	3,82795	4,76424
H	-2,87054	5,96401	5,78316
H	-5,32375	5,68621	5,95925

22-NH$_2$ {[W(CO)$_5$]PNH$_2$}

15

Energy = -1031.662193219029

ZPE = 0.06699243

P	-1,78053	2,17862	0,89423
C	1,08881	0,54338	3,98194
O	1,82094	0,11850	4,76989
C	1,36260	1,77723	1,28846
O	2,20429	2,05738	0,54851
C	-0,02796	3,23395	3,34671
O	0,04398	4,31768	3,74048
C	-1,81315	0,93139	3,78513
O	-2,72826	0,70775	4,45355
C	-0,42446	-0,53421	1,71259
O	-0,56971	-1,57304	1,22871
N	-1,27846	3,61002	0,24911
H	-0,42420	4,10479	0,49413
H	-1,83429	4,08121	-0,45985
W	-0,18930	1,32934	2,57181

22-NMe$_2$ {[W(CO)$_5$]PNMe$_2$}

21

Energy = -1110.326669544871

ZPE = 0.12251303

P	-1,40373	1,68157	-0,19626
N	-0,51817	1,46568	1,18578
C	0,89069	1,07415	1,31974
H	0,95335	0,14708	1,89956
H	1,32626	0,92606	0,33535
H	1,43352	1,86125	1,85404
C	-1,16183	1,67834	2,49773
H	-1,10599	0,75313	3,08099
H	-0,63006	2,47019	3,03592
H	-2,20284	1,96317	2,34581
C	1,43014	2,37172	-1,79550
O	2,36210	2,97832	-1,48092
C	-1,15910	3,05226	-2,96831
O	-1,68011	4,02448	-3,31285
C	0,50487	1,04801	-4,25149
O	0,93696	0,90048	-5,31562
C	0,62674	-0,45674	-1,72751
O	1,10225	-1,44888	-1,37391
C	-1,94470	0,26954	-2,90543
O	-2,89973	-0,30187	-3,21654
W	-0,24493	1,30476	-2,36139

22-NPh$_2$ {[W(CO)$_5$]PNPh$_2$}

35

Energy = -1494.042914613830

ZPE = 0.22548927

P	-0,76131	0,52187	0,40244
C	1,27209	-3,48114	0,69735
O	1,81478	-4,50233	0,64532
C	2,00091	-0,76851	-0,02200
O	2,94665	-0,26650	-0,45342
C	1,09533	-1,33301	2,65489
O	1,59617	-1,22065	3,68852
C	-1,34641	-2,55298	1,63455
O	-2,26395	-3,04859	2,12854
C	-0,39318	-2,06295	-1,12377
O	-0,77058	-2,30224	-2,19015
W	0,31440	-1,66895	0,76800
N	-0,97779	1,52513	1,74363
C	-1,34152	2,90493	1,54057
C	-2,30127	3,49865	2,36981
C	-0,74334	3,64125	0,51261
C	-2,67538	4,82216	2,14894
H	-2,75684	2,92216	3,16831
C	-1,12810	4,96381	0,29731
H	0,02987	3,17957	-0,09364
C	-2,09487	5,55756	1,11167

H	-3,42730	5,27761	2,78653
H	-0,65639	5,53488	-0,49675
H	-2,38612	6,59060	0,94725
C	-0,85265	1,12796	3,12348
C	0,05317	1,79706	3,95069
C	-1,65594	0,10312	3,62566
C	0,17192	1,41228	5,28428
H	0,66252	2,59860	3,54496
C	-1,53417	-0,27271	4,96249
H	-2,38191	-0,37032	2,97412
C	-0,61757	0,37665	5,79171
H	0,88630	1,91842	5,92659
H	-2,16137	-1,06723	5,35534
H	-0,52226	0,08144	6,83228

22-NCy$_2$ {[W(CO)$_5$]PNCy$_2$}

47

Energy = -1501.295167090530

ZPE = 0.36401837

P	-1,15945	0,35096	1,41314
C	1,08109	-3,07299	-0,52448
O	1,58463	-3,99820	-1,00703
C	1,18288	-0,20396	-1,00712
O	1,72978	0,45490	-1,78291
C	1,74538	-1,27307	1,68975
O	2,60149	-1,20020	2,46371
C	-0,79184	-2,69355	1,62888
O	-1,34933	-3,40949	2,34454
C	-1,37937	-1,59516	-0,98626
O	-2,26931	-1,69536	-1,71680
N	-0,40357	1,73281	1,94376
W	0,20136	-1,43504	0,33007
C	-1,28642	2,65153	2,74912
C	-1,14368	2,40304	4,26073
C	-1,17502	4,14010	2,40429
H	-2,29882	2,33111	2,47607
C	-2,21697	3,19609	5,02000
H	-0,15316	2,70809	4,61029
H	-1,24803	1,32845	4,45068
C	-2,24840	4,92252	3,17952
H	-0,18660	4,52758	2,67477
H	-1,30999	4,28446	1,32774
C	-2,13351	4,69178	4,69104
H	-2,09932	3,03087	6,09713
H	-3,21048	2,81803	4,74163
H	-2,15598	5,98909	2,94514
H	-3,24230	4,60210	2,83782
H	-2,92299	5,24074	5,21744
H	-1,17199	5,08827	5,04666
C	1,03224	2,04861	1,69778
C	1,22660	3,06353	0,55530
C	1,82622	2,44337	2,94962
H	1,44330	1,10127	1,33859
C	2,72055	3,18626	0,22169
H	0,84327	4,04520	0,84453
H	0,65740	2,72954	-0,31884
C	3,31540	2,57833	2,59464
H	1,46612	3,39851	3,34714
H	1,68968	1,68462	3,72692
C	3,53213	3,58599	1,45973
H	2,85347	3,91983	-0,58152
H	3,09141	2,22503	-0,15691
H	3,87281	2,87843	3,48920
H	3,70411	1,59786	2,28782
H	4,59756	3,64941	1,20963
H	3,21851	4,58480	1,79484

22-N(SiH$_3$)$_2$ {[W(CO)$_5$]PN(SiH$_3$)$_2$}

21

Energy = -1613.162081395819

ZPE = 0.09704875

P	-0,94194	-0,51466	2,14674
C	1,12534	-2,65604	-1,22811
O	1,60928	-3,27484	-2,07451
C	0,56210	0,19163	-0,79440
O	0,72159	1,14068	-1,43230
C	2,11990	-1,29711	1,19177
O	3,14675	-1,17065	1,70080
C	-0,03763	-3,29610	1,33487
O	-0,21719	-4,28217	1,90762
C	-1,58014	-1,78377	-0,60452
O	-2,61231	-1,92320	-1,10045
N	-0,55977	1,04599	2,64528
W	0,27151	-1,54406	0,28803
Si	-1,60006	1,60382	3,99378
H	-1,44677	3,07658	4,05517
H	-3,00065	1,23692	3,70641
H	-1,13982	0,98928	5,25804
Si	0,69767	2,15259	2,03643
H	1,81759	1,36562	1,49296
H	0,10865	3,02290	0,99529
H	1,14115	2,96871	3,18878

Table 7.3 More free enthalpy values for computed chloride abstractions (scheme 3.4.3). Single-point calculations at the PW6B95-D3/CPCM(THF)/def2-QZVP level with correction values (thermal, entropic and ZPE) at the TPSS-D3/CPCM(THF)/def2-TZVP level of theory.

		Phosphanide complexes **5a$^-$**		Phosphinidene complexes **22**		
[M]	**R**	**MBO(P-R)**	**MBO(P-M)**	**MBO(P-R)**	**MBO(P-M)**	**ΔG / kcal mol^{-1}**
$Cr(CO)_5$	NH_2	1,181	0,713	1,417	0,950	-15,32
$Cr(CO)_5$	NMe_2	1,263	0,705	1,554	0,911	-13,40
$Cr(CO)_5$	*t*-bu	0,985	0,676	0,995	1,135	-17,68
$Mo(CO)_5$	NH_2	1,184	0,832	1,418	1,086	-3,66
$Mo(CO)_5$	NMe_2	1,262	0,836	1,530	1,025	-12,59
$Mo(CO)_5$	*t*-bu	0,981	0,826	0,990	1,338	-31,35
$Fe(CO)_4$	Me	1,009	0,649	0,995	1,519	-22,03
$Fe(CO)_4$	Ph	1,025	0,587	1,111	1,382	-22,10
$Fe(CO)_4$	Anth	0,971	0,627	1,122	1,371	-20,61
$Fe(CO)_4$	NPh_2	1,173	0,602	1,351	1,069	-16,66
$Fe(CO)_4$	NCy_2	1,357	0,656	1,585	0,952	-10,68
$Fe(CO)_4$	$N(SiH_3)_2$	1,052	0,564	1,376	1,019	-21,14
$Fe(CO)_4$	SiH_3	1,039	0,592	1,022	1,455	-22,74
$Fe(CO)_4$	Cl	0,943	0,635	1,022	1,480	-22,04
$Fe(CO)_4$	F	0,862	0,735	0,861	1,627	-22,51
$Fe(CO)_4$	OH	1,062	0,667	1,070	1,482	-17,59
$Fe(CO)_4$	SH	1,163	0,591	1,273	1,376	-18,07
$W(CO)_5$	Cl	0,904	0,759	1,039	1,398	-28,87
$W(CO)_5$	F	0,821	0,869	0,894	1,505	-28,84
$W(CO)_5$	PH_2	1,061	0,708	1,142	1,296	-15,59
$W(CO)_5$	SH	1,157	0,714	1,490	1,076	-26,26

Table 7.4. The B3LYP-D3/def2-TZVP/COSMO(THF) optimized Cartesian coordinates (in Å). Each structure is labelled by its specific name, followed by its number of atoms, its single-point-energy (in hartrees), and the atomic coordinates.

47a-Me (+1/2)
38
Energy = -1113.353591519380
ZPE = 0.30766487

P	-0,70759	0,06759	-0,97250
C	-2,25859	0,09088	0,00195
H	-2,63085	1,11448	0,02020
H	-3,01930	-0,55074	-0,44924
H	-2,08742	-0,23887	1,02954
C	-0,20207	-1,63210	-0,91473
C	-0,88940	-2,67578	-0,24880
C	0,99527	-1,95797	-1,60278
C	-0,42137	-3,96440	-0,28705
H	-1,79037	-2,46370	0,30819
C	1,48114	-3,23991	-1,61773
H	1,52833	-1,17955	-2,13474
C	0,78141	-4,28865	-0,96759
H	-0,94600	-4,73702	0,25615
H	2,37687	-3,46586	-2,17745
C	1,27250	-5,63055	-0,99569
C	2,69282	-5,88940	-1,09874
C	3,62877	-5,05288	-0,45687
C	3,16507	-6,99875	-1,82967
C	4,98209	-5,32599	-0,53516
H	3,28024	-4,22318	0,14163
C	4,52158	-7,24840	-1,92662
H	2,46106	-7,63068	-2,35209
C	5,43184	-6,41888	-1,27428
H	5,68959	-4,69440	-0,01484
H	4,87411	-8,08741	-2,51133
H	6,49215	-6,62560	-1,33983
C	0,35720	-6,74871	-0,91974
C	0,72776	-7,92833	-0,24151
C	-0,91358	-6,68847	-1,52802
C	-0,14900	-8,99400	-0,15740
H	1,68713	-7,97834	0,25315
C	-1,77429	-7,76884	-1,46189
H	-1,19444	-5,80928	-2,09031
C	-1,39833	-8,91944	-0,77085
H	0,13621	-9,88362	0,38791
H	-2,73649	-7,72209	-1,95392
H	-2,07817	-9,75953	-0,71294

47a-NH$_2$ (+1/2)
37
Energy = -1129.431899935761
ZPE = 0.29691929

P	-0,82649	-0,01197	-1,16777
C	-0,33544	-1,68992	-1,05441
C	-1,04688	-2,75217	-0,44237
C	0,91925	-1,98331	-1,65075
C	-0,54521	-4,02424	-0,44746
H	-1,99116	-2,57407	0,05397
C	1,43281	-3,25296	-1,63292
H	1,47482	-1,19160	-2,13964
C	0,71588	-4,32659	-1,03856
H	-1,09302	-4,80958	0,05232
H	2,37535	-3,45081	-2,12127
C	1,23484	-5,65209	-1,02753
C	2,66896	-5,89454	-1,09965
C	3,58369	-5,06392	-0,42598
C	3,16918	-6,99205	-1,82497
C	4,94279	-5,32523	-0,47427
H	3,21678	-4,23888	0,16879
C	4,53072	-7,23539	-1,88877
H	2,48225	-7,63259	-2,36039
C	5,42151	-6,40739	-1,20959
H	5,63126	-4,69123	0,06895
H	4,90043	-8,07143	-2,46777
H	6,48444	-6,60732	-1,24936
C	0,34283	-6,80025	-0,94304
C	0,70810	-7,93050	-0,18823
C	-0,88769	-6,81938	-1,62563
C	-0,13638	-9,02411	-0,10021
H	1,64466	-7,92811	0,35170
C	-1,71860	-7,92516	-1,55245
H	-1,16659	-5,97784	-2,24468
C	-1,35028	-9,02706	-0,78402
H	0,14978	-9,87649	0,50185
H	-2,65155	-7,93406	-2,10062
H	-2,00427	-9,88723	-0,72269
N	-2,28984	0,05947	-0,44320
H	-2,76393	0,95042	-0,38631
H	-2,79937	-0,70727	-0,02548

48a-Me (+1/2)
49
Energy = -1747.260056823422
ZPE = 0.34939124

P	-0,76202	0,07368	-0,92043
C	-2,37291	0,12310	-0,08335
H	-2,75293	1,14123	-0,13967
H	-3,08492	-0,55045	-0,56105
H	-2,26535	-0,15636	0,96669
C	-0,22562	-1,59250	-0,94317
C	-0,94711	-2,64495	-0,32469
C	0,98963	-1,91600	-1,59875
C	-0,47648	-3,93098	-0,35409
H	-1,86652	-2,43785	0,20297
C	1,46586	-3,19743	-1,61559
H	1,54612	-1,14364	-2,10889
C	0,75204	-4,25727	-0,99151
H	-1,02286	-4,70324	0,16718
H	2,37572	-3,41583	-2,15443
W	0,52586	2,03705	-1,50287
C	-1,11185	2,90670	-2,44604
O	-2,00471	3,39352	-2,95951
C	1,64633	3,74052	-1,84288
O	2,26802	4,67910	-2,02246
C	1,18120	1,24347	-3,30765
O	1,54540	0,81494	-4,29918
C	2,15944	1,16873	-0,56613
O	3,04572	0,67042	-0,05023
C	-0,13592	2,87767	0,27480
O	-0,51186	3,33912	1,24693
C	1,25482	-5,58883	-1,00181
C	2,68051	-5,83956	-1,13561
C	3,62805	-5,01160	-0,50381
C	3,14075	-6,93658	-1,88894
C	4,98191	-5,27462	-0,62092
H	3,29113	-4,19104	0,11418
C	4,49661	-7,17888	-2,02349
H	2,42663	-7,57123	-2,39466
C	5,42041	-6,35310	-1,38653
H	5,69797	-4,64477	-0,10982
H	4,83691	-8,01099	-2,62545
H	6,47983	-6,55237	-1,48276
C	0,36174	-6,72750	-0,87573
C	0,76570	-7,86638	-0,15197
C	-0,90925	-6,73133	-1,48212
C	-0,07937	-8,95397	-0,02005
H	1,73136	-7,87203	0,33350
C	-1,74018	-7,83250	-1,36687
H	-1,21801	-5,88451	-2,07898
C	-1,33212	-8,94245	-0,63004
H	0,23554	-9,81219	0,55869
H	-2,70456	-7,83256	-1,85735
H	-1,98722	-9,79874	-0,53545

48a-NH_2 (+1/2)

48

Energy = -1763.330639983942

ZPE = 0.33829431

P	-0,86070	0,01642	-0,95767
C	-0,31741	-1,64091	-0,92383
C	-1,05683	-2,71758	-0,37588
C	0,95402	-1,92105	-1,48082
C	-0,55985	-3,99312	-0,40454
H	-2,00970	-2,54938	0,10609
C	1,45173	-3,19564	-1,50169
H	1,53938	-1,12515	-1,91639
C	0,71277	-4,28756	-0,97112
H	-1,12794	-4,78665	0,05802
H	2,40620	-3,37870	-1,97185
W	0,35774	2,02148	-1,46207
C	-1,19981	2,70053	-2,65507
O	-2,05896	3,06616	-3,30786
C	1,43082	3,75136	-1,84078
O	2,02953	4,69674	-2,04885
C	1,25708	1,15762	-3,11826
O	1,75639	0,69160	-4,03089
C	1,91766	1,32738	-0,28542
O	2,77481	0,92377	0,34808
C	-0,54134	2,95947	0,15745
O	-1,05294	3,48064	1,03223
C	1,22974	-5,61426	-0,99851
C	2,66563	-5,85233	-1,09748
C	3,58946	-5,06019	-0,39240
C	3,15657	-6,90025	-1,89697
C	4,94952	-5,30650	-0,48677
H	3,23072	-4,27394	0,25779
C	4,51848	-7,12854	-2,00610
H	2,46137	-7,51366	-2,45359
C	5,41960	-6,33574	-1,29930
H	5,64534	-4,70013	0,07841
H	4,87998	-7,92500	-2,64341
H	6,48290	-6,52195	-1,37757
C	0,34364	-6,76985	-0,93537
C	0,72489	-7,91387	-0,21022
C	-0,89148	-6,78689	-1,60887
C	-0,10808	-9,01794	-0,14014
H	1,66804	-7,91611	0,31844
C	-1,71235	-7,90171	-1,55260
H	-1,18440	-5,93482	-2,20697
C	-1,32832	-9,01739	-0,81229
H	0,19276	-9,88149	0,43861
H	-2,64991	-7,90677	-2,09314
H	-1,97379	-9,88486	-0,76479
N	-2,41204	0,01522	-0,46531

H	-2,91497	0,88596	-0,37699
H	-2,96745	-0,81022	-0,29324

47b-Me (0/1)

38

Energy = -1113.533092648807

ZPE = 0.30615266

P	-0,64986	0,11771	-0,78252
C	-2,35810	0,10230	-0,06791
H	-2,70669	1,13392	-0,01398
H	-3,05430	-0,46244	-0,69151
H	-2,37160	-0,31730	0,94032
C	-0,18700	-1,53782	-0,81999
C	-0,97873	-2,65698	-0,37935
C	1,12181	-1,86210	-1,33582
C	-0,52589	-3,93169	-0,45532
H	-1,95849	-2,47633	0,04067
C	1,58897	-3,13082	-1,38180
H	1,74084	-1,05330	-1,70772
C	0,79295	-4,25724	-0,94776
H	-1,14946	-4,73208	-0,08315
H	2,56714	-3,31793	-1,80063
C	1,26066	-5,55861	-0,98915
C	2,69053	-5,87263	-1,16163
C	3,68095	-5,19579	-0,43589
C	3,09046	-6,90040	-2,02838
C	5,02205	-5,52332	-0,58344
H	3,39021	-4,42644	0,26675
C	4,43166	-7,21834	-2,18603
H	2,34021	-7,44301	-2,58849
C	5,40407	-6,53145	-1,46354
H	5,76927	-4,99645	-0,00336
H	4,71991	-8,00550	-2,87130
H	6,44980	-6,78672	-1,57879
C	0,35804	-6,71754	-0,85821
C	0,70029	-7,78945	-0,02135
C	-0,83368	-6,80259	-1,59101
C	-0,13369	-8,89109	0,10245
H	1,62252	-7,74640	0,54326
C	-1,66104	-7,91252	-1,47884
H	-1,09562	-6,00214	-2,27011
C	-1,31830	-8,95790	-0,62707
H	0,14129	-9,70085	0,76655
H	-2,57090	-7,96514	-2,06340
H	-1,96441	-9,82199	-0,53814

47b-NH_2 (0/1)

37

Energy = -1129.598513235519

ZPE = 0.29483286

P	-0,80332	0,03434	-1,03616
C	-0,32816	-1,60695	-0,99052
C	-1,11586	-2,73549	-0,57362
C	1,01784	-1,90199	-1,41472
C	-0,62677	-3,99858	-0,59765
H	-2,12333	-2,58432	-0,20666
C	1,51726	-3,15987	-1,41372
H	1,64286	-1,08439	-1,75827
C	0,72595	-4,30525	-1,01318
H	-1,25301	-4,80605	-0,24598
H	2,52559	-3,32328	-1,76506
C	1,22103	-5,59613	-1,01458
C	2,66342	-5,88412	-1,14312
C	3,62251	-5,19461	-0,38776
C	3,11039	-6,90108	-1,99972
C	4,97360	-5,49700	-0,49679
H	3,29900	-4,42981	0,30587
C	4,46117	-7,19802	-2,11685
H	2,38687	-7,45610	-2,58295
C	5,40106	-6,49675	-1,36580
H	5,69362	-4,95699	0,10570
H	4,78201	-7,97937	-2,79465
H	6,45419	-6,73303	-1,45066
C	0,34186	-6,77565	-0,88803
C	0,68226	-7,82326	-0,01944
C	-0,82410	-6,91190	-1,65445
C	-0,12384	-8,94654	0,09965
H	1,58556	-7,74558	0,57193
C	-1,62722	-8,04004	-1,54314
H	-1,08710	-6,13342	-2,35855
C	-1,28444	-9,06082	-0,66182
H	0,15390	-9,73611	0,78696
H	-2,51751	-8,12723	-2,15365
H	-1,90990	-9,94027	-0,57493
N	-2,38606	0,07931	-0,51353
H	-2,86450	0,96534	-0,48913
H	-2,96322	-0,71584	-0,28743

48b-Me (0/1)

49

Energy = -1747.437916364015

ZPE = 0.34835545

P	-0,77428	0,06955	-0,88594
C	-2,44936	0,13778	-0,15501
H	-2,82175	1,15485	-0,26570
H	-3,13358	-0,54167	-0,66337
H	-2,42215	-0,10995	0,90741
C	-0,22905	-1,54932	-0,86020

C	-1,00227	-2,65360	-0,36000
C	1,07115	-1,87059	-1,38383
C	-0,53612	-3,92626	-0,40258
H	-1,97058	-2,46628	0,08280
C	1,54191	-3,13845	-1,41153
H	1,68416	-1,07502	-1,78216
C	0,76563	-4,25779	-0,93241
H	-1,13981	-4,71650	0,01998
H	2,51121	-3,32583	-1,84904
W	0,55605	2,12380	-1,45143
C	-0,92813	2,78406	-2,72903
O	-1,73724	3,15974	-3,44605
C	1,63388	3,79895	-1,81322
O	2,24969	4,74932	-2,01629
C	1,48433	1,20055	-3,04964
O	2,00337	0,71200	-3,94533
C	2,02738	1,41807	-0,17985
O	2,83207	1,01466	0,52562
C	-0,39382	3,07838	0,11560
O	-0,92550	3,61563	0,97521
C	1,24197	-5,55751	-0,97981
C	2,66384	-5,85514	-1,23263
C	3,68756	-5,17676	-0,55677
C	3,02212	-6,86159	-2,14133
C	5,02128	-5,48014	-0,79540
H	3,43059	-4,42317	0,17569
C	4,35499	-7,15435	-2,39046
H	2,24555	-7,40421	-2,66434
C	5,36108	-6,46468	-1,71847
H	5,79620	-4,95125	-0,25495
H	4,61084	-7,92269	-3,10908
H	6,40098	-6,69873	-1,90763
C	0,36481	-6,72545	-0,78963
C	0,78711	-7,79773	0,01052
C	-0,87920	-6,82511	-1,42850
C	-0,01703	-8,91328	0,18999
H	1,74954	-7,74378	0,50213
C	-1,67769	-7,94873	-1,26029
H	-1,20505	-6,02759	-2,08268
C	-1,25350	-8,99424	-0,44600
H	0,32188	-9,72292	0,82396
H	-2,62881	-8,01252	-1,77365
H	-1,87685	-9,86952	-0,31467

48b-NH_2 (0/1)

48

Energy = -1763.499261089699

ZPE = 0.33695839

P	-0,88589	0,00597	-1,00007
C	-0,34773	-1,60158	-0,94808
C	-1,13606	-2,72763	-0,52357
C	0,99625	-1,89037	-1,37584
C	-0,64253	-3,98916	-0,54726
H	-2,13515	-2,57157	-0,13817
C	1,48986	-3,14876	-1,38824
H	1,62526	-1,07940	-1,71556
C	0,70306	-4,29495	-0,98480
H	-1,26154	-4,79451	-0,17896
H	2,49449	-3,30813	-1,75031
W	0,39120	2,09461	-1,41774
C	-1,07156	2,78028	-2,70635
O	-1,87247	3,16835	-3,42520
C	1,46430	3,79441	-1,70572
O	2,07602	4,75236	-1,86753
C	1,36717	1,22822	-3,02268
O	1,90644	0,76502	-3,91809
C	1,84275	1,37959	-0,12579
O	2,63652	0,97792	0,59135
C	-0,59575	2,99504	0,16068
O	-1,14010	3,50781	1,02618
C	1,20393	-5,58290	-1,00583
C	2,64285	-5,85964	-1,19304
C	3,62721	-5,18131	-0,46137
C	3,05824	-6,84960	-2,09538
C	4,97482	-5,46581	-0,64052
H	3,32833	-4,43837	0,26626
C	4,40497	-7,12750	-2,28283
H	2,31380	-7,39542	-2,66066
C	5,37104	-6,43556	-1,55681
H	5,71668	-4,93390	-0,05783
H	4,70232	-7,88570	-2,99655
H	6,42149	-6,65595	-1,69846
C	0,34172	-6,77019	-0,84890
C	0,73444	-7,81600	-0,00038
C	-0,85519	-6,91695	-1,56340
C	-0,05170	-8,94907	0,15074
H	1,66244	-7,72875	0,54979
C	-1,63778	-8,05598	-1,42092
H	-1,15826	-6,14073	-2,25358
C	-1,24313	-9,07487	-0,55946
H	0,26617	-9,73729	0,82188
H	-2,55290	-8,15290	-1,99178
H	-1,85295	-9,96250	-0,44847
N	-2,47036	0,07095	-0,50843
H	-2,94898	0,95434	-0,59191
H	-3,08526	-0,72773	-0,56033

47c-Me (0/3)

38

Energy = -1113.514397493389

ZPE = 0.30512551

P	-0,74657	0,07311	-1,08738
C	-2,17210	0,12467	0,07967
H	-2,57708	1,13673	0,07770
H	-2,96161	-0,56733	-0,22420
H	-1,86800	-0,12491	1,09917
C	-0,21802	-1,65421	-0,99355
C	-0,77026	-2,63382	-0,15199
C	0,83974	-2,04310	-1,83686
C	-0,28926	-3,93330	-0,15688
H	-1,58000	-2,38314	0,51940
C	1,31902	-3,34057	-1,83853
H	1,28481	-1,31277	-2,50324
C	0,76411	-4,32023	-0,99917
H	-0,72882	-4,66404	0,50941
H	2,12731	-3,60995	-2,50547
C	1,27430	-5,69971	-1,00629
C	2,70902	-5,91462	-1,04671
C	3,59724	-4,99717	-0,44611
C	3,27498	-7,02998	-1,69943
C	4,96758	-5,19673	-0,47790
H	3,19682	-4,13357	0,06718
C	4,64664	-7,21989	-1,73848
H	2,62602	-7,73401	-2,20158
C	5,50405	-6,30931	-1,12368
H	5,62268	-4,48373	0,00722
H	5,05207	-8,07837	-2,25948
H	6,57523	-6,46241	-1,15142
C	0,34044	-6,80552	-0,97010
C	0,68394	-8,04731	-0,39078
C	-0,96426	-6,67917	-1,49705
C	-0,22009	-9,09520	-0,34651
H	1,66187	-8,17122	0,05257
C	-1,86225	-7,73255	-1,45630
H	-1,25957	-5,74691	-1,95840
C	-1,49917	-8,94946	-0,88121
H	0,06983	-10,0300	0,11716
H	-2,85098	-7,60833	-1,88031
H	-2,20379	-9,77034	-0,84606

47c-NH_2 (0/3)

37

Energy = -1129.579701996324

ZPE = 0.29430878

P	-0,82212	0,03690	-1,12708
C	-0,27438	-1,68462	-1,03123
C	-0,84757	-2,67506	-0,21872
C	0,83271	-2,04761	-1,81890
C	-0,34874	-3,96847	-0,21213
H	-1,67524	-2,43349	0,43541
C	1,33317	-3,33678	-1,80302
H	1,29611	-1,30838	-2,46319
C	0,74921	-4,33650	-1,00507
H	-0,80733	-4,70790	0,43128
H	2,17648	-3,58689	-2,43300
C	1,26717	-5,70976	-1,00830
C	2,70237	-5,92758	-1,04365
C	3,59299	-5,01971	-0,43281
C	3,26502	-7,04296	-1,69928
C	4,96250	-5,22791	-0,45898
H	3,19499	-4,15766	0,08499
C	4,63553	-7,24189	-1,73236
H	2,61379	-7,74149	-2,20631
C	5,49551	-6,34008	-1,10823
H	5,61969	-4,52249	0,03438
H	5,03802	-8,10076	-2,25510
H	6,56583	-6,50023	-1,13063
C	0,34004	-6,82415	-0,97561
C	0,68203	-8,05200	-0,36791
C	-0,95184	-6,72025	-1,53612
C	-0,21293	-9,10809	-0,32542
H	1,65190	-8,15887	0,09739
C	-1,84081	-7,78169	-1,49785
H	-1,24381	-5,79922	-2,02154
C	-1,48050	-8,98419	-0,89176
H	0,07521	-10,0320	0,16077
H	-2,81989	-7,67517	-1,94833
H	-2,17816	-9,81109	-0,85820
N	-2,34766	-0,06469	-0,40038
H	-2,89801	0,78182	-0,39119
H	-2,91765	-0,89598	-0,48428

48c-Me (0/3)

49

Energy = -1747.419746245859

ZPE = 0.34691433

P	-0,99444	0,05366	-1,22176
C	-2,40990	0,16350	-0,07345
H	-2,86502	1,14571	-0,19521
H	-3,15420	-0,60232	-0,29284
H	-2,08442	0,05835	0,96406
C	-0,39789	-1,63856	-1,13624
C	-0,89034	-2,59179	-0,23369
C	0,62498	-2,02734	-2,01605
C	-0,36584	-3,87397	-0,20356
H	-1,67274	-2,33162	0,46581
C	1,14543	-3,30545	-1,98284
H	1,01322	-1,32094	-2,73737
C	0,66719	-4,26335	-1,07151

H	-0,74770	-4,58428	0,51739
H	1,92722	-3,57795	-2,67851
W	0,61900	1,95484	-1,44933
C	-0,84728	3,12546	-2,32515
O	-1,66492	3,76262	-2,80866
C	1,97497	3,46674	-1,43829
O	2,75664	4,30848	-1,40247
C	1,27180	1,34567	-3,31533
O	1,64700	1,01784	-4,34551
C	2,03375	0,71573	-0,59251
O	2,80910	0,01687	-0,12635
C	-0,05056	2,57522	0,40389
O	-0,43247	2,91825	1,42624
C	1,23511	-5,61278	-1,03109
C	2,66778	-5,78012	-1,19879
C	3,57387	-4,79484	-0,75277
C	3,20895	-6,91939	-1,82991
C	4,94037	-4,94594	-0,92080
H	3,19326	-3,91463	-0,25278
C	4,57572	-7,06216	-2,00476
H	2,54132	-7,68066	-2,20896
C	5,45267	-6,07945	-1,54965
H	5,61186	-4,17883	-0,55559
H	4,96080	-7,94043	-2,50775
H	6,52035	-6,19435	-1,68549
C	0,36218	-6,75429	-0,83486
C	0,80665	-7,91520	-0,16745
C	-0,97014	-6,74402	-1,29977
C	-0,03158	-9,00195	0,01917
H	1,81283	-7,94469	0,22714
C	-1,80180	-7,83706	-1,11981
H	-1,33971	-5,87494	-1,82678
C	-1,34031	-8,97432	-0,45926
H	0,33413	-9,87362	0,54758
H	-2,81467	-7,80668	-1,50185
H	-1,99283	-9,82602	-0,31649

48c-NH_2 (0/3)

48

Energy = -1763.482370715514

ZPE = 0.33648010

P	-1,14355	-0,00280	-1,71698
C	-0,55407	-1,69929	-1,55524
C	-0,97155	-2,57168	-0,54345
C	0,43410	-2,13415	-2,44934
C	-0,40962	-3,83275	-0,42727
H	-1,71360	-2,25367	0,17665
C	1,00490	-3,38556	-2,31889
H	0,75588	-1,48683	-3,25564
C	0,60155	-4,26864	-1,30010
H	-0,73330	-4,48351	0,37389
H	1,76266	-3,69935	-3,02375
W	0,48401	1,83881	-1,11419
C	-0,28942	3,13850	-2,52740
O	-0,71131	3,86066	-3,30909
C	1,82385	3,21484	-0,47284
O	2,58320	3,98354	-0,07803
C	1,83861	1,12924	-2,50274
O	2,59850	0,74212	-3,26716
C	1,21487	0,47716	0,25817
O	1,60784	-0,29580	1,00405
C	-0,88745	2,54247	0,25651
O	-1,65576	2,93006	1,01222
C	1,21940	-5,58448	-1,14703
C	2,64647	-5,73444	-1,36396
C	3,53996	-4,67368	-1,10283
C	3,19636	-6,93772	-1,85447
C	4,90143	-4,81094	-1,31659
H	3,15546	-3,74359	-0,70777
C	4,55791	-7,06836	-2,07364
H	2,53817	-7,76298	-2,08805
C	5,42171	-6,00796	-1,80538
H	5,56306	-3,98285	-1,09484
H	4,94894	-7,99936	-2,46487
H	6,48550	-6,11297	-1,97559
C	0,39396	-6,72215	-0,77659
C	0,89242	-7,76369	0,03190
C	-0,94299	-6,82133	-1,21282
C	0,09824	-8,84509	0,37864
H	1,90500	-7,70361	0,40673
C	-1,73051	-7,90943	-0,87340
H	-1,35151	-6,04371	-1,84386
C	-1,21638	-8,92975	-0,07547
H	0,50333	-9,62410	1,01252
H	-2,74862	-7,96715	-1,23792
H	-1,83323	-9,77817	0,19164
N	-2,61596	-0,03612	-0,90904
H	-3,09598	0,84615	-0,80131
H	-3,25399	-0,80168	-1,08529

47d-Me (-1/2)

38

Energy = -1113.634204707530

ZPE = 0.30413143

P	-0,69333	0,16721	-0,90337
C	-2,34276	0,11673	-0,03249
H	-2,73193	1,13606	0,00557
H	-3,07434	-0,50374	-0,55799
H	-2,26134	-0,25125	0,99438
C	-0,19234	-1,53376	-0,88597

C	-0,91673	-2,61963	-0,32336
C	1,05221	-1,88882	-1,48394
C	-0,45351	-3,91424	-0,36356
H	-1,86220	-2,43041	0,16897
C	1,52121	-3,17569	-1,51230
H	1,64607	-1,10654	-1,94755
C	0,79122	-4,27176	-0,95679
H	-1,04720	-4,68837	0,10527
H	2,46546	-3,37388	-2,00231
C	1,27336	-5,61464	-0,99385
C	2,70353	-5,89666	-1,11765
C	3,68011	-5,11045	-0,47194
C	3,17546	-6,98844	-1,87621
C	5,03353	-5,39493	-0,57870
H	3,35987	-4,27635	0,13819
C	4,52825	-7,27370	-1,98280
H	2,45972	-7,61337	-2,39452
C	5,47394	-6,47988	-1,33533
H	5,75097	-4,77304	-0,05580
H	4,84957	-8,11734	-2,58275
H	6,53027	-6,70330	-1,41658
C	0,35781	-6,75033	-0,90083
C	0,72001	-7,93214	-0,21935
C	-0,92221	-6,73528	-1,49422
C	-0,13808	-9,01731	-0,13007
H	1,69131	-7,98499	0,25480
C	-1,78147	-7,82046	-1,40386
H	-1,23108	-5,85938	-2,04891
C	-1,40113	-8,97388	-0,71942
H	0,17655	-9,90195	0,41161
H	-2,75272	-7,77181	-1,88257
H	-2,07222	-9,82069	-0,64941

47d-NH_2 (-1/2)

37

Energy = -1129.690431277462

ZPE = 0.29289111

P	-0,83709	0,07944	-1,05955
C	-0,29271	-1,59812	-0,97752
C	-1,01490	-2,68577	-0,41909
C	0,97492	-1,93082	-1,53453
C	-0,52553	-3,97117	-0,43050
H	-1,96709	-2,49566	0,06133
C	1,46711	-3,20936	-1,53379
H	1,56635	-1,14425	-1,99481
C	0,74024	-4,31582	-0,99046
H	-1,11430	-4,74948	0,03755
H	2,42932	-3,39398	-1,99279
C	1,24436	-5,65086	-1,00578
C	2,68125	-5,90894	-1,09758
C	3,63449	-5,09986	-0,44297
C	3,19055	-6,99996	-1,83476
C	4,99458	-5,36061	-0,52147
H	3,28966	-4,26448	0,15206
C	4,54976	-7,26313	-1,91154
H	2,49699	-7,64388	-2,36016
C	5,47038	-6,44604	-1,25624
H	5,69020	-4,71940	0,00801
H	4,89634	-8,10789	-2,49603
H	6,53188	-6,65144	-1,31490
C	0,34656	-6,79987	-0,92292
C	0,71860	-7,97973	-0,24018
C	-0,93027	-6,80827	-1,52687
C	-0,12191	-9,07914	-0,16136
H	1,68609	-8,01945	0,24307
C	-1,77291	-7,90690	-1,44512
H	-1,25011	-5,93787	-2,08414
C	-1,38149	-9,05682	-0,76022
H	0,20366	-9,95940	0,38147
H	-2,74066	-7,87193	-1,93261
H	-2,03945	-9,91443	-0,69726
N	-2,44250	-0,03680	-0,37058
H	-2,88669	0,87355	-0,35345
H	-3,06207	-0,67831	-0,85672

48d-Me (-1/2)

49

Energy = -1747.559348563914

ZPE = 0.34631396

P	-1,13046	0,06850	-2,07046
C	-2,58230	0,18138	-0,91497
H	-2,98772	1,19110	-0,99698
H	-3,36431	-0,52240	-1,20990
H	-2,32811	0,00341	0,13136
C	-0,49976	-1,59911	-1,73626
C	-1,03930	-2,49725	-0,79953
C	0,59976	-2,05950	-2,49041
C	-0,49948	-3,75671	-0,60833
H	-1,88007	-2,19930	-0,18763
C	1,15165	-3,30294	-2,28990
H	1,02941	-1,41009	-3,24509
C	0,62686	-4,20275	-1,33078
H	-0,92900	-4,40202	0,14697
H	1,99488	-3,60997	-2,89427
W	0,73795	1,76181	-1,15727
C	-0,56322	3,20302	-1,83087
O	-1,31911	3,98114	-2,21483
C	2,07332	3,10316	-0,52099
O	2,84275	3,88519	-0,13674
C	1,60979	1,63007	-3,01544

O	2,09406	1,53313	-4,05450
C	1,89042	0,18356	-0,51365
O	2,52028	-0,70194	-0,14138
C	-0,19337	1,74416	0,67214
O	-0,70825	1,71020	1,70052
C	1,22243	-5,49798	-1,09314
C	2,65809	-5,68251	-1,25731
C	3,56714	-4,64245	-0,97207
C	3,19845	-6,90390	-1,70875
C	4,93275	-4,81421	-1,13372
H	3,18808	-3,69904	-0,60342
C	4,56448	-7,07132	-1,87425
H	2,52931	-7,71884	-1,94986
C	5,44392	-6,02850	-1,58869
H	5,60482	-3,99857	-0,89616
H	4,94659	-8,01809	-2,23641
H	6,51074	-6,16058	-1,71713
C	0,39114	-6,62161	-0,67818
C	0,86351	-7,59714	0,22229
C	-0,92215	-6,77697	-1,16528
C	0,06753	-8,66295	0,61325
H	1,86086	-7,49917	0,62968
C	-1,71409	-7,84683	-0,77850
H	-1,30843	-6,05433	-1,87113
C	-1,22681	-8,79885	0,11485
H	0,45510	-9,38941	1,31722
H	-2,71464	-7,94407	-1,18215
H	-1,84607	-9,63353	0,41802

48d-NH_2 (-1/2)

48

Energy = -1763.615507387697

ZPE = 0.33536895

P	-1,28178	-0,00404	-2,16292
C	-0,63065	-1,66323	-1,83475
C	-1,18849	-2,57122	-0,92155
C	0,50930	-2,08940	-2,54512
C	-0,62226	-3,81454	-0,70503
H	-2,07059	-2,28352	-0,36486
C	1,08421	-3,31783	-2,32011
H	0,95056	-1,43282	-3,28571
C	0,54598	-4,22876	-1,37908
H	-1,06478	-4,47220	0,03203
H	1,95672	-3,60520	-2,89170
W	0,61510	1,64549	-1,19391
C	-0,44614	3,06217	-2,23439
O	-1,07757	3,81541	-2,83291
C	1,95634	2,96068	-0,50955
O	2,72467	3,73067	-0,10116
C	1,73055	1,23150	-2,87168
O	2,34817	0,98245	-3,81052
C	1,49926	0,05945	-0,22276
O	1,97105	-0,83552	0,32107
C	-0,60413	1,90080	0,43105
O	-1,32334	1,99615	1,32592
C	1,17111	-5,50483	-1,11760
C	2,61813	-5,63915	-1,22807
C	3,47816	-4,57373	-0,89094
C	3,21707	-6,83193	-1,68052
C	4,85403	-4,69367	-1,00560
H	3,05143	-3,65140	-0,52073
C	4,59337	-6,94772	-1,79938
H	2,58629	-7,66472	-1,96102
C	5,42406	-5,88025	-1,46366
H	5,48728	-3,85926	-0,72957
H	5,02207	-7,87304	-2,16478
H	6,49877	-5,97209	-1,55651
C	0,36316	-6,65722	-0,74102
C	0,83926	-7,63021	0,16066
C	-0,93028	-6,84674	-1,26848
C	0,06607	-8,72531	0,51419
H	1,82071	-7,50699	0,59870
C	-1,69928	-7,94535	-0,91823
H	-1,31827	-6,12761	-1,97687
C	-1,20867	-8,89421	-0,02327
H	0,45580	-9,44896	1,21987
H	-2,68428	-8,06758	-1,35219
H	-1,81016	-9,75151	0,25111
N	-2,70246	0,00041	-1,15260
H	-2,55869	0,21097	-0,17181
H	-3,39835	0,63982	-1,51393

47e-Me (-2/1)

38

Energy = -1113.693668772890

ZPE = 0.30090136

P	-0,89894	0,01741	-1,23926
C	-2,00719	0,12731	0,27286
H	-2,43800	1,13195	0,29426
H	-2,83646	-0,58887	0,25239
H	-1,46792	-0,02131	1,21506
C	-0,29740	-1,68882	-1,11692
C	-0,63689	-2,61420	-0,10504
C	0,59428	-2,18222	-2,10137
C	-0,12245	-3,90759	-0,08386
H	-1,31020	-2,31655	0,68959
C	1,09363	-3,47253	-2,07241
H	0,88991	-1,52296	-2,91359
C	0,75582	-4,38956	-1,06019
H	-0,41860	-4,57567	0,71945

H	1,77379	-3,79338	-2,85546
C	1,29231	-5,77709	-1,03361
C	2,71505	-5,93770	-0,98284
C	3,56697	-4,86074	-0,57949
C	3,41598	-7,12591	-1,35954
C	4,94452	-4,97155	-0,53378
H	3,10879	-3,92352	-0,29400
C	4,79642	-7,22447	-1,31445
H	2,85721	-7,96987	-1,73701
C	5,59493	-6,15778	-0,89230
H	5,52751	-4,11657	-0,20517
H	5,26317	-8,15303	-1,62936
H	6,67363	-6,24324	-0,85267
C	0,34660	-6,85402	-1,05466
C	0,61684	-8,18685	-0,61272
C	-0,99988	-6,64617	-1,49270
C	-0,34143	-9,18667	-0,62695
H	1,59053	-8,42091	-0,20768
C	-1,94789	-7,65240	-1,50578
H	-1,28245	-5,65810	-1,82998
C	-1,64225	-8,95016	-1,07973
H	-0,07048	-10,17298	-0,26219
H	-2,94803	-7,42433	-1,86140
H	-2,38556	-9,73739	-1,09307

47e-NH_2 (-2/1)

37

Energy = -1129.747705410071

ZPE = 0.29017177

P	-1,04295	-0,09781	-1,42698
C	-0,39598	-1,78721	-1,24774
C	-0,73992	-2,69181	-0,22339
C	0,53310	-2,27120	-2,19746
C	-0,19552	-3,96962	-0,15989
H	-1,44523	-2,36565	0,53268
C	1,06268	-3,54967	-2,12723
H	0,83377	-1,62223	-3,01703
C	0,71926	-4,45185	-1,10571
H	-0,49476	-4,62918	0,64965
H	1,77037	-3,87076	-2,88553
C	1,28232	-5,82798	-1,04165
C	2,70693	-5,96059	-0,96580
C	3,53130	-4,86214	-0,56308
C	3,43717	-7,13903	-1,31717
C	4,90978	-4,94493	-0,49471
H	3,04998	-3,93083	-0,29693
C	4,81852	-7,20933	-1,25040
H	2,90131	-7,99831	-1,69331
C	5,58924	-6,12200	-0,82923
H	5,47061	-4,07468	-0,16757
H	5,30830	-8,13185	-1,54771
H	6,66874	-6,18515	-0,77269
C	0,35865	-6,92370	-1,06405
C	0,64791	-8,24567	-0,60128
C	-0,98496	-6,74802	-1,52498
C	-0,29077	-9,26381	-0,61609
H	1,61993	-8,45594	-0,17959
C	-1,91329	-7,77239	-1,53807
H	-1,28153	-5,77000	-1,87885
C	-1,58935	-9,05836	-1,09030
H	-0,00615	-10,2400	-0,23488
H	-2,91241	-7,56815	-1,91067
H	-2,31741	-9,85974	-1,10329
N	-2,16085	0,00214	-0,04221
H	-1,90540	0,72855	0,61472
H	-3,11975	0,16209	-0,32398

48e-Me (-2/1)

49

Energy = -1747.636647854056

ZPE = 0.34390309

P	-1,26673	0,05486	-1,62420
C	-2,51363	0,06453	-0,23836
H	-3,02245	1,02921	-0,25445
H	-3,26007	-0,71778	-0,39749
H	-2,07732	-0,07127	0,75354
C	-0,53381	-1,61155	-1,43857
C	-0,80131	-2,49992	-0,38870
C	0,34711	-2,07280	-2,43186
C	-0,21692	-3,75892	-0,33198
H	-1,45848	-2,20232	0,41804
C	0,93331	-3,32385	-2,36842
H	0,57185	-1,42995	-3,27695
C	0,67681	-4,22278	-1,31189
H	-0,44922	-4,40579	0,50654
H	1,60733	-3,63015	-3,15993
W	0,61800	1,83345	-0,88157
C	0,15667	2,81667	-2,61448
O	-0,15380	3,31035	-3,61000
C	1,98671	3,13719	-0,24535
O	2,77773	3,89138	0,15868
C	2,06790	0,77383	-1,88913
O	2,89799	0,20745	-2,44842
C	0,74655	0,51320	0,68799
O	0,74890	-0,27140	1,52832
C	-0,82968	2,89276	0,10760
O	-1,63318	3,50135	0,66866
C	1,29952	-5,55459	-1,24111
C	2,70782	-5,67426	-1,51770
C	3,59763	-4,56851	-1,37908

C	3,32444	-6,87611	-1,97211
C	4,95036	-4,66028	-1,65640
H	3,19911	-3,62237	-1,03792
C	4,67905	-6,96081	-2,24727
H	2,70875	-7,74971	-2,13705
C	5,52365	-5,85845	-2,09255
H	5,57399	-3,78245	-1,52075
H	5,08344	-7,90306	-2,60379
H	6,58280	-5,92905	-2,30616
C	0,47384	-6,68316	-0,89334
C	0,96959	-7,86553	-0,27200
C	-0,93128	-6,68571	-1,13392
C	0,15082	-8,93306	0,05769
H	2,01988	-7,92294	-0,02026
C	-1,74373	-7,75583	-0,80338
H	-1,37619	-5,81837	-1,60346
C	-1,22124	-8,90626	-0,20447
H	0,58910	-9,79984	0,54242
H	-2,80455	-7,69818	-1,02590
H	-1,85763	-9,74421	0,05087

48e-NH_2 (-2/1)

48

Energy = -1763.692305780888

ZPE = 0.33293141

P	-1,11342	-0,04318	-2,43136
C	-0,48694	-1,69371	-1,97792
C	-1,04284	-2,51115	-0,98645
C	0,62167	-2,21079	-2,66874
C	-0,50767	-3,75768	-0,68980
H	-1,90248	-2,16407	-0,42802
C	1,15088	-3,45261	-2,37116
H	1,07676	-1,62266	-3,45960
C	0,61487	-4,27955	-1,35867
H	-0,96363	-4,34662	0,09764
H	2,00636	-3,80647	-2,93404
W	0,64381	1,75071	-1,41692
C	-1,00445	2,91086	-1,05734
O	-1,94440	3,55084	-0,86197
C	1,83243	3,11398	-0,57461
O	2,51021	3,90937	-0,05988
C	0,76421	2,51500	-3,30705
O	0,78465	2,89380	-4,39759
C	2,26639	0,54934	-1,82693
O	3,18788	-0,10010	-2,05463
C	0,20917	0,61930	0,23959
O	-0,11643	-0,06801	1,10462
C	1,19404	-5,58684	-1,02159
C	2,62901	-5,71692	-0,96050
C	3,47910	-4,59744	-0,72434
C	3,31536	-6,95080	-1,14975
C	4,85823	-4,70407	-0,67984
H	3,02789	-3,62678	-0,56869
C	4,69578	-7,05117	-1,10222
H	2,73995	-7,84096	-1,36487
C	5,49865	-5,93266	-0,86421
H	5,44696	-3,81281	-0,48769
H	5,15699	-8,01974	-1,26808
H	6,57769	-6,01441	-0,82704
C	0,30882	-6,69029	-0,73727
C	0,65565	-7,77432	0,11808
C	-1,00489	-6,76395	-1,28335
C	-0,21131	-8,82123	0,38404
H	1,62343	-7,76873	0,60104
C	-1,86759	-7,81238	-1,01423
H	-1,33572	-5,97210	-1,94241
C	-1,48936	-8,86710	-0,17843
H	0,11017	-9,61065	1,05622
H	-2,85133	-7,81474	-1,47277
H	-2,16463	-9,68757	0,02949
N	-2,57219	0,00768	-1,45747
H	-2,42219	0,13302	-0,46109
H	-3,16707	0,76453	-1,77209

47f-Me (-2/3)

38

Energy = -1113.635458967413

ZPE = 0.29702859

P	-0,72842	0,19511	-0,93389
C	-2,34175	0,12713	0,01703
H	-2,74487	1,14192	0,05693
H	-3,09036	-0,51162	-0,46231
H	-2,21332	-0,22217	1,04644
C	-0,20734	-1,51461	-0,91111
C	-0,90154	-2,59067	-0,29826
C	1,01003	-1,87838	-1,55408
C	-0,43136	-3,88848	-0,33199
H	-1,82885	-2,39636	0,22605
C	1,48319	-3,16822	-1,57522
H	1,58229	-1,10292	-2,05592
C	0,78361	-4,24791	-0,96637
H	-0,99841	-4,66322	0,16867
H	2,40804	-3,38182	-2,09571
C	1,27309	-5,60395	-0,99400
C	2,69425	-5,87620	-1,11343
C	3,68989	-5,06932	-0,50519
C	3,16914	-7,05461	-1,80035
C	5,03739	-5,36109	-0,58024
H	3,37368	-4,19567	0,05337
C	4,52183	-7,33957	-1,87937

H	2,45167	-7,70285	-2,28434
C	5,48435	-6,51715	-1,28394
H	5,75541	-4,70749	-0,09674
H	4,84118	-8,22465	-2,42283
H	6,53829	-6,75904	-1,34562
C	0,35370	-6,72430	-0,90073
C	0,74463	-7,95393	-0,24981
C	-0,93192	-6,72126	-1,49995
C	-0,11536	-9,03761	-0,19493
H	1,71379	-8,00894	0,22663
C	-1,78354	-7,80694	-1,44964
H	-1,24911	-5,83102	-2,03130
C	-1,38539	-9,00221	-0,78104
H	0,20667	-9,93767	0,32184
H	-2,75648	-7,74830	-1,92557
H	-2,04222	-9,86239	-0,73865

47f-NH_2 (-2/3)

37

Energy = -1129.689847230464

ZPE = 0.28603730

P	-0,91182	0,07789	-1,18592
C	-0,34532	-1,61762	-1,09553
C	-1,03459	-2,68780	-0,47380
C	0,89915	-1,96050	-1,69084
C	-0,53215	-3,97213	-0,45601
H	-1,98152	-2,47254	0,00692
C	1,40473	-3,23896	-1,65994
H	1,46756	-1,18476	-2,19794
C	0,71278	-4,31766	-1,04308
H	-1,09409	-4,74871	0,04811
H	2,35072	-3,44396	-2,14478
C	1,23815	-5,66029	-1,01914
C	2,66942	-5,89649	-1,08748
C	3,62318	-5,04783	-0,47117
C	3,19743	-7,07438	-1,73697
C	4,98080	-5,30049	-0,50241
H	3,26553	-4,17159	0,05772
C	4,56005	-7,32052	-1,77195
H	2,51301	-7,75197	-2,22846
C	5,48069	-6,45837	-1,16782
H	5,66545	-4,61544	-0,01411
H	4,92061	-8,20637	-2,28780
H	6,54259	-6,67008	-1,19571
C	0,34726	-6,80337	-0,92754
C	0,75253	-8,00687	-0,23801
C	-0,92082	-6,84766	-1,55969
C	-0,07925	-9,11308	-0,18322
H	1,70874	-8,02401	0,26645
C	-1,74437	-7,95543	-1,50857
H	-1,24735	-5,97730	-2,11761
C	-1,33206	-9,12493	-0,80450
H	0,25221	-9,99285	0,36174
H	-2,70546	-7,93325	-2,01086
H	-1,96637	-10,00186	-0,76111
N	-2,46912	-0,00992	-0,34078
H	-2,51214	0,62469	0,44711
H	-3,25250	0,19956	-0,94770

48f-Me (-2/3)

49

Energy = -1747.588478778939

ZPE = 0.34311989

P	-1,32880	-0,00754	-2,03551
C	-2,66795	0,13713	-0,74882
H	-3,06738	1,15133	-0,80550
H	-3,48844	-0,56365	-0,92482
H	-2,28803	-0,01314	0,26408
C	-0,69266	-1,64579	-1,74890
C	-1,16699	-2,56864	-0,78376
C	0,43377	-2,07149	-2,50731
C	-0,57122	-3,79609	-0,59328
H	-2,01011	-2,30224	-0,15948
C	1,04050	-3,28364	-2,29801
H	0,82978	-1,40891	-3,26791
C	0,56671	-4,20869	-1,33019
H	-0,96240	-4,45370	0,17338
H	1,89515	-3,55418	-2,90545
W	0,86457	1,76954	-1,12281
C	-0,20224	3,19006	-2,13601
O	-0,82547	3,98304	-2,72142
C	2,22874	3,03040	-0,50955
O	3,03539	3,79425	-0,13282
C	1,83623	1,25769	-2,85531
O	2,37688	0,95438	-3,84658
C	1,73162	0,14879	-0,20238
O	2,22195	-0,76400	0,32528
C	-0,28938	2,07414	0,54164
O	-0,93286	2,25516	1,50018
C	1,20548	-5,48089	-1,10280
C	2,64271	-5,62096	-1,29045
C	3,52453	-4,54965	-1,02702
C	3,22154	-6,82232	-1,75401
C	4,89152	-4,67337	-1,21751
H	3,11855	-3,61866	-0,65467
C	4,58888	-6,94256	-1,94613
H	2,57787	-7,66118	-1,98325
C	5,43935	-5,86962	-1,68063
H	5,53765	-3,83213	-0,99611
H	4,99534	-7,87672	-2,31613

H	6,50734	-5,96391	-1,83200
C	0,41656	-6,63289	-0,68978
C	0,93159	-7,62179	0,17660
C	-0,91082	-6,81161	-1,13777
C	0,17198	-8,71417	0,56483
H	1,93765	-7,51172	0,55925
C	-1,66768	-7,90623	-0,75097
H	-1,33423	-6,08256	-1,81500
C	-1,13565	-8,87046	0,10432
H	0,59799	-9,44677	1,24043
H	-2,67845	-8,01402	-1,12688
H	-1,72767	-9,72504	0,40695

48f-NH_2 (-2/3)

48

Energy = -1763.645737294563

ZPE = 0.33219149

P	-1,47260	-0,04941	-2,38142
C	-0,90307	-1,71268	-2,11377
C	-1,41973	-2,61403	-1,15263
C	0,25249	-2,14451	-2,82070
C	-0,80691	-3,81835	-0,88700
H	-2,30138	-2,32732	-0,59330
C	0,87288	-3,33306	-2,53576
H	0,67204	-1,50129	-3,58547
C	0,38625	-4,22042	-1,53946
H	-1,21898	-4,45600	-0,11442
H	1,76119	-3,60766	-3,09056
W	0,84109	1,39558	-1,09112
C	0,00177	3,00676	-2,03231
O	-0,50434	3,90528	-2,57490
C	2,28957	2,40667	-0,25155
O	3,15588	3,01008	0,25943
C	1,91013	0,94290	-2,78154
O	2,51581	0,68183	-3,74640
C	1,43974	-0,38333	-0,25807
O	1,77414	-1,37803	0,23833
C	-0,43457	1,63930	0,48986
O	-1,15968	1,76610	1,40162
C	1,08755	-5,42900	-1,18681
C	2,54241	-5,47106	-1,27731
C	3,32206	-4,32206	-1,02080
C	3,23756	-6,64834	-1,62604
C	4,70470	-4,35165	-1,10887
H	2,82458	-3,40619	-0,73413
C	4,62097	-6,67408	-1,71639
H	2,67446	-7,54603	-1,84506
C	5,37004	-5,52644	-1,45896
H	5,26984	-3,45206	-0,89465
H	5,12012	-7,59366	-1,99915
H	6,45036	-5,54689	-1,53008
C	0,36030	-6,59621	-0,71456
C	0,90547	-7,48167	0,24184
C	-0,93772	-6,89493	-1,18560
C	0,20251	-8,58755	0,69249
H	1,88832	-7,27734	0,64517
C	-1,63780	-8,00289	-0,73541
H	-1,38288	-6,24892	-1,92996
C	-1,07687	-8,86270	0,20843
H	0,65001	-9,23652	1,43634
H	-2,62698	-8,20381	-1,13007
H	-1,62490	-9,72768	0,56028
N	-2,81773	0,04625	-1,25076
H	-2,51111	0,27246	-0,30896
H	-3,44847	0,78474	-1,53975

7.3 List of abbreviations

12c4, c	12-crown-4
Å	Ångström (1 Å = 10^{-10} m)
Abs.	absorption
Anth	anthracenyl
Ar	3,5-*tert*-butyl-pheny
Ar*	2,6-bis[(4-*tert*-butylphenyl)methyl]-4-methylphenyl
ATP	adenosine triphosphate
BDE	bond dissociation energy
bisyl	bis(trimethylsilyl)methyl
br	broad
Bu	butyl
CAAC	cyclic(alkyl)(amino)carbene
calc.	calculated
CHT	phospha-cycloheptatriene
Cp	cyclopentadienyl
Cp*	pentamethylcyclopentadienyl
CV	cyclo voltammetry
(Cw-)EPR	(continuous wave) electron paramagnetic resonance
Cy	cyclohexyl
d	dublet
Dmp	2,6-dimesitylphenyl
DNA	deoxyribonucleic acid
DOSY	Diffusion Ordered Spectroscopy
DRA	distonic radical anion
e	electron
EA	elemental analysis
E, C	electronical, chemical
e.g.	exempli gratia
Et	ethyl
eq.	equivalents
Fc	ferrocene

FWHM	full width at half maximum
GIAO	Gauge Included Atom Orbitals
HOMA	Harmonic Oscillator Measure of Aromaticity
HOMO	highest occupied molecular orbital
i.e.	id est
IR	infrared spectroscopy
Irr	irreversible
KHMDS	potassium hexamethyldisilazide
L	(co)-ligand
LDA	Lithium diisopropylamine
LUMO	lowest unoccupied molecular orbital
MBO	Mayer bond order
Me	methyl
Mes*	2,4,6-*tert*-butyl-phenyl
MS	mass spectrometry
MO	molecular orbital
m.p.	melting point
MS	mass spectrometry
NCD	phospha-norcaradiene
NICS	nucleus independent chemical shift
opt	optimized (during calculation)
OTf	triflate (trifluoromethane sulfonate)
Ph	phenyl
p*K*b	base constant
ppm	parts per million
Pr	propyl
q	quartet
Q	charge
red/ox	reduction/oxidation
r.t.	room temperature
s	singlet
S	spin state
sat	satellite

SET	single electron transfer
solv.	solvent
SOMO	single occupied molecular orbital
t	triplet
(TD-)DFT	(time-dependent) density functional theory
THF, t	tetrahydrofurane
Tol	tolyl
Trt/trityl	triphenylmethyl
TS	transition state
VDD	Voronoi Deformation Density
vs.	versus
VT	variable temperature
WBI	Wiberg bond index
WCA	weakly coordinating anion
WTMAD	weighted total mean absolute deviation
ZPE	zero-point-energy